Geotechnical and hydrogeological characterization of residual soils in the vadose zone

by

Jan Johannes Gerhardus Vermaak

submitted in partial fulfilment
of the requirements for the degree

Philosophiae Doctor

in the

Faculty of Science
University of Pretoria
Pretoria

February 2000

Geotechnical and hydrogeological characterisation of residual soils in the vadose zone

by

Jan Johannes Gerhardus Vermaak

Promoter: Professor A. van Schalkwyk
Faculty: Science
Department: Earth Sciences
Degree: Philosophiae Doctor

ABSTRACT

Groundwater is an important natural resource and ought to be protected. Groundwater recharge and contamination are two important aspects in groundwater management. Both these aspects apply to the vadose zone.

The research aimed to narrow the knowledge gap between practising geohydrologists and engineering geologists, both frequently involved in vadose zone investigations for geohydrological and engineering purposes respectively.

The vadose zone is the portion of the geological profile above the groundwater surface and is usually characterised by unsaturated conditions. Matrix forces counteract the force of gravitation to hold liquid in the porous medium and are reflected by hydraulic heads lower than atmospheric pressure (suction). The unique relationship between soil-water content and suction is presented by soil-water characteristic curves.

Flow of liquids is directly proportional to the hydraulic gradient and the hydraulic conductivity and is affected by the geometric properties of the pore channels. In unsaturated soils, flow is governed by both matrix and gravitational forces. Preferential flow is the process by which water and solutes move along preferred pathways through a porous medium.

Important hydrogeological properties, such as porosity, hydraulic conductivity and soil-water retention characteristics, can be estimated from geotechnical data. Unsaturated hydraulic conductivity can also be estimated from soil-water characteristic curves and saturated hydraulic conductivity.

The experimental procedures comprised analyses of existing hydrogeological data, laboratory tests and field experiments. The geotechnical data were used to predict important hydrogeological properties and these predictions were compared to experimentally derived hydrogeological properties. The effects of preferential flow and soil variability were also investigated.

Predictions of porosity, hydraulic conductivity and soil-water retention characteristics lack precision, owing mostly to the natural variability in hydrogeological properties and inherent errors of the empirical models. Accurate predictions of unsaturated hydraulic conductivity

were based on experimentally derived saturated hydraulic conductivity and soil water characteristic data.

The study area is located in Midrand and is underlain by granitoid rocks that had been subjected to a number of geomorphologic events. The land system classification approach was used to delineate the hydrogeological units. The different hydrogeological characteristics can be attributed mainly to the position of the hydrogeological units in respect of the topographical setting, the geomorphologic history and the underlying geology. A conceptual hydrogeological model was constructed for each of the hydrogeological zones and its significance in respect of groundwater recharge and vulnerability discussed.

The research has shown that geohydrological properties can be estimated from geotechnical data with various degrees of accuracy. Predictions of hydraulic conductivity, soil water retention characteristics and porosity are not suitable for site-specific investigations, but it can be used during the feasibility phases. In cases where saturated hydraulic conductivity and soil-water retention characteristics have been experimentally derived, estimations of unsaturated hydraulic conductivity are adequate for site-specific investigations. The land system approach can be used to delineate areas of similar geohydrological characteristics and these can be used in the compilation of aquifer vulnerability and groundwater recharge maps.

(478 words)

Die geotegniese en hidrogeologiese karakterisering van residuele gronde in die vadose sone

deur

Jan Johannes Gerhardus Vermaak

Promotor: Professor A. van Schalkwyk
Fakulteit: Natuurwetenskappe
Departement: Aardwetenskappe
Graad: Philosophiae Doctor

UITTREKSEL

Grondwater is 'n belangrike natuurlike hulpbron en behoort beskerm te word. Die bepaling van grondwateraanvulling en die omvang van grondwaterkontaminasie is twee belangrike aspekte van grondwaterbestuur. Beide hierdie aspekte is by die vadose sone van toepassing.

Daar is met die navorsing beoog om die kennisgaping wat tussen ingenieursgeoloë en geohidroloë bestaan te vernou. Ondersoeke in die vadose sone word deur beide ingenieursgeoloë en geohidroloë gedoen ten einde die geohidrologiese en ingenieurseienskappe van die grond te bepaal.

Die gedeelte van die geologiese profiel wat bokant die grondwatervlak voorkom, staan as die vadose sone bekend. Beide matriks- en gravitasiekragte word op die grondvog uitgeoefen. Die feit dat die hidrostatiese drukhoogte laer as atmosferiese druk is, word aan dié kragte toegeskryf ('n suigspanning word dus uitgeoefen). Die grondvog karakteristiekekurwe weerspieël die unieke verhouding tussen voginhoud en hidrostatiese drukhoogte in onversadigde gronde.

Die geometriese eienskappe van die poriekanale beïnvloed vloei in gronde. Hierdie vloei is direk proporsioneel tot die hidrouliese gradiënt en die hidrouliese konduktiwiteit. Vloei in onversadigde gronde word deur beide matriks- en gravitasiekragte beïnvloed. Die proses waarvolgens water langs voorkeurpaaie vloei staan bekend as voorkeurvloei.

Skattings van belangrike hidrogeologiese eienskappe, soos byvoorbeeld die porositeit, hidrouliese konduktiwiteit en grondvogretensie karakteristieke, kan gemaak word met behulp van geotegniese data. Skattings van die onversadigde hidrouliese konduktiwiteit kan gemaak word indien die grondvogretensie karakteristieke en versadigde hidrouliese konduktiwiteit bekend is.

Gedurende die navorsing is analises gemaak van bestaande hidrogeologiese data en laboratoriumtoetse, en veld-eksperimente is uitgevoer. Die geotegniese data is gebruik om voorspellings te maak van belangrike hidrogeologiese eienskappe. Die voorspellings is daarna vergelyk met waardes wat eksperimenteel verkry is. Die effek van voorkeurvloei en variasie van grondeienskappe is ook bestudeer.

Die porositeit, hidrouliese konduktiwiteit en grondvogretensie karakteristieke kon nie akkuraat voorspel word nie as gevolg van natuurlike variasie in geohidrologiese eienskappe

en inherente foute van die impiriese modelle. Die onversadigde hidrouliese konduktiwiteit kon wel akkuraat voorspel word deur gebruik te maak van die versadigde hidrouliese konduktiwiteit en grondvogretensie karakteristieke wat eksperimenteel bepaal is.

Die studie-area, geleë te Midrand, word onderlê deur granitiese gesteentes. Die gesteentes het verskeie geomorfologiese periodes deurgemaak. Die landsisteem klassifikasiestelsel is gebruik om hidrogeologiese eenhede te bepaal. Die posisie van die hidrogeologiese eenhede ten opsigte van die topografie, geomorfologiese geskiedenis en onderliggende geologie bepaal grootliks die geohidrologiese kenmerke van die eenhede. 'n Konsepsuele model is vir elke hidrogeologiese eenheid opgestel en die belangrikheid van die eenhede, ten opsigte van grondwater aanvulling en kwesbaarheid, is bespreek.

Die navorsing het getoon dat voorspellings van geohidrologiese eienskappe met verskeie grade van akkuraatheid gemaak kan word. Voorspellings van hidrouliese konduktiwiteit, grondvogretensie karakteristieke en porositeit is nie vir gedetailleerde terrein ondersoeke geskik nie, maar kan gebruik word tydens uitvoerbaarheidsondersoeke. Waar hidrouliese konduktiwiteit en grondvogretensie karakteristieke eksperimenteel bepaal is, kan akkurate voorspellings van onversadigde hidrouliese konduktiwiteit gemaak word. Die landsisteem klassifikasiestelsel kan gebruik word om hidrogeologiese eenhede te bepaal wat gebruik kan word om grondwateraanvullings- en kwesbaarheidskaarte op te stel.

(482 woorde)

ACKNOWLEDGEMENTS

- I would like to thank my promoter, Prof. A. van Schalkwyk, for his guidance and valuable support during the period of this study.

- I appreciate the opportunity given to me by the Water Research Commission to conduct the research and to use it for this thesis

- This project was only possible with the co-operation of many individuals and institutions. I therefore wish to record my sincere thanks to the following:

  - The Department of Water Affairs for their contributions in conducting laboratory geotechnical tests and making equipment available during the course of the project.

  - The Council for Geoscience and CSIR (Transportek) for making geotechnical data available for use in the project.

  - Dr J Annendale for making equipment available for use by the research team.

  - Prof. S Lorentz for contributing in literature and the value discussion regarding unsaturated soils.

  - Mr P Aucamp and C McKnight for their contributions to the research team.

  - The University of Pretoria, CONCOR Ltd., Department of Water Affairs and the Council for Geoscience for providing sites for the field experiments.

  - The many persons and institutions that provided assistance during the course of the field experiments.

- I would like to thank my employers, Yates Consulting (Pty) Ltd., for their support during the latter part of my study period.

- The support of my parents during my study period is greatly appreciated.

TABLE OF CONTENTS

LIST OF FIGURES

LIST OF TABLES

LIST OF SYMBOLS

A	Area (m^2) [L^2], Activity of soil (-) [-]
α_w	Contact angle between water and glass (deg) [-]
C	Percentage clay content (%) [-]
C_k	Permeability change index (-) [-]
C_c	Coefficient of curvature (-) [-]
C_u	Coefficient of uniformity (-) [-]
CV	Coefficient of variability (%) [-]
d	Diameter of liquid surface curvature, depth to groundwater level (m) [L]
D	Diameter of grain (m) [L]; Fractal dimension (-) [-]
D_x	Sieve size of where x per cent of mass of soil have passed through (m) [L]
D_{10}	Effective grain diameter (m) [L]
e	Void ratio (-) [-]
ε	Porosity (-) [-]
f	fluidity (m^{-1} s^{-1}) [$L^{-1}T^{-1}$]
G	Percentage gravel content (%) [-]
g	Gravitational force (m s^{-2}) [LT^{-2}]
γ_w	Unit weight of water (N) [$ML^{-2}T^{-2}$]
h	hydraulic head (m) [L]
η	Viscosity of a fluid (kg m^{-1} s^{-1}) [$ML^{-1}T^{-1}$]
h_c	Capillary height (m) (L)
h_f	Hydraulic head at the wetting front (m) (L)
h_p	Piezometric head or Hubert's potential (m) [L]
i	Infiltration rate (m s^{-1}) [LT^{-1}]

I	Cumulative infiltration rate (m s^{-1}) [LT^{-1}]
i_c	Final infiltration rate (m s^{-1}) [LT^{-1}]
i_o	Initial infiltration rate (m s^{-1}) [LT^{-1}]
K	Hydraulic conductivity (m s^{-1}) [LT^{-1}]
k	Intrinsic hydraulic conductivity or permeability (m^2) [L^2]
K_s	Saturated hydraulic conductivity (m s^{-1}) [LT^{-1}]
K_r	Relative hydraulic conductivity (-) [-]
l	Length (m) [L]
L_f	Depth to the wetting front (m) [L]
v	Darcian velocity (m s^{-1}) [LT^{-1}]
v_s	Seepage velocity or true velocity of flow (m s^{-1}) [LT^{-1}]
M	Percentage silt content (%) [-]
N_{re}	Reynolds number (-) [-]
OM	Percentage organic matter (%) [-]
p	Pressure (Pa or N m^{-2}) [$MT^{-2}L^{-1}$]
ρ	Density (kg m^{-3}) [ML^{-3}]
ρ_f	Density of the fluid (kg m^{-3}) [ML^{-3}]
ρ_w	Density of water (kg m^{-3}) [ML^{-3}]
ρ_d	Dry density of soil (kg m^{-3}) [ML^{-3}]
p_0	Atmospheric pressure, by convention considered to be equal to nil (Pa or N m^{-2}) [$MT^{-2}L^{-1}$]
PI	Plasticity index (%) [-]
Q	Rate of flow (m^3s^{-1}) [L^3T^{-1}]
q	Specific discharge, Darcian flux or flux (cubic metre per square metre area) (m s^{-1}) [LT^{-1}]
q_{zo}	Specific discharge at groundwater surface depth (m s^{-1}) [L T^{-1}]
θ	Volumetric water content (m^3 m^{-3}) [-]
Θ	Effective degree of saturation (m^3 m^{-3}) [-]
θ_0	Initial volumetric water content (m^3 m^{-3}) [-]

θ_a Residual air content ($m^3\ m^{-3}$) [-]

θ_r Residual water content or specific retention ($m^3\ m^{-3}$) [-]

θ_s Saturated water content ($m^3\ m^{-3}$) [-]

Q_{tot} Total quantity of flow over time t (m^3) [L^3]

r Radius of the liquid surface curvature (m) [L]

R Radius of the narrow tube or pore radius (m) [L]

ρ_d Dry density of an undisturbed soil sample or *in situ* soil ($kg\ m^{-3}$) [ML^{-3}]

ρ_g Density of the gas ($kg\ m^{-3}$) [ML^{-3}]

ρ_l Density of the liquid ($kg\ m^{-3}$) [ML^{-3}]

ρ_w Density of water ($kg\ m^{-3}$) [ML^{-3}]

r Radius of the liquid radius curvature (m) [L]

R Radius of the capillary/soil pore (m) [L]

RE Recharge ($m\ s^{-1}$) [LT^{-1}]

R_{eff} Effective pore radius (m) [L]

σ Surface tension of a liquid ($N\ m^{-1}$) [MT^{-2}]

S Percentage sand content (%) [-]

S_s Specific Storage (m^{-1}) [L^{-1}]

SG Specific gravity (-) [-]

t Time (s) [T]

T Temperature (°C) []

τ_s Shearing stress ($N\ m^{-2}$) [$MT^{-2}L^{-1}$]

Tt Travel time of liquids flowing through the vadose zone (s) [T]

u Velocity ($m\ s^{-1}$) [LT^{-1}]

$\overline{u}$ Average velocity ($m\ s^{-1}$) [LT^{-1}]

u_a Pore air pressure (Pa or $N\ m^{-2}$) [$MT^{-2}L^{-1}$]

u_w Pore water pressure (Pa or $N\ m^{-2}$) [$MT^{-2}L^{-1}$]

V_{dz} Deficiency zone or storage capacity of the vadose zone (m^3) [L^3]

w Mass of sample (kg) [M]

W Sources/Sinks discharges (cubic meter water per cubic meter soil) (s^{-1}) [T^{-1}]

ψ Soil suction (Pa or N m^{-2}) [$MT^{-2}L^{-1}$]

ψ_b Bubbling pressure (Pa or N m^{-2}) [$MT^{-2}L^{-1}$]

ψ_a Air entry value (Pa or N m^{-2}) [$MT^{-2}L^{-1}$]

z Vertical distance or depth (measured from the groundwater surface positively upwards) (m) [L]

z_0 Distance to the groundwater level (m) [L]

z_{dz} Depth of the deficiency zone (m) [L]

z_{dz} Depth of the deficiency zone (m) [L]

CHAPTER 1

INTRODUCTION

It is well known that South Africa is a water-poor country (Department of Water Affairs and Forestry, 1986; Reynders, 1991; Parsons & Jolly, 1994). Due to a rapidly expanding population, increased consumption of water by the industrial sector and general upliftment in living standards of South African people, it is believed that the demand for water will in the future increase significantly.

The South African government's objectives as regards the management of water resources are "to achieve optimum, long term, environmentally sustainable social and economic benefit for society from their use" (Braune & Dziembowski, 1997). The Department of Water Affairs and Forestry (South Africa) has recognised that a holistic approach should be followed in the management of water resources (Braune & Dziembowski, 1997). This implies an integrated approach to management, with regard to both quantity and quality, for all water resources, i.e. surface and sub-surface water.

The importance of groundwater in South Africa is well-documented (Braune, 1990; Reynders, 1991; Parsons & Jolly, 1994). Approximately 65 per cent of the area in South Africa relies on this water source in one way or another (Braune, 1990). Groundwater is an important source of water for many rural communities, especially those that have been disadvantaged.

While rapid growth puts ever-increasing demands on groundwater as a source of urban, agricultural and rural water supply, it also causes deterioration in groundwater quality, mainly due to poor groundwater management, waste disposal, mining and agricultural activities.

The government's commitment to ensure that every person has access to clean drinking water should include the protection and efficient management of groundwater, to ensure its use as a sustainable resource for both groundwater users, and indirectly for surface water users. Groundwater management should thus strive towards ensuring that a sustainable source of water of an acceptable degree of quality is maintained. This implies that an assessment of groundwater recharge and vulnerability should be an integral part of the management of groundwater resources. Unfortunately, both aspects are as yet poorly understood. This is partly because these processes take place in the vadose zone, an area that has been largely neglected by the geohydrological community.

Much of the theoretical knowledge regarding unsaturated flow and soil-moisture retention is based on investigations conducted largely to determine the moisture retention characteristics for agricultural purposes. However, during the last two decades, this knowledge has primarily been applied to liquid flow and contaminant transport investigations. The theoretical aspects of fluid movement and contaminant transport through the vadose zone are fairly well established and have been proven by numerous vadose zone investigations. However, soil scientists have traditionally focussed on the top 1.2 metres of the soil profile and very little investigations have been conducted in deeper soil profiles, with the result that very little is known about the hydrogeological characteristics for major parts of the vadose zone.

Engineering geologists have also traditionally been involved with investigations regarding the vadose zone primarily for engineering purposes. In most cases, geotechnical investigations comprise an

assessment of the weathered geological profile that usually constitutes a portion of the vadose zone. Engineering geologists and geotechnical engineers are mainly interested in soil and/or rock material strength, possible volumetric changes and permeability of materials.

More recently, a general awareness of the environment has compelled engineering geologists to address environmental aspects in many geotechnical investigations. These investigations include developments of waste disposal sites, underground and surface storage facilities as well as pipelines for the storage and transmission of hazardous fluids, water purification works, cemeteries, low cost housing, developments where no sewage services are available and industrial developments.

Depending on the purpose of the investigation, engineering geologists may be required to assess soil conditions for

i. Regional areas (e.g. planning for residential and industrial developments)

ii. Local areas (e.g. residential developments)

iii. Site-specific areas (e.g. foundation investigations).

A large number of proven geotechnical methods and techniques have been developed to assess soil and rock conditions for these situations. These methods may include aerial photo interpretation, description of soil profiles and a number of *in situ* and laboratory tests.

Standard geotechnical tests, such as soil profile descriptions and foundation indicator tests, are conducted at almost every geotechnical investigation. In the case of geotechnical investigations for residential purposes, these geotechnical data may cover large areas. These data are stored for record keeping purposes and are generally available from the relevant engineering and engineering geology institutions. In addition, a number of mainly public institutions have established large geotechnical data sets, mainly for general development and transport planning purposes. This information is generally available from the relevant institutions, in formats varying from hardcopy reports and maps to electronic databases and from Geographical Information Systems (GIS). This information can be used in hydrogeological investigations.

The current groundwater situation can be summarised as follows:

- The importance and vulnerability of groundwater requires that the resource should be effectively managed. This entails an accurate assessment of groundwater recharge and its vulnerability to contamination.

- The geohydrological community has traditionally been involved in the exploration of groundwater resources, groundwater exploitation and the assessment of possible contamination pathways within the groundwater regime. However, due to a lack of knowledge and information regarding the vadose zone, groundwater recharge and vulnerability could often not be accurately assessed.

- The soil science community has contributed significantly to the understanding of unsaturated flow processes. In addition, soil data are available from mainly public sector institutions. However, soil data have traditionally been collected for agricultural purposes, therefore ignoring the deeper soil and rock profile constituting a major portion of the vadose zone.

- Engineering geologists have been traditionally involved in assessing soils and rocks for engineering purposes. Many of these structures, such as waste disposal sites, can adversely affect groundwater. The engineering geologists are therefore required to assess the contamination potential for these structures, often lacking knowledge to accurately assess the situation.

- On the other hand, engineering geologists are in possession of large geotechnical data sets and have the knowledge and expertise to accurately assess geotechnical characteristics for large areas. These

data sets and geotechnical techniques can be used to assess groundwater recharge and contamination and will assist geohydrologists to accurately assess the sustainability and vulnerability of groundwater resources.

The research aims to bridge the knowledge gap between practising geohydrologists involved in groundwater recharge and contamination investigations and engineering geologists frequently involved in similar investigations from an engineering point of view. It also aims to incorporate the wealth of existing geotechnical data to estimate important hydrogeological properties. These estimated properties could be used, in conjunction with relevant climatic and geohydrological information, to estimate groundwater recharge and contamination for use in aquifer vulnerability studies and recharge assessments.

1.1 Aims of this study

The hydrogeological properties of soil, climate and vegetation are the main aspects that need to be considered in the assessment of water flow in the vadose zone. Water infiltrates the vadose zone mainly because of precipitation and irrigation. In addition, water is removed from the soil by means of evaporation and transpiration processes. The portion of water not removed by evapotranspiration processes reaches the groundwater and is termed recharge. Rainfall events are erratic and, as such, water flow in the vadose zone is dynamic. This implies high variability in annual recharge that will mainly be a function of rainfall patterns.

The rate at which water infiltrates into, or is removed from the soil will mainly be a function of the hydrogeological properties of the vadose zone. The term "*hydrogeological properties of the vadose zone*" refers to mainly physical properties of soils and rocks that constitute the vadose zone and are affecting the rate at which water is flowing through it. Flow in the vadose zone is a function of *inter alia* moisture content, which implies that the rate of water flow through the vadose zone is determined by complex functions of precipitation and evapotranspiration processes. Considering the highly erratic characteristics of rainfall, it is the author's opinion that these complex relationships can only be described, understood and predicted by means of numerical modelling.

Since infiltration and evapotranspiration theory is well-established (Ward, 1975; Bodman & Colman, 1943; Philip, 1964; Penman, 1963, Horton, 1933), it was decided not to consider climate as part of the project. Rather, it was decided to focus on estimating hydrogeological properties from readily available geotechnical data, thereby providing inputs, which together with climatic inputs, infiltration, redistribution and evapotranspiration theory, could be used in the assessment of groundwater recharge, vulnerability and other processes occurring in the vadose zone.

The aims of this research were:

- To identify those hydrogeological properties important in the assessment of saturated and unsaturated flow occurring in the vadose zone
- To establish relationships between readily available geotechnical data and the hydrogeological properties of residual soils that occur within the vadose zone
- To apply the above-mentioned results in the hydrogeological characterisation of the vadose zone for a specified study area.

The initial approach was to obtain direct relationships between geotechnical and hydrogeological properties as described by established one-dimensional flow equations through the soil matrix of the vadose zone. However, it soon became apparent that preferential flow could have a major impact on flow of fluids and solute transport through the vadose zone. It has also been established that the spatial distribution and variability of soil properties could have a significant impact on recharge within a regional

area. Research was conducted on three aspects regarding the hydrogeology of the vadose zone, namely: pedotransfer functions, preferential flow and hydrogeological characterisation on a field scale (**Figure 1.1**).

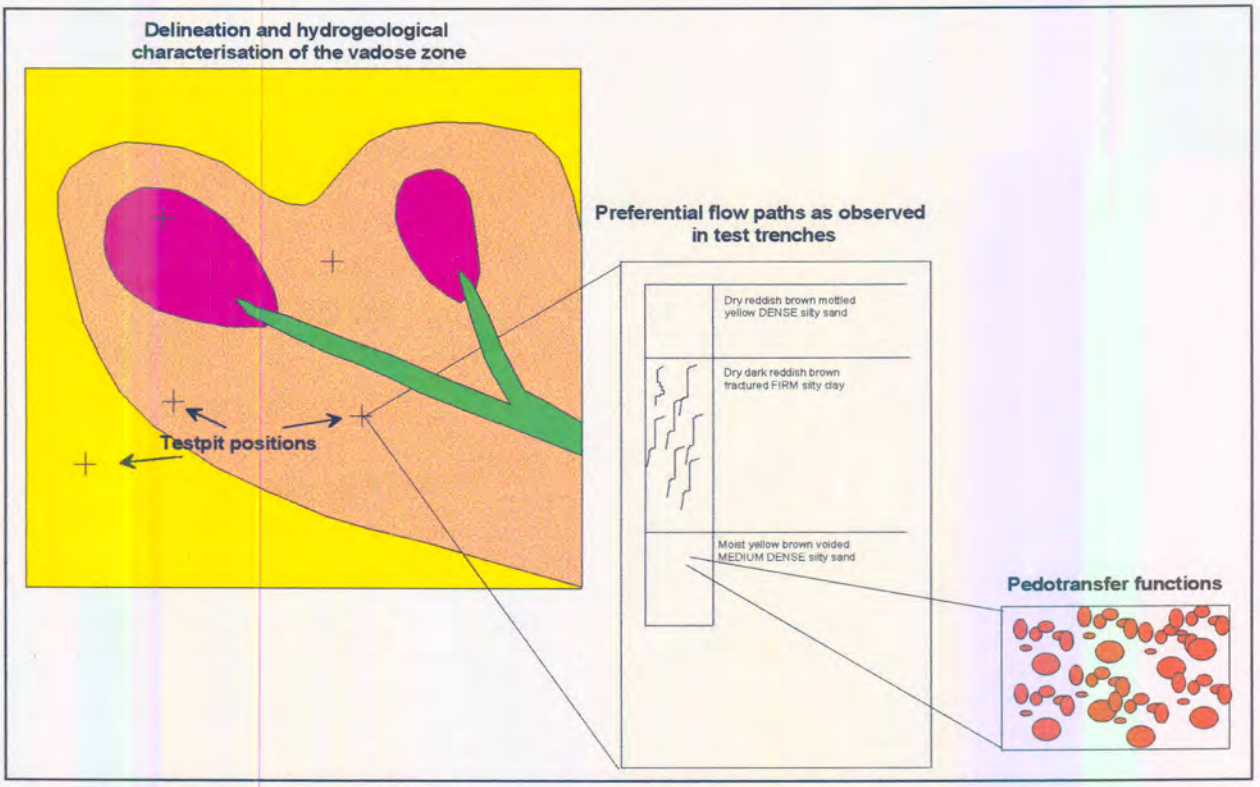

Figure 1.1: Three aspects considered regarding flow in the vadose zone

Pedotransfer functions refer to methods and techniques to estimate important hydrogeological parameters from widely available soil data such as particle-size distribution and Atterberg limits. These functions are based on point source soil samples and generally represent flow characteristics through specific soil layers within the vadose zone. Pedotransfer functions are typically empirical in nature.

Preferential flow represents flow mechanisms where fluids by-pass the soil matrix. In this investigation, the impact of macropore channelling was assessed for three different residual soils.

Both pedotransfer functions and preferential flow were considered in the compilation of a map indicating units of similar hydrogeological characteristics of the vadose zone. This map can be used in groundwater recharge and vulnerability assessments and indicates how geotechnical data can be applied to assist in the assessment of groundwater recharge and vulnerability. Aspects such as attenuation and climate were not considered in the compilation of this map.

It can be seen that the three above-mentioned aspects account for the effect of scaling within the vadose zone. Pedotransfer functions are used to determine hydrogeological parameters for specific soil layers within the vadose zone. Preferential flow accounts for preferred flow through the vadose zone and, in the case of macropore channelling, it can generally be observed in soil profiles. Hydrogeological characterisation implies that units with similar hydrogeological characteristics can be presented by means of either electronic or hardcopy maps.

1.2 Approach

In compiling this thesis, it was taken into consideration that the results could be applicable to a broad spectrum of scientists involved in groundwater research. These scientists include engineering geologists

who may not be fully versed in geohydrology and geohydrologists who may not be acquainted with aspects of engineering geology. Likewise, these scientists might not possess knowledge on unsaturated and preferential flow processes occurring in the vadose zone. For this reason, the thesis contains an extensive literature survey, covering aspects ranging from basic textbook information to frontline research findings.

This thesis incorporates the extensive literature study and the application of the research findings to the study area.

Chapters 2, 3 and 4 contain an extensive literature study. Chapter 2 covers basic aspects of the vadose zone, theory of flow through saturated and unsaturated soil, preferential flow, groundwater recharge and vulnerability and numerical unsaturated flow modelling. Chapter 3 describes the general aspects, methods and techniques applied during engineering geology investigations, and also discusses the availability of geotechnical data. Chapter 4 covers relationships between geotechnical data and hydrogeological properties of soils in the vadose zone. Both saturated and unsaturated properties are considered.

Chapter 5 describes the experimental procedures. Those include five field studies conducted at three different areas in South Africa, laboratory experiments and analyses of data sets obtained from the literature. Chapter 6 discusses the results of the experiments.

Chapter 7 describes the application of the above-mentioned relationships in a regional hydrogeological investigation of a study area located in Midrand, South Africa. A map of the study area, depicting zones of similar soil types, has been compiled in GIS and is included as Drawing 1 at the back of the thesis.

CHAPTER 2

GEOHYDROLOGICAL CHARACTERISTICS OF THE VADOSE ZONE

2.1 Behaviour of a fluid in a porous medium

Porous media such as soil and rock are generally three-phase systems, comprising solids, liquids and gasses. Saturated porous media refer to the situation where almost all gases have been replaced by liquid. Unsaturated porous media refer to the situation where both gasses and liquids are present in between the porous medium.

2.1.1 Saturated porous media

Saturated conditions refer to a two-phase system comprising solids and liquids. The liquids are subjected to gravitational force. The behaviour of the liquids is primarily governed by the Fundamental Theorem of Fluid Statics, stating that the difference of pressure in a fluid in a vertical direction can be represented by the following equation:

$$\frac{\delta p}{\delta z} = -\rho_f \cdot g \qquad [2\text{-}1]$$

Equation 2-1 can be applied to calculate any pressure, p, at height, z, at a given pressure p_0, and height, z_0, provided that the density is a constant or a known function of both pressure and height as is shown in the following equation.

$$\int_{p_0}^{p} \frac{\delta p}{\rho_f . g} = \int_{z_0}^{z} \delta z = z - z_0$$

or

$$z = z_0 + \int_{p_0}^{p} \frac{\delta p}{\rho_f \cdot g} \qquad [2\text{-}2]$$

If the fluid is incompressible or the effect of pressure and density is negligible, Equation 2-2 is simplified as follows:

$$z = z_0 + \frac{(p - p_0)}{\rho_f \cdot g} \qquad [2\text{-}3]$$

The pressure at the groundwater surface is equal to atmospheric pressure. In subsurface flow studies, the value of atmospheric pressure, p_0, is by convention considered to be nil. Height, z, is known as the pressure head, piezometric head or Hubert's potential, h_p, and pressure, p, is the difference between pore-water and pore-air pressure. Since pore-air pressure is usually equal to atmospheric pressure (nil), pressure, p, is equal to pore-water pressure, u_w, Equation 2-3 can then be expressed as follows:

$$h_p = \frac{u_w}{\gamma_w} \qquad [2\text{-}4]$$

2.1.2 Unsaturated porous media

Unsaturated conditions refer to a three-phase system comprising solids, liquids and gasses. Under these conditions, the voids are filled mainly by gas, since most of the liquid has been removed because of gravitational force. Forces that counteract the force of gravitation to hold liquid in the porous medium are called *matrix forces*. These forces include *capillary* and *adsorption forces* and *electrical forces on a molecular level.*

In soil-plant environments, the matrix forces may include the effect of osmotic forces. Osmotic forces refer to the attraction of solute ions or molecules to water. If pure water is separated from water containing solutes, by a membrane that is not permeable for solutes, water molecules will move towards the solute water mixture and this will cause a higher pressure in the solute water side of the membrane. Since osmotic suction has little effect on movement of water through a porous medium, osmotic forces have been omitted for purposes of this study.

Capillary forces

A wetting liquid, such as water, will rise in a capillary tube, caused by the difference in pressure between the liquid and gas within the tube. The difference in pressure occurs owing to curvature on the liquid-gas interface, known as the meniscus, in a capillary tube.

The relationship between pressure difference, dp, and a double-curved surface element on the liquid-gas interface (such as the curvature that occurs in a capillary tube) is expressed by Laplace's equation:

$$dp = \sigma\left(\frac{1}{r_1} + \frac{1}{r_2}\right) \qquad [2\text{-}5]$$

If the radii are equal in length, Equation 2-5 is simplified to:

$$dp = \frac{2 \cdot \sigma}{r} = \frac{4 \cdot \sigma}{d} \qquad [2\text{-}6]$$

The pressure difference within the capillary tube can be expressed as:

$$dp = \frac{2 \cdot \sigma \cdot \cos(\alpha_w)}{R} \qquad [2\text{-}7]$$

The height, h_c, to which the liquid rises in the tube is controlled by the downward force caused by the weight of the liquid, and can be calculated as follows:

$$h_c = \frac{2 \cdot \sigma \cdot \cos(\alpha)}{(\rho_l - \rho_g) \cdot g \cdot R} \qquad [2\text{-}8]$$

The density of the gas, ρ_g, is generally ignored. From Equations 2-7 and 2-8 we obtain the following:

$$h_c = \frac{dp}{\rho_l \cdot g} \qquad [2\text{-}9]$$

dp has a negative value, which implies that the pressure beneath the meniscus in the capillary tube is lower than atmospheric pressure and that the liquid will rise in the tube.

Equations 2-4 and 2-9 can be combined to yield an equation that is applicable in both saturated and unsaturated conditions:

$$h = \frac{u_w}{\gamma_w} \qquad [2\text{-}10]$$

Hydraulic head, h, and pore-water pressure, u_w, have negative values in unsaturated conditions. Capillary forces can also be expressed in terms of soil suction, ψ

$$\psi = u_a - u_w \qquad [2\text{-}11]$$

The pore-air pressure, u_a, is usually equal to atmospheric pressure and is therefore omitted.

A porous medium, such as soil, can be compared to a bundle of capillary tubes, with varying and irregular radii, tied together. A concave meniscus extends from grain to grain across each pore channel. The radius of each curvature reflects the pressure difference between the liquid and the gas (Freeze & Cherry, 1979). Forces that hold liquid in a porous medium owing to capillary action are called capillary forces. Capillary forces are approximately inversely proportional to effective pore diameter, R_{eff} (Hillel, 1980), to be expressed as follows:

$$R_{eff} = \frac{2 \cdot \sigma \cdot \cos(\alpha_w)}{\rho_f \cdot g \cdot h} \qquad [2\text{-}12]$$

R_{eff} represents the radius of a hypothetical bundle of capillary tubes on a macroscale. On a microscale, however, great variations occur caused by variations in pore size. Ward (1975) states that the concept of soil being compared to a bundle of capillary tubes tied together, is totally inadequate in describing soil-water movement in unsaturated soils. He maintains that water movement in unsaturated soils mainly takes place through films of water in the irregularly shaped inter-particle voids.

Adsorption forces

In addition to capillary forces, the adsorption of liquid molecules onto solid particles is also an important force. Surface tension forces occur on the solid-liquid and solid-gas interfaces. The force that attracts a

fluid to a solid surface is known as adhesion. Adsorbed liquids are held very tightly to the solid particles and cannot be removed, except by external forces such as evaporation (Hillel, 1980). Water that is adsorbed onto soil grains is called hygroscopic or adsorbed water.

The volume of water that is adsorbed onto soil grains is directly proportional to the specific surface of the soil, which in turn is inversely proportional to the grain size of the soil. Clay minerals have much higher specific surfaces than silt or sand grains, due to their relatively small sizes. Certain clay minerals, especially smectites, possess large adsorption areas because of their ability to incorporate water into their crystal lattices.

Electrical forces at molecular level

Since water is a bipolar molecule, it is attracted to soil grains resulting from the net electrical charges that may occur on the surfaces of soil grains, especially clay minerals. Permanent negative charges occur on the surfaces of clay minerals, caused by isomorphous substitution. Net electrical charges also occur on the edges of clay minerals and on the surfaces of allophane and hydroxides of iron and aluminium, due to their incomplete crystal lattices (White, 1989). This phenomenon is partly responsible for water being held in the soil matrix, particularly of clay soils. It is also partly responsible for the cohesion and plasticity of clay soils.

The charges on a mineral surface can be calculated by measuring the difference in moles of charge contributed, per unit mass, by cations and anions adsorbed from an electrolyte solution at a known pH. The cations and anions adsorbed, are known as the Cation Exchange Capacity (CEC) and Anion Exchange Capacity (AEC), respectively, and are expressed as cmols charge per kilogram. Typical cation exchange capacities of common clay minerals are shown in **Table 2.1**.

Table 2.1 Typical values of some properties of common clay minerals (White, 1989; Holtz & Kovacs, 1981)

	Kaolinite	Illite	Chlorite	Montmorillonite	Vermiculite
Thickness (nm)	50-2000	30	30	3	NA
Diameter (nm)	300-4000	1000	1000	100-1000	NA
Specific surface (km^2/kg)	0.015	0.08	0.08	0.8	NA
CEC $cmol_{(+)} \cdot kg^{-1}$	3-20	10-40	NA	80-120	100-150
Plasticity	Low	Medium	Medium	High	Medium
Swelling/ Shrinkage	Low	Medium	Low	High	NA

NA = Not available

2.2 The vadose zone

The vadose zone is the portion of the geological profile above the groundwater (phreatic) surface. Voids within the profile are usually, but not always, partially filled by liquid and partially by gas. The terms 'unsaturated zone', 'capillary zone' and 'zone of aeration' are frequently used in literature referring to this portion of the soil profile. To understand the concepts affecting moisture distribution and flow through the vadose zone, knowledge of the processes and forces that govern liquid flow through a porous medium is essential.

Figure 2.1 indicates a homogeneous soil profile through the vadose zone, under static conditions. The effect of evapotranspiration has been omitted. The vadose zone can be divided into three sub-zones namely, the *capillary fringe*, *capillary zone* and *discontinuous zone* (Martin & Koerner, 1984a) as indicated in the figure.

The **capillary fringe** is a zone that occurs directly above the groundwater surface. The zone is completely saturated and subjected to negative pressure. The thickness of the capillary fringe, h_d is analogous to the height of capillary rise. The specific diameter of the capillaries is inversely proportional to the effective pore diameter of the soil (Martin & Koerner, 1984a). The effective pore diameter is dependent on the gradation (soil texture), porosity and other factors. The capillary fringe will be thick in fine-grained soils and thin in coarse-grained soils.

The **capillary zone** consists of soil in which the pores are filled with air and water. Matrix forces hold the water in the soil. Water fills the small pores, while air fills the large pores in the soil. As the pore-water pressure decreases with distance above the groundwater surface, the radius of the curved water surface decreases and the water consequently retreats into smaller pores. This leads to a decrease in water content. Fine-grained soils can retain high water contents for considerable distances above the groundwater surface (Martin & Koerner, 1984a).

In the **discontinuous zone**, water is only retained as adsorbed water, since the pore-water pressure is too low to sustain capillary water. Water is strongly adsorbed on each soil particle. This water can be removed by evaporation.

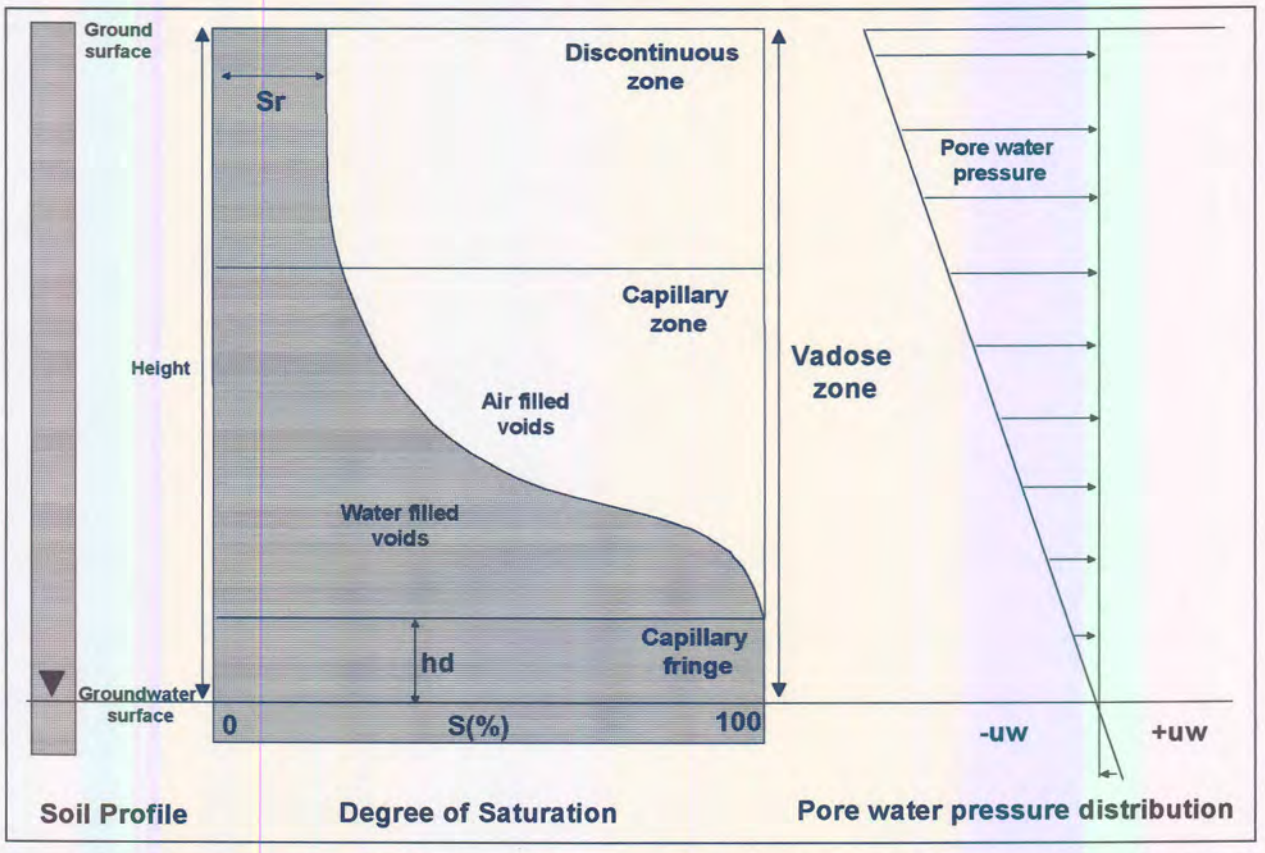

Figure 2.1: The vadose zone indicating soil-water content – pore-water pressure relationship (after Martin and Koerner, 1984a)

Specific retention and storage capacity

Specific retention, θ_r, can be defined as "the volume of water that is retained by a unit volume of soil against the force of gravity during drainage" (Everett, Wilson & Hoylman, 1984). This minimum water content is known as specific retention, field capacity or residual water content and can be determined from soil-water characteristic curves (section 2.3). The concept of specific retention is controversial since it does not exist (Edworthy, 1989). Drainage never really ceases but drainage rates decrease progressively until the drainage rate is practically equal to nil. There is no definite point where the water

flow ceases. The extreme variability in unsaturated flow rates, as well as the existence of preferential pathways, considerably complicates the determination of specific retention.

Specific retention is reached in a static situation, i.e. no external factors are considered. However, in field situations evapotranspiration is responsible for a decrease in water content lower than the specific retention value. This zone of water deficiency can reach considerable depths in arid and semiarid environments (Martin & Koerner, 1984a). In the case that water reaches these zones, it will be retained in the soil because of the high sorption of the soil. The maximum volume of water that can be accommodated in the deficiency zone, V_{dz}, also known as the storage capacity of the vadose zone, can be approximated by the following equation (Everett *et al.*, 1984):

$$V_{dz} = (\theta_r - \theta_s) z_{dz} \cdot A \qquad [2\text{-}13]$$

The disposal of hazardous waste in zones of water deficiency seems to be feasible, since leachate will be retained in the soil matrix because of the high sorption of the soil (Martin & Koerner, 1984b; Levin, 1988). However, downward migration of leachate will continue, albeit at a very slow rate. Calculations of storage capacity may be inaccurate because of complications in determining the specific retention value of the soil. The existence of preferential pathways may cause rapid movement of liquid waste and leachate along these pathways.

2.3 Soil-water characteristic curves

When soil suction is slowly increased on a fully saturated non-shrinking soil, either by applying suction on the liquid phase or by exerting pressure on the gas phase, the liquid will begin to retreat below the soil surface. Large pores will be emptied and a curved liquid surface, initially with a large radius, will develop. At low suctions, only large pores are partially filled with gas, while smaller pores are filled with liquid. With increasing suction, the radius of the curved liquid surface becomes smaller in accordance with Laplace's equation, and the liquid retreats into smaller pores. This results in a decrease in water content. Water in large pores is held less tightly and drains more easily.

A similar process is observed in shrinking soils such as clay with a high smectite content. However, under low suction the material will shrink, resulting in a reduction in pore size. Although water will drain from the soil at these pressures, the material will still be completely saturated. Under increasing suction, pores will begin to fill with gas and the process described above will develop. However, in field soils, cycles of shrinkage and heaving will cause cracks to develop. At very low suctions, a portion of the water will drain through cracks, resulting in a decrease in water content. After the water has drained through the cracks, the drainage rate becomes much slower, with a progressively higher suction.

The unique relationship between water content and soil suction for a specific soil is presented by soil-water characteristic curves. **Figure 2.2** shows typical adsorption and desorption soil-water characteristic curves for silty sand. A number of parameters can be defined from these curves, namely the saturated water content, θ_s, residual water content, θ_r, the air-entry or bubbling pressure, ψ_a, and the residual air content, θ_a.

The difference between adsorption (wetting) and desorption (drying) cycles may be attributed to hysteresis. This phenomenon is caused by the 'ink bottle' effect where many pores have narrow connections or entry channels to adjacent pores. This means that, when drying, pores will not drain until suctions are large enough to drain water from the entry channel. Likewise, with wetting, water will not enter a pore until equal suctions are reached. The water content will therefore be lower for wetting cycles at equal suction values. The difference between wetting and drying cycles at saturation can be attributed to air entrapment during the wetting cycle. With time, air bubbles trapped in pores will be released and the water content will be equal to the saturated water content. The drying curve is usually employed in experimental studies. Many researchers feel that the wetting cycle gives a better indication of pore-size distribution than the drying cycle, since the former is governed by the size of the pore while the latter is

governed by the size of the entry channel (Ward, 1975). However, because of experimental difficulties involving the wetting cycle, many researchers prefer to use the drying curve in their studies.

Figure 2.3 indicates typical drying soil-water retention curves for sand, silty sand and clay respectively. Soil-water characteristic curves generally have an inverse-S shape and three sections can be identified, namely a gradual slope at low soil suctions, a steeper slope at increasing suctions and again a gradual slope at high soil suctions. The differences between the soil-water characteristic curves of different soils are attributed mainly to differences in pore-size distribution in each soil. The curves are sensitive to changes in soil density and disturbances of soil structures (Miyazaki, 1993).

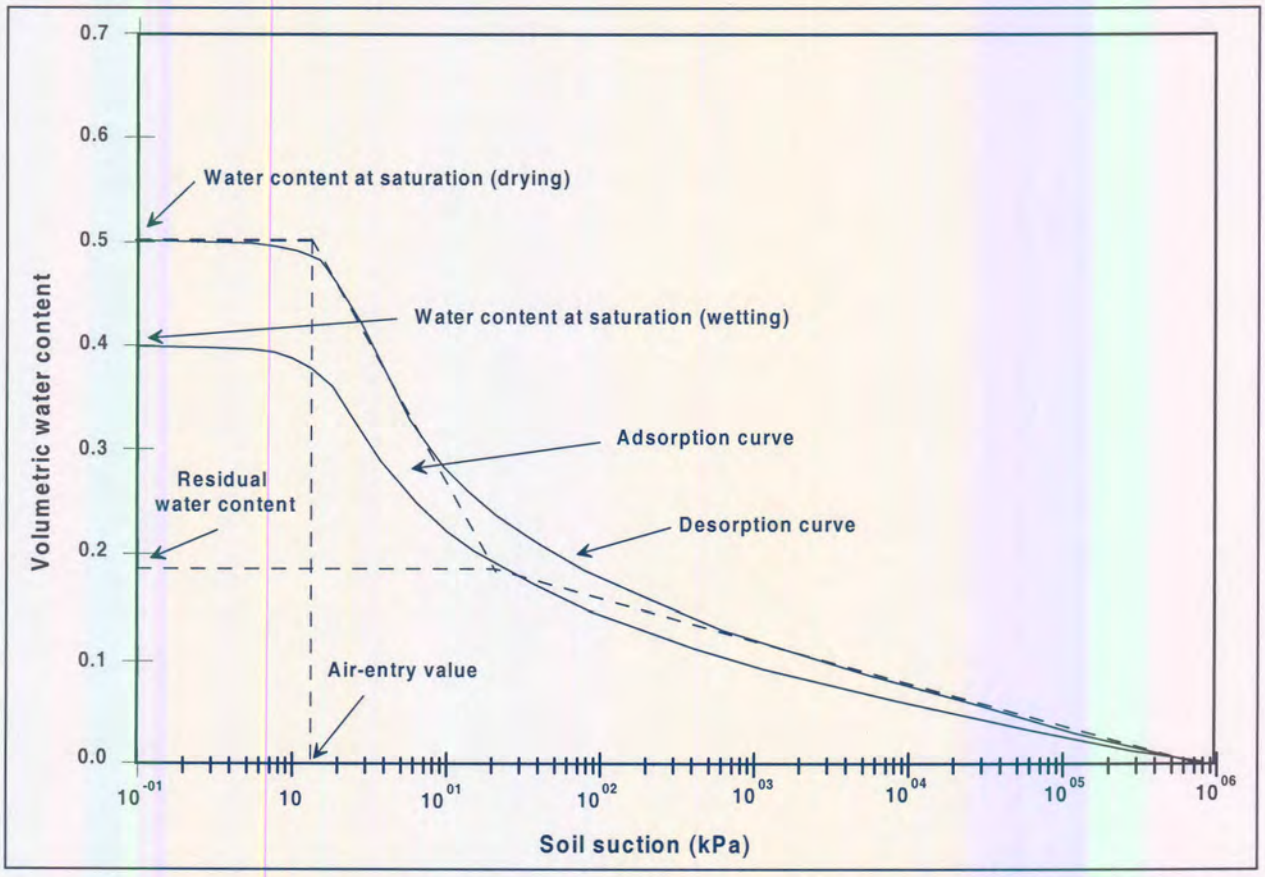

Figure 2.2: Typical soil-water characteristic curve for a silty sand (after Fredlund & Xing, 1994)

Since the soil suction, ψ, is inversely proportional to pore-water pressure, u_w, and hydraulic head, h, and proportional to effective pore-size, R, water content can be related to either of the above-mentioned parameters.

Soil-water characteristic curves are frequently used by the agricultural soil science and geotechnical communities in vadose zone studies (Martin & Koerner, 1984a; Everett *et al.*, 1984; Fredlund & Xing, 1994, Leong & Rahardjo, 1997). Soil-water retention data may be available from agricultural soil science institutions and many soils laboratories are equipped to determine soil-water retention characteristics.

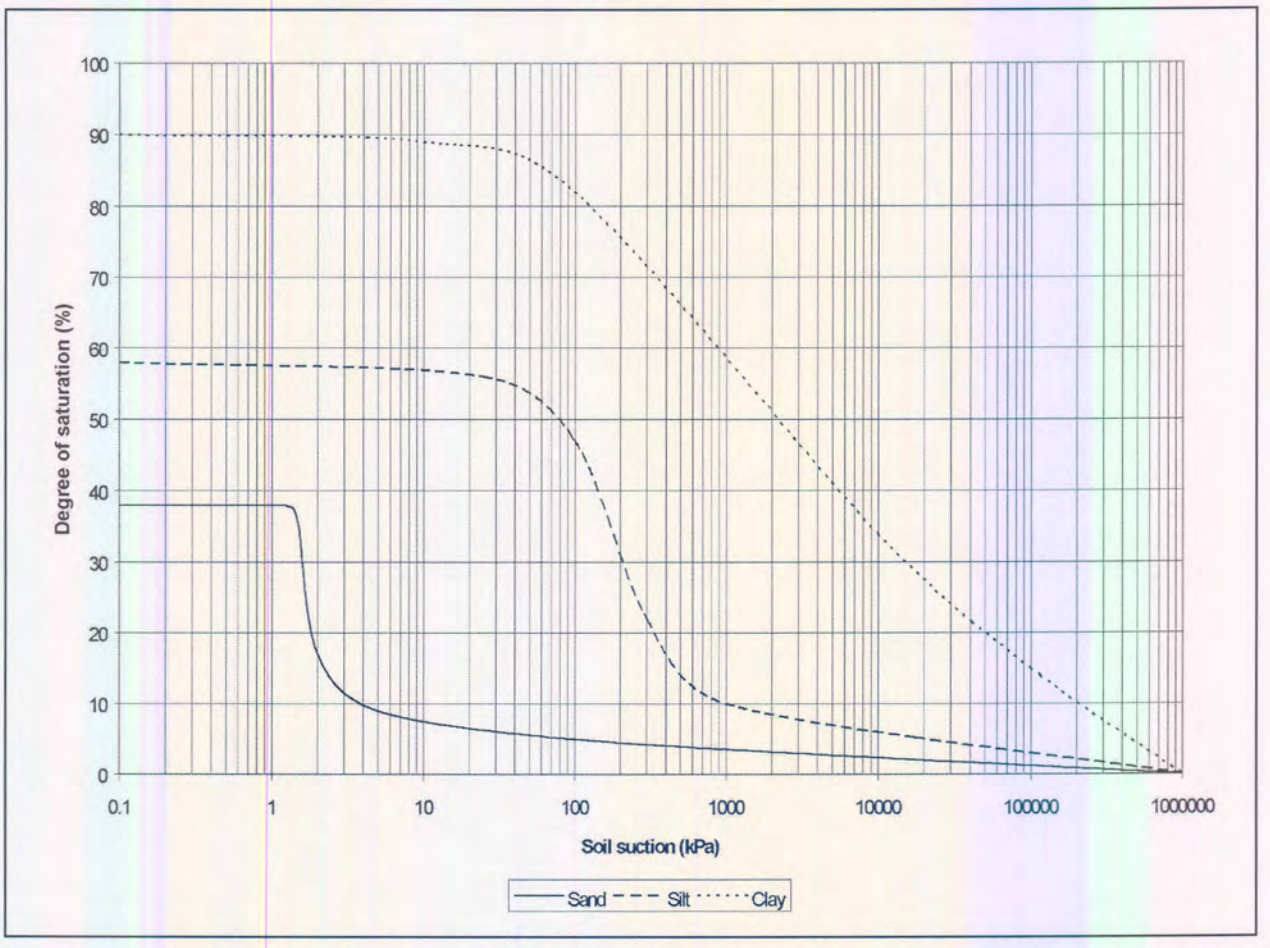

Figure 2.3: Typical soil-water characteristic curves for a sand silt and clay (Modified after Brady, 1974)

2.4 Flow of a liquid in a porous medium

Liquid in a porous medium possesses different forms of energy, largely due to the effects of gravitational and matrix forces. Energy in liquid is generally expressed in terms of a difference in liquid pressure and therefore a difference in the hydraulic head.

The hydraulic gradient, *dh/dl*, represents the loss of hydraulic head between two points, and can be expressed as:

$$\frac{dh}{dl} \text{ or } \frac{dh}{dz} \qquad [2\text{-}14]$$

In this context, the equation represents a one-dimensional vertical situation in which z is measured positive downwards.

If, in a continuous area of liquid, there is a difference in the amount of energy between two points, the flow of liquid will occur in the direction of lesser energy (Bell, 1993). Other things being equal, and on condition that laminar flow exists, the velocity of flow between two points is directly proportional to the difference in hydraulic head between them (Das, 1990).

2.4.1 Steady-state saturated flow

Flow through soil is a complicated process, inhibited by numerous restrictions, bottlenecks, and occasional "dead end" spaces. It is therefore too complicated to describe in microscopic detail, and is rather described in terms of a macroscopic flow vector. The detailed flow pattern is ignored and the conducting body is treated as though it were a uniform medium, with the flow spread out over the entire cross-section, solids and pore space alike (Hillel, 1980).

Darcy's empirical expressions describe steady-state macroscopic flow of fluids through a porous medium. Darcy (1856), while observing the flow of water through sand filters, related the macroscopic velocity (also known as the Darcian velocity), v, to the hydraulic gradient (Hazen, 1930).

$$v = -K\frac{dh}{dz} \qquad [2\text{-}15]$$

The flow of liquid is therefore directly proportional to the driving force acting on the liquid (i.e., the hydraulic gradient) and also to the ability of the conducting medium to transmit the liquid (i.e., the hydraulic conductivity) (Hillel, 1980). The minus or negative symbol is used by convention and indicates that flow occurs in the direction of decreasing hydraulic head.

The total quantity of flow, Q_{tot}, is the volume of water that flows through an area within a given time. It can be expressed as:

$$Q_{tot} = -K\frac{dh}{dz}A \cdot t \qquad [2\text{-}16]$$

The steady-state rate of flow, Q, through an area can be expressed as:

$$Q = -K\frac{dh}{dz}A \qquad [2\text{-}17]$$

Macroscopic velocity, v, is a macroscopic quantity. The conducting body is treated as though it were a uniform medium, with the flow spread out over the entire cross-section, solids and pore space alike (Hillel, 1980). The cross-sectional area of flow, however, includes both solids and voids (Everett *et al.*, 1984). The real area through which flow takes place is therefore smaller than the entire cross-sectional area, suggesting greater actual velocity values. In addition, the length of the liquid body flowing through the soil is much longer because of the tortuous nature of the pore passages, implying even higher actual velocity values. The seepage rate or true velocity of flow, v_s, is the microscopic tortuous flow of the liquid and can be approximated by means of the following equation:

$$v_s = -\frac{K}{\theta_s}\frac{dh}{dz} \qquad [2\text{-}18]$$

Since the water content at saturation is approximately equal to the porosity of the soil, ε, Equation 4-5 can be expressed as:

$$v_s \approx -\frac{K}{\varepsilon}\frac{dh}{dz} \qquad [2\text{-}19]$$

Tortuosity is the average ratio of the actual flow of liquid along pore passages to the physical straight length of the flow path. The value of tortuosity will always be greater than one.

Specific discharge, q, also known as the flux or Darcian flux, is the volume of fluid discharge per unit area per unit time. It has the same value and units as Darcian velocity:

$$q = -K\frac{dh}{dz} \qquad [2\text{-}19]$$

Specific discharge differs from macroscopic velocity in that it does not represent the velocity of the liquid, but rather the discharge rate of the liquid. However, the value of specific discharge is numerically equal to macroscopic velocity.

Limitations of Darcian expressions

Darcian expressions describe the one-dimensional, steady-state flow of an incompressible fluid through a homogeneous porous medium. The flow of fluids in field soils is much more complicated. Certain assumptions have to be made when Darcian expressions are applied (Daniel, 1989):

- The porous medium is homogeneous and isotropic.
- One-dimensional flow takes place.
- The fluid is incompressible.
- A steady-state of flow exists.
- Flow in the porous medium is laminar.
- There is no interaction between the fluid and the porous medium.
- The porous medium remains physically stable.
- Atmospheric pressure and fluid temperature are constant.

In addition to the above-mentioned constraints, the relationship between hydraulic gradient and quantity of flow is not always linear, as many authors have found (Scheidegger, 1957; Childs, 1969; Swartzendruber, 1962; Miller & Low, 1963; Mabula, 1997). At high velocities, the flow may become turbulent and the hydraulic potential may become less effective in inducing flow. At low velocities water in close vicinity to particles becomes rigid and resists flow, probably due to adsorption forces.

Darcian expressions have been validated in both sandy soils and clayey soils by laboratory and *in situ* experiments (Tavenas, Jean, LeBlond & Leroueil, 1983b; Daniel, 1989), indicating that although not all the assumed criteria are met, a reasonably accurate value of hydraulic conductivity can be obtained.

2.4.2 Unsaturated flow

Flow in unsaturated media is more complex than in saturated media. Complex relationships exist between hydraulic conductivity, moisture content and soil suction, and these are further complicated by hysteresis. The basic Darcian principles also apply to unsaturated conditions, i.e. flow takes place in the direction of decreasing potential, the rate of flow is proportional to the hydraulic gradient and is affected by the geometric properties of the pore channels. However, soil moisture in unsaturated soil is subject to pressures lower than atmospheric pressure and the flow is governed by both matrix and gravitational forces.

An important difference between the flow of liquid in saturated and in unsaturated conditions is reflected by hydraulic conductivity values. Under saturated conditions almost all the pores are filled with liquid,

except for approximately 5 per cent of the pore volume occupied by entrapped air (Hillel, 1980), and are therefore conductive. As the soil desaturates, some pores are filled with air and the soil becomes less conductive. The larger, more conductive pores drain first, with the result that the liquid flows only in the smaller pores. The water has to circumvent empty pores, resulting in an increase in tortuosity. Transition from saturated to unsaturated conditions usually entails an initial sharp drop in hydraulic conductivity, especially in sand (Hillel, 1980).

The hydraulic conductivity in unsaturated porous media is a non-linear function of volumetric water content, $K(\theta)$. Since the volumetric water content is a function of hydraulic head, $\theta(h)$, (as shown in soil-water characteristic curves), the unsaturated hydraulic conductivity is also a function of hydraulic head. Unsaturated hydraulic conductivity can also be expressed as a function of soil suction, $K(\psi)$, pore-water pressure, $K(u_w)$, and effective pore radius $K(R_{eff})$.

Darcian expressions are valid in unsaturated porous media. Both liquid and gas fill the voids but liquid flow is confined to spaces occupied by liquid.

The rate of flow, Q, in unsaturated porous media can be expressed as:

$$Q = -K(\theta)\frac{dh}{dz}A \qquad [2\text{-}20]$$

where volumetric water content can be substituted by hydraulic head, soil suction, pore-water pressure or effective pore radius.

The cross-sectional area of flow includes solids, liquid and gas. The seepage rate, v_s, in unsaturated conditions can therefore be expressed as:

$$v_s = \frac{K(\theta)}{\theta}\frac{dh}{dz} \qquad [2\text{-}21]$$

(Everett *et al.*, 1984)

2.4.3 Transient flow of water through the vadose zone

Rainfall events are erratic, not only in frequency but also in duration and intensity. These factors have a great effect on the infiltration and redistribution of water flowing through the vadose zone. On the other hand, evaporation and transpiration are less erratic, especially in areas where the climate is characterised by relatively small climatic variations. While rainfall events are time-specific, evaporation and transpiration take place continuously.

Soil-water movement during infiltration

While precipitation or irrigation events take place, water infiltrates the soil. Soil layers close to ground surface will become saturated and downward movement of a zone with higher volumetric water content occurs. The downward movement is caused by both gravitational forces and a suction gradient between the top saturated soil layers and the bottom drier soil layers. Bodman & Colman (1943) identified a number of zones that can be distinguished during infiltration.

The saturated zone at ground surface is approximately one centimetre thick. Immediately below this is the transition zone of a few centimetres in thickness and characterised by a fairly sharp decrease of volumetric water content with depth. The transmission zone occurs below the transition zone and is characterised by little variation in moisture content with depth. The transmission zone, as the name implies, transmits water from the transition zone to the underlying wetting zone. The wetting zone is characterised by a sharp decrease in volumetric water content with depth. The wetting front marks the

limit between the wetted soil profile and the underlying dry soil (Ward, 1975). The sharp decrease in volumetric water content implies that a high suction gradient exists in the wetting zone.

With continuing infiltration, the length of the transmission zone increases and little changes in water content take place in the saturated, transition and transmission zones. However, within the wetting zone, the high suction gradient causes an initial rapid movement of water. With time (that implies deeper soil profiles) the suction gradient decreases and the sharp boundary between the wetted and dry soil of the wetting zone becomes less well defined. Ward (1975) argues that as volumetric water content approaches values similar to the transmission zone, the effect of the suction gradient on downward movement of water becomes of lesser importance and the gravitational force becomes the main downward driving force. Since the gravitational gradient has a value of one, downward flux will approximate the value of the saturated hydraulic conductivity.

Infiltration in field soils is more complex than the above-mentioned conceptual processes. Reasons for this include non-uniform soil and water content properties, the effect of hysteresis, boundary conditions that vary with time and the effect of preferential flow paths.

Experiments have shown that the final infiltration rate in field soils is one-half to two-thirds of the saturated hydraulic conductivity (Miyazaki, 1993). This discrepancy can probably be explained by the fact that large volumes of entrapped air occur within the field soil as opposed to laboratory determined saturated hydraulic conductivity, where the sample is usually saturated from the bottom up, thereby minimising entrapped air (Miyazaki, 1993). The difference between the saturated hydraulic conductivity and the final infiltration rate can thus be attributed to entrapped air obstructing the flow of water in field soils

Various equations were derived to describe infiltration of water into soil. These can be classified as empirically and physically based methods. Empirical equations describe the infiltration curve applying two or more fitting parameters. These equations are discussed by Miyazaki (1993).

The Green-Ampt (1911) equation was the first to describe infiltration into soil on the basis of physical methods. The model assumes a piston-like moisture profile and the wetting front is represented by a sharp transition between the saturated soil and the underlying unsaturated soil. The reliability of the Green-Ampt equation relies on the accurate description of the hydraulic head at the wetting front. The vagueness in definition of this parameter has lowered the theoretical reliability of this equation (Miyazaki, 1993). Although the Green-Ampt equation has been derived from the oversimplified assumption of piston-like movement of water through soil, it is still used because of its ability to predict the infiltration rate with no less validity than equations based on the more realistic movement of water through soil.

The equation derived by Phillip (1969) is sometimes used to predict infiltration rates. The method is restricted to particular initial and boundary conditions and to uniform soils. It is very cumbersome and requires knowledge of unsaturated hydraulic conductivity relations in terms of both volumetric water content and soil suction. (Miyazaki, 1993).

Soil-water movement during redistribution

After the infiltration process has ended, infiltrated water continues to move downwards through the soil profile. The downward flow is termed redistribution or the drainage stage. Water, and therefore also the wetting front, continues to move downwards through the soil profile under gravitational and suction forces. However, as water moves downwards, water in the upper zones begins to drain and the transmission zone subsequently becomes a drainage zone (Ward, 1975). The hydraulic conductivity decreases with lower volumetric water content and subsequently, the water (and therefore also the wetting front) moves downwards at a lower rate. The hydraulic gradient in this zone is slightly higher than one, while the hydraulic gradient at the wetting front is much higher (Miyazaki, 1993). A large quantity of downward flow thus takes place around the wetting front, while less downward flow occurs in the wetted front. At volumetric water content values close to field capacity, very little downward movement of water is taking place. The permeability of the soil and the initial volumetric water content are two

important factors which affect redistribution. Wierenga (1995) has shown that soils with a higher initial water content allow recharge to take place much more quickly than drier soils in similar conditions.

Soil water movement during evapotranspiration

After infiltration has ended, evaporation takes place and results in the removal of water from the surface layers. Evaporation and redistribution processes occur simultaneously, and while redistribution will result in a lower rate of downward movement of water, evaporation causes an upward movement of water due to a suction gradient between the drier surface layers and the wetter deeper soil layers. Evaporation is affected by temperature, relative humidity and wind velocity, as well as hydrogeological properties such as the unsaturated hydraulic conductivity and the hydraulic gradient. Three distinct patterns for rate of evaporation can be identified, depending on the evaporation potential of the soil. These include:

i A constant-rate stage where the evaporation rate does not change with time,

ii The first falling-rate stage where evaporation rate decreases linearly with time and

iii A second falling-rate stage where the evaporation rate decreases exponentially with time

(Miyazaki, 1993).

It is difficult to estimate rates of evaporation and transpiration in the vadose zone due to the many factors affecting evaporation rate and the difficulties in measuring these factors. Water movement during redistribution and evapotranspiration is graphically represented in **Figure 2.4**.

The value of the hydraulic gradient in the vadose zone

Flow of water within the vadose zone is caused mainly by rainfall events and evapotranspiration. These events cause a positive (downward flow) and negative (upward flow) hydraulic gradient respectively within the vadose zone. Miyazaki (1993) states that large positive hydraulic gradients only occur at the wetting front while the hydraulic gradient in the wetted zone is almost equal to one. Miyazaki (1993) maintains that in the case of gravity-dominant flow in deep soils (not affected by evapotranspiration), hydraulic gradients tend to equal one. According to Wierenga (1995) hydraulic gradients in moist soils is almost equal one and do not change much. Based on approximations over long periods of time, Unlu, Kemblowski, Parker, Stevens, Chong & Kamil (1992) suggest that the value of the hydraulic gradient can be assumed to be one, since conditions of vertical flow prevail.

In contrast, Miyazaki (1993) states that these conditions may only prevail in regions where the annual precipitation exceeds annual evaporation. In semi-arid and arid regions or regions characterised by distinct wet and dry seasons, evaporation can cause the surface soil layers to dry out, causing a negative hydraulic gradient. In addition, the effect of ponding must be considered. Ponding can result in relatively large positive hydraulic gradients. Perched groundwater levels may also result in relatively large hydraulic gradients. Further investigations should be conducted on the effect of hydraulic gradients within the vadose zone under South African conditions.

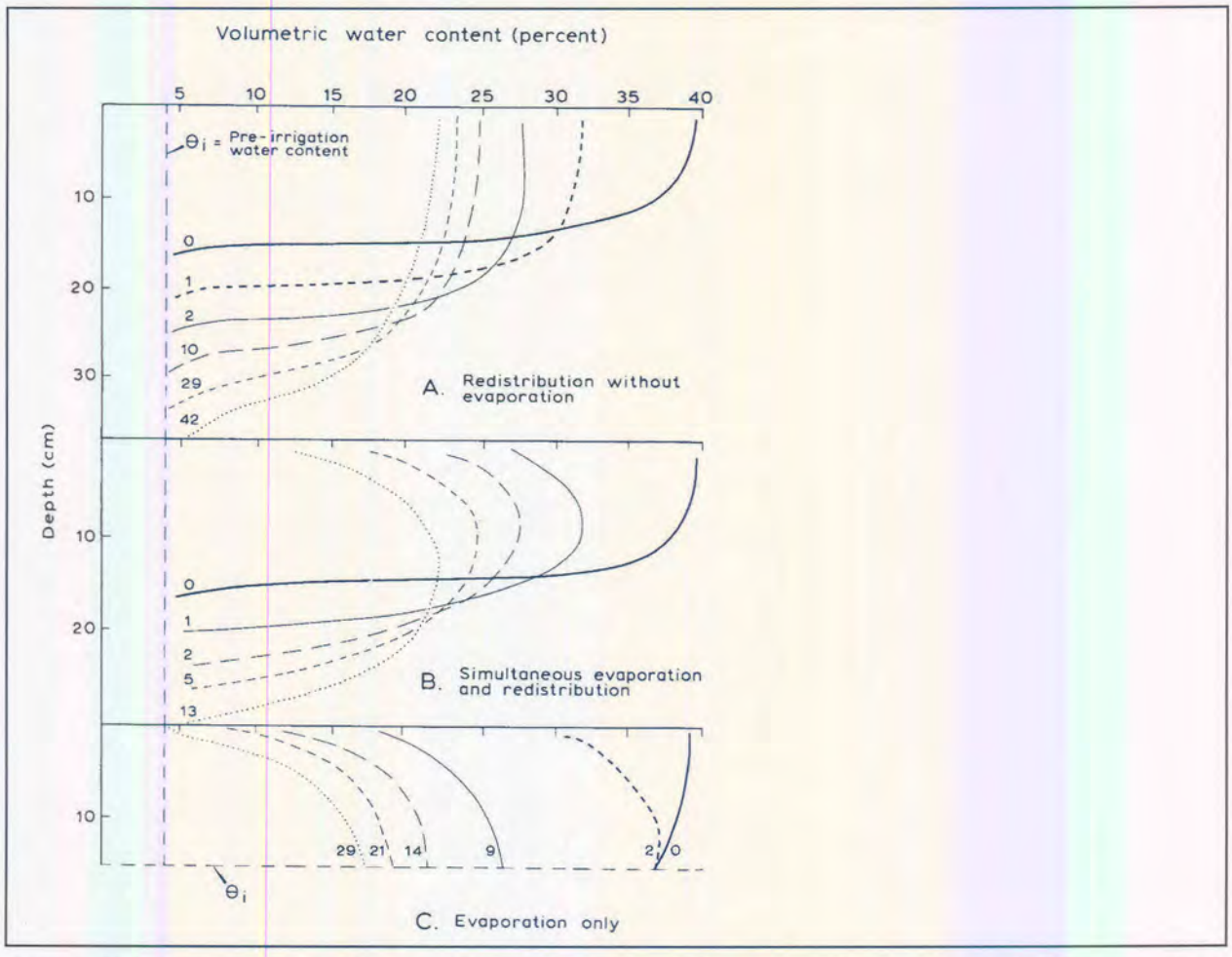

Figure 2.4: Soil-water content profiles during redistribution and evapotranspiration (numbers indicate days after wetting) (after Ward, 1975)

Upward movement of soil-water

The effect of evaporation and transpiration causes a suction gradient to develop between the lower wetter zones and the upper dried-up zones. The suction forces cause upward movement of soil-water up to the root zone from where it is released to the atmosphere by evaporation and transpiration processes. The rate at which upward movement of soil-water occurs, is controlled by various factors, the most important being the permeability of soil, the rate of drying of the surface layers, the density of the plant root system and the depth to the groundwater level. Penman (1948) has shown that in the case of slowly drying soil surfaces, the rate of upward movement of soil-water will keep pace with the rate at which soil-water is removed from soil surfaces by evaporation processes. However, in the case where drying occurs rapidly, upward movement of soil-water will be constrained by the reduced hydraulic conductivity at the dry (hence less permeable) surface layers. In extreme cases, evaporation losses from soils may become negligible even though soil-water contents at a few centimetres depth are still high. The depth to the groundwater surface is a major factor in the upward movement of soil-water. Wind (1961) has shown that the rate of upward movement of soil water is mainly a factor of groundwater level rather than the suction imposed at the soil surface. High rates of water movement will therefore occur where the groundwater is shallow (<60cm) This aspect is more pronounced in coarse-grained soils than in fine-grained soils.

Wind (1961) also shows that the rate of upward water movement is sensitive to the juxtaposition of different horizons in the soil profile. In wet conditions, the hydraulic conductivity of clay soils is low while in drier conditions, the hydraulic conductivity of clay soils can be higher than sandy soils. As such,

sandy soil overlying a clayey soil will result in low rates of upward soil-water movement. According to Wind (1961), the highest rate of upward movement of soil water will occur in a soil profile comprising of a lower sandy soil horizon overlain by a silty soil horizon with a clay horizon at the surface.

In conclusion, it can be stated that in humid areas, where rainfall exceeds evaporation, downward movement of soil-water will dominate. This results in the leaching of soluble minerals from the top soil layers and the accumulation of these minerals in lower soil profiles. These processes can eventually result in the development of iron and aluminium-rich horizons and even the development of hardpan ferricrete.

In dry areas, where evaporation exceeds rainfall, upward movement of water will dominate. This can cause upward transport of soluble minerals and the eventual development of typically lime-rich soil horizons. These processes can lead to the accumulation of salts on the surface layers.

2.4.4 Numerical simulation modelling of unsaturated flow

Simulation can be defined as the application of models as a substitute for the study of real or hypothesised systems. These models may comprise either physical or numerical models. With advances in the processing capabilities of personal computers, most researchers have focussed on the development of easy to construct and low-cost numerical models. Simulation modelling is a powerful tool for understanding a particular problem and in some instances to understand what the problem is. Time can either be stretched or compressed for processes that happen too fast for observation or too slowly for practical observation. Ultimately, numerical models can be used as a prediction and decision-making tools. A number of "what if..." scenarios can be simulated and the relevant designs can be optimised for the particular problem.

Since flow in the vadose zone is dynamic and transient in nature, numerical modelling by means of computer models offers the best tool to understand, simulate and ultimately predict flow of water and solutes through the vadose zone. Since flow in the vadose zone is predominantly downward (or upward), it can be presented by a one-dimensional model. Transient flow in the vadose zone can be described by the Richard's equation, which is based on Darcy's law (modified from Feddes, Kowalik & Zaradny, 1978):

$$\frac{\partial \psi}{\partial t} = \frac{1}{\theta'(\psi)} \cdot \frac{\partial}{\partial z}\left[K(\psi)\left(\frac{\partial \psi}{\partial z} \right) + 1 \right] - \frac{S(\psi)}{\theta'(\psi)} \qquad [2\text{-}22]$$

where $S(\psi)$ is a sink term and represents the volume of water taken up by plant roots (volume water per volume soil per unit time). Water uptake by plant roots does not constitute part of the research and as such, readers are referred to Feddes *et al* (1978).

A boundary condition is defined at the top of the system where water infiltrates the system by means of precipitation or irrigation and where water leaves the system by means of evapotranspiration. Evapotranspiration can be directly measured or can be calculated by means of a number of equations of which the Penman (1948) equation is the most popular. Rainfall is measured directly. Another boundary condition is defined at the bottom of the system and this will depend on the particular situation.

A number of numerical solution schemes can be used to simulate flow of water in the vadose zone. The finite-difference technique is the most frequently used technique to solve the extended Richard's equation. Other techniques, including the finite element method, are also used to simulate flow of water through the vadose zone. Wates, Rykaart, Vermaak & Bezuidenhout (1999) identified forty-five models capable of handling unsaturated flow conditions. The most popular models include HELP, FEMWATER, LANDFIL, SEEP/W and ACRU. However, many of these models are analytical models and can not simulate dynamic conditions. The conceptual unsaturated flow model is shown in **Figure 2.5**.

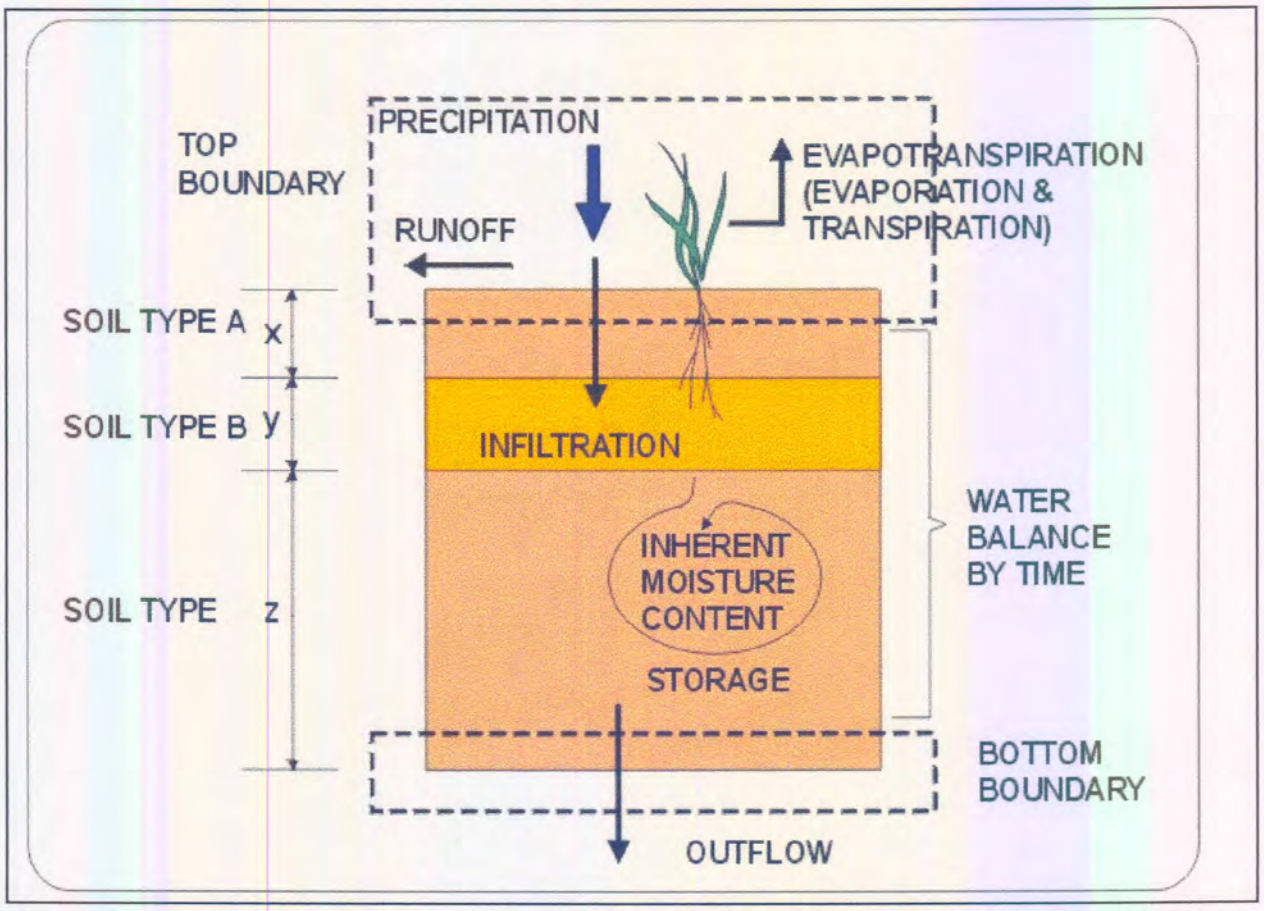

Figure 2.5 Conceptual unsaturated flow model for a layered soil (after Wates *et al*, 1999)

2.4.5 Saturated hydraulic conductivity

Saturated hydraulic conductivity represents the factors, other than the hydraulic gradient, which affect the flow of liquid through a porous medium. Three important factors have to be considered:

- Properties of the fluid
- Properties of the porous medium (soil or rock)
- Interaction between the fluid and the porous medium

Interaction between the fluid and the porous medium generally refers to electric forces at molecular level. These forces may be an important factor in saturated hydraulic conductivity, especially in clayey soils. However, in sandy soils, these forces do not generally have a significant effect on saturated hydraulic conductivity. In these instances, saturated hydraulic conductivity, K, can be described in terms of the properties of the fluid medium, known as fluidity, f, and in terms of properties of the porous medium, known as intrinsic hydraulic conductivity or permeability, k:

$$K = kf \qquad [2\text{-}23]$$

Fluidity is inversely proportional to viscosity:

$$f = \frac{\rho_f g}{\eta} \qquad [2\text{-}24]$$

The density of most liquids is nearly constant, although it may vary somewhat due to the effect of temperature and solute concentration, but the viscosity value varies due to the effect of temperature.

Equation 2-24 indicates that saturated hydraulic conductivity will vary in accordance with the type of liquid. The petroleum industry uses Equation 2-24 to differentiate between the velocity of flow of oil, water and methane gas.

Intrinsic permeability represents all factors associated with the porous medium which affects saturated hydraulic conductivity. Intrinsic permeability is a factor of grain-size distribution, structure, density and other properties of the soil. It depends primarily on the size of the conducting pores as well as on the porosity of the soil.

In a case where the porous medium consists of a bundle of straight tubes with equal and constant diameters, the intrinsic permeability can be calculated from Equation 2-25 that is based on Poiseuille's law:

$$k = 0.125 \cdot R^2 \qquad [2\text{-}25]$$

It is much more difficult to determine the intrinsic permeability for soils and rocks because of the irregular geometry of the pores and because pore-size distributions depend on grain-size distribution, packing, the shape of the grains and various other factors.

The effect of electro-chemical forces at molecular level

Electro-chemical forces have already been discussed (Section 2.1.2) with regard to their effect on retaining fluids in unsaturated soil. These forces play an important role in flow through soils with active particle surfaces, such as clays. The flow of fluids through these soil types will strongly depend on the electro-chemical properties of the fluid.

Fernandez and Quigley (1985) found that the hydraulic conductivity of clayey soils was strongly influenced by the physico-chemical properties of liquid hydrocarbons. They ascribed this to the electro-chemical reactions between the liquid and the soil media, especially clay minerals.

Fernandez and Quigley (1985) found that liquids with a relatively high dielectric constant, such as water, inhibited flow through the clay. The hydraulic conductivity of water (with a dielectric constant of 80) flowing through a clayey soil (with a void ratio of 0.8) was measured at 5×10^{-9} m·s^{-1}. The hydraulic conductivity of liquid hydrocarbons (with a dielectric constant of 2) flowing through the same soil was measured at 1×10^{-4} m·s^{-1}.

Equation 2-23 does not apply to these conditions, because the effect of the dielectric constant on the double clay layers completely swamps the effects of fluid viscosity and density.

Fernandez and Quigley (1985) found no changes in hydraulic conductivity when water-insoluble liquids with a low dielectric constant were used in a water-wet compacted clayey soil sample. These hydrophobic liquids were probably forced through micro-channels or macropores, displacing only 10% of the pore water from the samples.

The use of water-soluble hydrocarbons in water-wet compacted clayey soil samples resulted in an up to ten-fold increase in hydraulic conductivity and the extensive removal of pore water, while permeation with liquid aromatics with a very low dielectric constant resulted in a thousand-fold increase in hydraulic conductivity.

Interaction between the liquid and porous medium can have a significant effect in cases where leachate is moving through clay.

2.5 Heterogeneity and the effect of scale

Heterogeneity of soils is defined in terms of the spatial variability in physical soil properties, such as bulk density, water content, grain-size distribution, pore-size distribution, consistency and other properties. Since all these properties are defined and measured with respect to an elementary volume, the definition of soil heterogeneity is expressed in terms of an elementary volume.

In general, the larger the elementary volume, the more physical properties are averaged in each elementary volume. Therefore, more homogeneous properties of a specific field soil are defined. On the other hand, the smaller the elementary volumes in the same field, the larger the differences in physical properties between the elementary volumes, resulting in defining more heterogeneous properties of a specific soil.

Figure 2.6 shows the value of a specific soil property within a number of elementary volumes with increasing sizes. It can be seen that the variability of the soil property decreases as elementary volumes increase. The elementary volume in which little variability exists, is known as the representative elementary volume (REV) (Bear, 1979). The larger the REV, the larger the heterogeneity of the soil within a specific field soil type.

Although the general theory for establishing REV has not yet been established, various authors have determined empirical REVs for various purposes. These tentatively acceptable empirical REV values (designated by representative lengths) are expressed in **Table 2.2**:

Table 2.2: Empirical REV designated for various purposes

REV (m)	Subject	Reference
REV > 1000	Hydrological modelling in a river basin	Wood, Sivapalan, Beven & Band (1988)
REV > 5	Water balance in a field with cracks	Inoue, Hasegawa & Miyazaki (1988)
REV > 0.5	Saturated hydraulic conductivity of a soil with macropores	Lauren, Wagnent, Bouma & Wosten (1988)
REV > 0.05	Bulk density, water content and solute concentration	Tokunaga and Sato (1975)
REV > 0.01	Microstructure	Cogels (1983)

The REV concept assumes statistical correlation of an intrinsic property independent of scale. As such, it assumes the porous medium to be composed of homogeneous material above some critical scale (Tyler and Wheatcraft, 1990). Although the REV concepts can be and have been applied at small to medium scale (millimetres to metres) in hydrogeological investigations, such correlations are limited at large field scale. Many intrinsic properties can be correlated in space due to differences in geology and soil formation processes. Serious errors could result in the averaging process if the REV approach is applied without consideration of the geology and soil formation processes. The spatial distribution of soils with similar physical and hydraulic properties can be identified, presented and quantified by means of their geological origin and topographical setting. These aspects are discussed under **Section 2.8**.

Miller & Miller (1956) applied the theory of similitude analyses to unsaturated hydraulic conductivity and hydraulic head. Two porous media can be described as Miller-similar if a defined scale factor can describe these media exactly relative to each other (Warrick, 1990, Sposito & Jury, 1990). Similar media exhibit microscopic structures that are similar in shape, but occur on different scales. According to Miller & Miller (1956), the unsaturated hydraulic conductivity – hydraulic head relationship of two similar media can be related by the equation:

$$\frac{K'(\lambda' h')}{\lambda'^2} = \frac{K(\lambda h)}{\lambda^2} \qquad [2\text{-}26]$$

where $K'(h')$ and $K(h)$ denotes the unsaturated hydraulic conductivity – hydraulic head relationship of two points within a specific field soil and λ is the characteristic length that relates the unsaturated hydraulic conductivities.

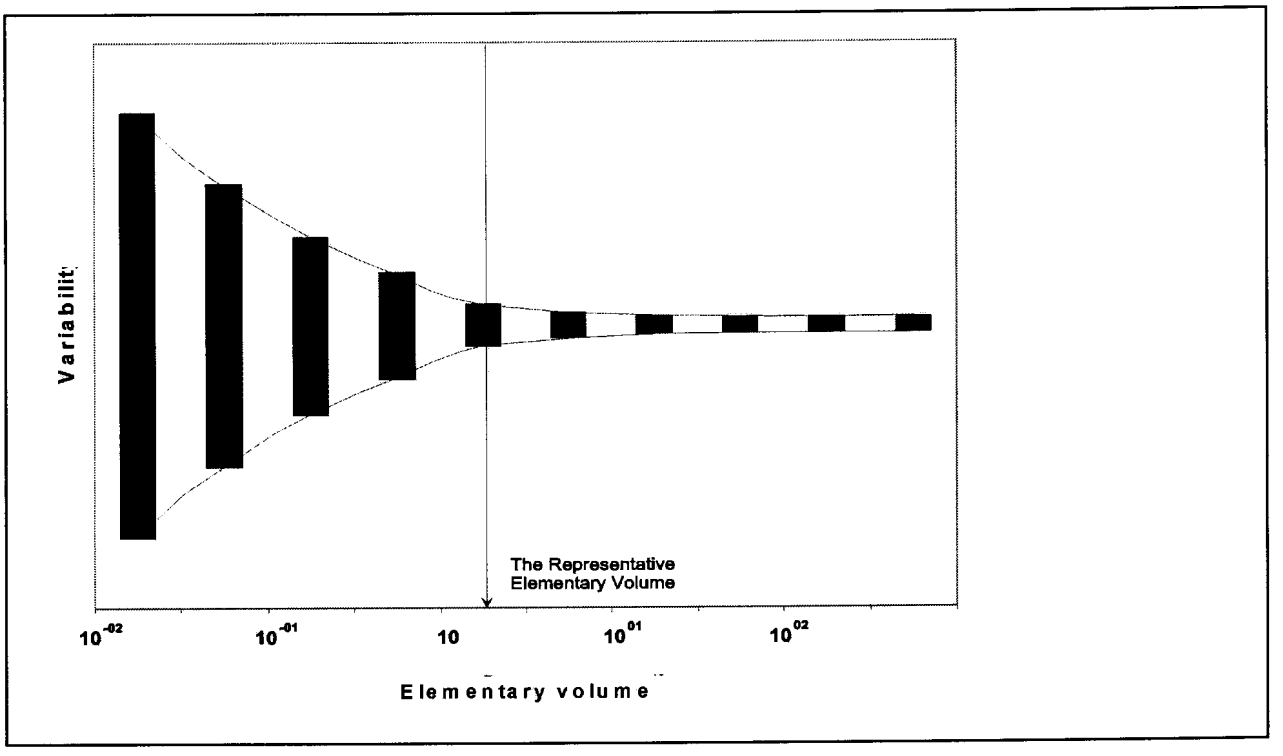

Figure 2.6: The Representative Elementary Volume (modified after Bear, 1979)

Similitude analyses have successfully been applied in describing unsaturated flow through heterogeneous field soils (Sposito & Jury, 1990; Youngs, 1990) using the modified Richard's equation. It has also been successfully applied to characterise the spatial variability of field soils. Warrick (1990) found that by applying scaling techniques in heterogeneous soils, the best fit could be applied to the soils with considerably more accuracy. Warrick recorded up to 80 per cent reduction in the Sum of Squares for scaled fitted data points compared to the unscaled fitted data. The results are indicated in **Figure 2.7**.

The basic principles and applications of scaling techniques are described by Hillel & Elrick (1990).

2.6 Hydrogeological properties important in the assessment of saturated and unsaturated flow through the vadose zone

The flow situation in the vadose zone varies according to climatic events, i.e. rainfall and evapotranspiration, as well as irrigation and other human activities. Since these events are generally erratic, flow in the vadose zone will be transient in nature and vary accordingly. Climatic events result in either the addition or removal of soil-water from the soil. All properties that are functions of soil-water, i.e., soil-suction gradient, soil-water retention characteristics and the unsaturated hydraulic conductivity, will vary accordingly.

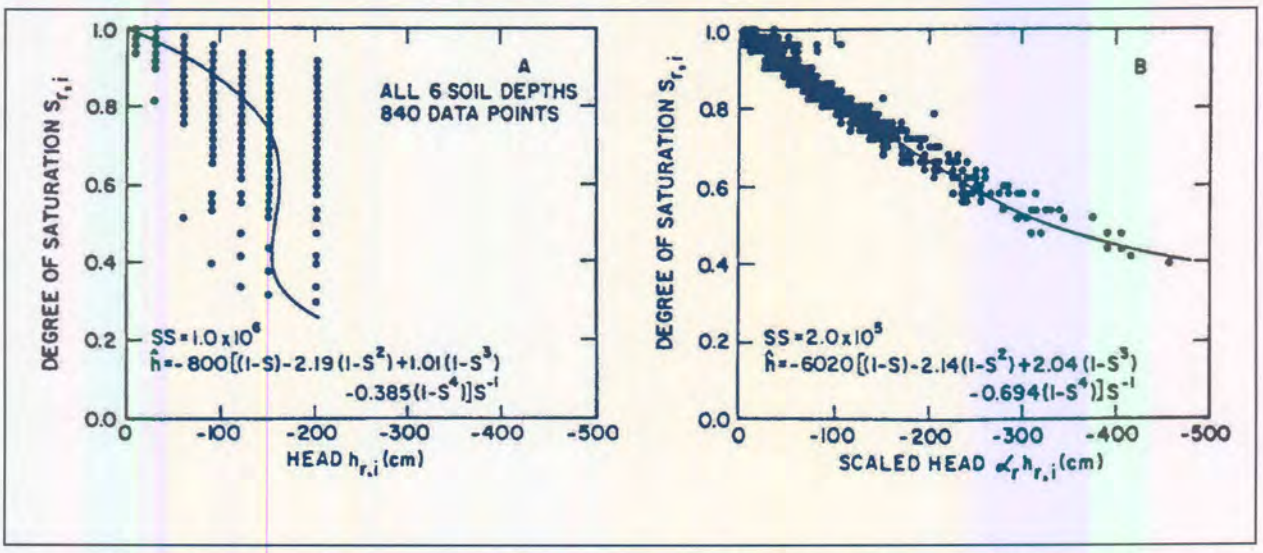

Figure 2.7: Soil-water retention data for fine loam: unscaled (A) and scaled (B) (after Warrick *et al.*, 1977)

The hydrogeological properties of importance in the assessment of saturated and unsaturated flow through the vadose zone, are summarised in **Table 2.3**. The properties described in **Table 2.3** refer to Darcian type flow mechanisms as described by the Richard's equation. These properties may not be relevant in the case of other flow mechanisms such as preferential flow.

Table 2.3: Hydrogeological properties affecting groundwater recharge and contamination

Property	Symbol	Application
Saturated hydraulic conductivity	K_s	Estimates of saturated and unsaturated flow
Hydraulic gradient	$\frac{dh}{dz}$	Estimates of saturated and unsaturated flow
Soil suction gradient	$\frac{d\psi}{dz}, \frac{d\theta}{dz}$	Estimates of saturated and unsaturated flow
Depth to groundwater level	D	Estimates of time before reaching the groundwater level
Volumetric water content	θ	Estimates of unsaturated flow
Soil suction/hydraulic head/ effective pore size	$\psi/h/R_{eff}$	Estimates of unsaturated flow
Soil-water /soil suction relationship	$\theta(\psi)$	Estimates of unsaturated flow and storage capacity
Specific retention	θ_r	Estimates of unsaturated flow and storage capacity
Saturated volumetric water content	θ_s	Estimates of unsaturated flow
Unsaturated hydraulic conductivity	$K(\theta)$, $K(\psi)$	Estimates of unsaturated flow
Dry density, porosity and void ratio	ρ_d, ε, e	Estimates of saturated and unsaturated flow

2.6.1 Characteristics of water movement through geological units

The geological framework will dictate the flow of water and contaminants through the vadose zone. According to Kramer and Keller (1995), the geological profile containing an aquifer may comprise materials hosting primary flow and materials hosting secondary flow. Primary flow can be compared to

matrix flow where water and contaminants flow through the soil matrix in accordance with Darcy's law. Secondary flow refers to water and contaminants preferentially flowing along discontinuities in the soil or rock mass.

Matrix flow will be hosted mainly in unconsolidated materials. These include deeply weathered residual material, alluvium and other transported material and many Quaternary deposits. Soils containing high, active clays where preferential flow along cracks may take place, can be exceptions. Other exceptions may be well-cemented geological formations and pedogenic materials that may be impermeable, except for occasional discontinuities in which preferential flow will take place.

Secondary flow is mainly hosted in rock masses. These include most igneous, sedimentary and metamorphic rocks of pre-Quaternary age. Discontinuities such as joints, fault zones, geological contacts, bedding planes, solution cavities and lava tubes occur naturally within the rock masses. Underground mining, oil and water extraction and other processes can cause other discontinuities to develop within the rock mass. Secondary flow may be more rapid in comparison to matrix flow and, in the case of solution cavities and lava tubes, may reach flow velocities of several metres per second.

2.7 Preferential flow

Preferential flow is the process by which water and solutes move along preferred pathways through a porous medium (Helling & Gish, 1991). In the case of flow through the vadose zone, water and solutes by-pass large parts of the soil matrix, conventional convection equations may not be valid and water flow may be faster (or slower) than anticipated. In addition, monitoring devices, such as suction lysimeters, may be located outside (or inside) preferential flow paths and may not yield representative readings.

In many cases preferential flow plays an important role in groundwater recharge and contamination. This may be the predominant factor in groundwater recharge, as shown by Van Tonder and Kirchner (1990) and Kirchner, Van Tonder & Lukas (1991).

Flury, Flürer, Jury and Leuenberger (1994) conducted field experiments on various soils in Switzerland to study the effect of preferential flow. A dye tracer was irrigated on the soil and the pathways of the tracer were described. Flury *et al.* stated that preferential flow was "the rule rather than the exception" and that in most soils, water by-passed a portion of the soil matrix. The extent of by-passing, differed but Flury *et al.* (1994) found that it was likely that during heavy rainstorms, water by-passed the soil matrix in most arable Swiss soils. Flury *et al.* (1994) also found that the (coloured) water penetrated much deeper into structured clayey soils than into non-structured soils. They warned that well-structured clayey soils might be susceptible to pesticide leaching.

2.7.1 Classification of preferential flow

The following types of preferential flow have been identified:

- Macropore channelling that includes
  - Channelling through bio-pores such as relict root structures and burrowing animals
  - Channelling through fractured soil
  - Channelling through relict rock structures
- Other preferential flow types such as
  - Fingering flow

- Funnelled flow
- Preferential flow due to water repellent soil
- Preferential flow along protruding structures in the ground

Preferential flow mechanisms are presented in **Figure 2.8**

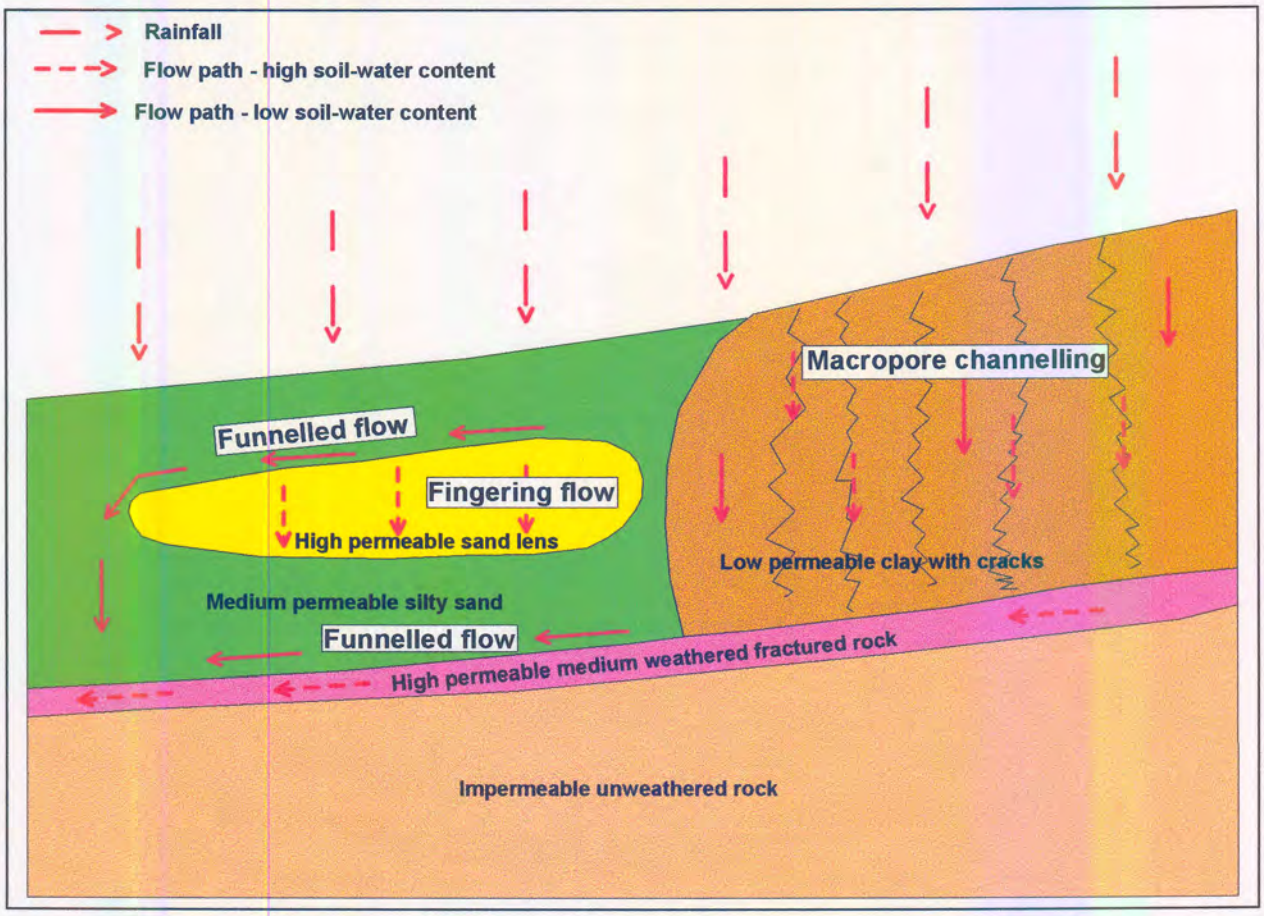

Figure 2.8: Conceptual preferential mechanisms indicating macropore channelling, funnelled flow and fingering flow

2.7.2 Macropore channelling

Macropore channelling refers to a liquid that by-passes the soil matrix via macropores. It can cause rapid water movement through the soil, with the result that the water by-passes the soil matrix and increases the flux value, resulting in a higher recharge rate. Pollutants may be transported through macropores in a very short travel time before the aquifer is reached. This may decrease the attenuation capacity of the vadose zone. Very little interaction between the fluid and soil matrix can also result in a decrease in attenuation, since attenuation processes such as dispersion and cation exchange are by-passed. Macropore channelling may be a very important factor in the flow process of water through soil.

Van Tonder and Kirchner (1990) conducted a recharge study of Karoo aquifers in South Africa. Data on both the phreatic and vadose zones were collected. A major flood occurred during the end of the study period and provided the opportunity to study recharge mechanisms in this semi-arid environment. No measurable matrix flow occurred in the flat-lying areas. However, much recharge took place, as was evident from higher groundwater levels. This lead to the conclusion that recharge occurred through

preferential pathways, probably through cracks in clay layers. Van Tonder and Kirchner stated that water could move downwards until the heavy clay layer is reached, after which water movement is predominantly horizontal. Water then moves down natural cracks occurring at specific locations. Recharge estimates, applying common models of water flow through unsaturated soils, do not apply in this situation.

2.7.3 Types of macropores

Macropores refer to openings in the soil which are larger than the pores occurring in the soil matrix. These voids are readily visible and may be continuous for several metres, both in vertical and horizontal directions. Macropores are generally classified according to their morphology and origin of the pores.

Fissures and fractures are generally caused by shrinking/heaving clays, chemical weathering and freeze/thaw cycles (Beven & Germann, 1982). The extent of shrinkage/heave can be predicted by determination of the activity of clay soils. A high plasticity index and clay fraction increases the activity of the soil. Cracks formed in shrinking and heaving soils depend on moisture content changes and may vary seasonally.

Processes causing the formation of discontinuities in clay are dynamic. In the case of desiccation, cracks appear during dehydration of the soils caused by evaporation processes. These cracks will close during hydration processes caused by precipitation events.

Formation of macropores by soil fauna and flora

Pores caused by soil fauna are normally tubular in shape with diameters of 1 – 500 mm (Beven & Germann, 1982). Various animal species, including insects (ants and termites), earthworms, moles, rodents and aardvarks, are responsible for burrowing holes. Most pores caused by soil fauna are close to the ground surface (up to one metre down), except for termite holes, which are known to extend down to the groundwater level. The types of species that occur in the soil depend on the properties of the soil and climate. Insects are found in acidic soils, while earthworms prefer low-acidic to neutral soils. Pores caused by soil flora are also generally tubular in form. These pores are generally caused by plant roots, alive or decayed (Beven & Germann, 1982). The extent and depth of the macropore network caused by soil flora are related to the plant species contingent to the climate of the area.

2.7.4 Other preferential flow mechanisms

Fingering flow

Fingering flow refers to the process where water or solutes move down the soil matrix in columnar structures, approaching velocities of saturated flow. Fingering is caused where the wetting front becomes unstable. This may occur for a number of reasons, including a change in hydraulic conductivity with depth and the compression of air ahead of the wetting front (Steenhuis & Perlange, 1990).

Fingering causes an increase in flow velocity within the more permeable zone. The lower travel time results in less contact time for attenuation processes to take place. In addition, large parts of the soil matrix are by-passed. Since fingering flow tends to be confined to certain areas in the soil profile, attenuation processes are also confined to these areas and the attenuation capacity of the soil will therefore be lower compared to soil where no fingering flow occurs.

Water flowing through a less permeable layer into a more permeable layer may cause wetting front instability. Water in the less permeable zone cannot enter the larger pores of the more permeable zone, due to a difference in pore water pressure. Water will not enter the larger pore as long as the suction at the bottom of the upper pore is greater than the suction of the lower pore. When the pore suction of the

top layers finally exceeds the suction of the pore layers at the bottom, water moves down into the coarse-grained layer. Because of the reduced flux in the coarse-grained layer (the flux cannot exceed that in the less permeable layer on top), the effect of gravity offsets the effect of the surface tension of the liquid. This causes wetting front instability. The wetting front splits and fingering takes place.

Wetting front instabilities may also occur due to low intensity rainfall which is much lower than is necessary for ponding to develop. Fingering flow can occur when soils are very permeable (coarse sand or gravel) or if soils are water-repellent.

Funnelled flow

Funnelled flow refers to the preferential flow of the water being 'funnelled' to flow laterally on top of coarse-grained soil layers (Kung, 1990). This phenomenon occurs because water in the less permeable zone cannot enter the larger pores of the more permeable zone because of a difference in pore water pressure. Water will not enter the larger pore as long as the pore suction at the bottom of the upper layer is greater than the pore suction at the top of the lower layer. Since vertical flow is impossible, the water will move laterally.

Funnelled flow also refers to the funnelling of water laterally on top of a less permeable zone. In this instance, the hydraulic conductivity of the underlying less permeable layer is too low to accept incoming water.

The funnelled water eventually moves downward in concentrated columnar flows when it reaches the edges of the coarse-grained (or fine-grained) layer. If the water content within the funnelled area is high enough, fingering within the coarse-grained soil may result.

Funnelling causes the decrease of the total flow area. Since most of the flow is concentrated in columnar structures, very little or no flow occurs in adjacent areas. Kung found that funnelled flow might be restricted to one-tenth of the total flow area. The subsequent increase in water content also causes an increase in flow velocity. Kung found that the steady-state flow velocity in the columnar structures increased 100 times.

2.8 Important aspects regarding unsaturated flow within field soils

The vadose zone represents the top portion of the geological profile. This zone is subjected to weathering, erosion, pedogenic and other processes, often resulting in a complex geological setting. The soils and rocks in the vadose zone are very rarely homogeneous and the situation presented in **Figure 2.1** is therefore rarely a reflection of the situation in the field.

The top portion of the geological profile can consist of thick layers of transported material, unweathered to completely weathered *in situ* material, poorly to well developed pedogenic soils with clearly defined soil layers, poorly to well developed pedocrete layers or a combination of the above-mentioned and other materials. A range of materials with a variety of physical properties may occur within this portion and significantly complicate studies of the vadose zone. The geological setting of the vadose zone has to be thoroughly understood before hydrogeological studies can be conducted.

The hydrogeological characteristics of specific geological materials are discussed in **Chapter 3**.

2.8.1 Shallow weathered and perched aquifers

Shallow weathered aquifers generally occur in a weathering profile overlying hard rock types. The groundwater is mainly stored within primary voids in the weathered zone. The depth of the shallow weathered aquifer may vary considerably depending on the climate, geological conditions and rock type.

Weathered zones in more humid areas could be more than 100m in thickness while thicknesses of less than 10m could be expected in dryer parts of South Africa. Shallow groundwater is recharged mainly by rainfall and influent (losing) streams. Groundwater stored within the weathered zone is, in most cases, hydraulically connected to deeper fractured aquifer systems. Shallow groundwater generally acts as storage for deeper fractured aquifer systems and provides base flow for streams and rivers.

Perched aquifers are defined as independent and isolated areas of groundwater situated above the groundwater level and separated from it by unsaturated soils/rocks; i.e. they occur in the vadose zone (Monkhouse, Steyn & Boshoff, 1983). Perched aquifer systems generally occur on top of clay lenses with low permeability. In South Africa, perched aquifers often occur on top of pedogenic layers such as hardpan ferricrete and calcrete.

The geotechnical fraternity in South Africa often uses the term "*perched aquifer*" incorrectly to describe shallow, (less than 5m), often seasonal, groundwater conditions. The engineering geologist records shallow seepage during the description of soil profiles since this could impact significantly on the development of the site and is generally not concerned with the hydraulic setting of the so-called, *perched aquifer*, relevant to deeper aquifer and surface water systems. Although this body of groundwater is frequently (but not always) located above the groundwater level, it is rarely independent and isolated and is normally hydraulically connected to surface water systems. These groundwater bodies are therefore not perched aquifers *sensu stricto*.

2.8.2 Hypothetical flow paths of contaminants seeping from a pollution source

Hypothetical flow paths of contaminants seeping from a pollution source are schematically represented in **Figure 2.9.** This figure represents a typical geological profile which comprises residual material overlying unweathered fractured bedrock. A fractured aquifer, developed in a highly weathered fractured fault zone, is located upstream of the site. Half the disposal area is underlain by impermeable hardpan ferricrete on which a perched water table has developed. The contaminants flow along the slope of the hardpan ferricrete (A). Funnelling flow occurs in more permeable weakly developed ferruginised material (B) and contaminants flow downwards until they reach impermeable hard rock. Contaminants flow preferentially through highly permeable materials to highly weathered and highly fractured materials (C) and enter the fractured rock aquifer (D). Contaminants may also flow along highly permeable leached relict rock structures (G) resulting from preferential weathering along these structures. On the other hand, in the event of lower water contents, contaminants may flow preferentially along the residual soil – highly leached zone interface. Fingering flow (I) may occur within the highly leached zone.

Figure 2.9 illustrates the complexity of aquifer recharge and contamination processes. Although it is not feasible to identify all these aspects on a regional scale, it may be possible to identify major recharge and contamination mechanisms.

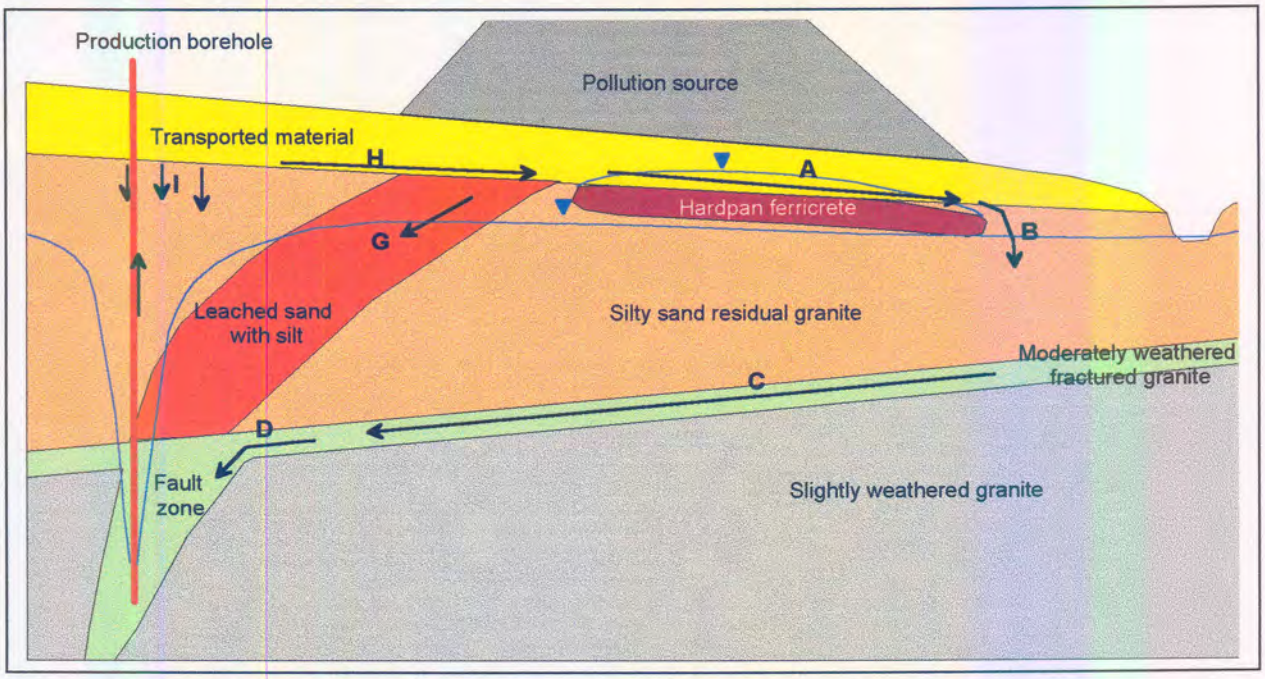

Figure 2.9: Hypothetical flow paths of contaminated water flowing through the vadose zone

2.9 Quantification of groundwater recharge

Groundwater recharge can be defined as the quantity of water flowing through the groundwater surface per unit time (Everett *et al.*, 1984), and is generally measured over a long period of time. It represents the portion of rainfall that reaches the groundwater surface and is frequently expressed as a percentage of mean annual rainfall (Bredenkamp, Botha, Van Tonder & Van Rensburg, 1995).

Groundwater recharge estimations are of great importance in groundwater management. In many parts of South Africa and other semi-arid regions of the world, future development and sustainable growth depend to a large extent on the availability of groundwater. In many rural areas groundwater is the sole or bulk water resource and, during droughts, often the only exploitable resource available (Bredenkamp *et al.*, 1995).

Many well-established methods for the quantitative estimation of groundwater recharge have been developed (Lerner *et al.*, 1990), but few can be applied with success to all the different climatic regions, especially to the semi-arid environments. Simmers (1988) states that no single comprehensive technique for the estimation of groundwater recharge can be identified from the available methods. Bredenkamp *et al.* (1995) suggest that it is preferable to average the results of the different methods.

The methodologies suitable for the estimation of groundwater recharge have been classified by Bredenkamp *et al.* (1995) in a number of categories and are discussed in detail by them and in many other hydrogeological textbooks.

2.9.1 Application of direct methods in the quantitative estimation of recharge

A flow model based on Darcy's law can be used to estimate groundwater recharge. However, conditions in the vadose zone are very complex and knowledge of a number of parameters is essential when recharge is estimated. These parameters include porosity, soil suction as a function of volumetric water content (i.e. the soil-water characteristic curve), saturated hydraulic conductivity and the residual water content.

Recharge can be expressed as the rate of flow per square metre and in the case that matrix flow is the dominant flow type, can be expressed as:

$$RE = q_{z_0} = -K(\theta)\frac{dh}{dz} \qquad [2\text{-}27]$$

where q_{z_0} is the specific discharge at groundwater surface depth.

The depth to the groundwater surface, volumetric water content, and hydraulic head are site-specific parameters and vary with time due to changing climatic conditions.

Bredenkamp *et al.* (1995) state that the unsaturated Darcy flow model fails as a practical method for estimating recharge because:

- Boundary conditions are difficult to determine and have to be approximated by sub-models. These models may apply only to part of the aquifer or for only part of the time.
- The lack of relevant precipitation and evaporation data is a practical restraint.
- The method relies on point measurements to derive values that cannot generally be extrapolated because of considerable variation in moisture content and hydraulic properties.

Freeze (1969) states that rainfall, with its influence on soil moisture conditions, is the main variable in recharge control. He also states that estimates of recharge based on saturated hydraulic conductivity and textural classification can be misleading.

Another drawback of the method is that preferential pathways and soil layering, frequently occurring in the vadose zone, have a major effect on fluid flow in the vadose zone and may render Darcy's law invalid.

Notwithstanding the above-mentioned criticism of direct methods in estimating recharge, recent advances in the processing capabilities of PCs and advances in unsaturated flow numerical modelling enables hydrogeologists to simulate and predict recharge processes.

2.10 Techniques for assessing aquifer vulnerability

Groundwater is polluted by many human activities, such as waste disposal and mining, as well as industrial and agricultural activities. The cleaning of polluted aquifers is technically very difficult and extremely expensive (Parsons & Jolly, 1994). It is therefore necessary to adopt a proactive approach to groundwater protection.

The concept of aquifer vulnerability originated from the assumption that the physical environment might provide some degree of protection against contaminants entering the ground surface (Vrba & Zaporozec, 1994). Contaminants enter the ground and are attenuated by a number of processes that are active in vadose and phreatic zones. Attenuation processes are discussed in section 2.10.1. Different physical environments have different capacities for the attenuation of contaminants.

Aquifer vulnerability maps indicating areas more (or less) sensitive to contamination will provide local, national and water authorities, as well as anybody involved in the planning and development, with knowledge concerning ways to site potential groundwater degrading activities away from vulnerable areas, or enable sites to be engineered in such a way that contamination is avoided. In South Africa and other developing countries, aquifer vulnerability maps can also promote the assessment of vulnerability in the case of informal settlements where services are lacking.

A number of methods have been developed to assess aquifer vulnerability. These include popular methods such as DRASTIC (Aller, Bennet, Lehr, Petty & Hacket, 1987), SINTACS (Civita, 1990) and GOD (Foster, 1987). The assessment of aquifer vulnerability does not constitute part of this research and readers are referred to Vrba and Zaporozec (1994) and Hearne, Wireman & Campbell (1991) for detailed discussions on aquifer vulnerability assessment and mapping.

Parsons and Jolly (1994) developed the Waste-Aquifer Separation Principle (WASP) to assess the effect of waste disposal sites on aquifers. This concept is based on the principle that waste and groundwater ought to be separated. Potential groundwater-degrading activities have to be situated away from vulnerable aquifers and such sites must be engineered to prevent infiltration of contaminants into the ground (Parsons & Jolly, 1994).

Three components have to be considered when pollution potential is assessed:

- Source of contamination (Threat factor)
- Pollution pathways (Barrier factor)
- Pollution receptor (Resource factor)

Figure 2.10 indicates the factors affecting groundwater resource pollution. The vadose zone acts as a barrier against pollution of the groundwater resource.

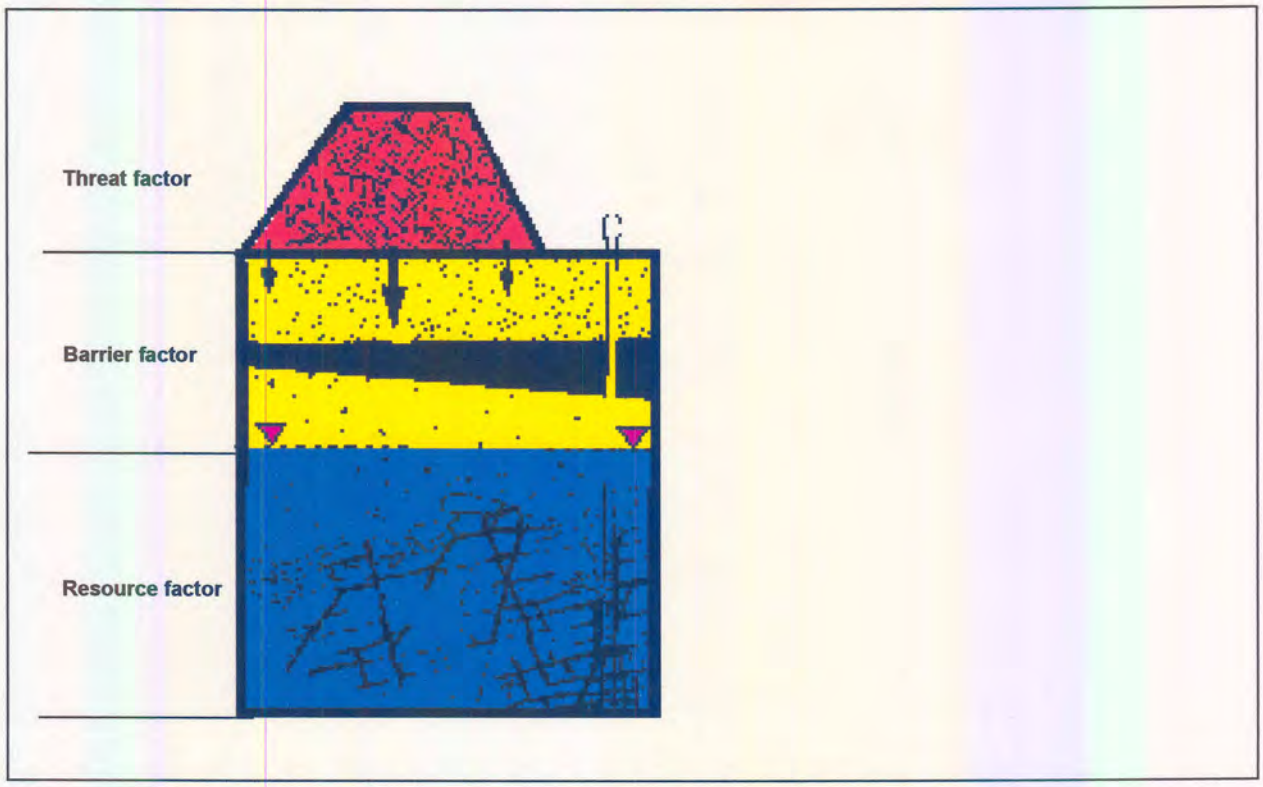

Figure 2.10: Factors that could have an effect on contamination of the groundwater resource (after Parsons and Jolly, 1994)

Parsons and Jolly (1994) use travel time to quantify the barrier factor which prevents the pollutants from a waste disposal site from reaching groundwater level. The travel time, also known as residence time, is the time it takes for the dissolved contaminant species to move to the groundwater surface. A longer travel time suggests that the contaminants are exposed to attenuation processes for a longer period, thus increasing the probability of complete attenuation before the contaminants reach the groundwater. The travel time can therefore be used to quantify the attenuation capacity of the vadose zone.

Travel time can be defined as:

$$Tt = \frac{d}{v_s} \qquad [2\text{-}28]$$

In a case where matrix flow is the predominant flow type of a specific area, Equation 2-28 can be written in Darcian terms:

$$Tt = \frac{z_{gs} \cdot \theta}{K(\theta)\frac{dh}{dz}} \qquad [2\text{-}29]$$

The depth to groundwater surface, volumetric water content and hydraulic gradient are site-specific parameters that vary with time due to changing climatic conditions. In addition, the saturated hydraulic conductivity may also vary, depending on the type of leachate moving through the soil. This is especially true in the case of hydrocarbon-based leachate moving through clay.

This simplistic approach may be criticised, since the most basic attenuation properties of the soil are not considered. Attenuation properties can either be an advantage or a disadvantage, depending on the type of contaminant that is involved. In the absence of attenuation processes, contamination is delayed and will resume after reaching the groundwater surface. In the case of a long travel time, specific discharge will be very low and dilution processes may be effective in preventing serious groundwater pollution. However, it has long been recognised in the hydrogeological fraternity that "*dilution is not the solution for pollution*". Attenuation processes have to be addressed in groundwater vulnerability studies. However, in the absence of relevant data, the travel time can be used to quantify the attenuation capacity of the vadose zone since long travel times are generally the result of a high clay content, which is a desirable property in attenuation.

2.10.1 Attenuation

When contaminants enter the ground, the dissolved contaminant species or leachate migrates downwards because of the water flow in the vadose zone. This process is known as advection. Several physical, chemical and biological processes that can improve the quality of the leachate take place in both the vadose and phreatic zones. These processes are known as attenuation processes. **Table 2.4** lists the types of attenuation processes that are operative in the vadose and phreatic zones.

Table 2.4 Types of attenuation processes (Sililo, Conrad, Murphy, Tredoux, Eigenhuis, Ferguson & Moolman, 1997)

Physical	Chemical	Biological
Dispersion	Hydrolysis	Aerobic biodegradation
(Ad)sorption	Dehydrohalogenation	Anaerobic biodegradation
Volatilisation	Precipitation	Hypoxic biodegradation
Filtration	Cation exchange	Nitrification
Dilution	Oxidation/reduction	Denitrification
Advection		Recarbonation (of high pH effluent)
		Cell synthesis

The effectiveness of these attenuation processes depends on:

- The properties of the contaminant species
- The properties of the soil medium
- Environmental factors (e.g. temperature)
- The travel time of the contaminants (the longer this period, the longer the contaminants are exposed to attenuation processes).

Because of the numerous interactions between different kinds of contaminants and the different kinds of soil media present, the evaluation of aquifer vulnerability is complicated. Some researchers have therefore suggested that a list of soil properties in the vadose zone may contribute either favourably or unfavourably to attenuation (Thorton, Lerner, Bright & Tellman, 1993):

Favourable properties

- A high clay and silt content increases the sorption capacity of organic and inorganic solutes.
- Particulate organic matter possesses a much higher cation exchange capacity (CEC) per unit weight, than clay. This can contribute favourably to the retention of leachate cations, especially of heavy metals.
- An alkaline pH enhances the immobilisation of heavy metals by hydroxides and/or carbonates. It also controls the effective CEC of the system.
- High levels of ferric oxide may contribute favourably to the attenuation of heavy metals in aerobic conditions.
- High levels of lime may also contribute favourably to attenuation.

Unfavourable properties

- High levels of soluble salts in the soil medium may mobilise toxic constituents.
- Adsorbed metals in contact with a reducing leachate may, in the presence of ferric oxide in the soil, be released through dissolution.

Attenuation processes are complex and are not yet fully comprehended. It is difficult to apply quantitative values to the above-mentioned properties, since attenuation is affected by the properties of both the soil and the contaminant.

It is generally accepted that pH is the primary variable in control of attenuation processes (Sililo *et al.*, 1997). Metal cations are adsorbed and precipitate as oxides, hydroxides and carbonates in high pH environments. Their mobility increases as pH decreases. The opposite is true for metal anions such as chromium, selenium and arsenic in some valence states. Some soils and rocks can resist pH changes where acidity or alkalinity is introduced. Important mechanisms include carbonate mineral buffering, exchangeable base cation buffering and buffering by alumina-silicate mineral decomposition in strongly acidic soils (McBride, 1994).

Sililo *et al.* (1998) are of the opinion that several attenuation processes operate in the soil/aquifer system and that these systems occur simultaneously and in certain cases compete with each other. The attenuation potential of a soil is not a fixed parameter, but a variable. However, Sililo *et al.* maintain that

a soil with a high level of adsorption surfaces, pH well-buffered in the neutral or higher range and a low level of dissolved organic carbon will successfully immobilise metals.

Sililo *et al.* verified said propositions with an investigation of the attenuation potential of six different soils with regard to an array of heavy metals and organic compounds. The strongest attenuation occurred in soils with high pH and CEC values. However, chromium - anionic in groundwater - was most strongly attenuated in acidic soils, while other metals were also attenuated in these soils due to a high sesquioxide content with a subsequent high adsorption potential.

Attenuation processes continue in the phreatic zone, mainly by means of dilution. The effectiveness of attenuation in the phreatic zone will be dependent on the rate of flow at the groundwater surface, i.e. the specific discharge or flux.

CHAPTER 3

GEOTECHNICAL INVESTIGATION METHODS AND THEIR HYDROGEOLOGICAL INTERPRETATIONS

Engineering geologists and geotechnical engineers are primarily concerned with the strength, potential volumetric change and permeability of soils and rocks. Engineering geologists use a variety of investigation methods to determine relevant soil and rock properties. Many of these methods involve the application of knowledge and experience in the fields of soil and rock mechanics and it is therefore difficult to derive direct correlation with hydrogeological properties. During the last few years, geohydrological investigations have become an important aspect of many engineering investigations, including waste disposal, mining activities (including mine tailings dams) and industrial development. Engineering geologists with training and experience in hydrogeology have become involved in these investigations to an increasing degree. Geotechnical methods and tests are described in detail in numerous textbooks and other publications (Jennings *et al.*, 1973; Brink, 1979; Holtz & Kovacs, 1981; Das, 1990; Bell, 1993)

Engineering geologists have traditionally been involved in the spatial distribution of geological materials with similar geotechnical properties. In particular, engineering geological investigations in assessing the geotechnical suitability for residential development and investigations concerned with the identification of geological materials for road construction purposes have greatly increased the engineering geologist's ability to determine the spatial distribution of geological materials.

Since many engineering geologists are mainly interested in the unconsolidated material overlying the bedrock, they need to consider the following processes in the assessment of geotechnical properties:

- The extent of weathering, which is mainly a function of climate;
- The time the material has been exposed to weathering processes, which implies that knowledge regarding paleo-climate could be necessary;
- Differences in geotechnical properties that could be ascribed to its topographical setting;
- Pedogenic processes

3.1 Geology

A thorough understanding of the geology is of paramount importance in any engineering geology investigation. Geological maps are widely available, and with his knowledge and experience of rock properties and its weathered products, the engineering geologist can predict possible geotechnical

problems even before visiting the site. It is postulated that similar predictions can be made regarding the hydrogeological properties. The hydrogeological characteristics depend on *inter alia* the geological material.

Most pre-Quaternary rocks in South Africa are characterised by two features, namely negligible primary porosity and varying secondary porosity caused by fracturing and weathering. These rocks are generally classified by geohydrologists as "*hard rocks*" (UNESCO, 1984). Hard, competent, impermeable rocks underlie most parts of South Africa. Some authors choose to exclude volcanic and carbonate rocks from the hard rock category (UNESCO, 1984). However, most volcanic and carbonate rocks in South Africa exhibit typical hard rock characteristics and have been included in the hard rock category. In the case of sedimentary rocks, competent impermeable hard rocks occur interbedded between impermeable fine-grained rocks such as shale, mudrocks and siltstone. These fine-grained rocks, although not classified as hard rocks, are also characterised by virtually no primary porosity and may also contain secondary porosity due to fracturing.

Rock masses are seldom homogeneous, but are intersected by joints, tension cracks, bedding planes, geological faults and other discontinuities. This causes more rock surface area to be exposed to weathering. Weathering etches along discontinuities and causes complex weathering profiles. Weathering is usually more intense along geological structures such as faults and often results in deeply weathered soils along these zones. Where three orthogonal joint sets are present in the rock mass, weathering along these joints may result in the development of corestones in the profile.

Flow through hard rocks is generally restricted to an interconnected system of fractures, joints and fissures within the rock mass. These discontinuities are mainly the result of large-scale tectonic events within the earth's crust. (UNESCO, 1984). Weathering processes have a significant effect on the flow and storage capacity of the discontinuities.

3.1.1 The weathering profile

While rocks are exposed to weathering processes, they go through a series of weathering stages before converted to residual soils. The weathering stages typically manifested within a soil/rock profile from the ground surface to unweathered rock are as follows (Geological Society Engineering Group, 1990):

- Residual soil (Stage VI) – The original structure of the material has been destroyed. A pedological soil profile with characteristic horizons has developed. Large volume changes have occurred, but the soils have not been transported significantly.

- Completely weathered (Stage V) – All rock material has decomposed or disintegrated into soil. The original structure of the rock is still intact and visible.

- Highly weathered (Stage IV) – More than half of the rock material has decomposed or disintegrated into soil. Discoloured rock is present as blocks or rounded core-stones.

- Moderately weathered (Stage III) – Less than half of the rock material has decomposed or disintegrated into soil. Fresh or discoloured rock is present as blocks or core-stones that fit together.

- Slightly weathered (Stage II) – Discoloration on the rock surface indicates weathering, especially along discontinuity surfaces.

- Unweathered (Stage I) – No visible sign of rock material weathering except perhaps slight discoloration along discontinuity surfaces.

The hydrogeological properties of a particular geological material will vary depending on the stage of weathering of the material. Weathering characteristics are a function of both climate and geology and therefore need to be assessed on a site-specific basis. However, the following trends can be identified:

Unweathered rock: Since the South African geology is dominated by "hard rocks", the unweathered rocks (igneous, sedimentary and metamorphic) are generally characterised by a low primary porosity and very low primary hydraulic conductivity. Preferential weathering frequently develops along joints, fractures and geological boundaries. The depth to unweathered rocks may therefore vary significantly over small distances, and this complicates unsaturated hydrogeological studies significantly.

Slightly weathered rock: Although weathering has not penetrated fractures and joints, discontinuities and rock surfaces are stained by weathering agents. The hydrogeological properties are similar to unweathered rocks, i.e., low primary porosity and low but definite primary hydraulic conductivity as indicated by the stained surfaces.

Moderately weathered rock: Less than half the rock material is decomposed or disintegrated to a soil. The rock could be highly fractured, which could result in very high permeabilities, typically up to 10 000 times higher than unweathered and slightly weathered rock. Moderately weathered rock typically has the highest hydraulic conductivities of all weathering stages in the soil profile resulting it to be the main pathway for contaminants originating from the surface. In particular, moderately weathered dolerite (termed fractured, boulder or gravel dolerite depending on the weathering stage and appearance) is characterised by high hydraulic conductivities. The material has been identified as the major contamination pathway of many pollution sources associated with coal mining in the Mpumalanga coal fields.

Highly weathered rock: More than half the rock has been decomposed or disintegrated into a soil. The rock is characterised by a high porosity, but unlike during the moderately weathered stage, the hydraulic conductivity depends on infilling between joints and fractures. In cases where the infilling has been decomposed to clay, hydraulic conductivity may be very low. In the case of disintegration to sand and gravel, the hydraulic conductivity may be very high. Dolerite generally disintegrates to granular (or sugar) dolerite with high expected hydraulic conductivities.

Completely weathered material: All rock material has been disintegrated or decomposed to a soil. However, the original rock structure is still intact. The hydraulic conductivity will be highly variable and flow of water will mainly occur along preferential pathways such as highly leached preferential weathering zones or disintegrated quartz veins. The field hydraulic conductivity is a function of *inter alia* climate and rock type.

Residual soil: All rock material has been disintegrated or decomposed to soil and the rock structure has been destroyed by pedogenic processes. This weathering stage is characterised by more uniform materials, compared with materials of the other weathering stages. Therefore, flow in residual soils generally conforms to traditional unsaturated flow theory. Hydraulic conductivities may be high in cases where disintegration is dominant, low in the case of decomposition and very low in cases where minerals have been weathered to predominantly clay minerals.

The contact between the weathered material and bedrock can be described as transitional, sharp, regular or irregular (Chorley, Schumm & Sugden, 1984).

Transitional contacts are commonly found in rocks with uniform structure and texture. Weathering susceptibility is limited to mineralogical level and the boundary between soil and bedrock is difficult to define. Arenaceous rocks of the Karoo Sequence generally exhibit transitional contacts in the more humid areas of South Africa.

Sharp contacts are characterised by thin (often only a few millimetres thick) contacts between bedrock and soil. These contacts are frequently referred to as a weathering front. Sharp contacts are associated with dense, mineralogically and structural uniform rocks, rocks susceptible to solution, basic rocks with a

low resistance to weathering and rocks with a low permeability or those with a permanent groundwater level close to surface (Chorley *et al.*, 1984). Basement granitoid rocks typically exhibit clearly defined weathering fronts. However, discontinuities in these rocks could result in preferential weathering along these zones and the weathering contact can then be described as irregular.

Regular contacts refer to contacts characterised by extensive jointed corestones, increasing in size with depth. Weathering stages are more clearly defined than with sharp and transitional contacts. The weathering of dolerite dykes and sills (occurring as intrusive bodies in Karoo rocks) may, to some degree, be described as regular. Extensive fracturing and jointing frequently occurs along the contact between bedrock and soils. .The regular contacts of dolerite are probably related to the jointing and low resistance to weathering of the bedrock material.

Irregular contacts refer to conditions where weathering depths may vary considerably. This occurs where the bedrock's susceptibility to weathering and degree of jointing vary spatially. Irregular contacts typically develop in intrusive igneous rocks.

3.1.2 The Weinert N-value

Weinert (1980) developed the N-value to differentiate between regions of similar weathering characteristics. The N-value is based on the climatic situation of a particular area and can be defined as:

$$N_W = \frac{12\,E_J}{P_a}$$

where N_W is the Weinert N-value, E_J is the total evaporation for the warmest month (in the case of southern hemisphere countries such as South Africa, this will generally be January) and P_a is the total annual precipitation. A map showing Weinert N-values for southern Africa is contained in **Figure 3.1**.

According to Weinert, physical weathering (disintegration) will predominate in areas where the N-value is larger than 5 and chemical weathering (decomposition) will predominate in areas where the N-values are less than 5. Chemical weathering will result in the formation of secondary minerals such as hydromica, clay minerals and sesquioxides. The type of secondary minerals that will develop will depend on the underlying geology, the time the rock has been exposed to weathering processess and climate and will be discussed in section 3.3. The weathering characteristics for areas of similar N-values are summarised in **Table 3.1**.

Table 3.1: Weathering characteristics as influenced by climate (Weinert, 1980)

N-value	Mode of weathering	Weathering characteristics	Principle secondary minerals
>10	Mainly disintegration	Thin weathering layer, No secondary minerals	Almost none
5-10		Few secondary minerals	Hydromica, illite
2-5	Mainly decomposition	Weathering profile deepens towards N=2, significant secondary minerals	Kaolinite, Montmorillonite
<2		Montmorillonite changes to Kaolinite in top soil layers, deep weathering profile	Kaolinite, Montmorillonite
<1		Montmorillonite and kaolinite change to sesquioxides, very deep weathering profiles	Kaolinite, Sesquioxides

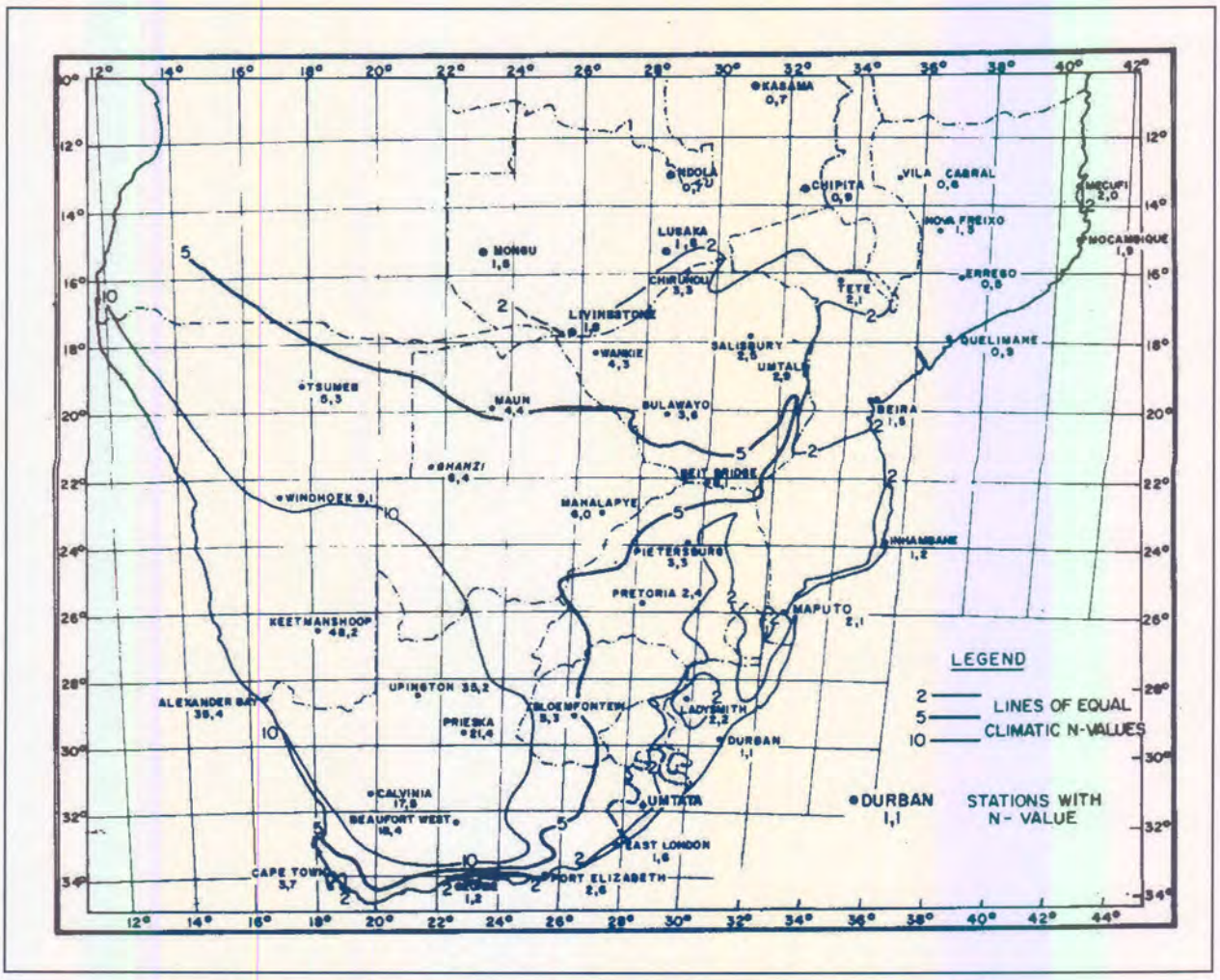

Figure 3.1: Map of South Africa indicating Weinert N-values (after Weinert, 1980)

3.2 Geomorphologic cycles

The present landscape in South Africa is the result of distinct geomorphologic cycles, ranging from the late Jurassic age to the present. Each cycle was initiated by a tectonic episode in which the land surface was uplifted, rifted, tilted or deformed in some way. With a new base level of erosion established after each cycle, renewed denudation proceeded, carving new landforms on top of the older ones (Brink, 1979).

Principal geomorphologic events in South Africa ranging from the Mesozoic age to present are summarised below (Partridge & Maud, 1987).

- Break-up of Gondwanaland by means of rift-faulting occurring in the late Jurassic/early Cretaceous to early Miocene age and manifested in the initiation of the Great Escarpment, owing to high absolute elevation of the southern African portion of Gondwanaland, also leading to the Enon-conglomerate Formation.

- African polycyclic erosion cycle occurring in the late Jurassic/early Cretaceous to early Miocene age, manifested in advanced planation throughout the subcontinent, resulting in erosion surfaces at two levels, above and below the Great Escarpment; also in the development of deep residual soil with extensive ferricrete and silcrete development and leading to the development of the Kalahari basin with the onset of sedimentation towards the end of the Cretaceous period

- Upliftment of 150-300 m comprising a slight westward tilting of the African erosion surface with limited coastal monoclinal warping and subsidence of the Bushveld Basin occurring at the end of the early Miocene age

- Post-African I erosion cycle occurring in the early mid Miocene to late Pliocene age, manifested by the development of the imperfectly planed Post-African I erosion surface and major deposition in the Kalahari basin

- Major upliftment event of up to 900 m, comprising an asymmetrical upliftment of the subcontinent and a major westward tilting of previous land surfaces of the interior, with monoclinal warping along the southern and eastern coastal margins, occurring in the Late Pliocene age.

- Post-African II erosion cycle of major valley incision occurring in the Late Pliocene to Holocene age, manifested in incision of coastal gorges, down-cutting and formation of higher terraces along interior rivers, formation of erosion surfaces and limited planation restricted to the eastern Lowveld region

- Quaternary cycle of climatic oscillations and glacio-eustatic sea-level changes occurring in the Late Pliocene to Holocene age, manifested in low-level marine beaches, coastal dune deposits, river terraces and deposits of the Kalahari sands

The hydrogeological properties of weathered materials and residual soils have mainly been influenced by the African and Post-African erosion cycles. The African polycyclic erosion cycle lasted for more than 100 million years. Soils and rocks have been exposed to weathering processes for very long periods resulting in the development of extensive weathering profiles. In addition, the palaeo-climate during the African erosion cycle was different than the present climate, with many areas in South Africa being wetter for long periods. Much of these soils have been removed by later erosion cycles but soils located on the African erosion surface are characterised by extensive pedocrete development and, particularly in areas underlain by granite, extensive kaolinisation (Partridge & Maud, 1987). In assessing the hydrogeological characteristics of residual soils, the geomorphic situation has to be considered.

It is not possible to discuss the effect of geomorphology for all geomorphic cycles since these will depend on the geology, topography, paleo-climate and present climate. These effects should be considered at site-specific and regional (1:50 000) investigations.

3.3 Land pattern classification

The preparation and compilation of any map, indicating the spatial distribution of various elements in the natural environment, imply that these elements can be classified according to the similarity of one or more physical attributes. The physical attributes within each of these classes should not vary significantly in order to allow the deduction of purposeful information. In addition, data collected for a particular land pattern class should be relevant for similar land patterns in other areas. In this way, the physical characteristics of particular land pattern classes can be extrapolated to similar land patterns in the investigation area, thereby making full use of available data and eliminating the need for the duplication of costly investigations on other similar land patterns.

The advantage of this approach is that, with the aid of remote sensing imagery, in particular aerial photographs, the properties of extensive land areas can be inferred at relatively low cost.

Several approaches have been developed in recognising the different land pattern classes. The two main approaches applied in South Africa are:

- The land system classification

- The land type classification

3.3.1 The land system classification approach

The land system classification system originated from soil engineering maps developed in the UK, South Africa and Australia for engineering purposes (Partridge, 1994). The nomenclature employed in this system closely resembles that of Christian and Stewart (1953). The system gained acceptance from approximately 1966 onwards, when it was adapted mainly for engineering purposes.

A land system is a large area with a recurring pattern of land forms, soils and hydrological regimes (Beaven, 1994). Land systems differ from other land systems by their distinctive physical attributes and can be recognised from aerial photos and other remote sensing techniques. Land systems are identified and mapped by their pattern of landforms, streams and vegetation. They are characterised by the following aspects (Beaven, 1994):

- They usually extend over an area of at least 100km^2 and can be mapped at scales of between 1:250 000 and 1: 1 000 000.
- The climate is uniform.
- Underlying geology is either uniform, or consists of closely related geological units (e.g. alternate layers of sandstone and mudstone) that can be mapped as a single unit.
- Recurrent land patterns can be recognised from aerial photo interpretations. Recurrent land systems may be situated thousands of kilometres from each other and still be named similarly, indicating that they possess similar physical attributes.
- Land systems are contiguous and no gaps of unclassified area occur between them.

Land systems are generally named after a town or village located within such a system. **Figure 3.2.** illustrates the Kyalami and surrounding land systems developed for the Gauteng area.

Land facets are defined as recognisable aspects of the landscape that together comprise a particular land system. These are geomorphologically related to each other. This means that they always occur in a certain relationships to each other. Land facets therefore occur in a particular sequence (e.g. crest, convex slope, concave slope), enabling engineers and geologists to identify land facets by their position in the landscape. Land facets are units of uniform slope, geology, soils, hydrological and hydrogeological conditions. Any deviation in a land facet should be simple and uniform. Land facets are characterised by the following aspects (Beaven, 1994):

- Non-related land facets may occur within a land system. These occur generally due to local geological features (such as intrusion structures) or particular hydrological features (such as pans).
- Land facets can generally be mapped at scales of between 1:10 000 and 1:100 000.
- Hydrological characteristics are consistent within a particular land facet.
- Land facets are named after the particular land form they are comprised of, e.g. hill crest, foot slope and river terrace. These units are not unique for all land systems.
- Land facets are contiguous and no gaps of unclassified land occur between them.

Land elements are the smallest unit in the land system classification methodology. Land elements are subdivisions of land facets and are often too small to be mapped at any practical scale. Yet, these features may have a significant effect on the aspect investigated. Examples include small rock outcrops, small dykes and oxbow lakes.

Variations within a land facet that cannot always be identified except from field investigations are termed variants. For example, residual soil from different rock types, concealed by transported soil, may have diverse physical properties. Although the area blanketed by the transported soil is described as a single land facet, different residual soils are described as different variants within the land facet.

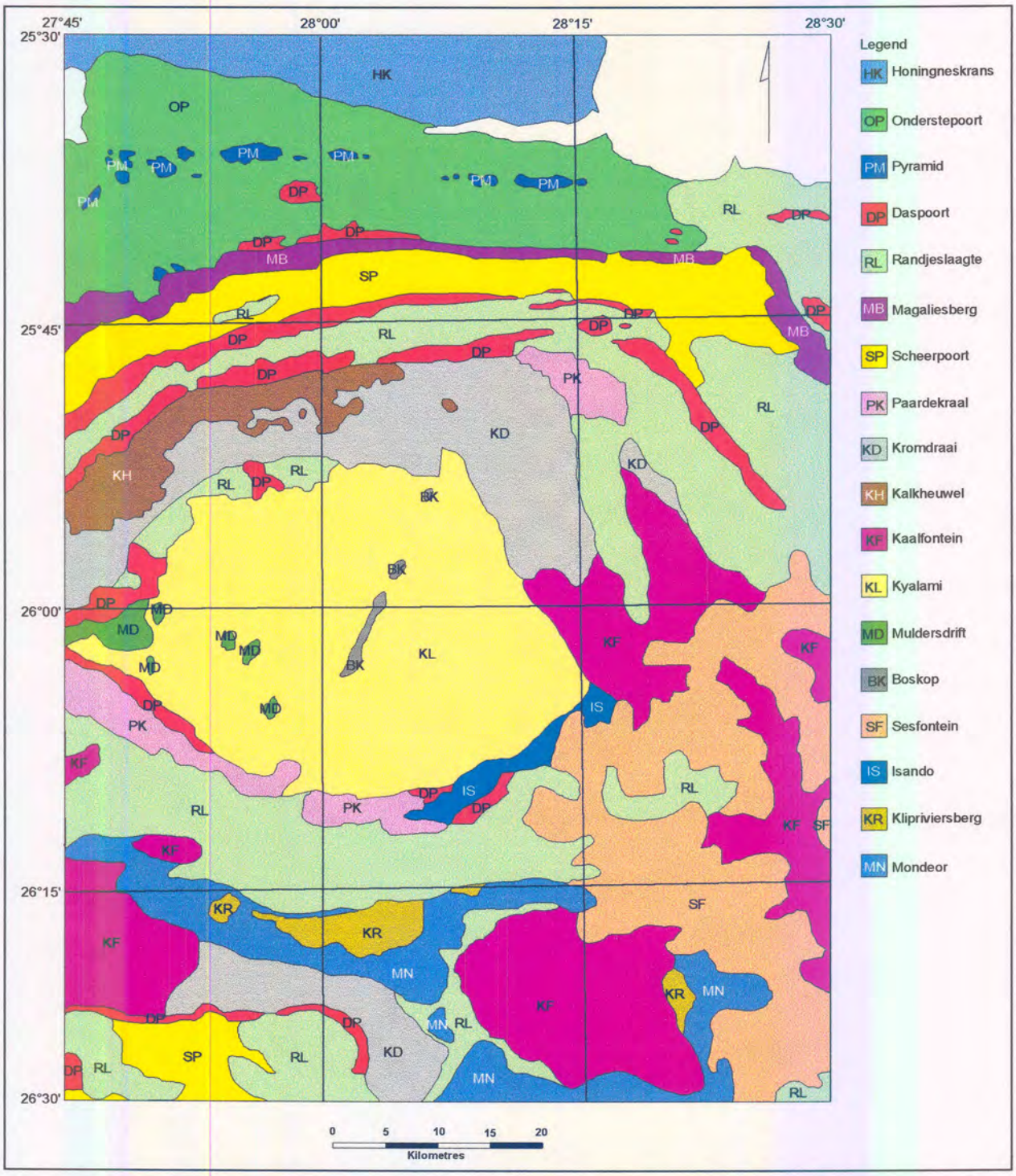

Figure 3.2: Land System map for the Gauteng Province area, South Africa (modified after Partridge, 1994)

The first stage in the assessment of the spatial characteristics of a particular area is to identify and define different mapping units. The scale and extent of the mapping depend on the intended use of the final presentation. In South Africa, national land system maps on a 1:250 000 scale are compiled by the

Institute for Soil, Climate and Water. Large parts of mainly urban areas are mapped for geotechnical purposes, generally at a scale of 1:10 000 or larger.

Land facets are mainly identified from stereoscopic aerial photo interpretations. The scale of the aerial photos chosen will depend on the level of detail required and the availability of the aerial photos. Other sources that can be used to identify land systems and land facets include satellite imagery, aerial colour photos and other remote sensing techniques.

3.3.2 The land type classification system

The land type classification system is similar to the land system classification system generally applied by the engineering fraternity. The land type classification system has been formulated by the Soil and Irrigation Research Institute of the South African Department of Agriculture during the 1970's.

Land type classification denotes an area to be depicted on a scale of approximately 1:250 000 and indicate areas characterised by a high degree of uniformity in respect of climate, terrain form and soil pattern. Land types are analogous to land systems, although differences do exist with regard to delineation of the land type. The chief criteria in land type delineation are pattern and density of the drainage system, relief, slope, profile and extent of every terrain unit.

A terrain unit is defined as any part of the land surface with a homogeneous form and slope, with other land units together comprising a particular land type. Five basic terrain units are used throughout the classification system, namely crest, scarp, midslope, footslope and valley bottom. These units are fixed: unlike the land facet approach, morphology and not genesis determines the delineation and description of terrain units. Variations in the form and sequence of the terrain units are generally indicated on an accompanying cross-section of the particular land type. Terrain units may further be subdivided into phases indicating variations within a specific terrain unit.

3.3.3 Parametric and analogue methods

The parametric and analogue methods differ from the land pattern method in that they identify a large feature in the landscape and subdivide it by weighting and rating separate data points within the feature.

The advantage of the parametric approach is that it reduces the physiographic bias associated with land pattern methods. However, grave disadvantages are associated with this approach. The first problem derives from choosing attributes to define the limits of a particular unit. The different attributes are rated and weighted according to their relevance for the aspect under investigation. In practical terms, the method proves to be less effective and requires much more effort than demarcating land units characterised by similar physical attributes. In addition, the method has proven to be very data intensive, thereby increasing the costs of deriving a parametric model. However, the increasing availability of data and recent progress in Geographical Information Systems may result in the increased application of parametric methods in mainly detailed investigations.

Analogue techniques are similar to parametric methods in that they identify a large feature in the landscape and subdivide it by assigning a rating to the relevant attributes within the land feature. Unlike the parametric method, analogue methods assign a numerical value to the particular attributes, which is entered into a mathematical equation, relating the attributes to the particular aspect investigated. LeGrand (1983) state that these methods may be suited to advanced stages in the investigation and are generally suited to site specific investigations where large amounts of data are available to numerically define the particular physical attribute.

3.4 Data collection and evaluation

After land patterns have been delineated for a specific investigation area, data must be collected to describe typical physical characteristics for a particular land facet. Soil data are usually collected by:

1. Excavating a number of testpits representative of the particular land facet,

2. Describing the soil profiles and

3. Collecting soil samples representative of the different soil horizons for laboratory testing.

Variability in soil properties for a particular land facet can be attributed to a number of reasons and has been discussed in preceding sections. These aspects should be taken into account during the processing and evaluation of data.

3.4.1 Data evaluation by means of GIS

After data collection has been completed, it should be recorded in a database in order to facilitate data evaluation and manipulation. For these purposes, data should preferably be recorded and presented within a spatial database framework. Recent advances in Geographical Information Systems (GIS) make it possible to evaluate point data within a land facet classification context.

GIS provides an invaluable tool for the capturing, processing, evaluation and presentation of spatial data. Digital photogrammetric work stations allow direct digital capturing of aerial photo interpretations. Information from adjoining studies can be incorporated within present studies, assisting in the interpretation (Murphy & Stiff, 1994). A major advantage of GIS is that different data source/layers can be overlain, thereby exposing patterns that may not have been noticed when the data sources were studied individually. Point data sources can be evaluated in terms of its positions within a particular land facet. With point data attributes captured in a database, data can be presented in terms of any of these attributes, thereby exposing patterns and assisting in the interpretation of the data.

Another major advantage of GIS is that data can be presented in any form required by the end user. Maps can be compiled on any scale to present any of the data digitally captured within GIS. However, data should not be presented at a scale larger than the scale in which the data were collected, as this may cause misinterpretation of the data for the particular area.

As is the case with any computerised tool, a major disadvantage of GIS is that the information presented may be based on insufficient data, thereby misleading the end user with regard to the quality and reliability of the end product.

3.5 Standard geotechnical investigation methods

An engineering geological investigation commences with a desk study during which all relevant information is gathered. Geological, topographical, orthophoto-, geohydrological, geophysical and other maps may be consulted to assess site conditions, then to be confirmed by a site visit. Aerial photographic interpretations serve to investigate the area from another angle and to identify geological structures such as faults.

Geophysical investigations are conducted for a number of reasons, but are applicable especially in dolomitic and geohydrological investigations. Gravimetric and Electromagnetic (EM) methods are commonly used in dolomitic investigations, while Vertical Electrical Resistivity (VER), as well as Magnetic and Seismic methods are used in geohydrological investigations.

Field investigations involve the mapping and excavation of a number of testpits on site. The soil profiles are described according to guidelines laid down by Jennings, Brink & Williams (1973). These allow for consistent soil profile descriptions for every type of soil. Percussion or rotary drilling may be conducted and drill cores are described according to guidelines by the Association of Engineering Geologists (1976). Small and large diameter auger drillings may also be conducted to extract samples or to describe soil profiles at greater depths. Samples for laboratory testing can be taken from the testpits, auger holes or drill cores.

In geohydrological investigations, the first step is usually to conduct a borehole census within a radius of a few kilometres from the proposed site. A data sheet containing information on borehole location, depth to groundwater level, borehole yield and groundwater use is completed for each borehole. Water samples are taken from a number of boreholes and tested for pH, electrical conductivity, total dissolved solids, major cations and anions, relevant microconstituents and bacteriological constituents.

During the geohydrological investigation, borehole pumping tests may be conducted to estimate the specific geohydrological characteristics of the aquifer. Step drawdown tests and constant-rate discharge tests are conducted, followed by recovery tests. Important geohydrological properties such as transmissivity, storativity and hydraulic conductivity can be obtained. From these data, estimates regarding the safe yield of the well can be made.

Geotechnical laboratory tests may be conducted to obtain index properties of the soil or rock material, in order to compare them with soils or rocks with similar properties of which the geotechnical behaviour is known. Certain geotechnical properties can be measured directly. Standard laboratory tests for geotechnical investigations are summarised in **Table 3.2**. Standard laboratory testing procedures are generally specified by the American Society for Testing and Materials (ASTM, various dates), the American Association of State Highway and Transportation Officials (AASHTO, 1974) and the British Standards Institution (1990).

The type of laboratory tests conducted depends on the nature and scope of the investigation. In general, index properties are derived for nearly all geotechnical investigations and are most widely available in the literature.

In addition to laboratory tests, *in situ* tests may be conducted to obtain additional information on the typical behaviour of soils and rocks. Standard in situ tests conducted during geotechnical investigations are listed in **Table 3.3** Standard *in situ* tests are generally specified by the American Society for Testing and Materials (ASTM).

Direct and indirect correlation with geohydrological parameters can be made from many of the above-mentioned profiling techniques, laboratory and in situ tests. However, not many of results of geotechnical testing are widely available. For purposes of this research, the focus is on those geotechnical data that are readily available. These are the following:

- Soil profile descriptions
- Particle-size distribution
- Atterberg limits

These aspects will be dealt with in more detail.

Table 3.2: Standard geotechnical laboratory tests.

Test	Properties determined	Reference
Soil index properties		BSI 1377 (1990)
Particle-size analysis	Grading, soil fractions, classifications	
Atterberg limits	Plasticity charts, soil classification	
Bulk density	Natural density	
Natural moisture content	With bulk density → dry density	
Specific gravity	With dry density → void ratio, porosity	
pH	PH	
Conductivity	Conductivity	
Dispersivity tests		Elges (1985)
Crumb test	Dispersive/non-dispersive	
Pin hole test	Degree of dispersiveness	
Double hydrometer	Percentage of dispersiveness	
Compaction tests		BSI 1377 (1990)
MOD-AASHTO/PROCTOR	Max. dry density, opt. moisture content	
California Bearing Ratio	Bearing capacity	
Rock strength/durability		AASHTO (1974)
Unconfined compressive strength	Rock strength	
ACV and 10 % FACT	Rock durability	
Water absorption	Degree of weathering	
Consolidation tests		BSI 1377 (1990)
Single oedometer	Degree and rate of consolidation	
Double oedometer	Degree and rate of consolidation	
Collapse potential	Collapse potential	
Swell potential	Swell potential	
Permeability tests		BSI 1377 (1990)
Constant head	Hydraulic conductivity	
Falling head	Hydraulic conductivity	
Triaxial and shear box tests		BSI 1377 (1990)
Unconsolidated undrained	Friction angle, cohesion	
Consolidated undrained	Friction angle, cohesion	
Consolidated drained	Friction angle, cohesion	
Quick shear box	Friction angle	
Slow drained shear box	Friction angle	

Table 3.3: Standard geotechnical *in situ* tests.

In situ test	Properties determined	References
Penetrometer tests		
Dynamic Cone Penetration (DPL)	Relative density, CBR, depth to bedrock	De Beer (1991)
Standard Penetration Test (SPT)	Effective angle of friction, relative density, compressibility, undrained shear strength (cohesive soils)	ASTM D1586-84
Dynamic Probing (DPM, DPH, DPSH)	Effective angle of friction, relative density, compressibility, shear strength	Melzer (1982)
Cone Penetration Testing (CPT) and Piezocone (CPTU)	Relative density, effective strength parameters, various moduli, Overconsolidation Ratio, permeability, sand type	ASTM 3441-86
***In situ* field density tests**		
Sand replacement	*In situ* density	ASTM D1556-82
Neutron meter	*In situ* density, *in situ* water content	ASTM D2922-81
Borehole tests		Houlsby (1976)
Single and double packer	Water loss	
Permeability tests		Daniel (1989)
Double ring infiltrometer	Hydraulic conductivity	
Constant or falling head borehole permeameters	Hydraulic conductivity	

3.5.1 Soil profile descriptions

The first assessment of soil properties commences with a systematic description of the soil profile. A systematic description of soil profiles is a widely used practice in South Africa, and the soil profile records are readily available. Most engineering geologists and geotechnical engineers use the guidelines developed by Jennings *et al.* (1973) to describe a soil profile.

Observations of a soil profile take place in trenches, test pits or large-diameter auger holes. Geological information of the top three to five metres is usually obtained. Auger holes, however, will provide geological information to depths in excess of 30 m. A soil profile usually consists of several layers/horizons that can be distinguished by changes in moisture content, colour, consistency, structure, soil type and origin. The individual layers are identified and their depths/thicknessess are recorded. The layers are then described by the MCCSSO method (Jennings *et al.*, 1973) on the basis of moisture content, colour, consistency, structure, soil type and origin.

Moisture content

The moisture content varies with time and rainfall events. The moisture content is described as dry, slightly moist, moist, very moist or wet. Wet soils are generally situated below the groundwater or perched groundwater levels. The moisture content must be interpreted in terms of grain-size. Sand with a water content of five to ten per cent may be described as 'wet', while a clay with the same water content may be described as 'slightly moist'. The term 'moist' usually describes a soil with a water content close to optimum. Dry and slightly moist soils require water if they are to be compacted effectively. Likewise, very moist and wet soils require drying before they can be effectively compacted.

Colour

The colour of soil is recorded to allow correlation of the same layer in different holes in the investigation area and it may be used to communicate with other people on the site. The colour of the soil depends on its moisture content. The colour is therefore described 'in profile', i.e. at natural water content, as well as 'wet', i.e. the colour of soil after it has been wetted.

Consistency

Soil consistency is a measure of the hardness or toughness of soil, i.e. the effort required to excavate the soil. It is also a rough measure of the soil's strength and density. The consistency of a soil depends on its moisture content, particularly with regard to cohesive soils. Soil consistency is described in different terms for granular and cohesive soils. The terms relating to consistency and their meanings are presented in **Table 3.4** and **3.5**:

Table 3.4: Consistency of granular soils (Jennings *et al.*, 1973)

Term	Description	Typical density (kg/m3)
Very Loose	Crumbles very easily when scraped with geological pick	< 1 450
Loose	Slight resistance to penetration with sharp end of geological pick	1 450 - 1 600
Medium dense	Considerable resistance to penetration with sharp end of geological pick	1 600 - 1 750
Dense	High resistance to penetration with sharp end of geological pick; requires many blows of the pick for excavation	1 750 - 1 925
Very dense	High resistance to repeated blows of geological pick; requires power tools for excavation	> 1 925

Table 3.5: Consistency of cohesive soils (Jennings *et al.* 1973)

Term	Description	Unconfined compressive strength (kN/m2)
Very soft	Pick head can easily be pushed in up to shaft of handle, easily remoulded by fingers	< 35
Soft	Easily penetrated by thumb, sharp end of pick can be pushed in by 30 to 40 mm, moulded by fingers with some pressure	35 – 75
Firm	Indented by thumb with effort, sharp end of pick can be pushed in up to 10 mm	75 – 150
Stiff	Slight indentation with sharp end of pick; requires hand pick for excavation	150 – 300
Very stiff	Slight indentation produced by blow of pick point; requires power tools for excavation	> 300

Structure

The structure of soil refers to the presence or absence of cracks, fissures and other structures not associated with the soil matrix. Granular soils generally exhibit a granular microstructure while the term voided is used for soils with a loosely-packed open microstructure.

Cohesive soils may exhibit a variety of structures:

The term *intact* indicates the absence of macrostructures. If the soil is firm, it may exhibit tension cracks when cut with a geological pick.

The term *fissured* indicates the presence of closed joints. The fissure surfaces are often stained with iron and manganese oxides. In residual soils, the fissures may coincide with relict joints or they may represent planes in which tension or shear has taken place.

The term *slickensided* indicates fissures with highly polished and glossy surfaces that are often striated. This indicates fairly recent shearing in the soil, probably due to heaving conditions.

The term *shattered* indicates the presence of open joints. The fragments usually consist of stiff to very stiff cubical, elongated or granular shapes. Shattered soil is usually associated with shrinkage or heaving conditions.

The term *microshattered* indicates small-scale shattering. The fragments are usually sand-sized. The soil appears to be granular but when wetted and rubbed on the palm of the hand, it breaks down into silt and clay.

Terms such as *stratified*, *laminated*, *foliated* and *warved* are generally used when soil shows relict structures of the parent material; they indicate the origin of the residual soil.

Soil type

The soil type is described in terms of the proportions of the various soil fractions, i.e. gravel, sand, silt or clay. A smaller proportion of soil fractions attains an adjectival function when the main soil fraction type is described, e.g. soil consisting mainly of sand with secondary silt is described as silty sand. A very small proportion of soil fractions is also recorded, e.g. a sandy soil with very little silt is described as sand with silt. Soil with approximately equal parts of soil fractions is described as silt-clay. Sand and gravel fractions are further described as fine, medium or coarse. A well-graded soil with secondary silt and little gravel is therefore be described as silty fine, medium and coarse sand with gravel.

The shapes of gravel, cobbles and boulders are recorded and described as rounded, subrounded or angular. The composition of these fractions is also recorded. The packing of soils with large proportions of gravel or pedogenic material is recorded. These soils are described as, e.g. 'Densely packed, rounded and subrounded quartz, coarse gravel and cobbles in a matrix of silty medium and coarse sand' or 'Loosely packed nodular ferricrete in a matrix of silty fine and medium sand'. Following this convention, consistent descriptions of soil profiles are possible.

Origin

Engineering geologists distinguish between transported and residual soils. The origin of transported soils is described by the mode of transport, i.e. hillwash, fine or coarse colluvium, alluvium, lacustrine, aeolian or beach deposits. A pebble marker usually occurs at the base of transported soil. The origin of residual soils is described in terms of the parent rock. The name of the formation of the parent rock should be included.

Notes

Additional information regarding the general conditions of the soil profile is recorded at the end of the description under the heading; 'notes'. Information regarding seepage, reasons for refusal of the machine, and samples taken, are usually recorded. Whereas descriptions of soil layers may be confirmed by laboratory tests, the information contained in the notes section is in many cases the only indication of shallow or perched groundwater conditions. In the absence of borehole logging data, these notes are the

only indication of weathering depths. Both the laboratory tests and the notes may be important in the characterisation of the vadose zone.

3.5.2 Soil index tests

Particle-size distribution

Several tests have been developed to analyse index properties of soil. These values are compared with the index properties of other soils to enable a prediction of soil behaviour. Mechanical analyses determine the range of grain sizes in a particular soil. Sieve analyses are conducted on particles larger than 0.075 mm, while hydrometer analyses are conducted on particles smaller than 0.075 mm. The methodology of these procedures is described by Das (1990) and several other authors. The results of the mechanical analysis can be presented on semi-logarithmic plots and are known as grain-size distribution curves. Several properties can be derived from particle-size distribution curves. Well-graded soils have a wide range of grain sizes and the curves are therefore smooth and generally concave. Soils with a uniform grain size have a small range of grain sizes and the curves are therefore steep. Gap-graded or skip-graded soils have a deficiency of certain grain sizes that may be caused by leaching or lessivage. Some parameters used for geotechnical purposes are obtained from particle-size distribution curves.

The grading modulus is a function describing the shape of the particle-size distribution curve. It can be defined as follows:

$$Gm = \frac{P_{2.0} + P_{0.425} + P_{0.075}}{100} \qquad [7\text{-}1]$$

where P is the percentage the material retained on sieve sizes 2 mm, 0.425 mm and 0.075 mm respectively. Soils with a high fine fraction will in general have a grading modulus value of less than 0.8, while soils with a low fine fraction will have a grading modulus value of more than 1.0.

The effective size, D_{10}, corresponds to the sieve size, where 10 per cent of the mass of the soil sample have passed through; 10 per cent of all the grains of the sample therefore have diameters smaller than the effective size. Other sizes frequently used are D_{60} and D_{30}, where 60 per cent and 30 per cent of all grains have diameters smaller than D_{60} and D_{30}, respectively.

The coefficient of uniformity, C_u, is a crudely shape parameter, and is defined as:

$$C_u = \frac{D_{60}}{D_{10}} \qquad [7\text{-}2]$$

C_u values of 2 to 3 correspond to uniform soils, such as beach sand, while C_u values of more than 15 correspond with well-graded soils (Das, 1990).

The coefficient of curvature, C_c, another shape parameter, is defined by:

$$C_c = \frac{(D_{30})^2}{(D_{10}) \cdot (D_{60})} \qquad [7\text{-}4]$$

C_c values of between 1 and 3 correspond to well-graded soils, while C_c values are higher than 6 for uniform sands, and higher than 4 for uniform gravel (Das, 1990).

Atterberg limits

The presence of water in the pores of especially clayey soils will significantly change the geotechnical properties of a specific soil. Soil consistency changes as water content increases and can be grouped into four basic states: solid, semi-solid, plastic and liquid, with water content increasing from the solid to the liquid state.

The specific water contents where the nature of a soil changes (e.g. from solid to semisolid), are known as the Atterberg limits. The Shrinkage Limit (SL) refers to transition from a solid to a semisolid state. The Plastic Limit (PL) refers to transition from a semisolid to a plastic state and the Liquid Limit (LL) the transition from a plastic to a liquid state. The Plasticity Index (PI) is the difference in moisture content between the liquid and the plastic limit.

The activity value of soils can be used to predict the heaving potential of clayey soils. The activity of soils is defined as:

$$A = \frac{PI}{C} \qquad [7\text{-}4]$$

Soil classification systems

The main purpose of soil classification systems is to group together soil types with similar behaviour patterns. Soils are generally classified according to their grain size. Gravel, sand, silt and clay are the main fractions to be distinguished. **Table 3.6** shows the classification system that is generally used in South Africa (Geological Society Engineering Group Working Party Report, 1990).

Table 3.6: Classification according to grain size (Geological Society Engineering Group Working Party Report, 1990)

Grain size (mm)	Classification	Mineralogical composition
< 0.002	Clay	Secondary minerals (clay minerals and sesquioxides)
0.002 – 0.074	Silt	Primary and secondary minerals
0.074 – 0.2	Fine sand	Primary minerals (mainly quartz)
0.2 – 0.6	Medium sand	
0.6 – 2.5	Coarse sand	
2.5 – 12	Fine gravel	Rocks (sometimes vein quartz)
12 – 50	Medium gravel	
50 – 200	Coarse gravel	
200	Boulders	Rocks

Natural soil usually consists of a mixture of various grain-sizes. For this reason, soils are usually classified in terms of their proportions of gravel, sand, silt and clay.

The Unified Soil Classification System (USCS), depicted in **Table 3.8**, is the most widely used classification system for geotechnical purposes. The USCS is based on the premise that the behaviour of a coarse-grained soil depends largely on its grain size, while the behaviour of a fine-grained soil depends on its plasticity. The soil is classified in terms of the results of mechanical analyses, after the Atterberg limits have been determined.

Coarse-grained soils are subdivided into gravel (G) and sand (S). They are further subdivided according to their gradation (well-graded (W) and poorly graded (P)), as well as according to the proportion of fines in the sample. Fine-grained soils are subdivided into silts (M) and clays (C) based on their plasticity

properties, and not on grain size. **Figure 3.3** shows the plasticity values of a fine-grained sample that are plotted on the plasticity chart.

Silts plot below the A-line, while clays plot above this line. Fine-grained soils are further classified according to the value of their liquid limit. Organic soils (O) and peat (Pt) are visually identified.

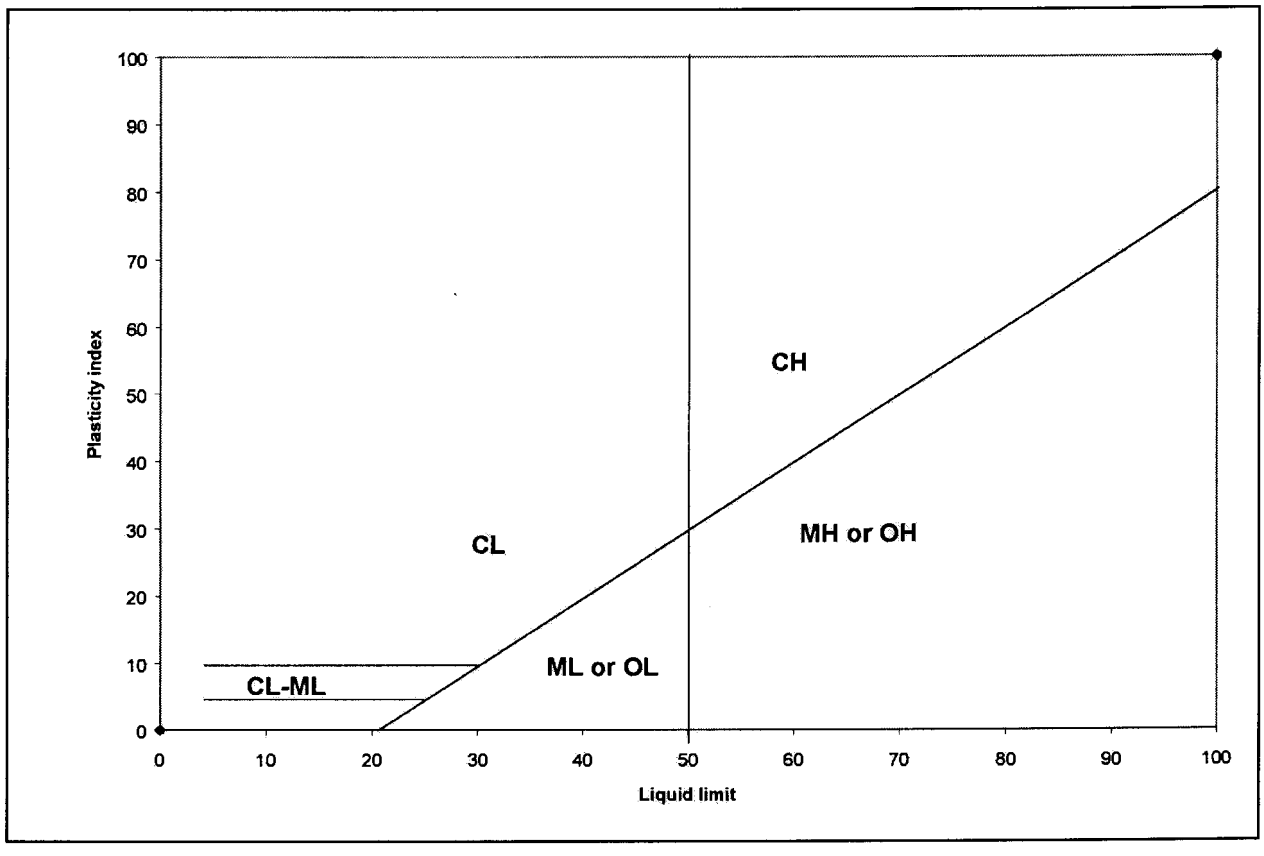

Figure 3.3: The plasticity chart

Table 3.8 contains a summary of the different USCS classes and indicates the criteria for distinguishing between the classes.

Another soil classification system frequently used is the AASHTO system. This system has been developed for use in the construction of roads and is also based on the grain size and plasticity of the soil. Holtz and Kovacs (1981) give a detailed description of the applicability of the AASHTO system in engineering work.

3.5.3 In situ permeability tests

In situ permeability tests provide the best means of obtaining the accurate hydraulic conductivity values of field soils and rock masses. Although laboratory permeability tests may provide accurate hydraulic conductivity values for compacted soils, they may not yield an accurate description of the geohydrological characteristics of field soils. Because of the small size of the laboratory sample and the spatial variability of geohydrological properties of field soils, they cannot be regarded as a representative. In addition, inaccurate measurements may result because of preferential flow along the sides of the 'undisturbed' samples. This is especially true for low-permeability soils.

Table 3.7: The Unified Soil Classification System (Holtz & Kovacs, 1981)

Major Division			Symbol	Description
Coarse-grained soil	Gravel	No fines	GW	Well-graded gravel, gravel-sand mixture, little fines
			GP	Poorly graded gravel, little fines
		With fines	GM	Silty gravel, gravel-sand-silt mixture
			GC	Clayey gravel, gravel-sand-clay mixture
	Sand	No fines	SW	Well-graded sand, gravelly sand with little fines
			SP	Poorly graded sand with little fines
		With fines	SM	Silty sand, sand-silt mixture
			SC	Clayey sand, sand-clay mixture
Fine-grained soil	Silt and clay LL<50		ML	Inorganic silt and very fine sand, silty or clayey fine sand, clayey silt with slight plasticity
			CL	Inorganic clay with low to medium plasticity, gravelly or sandy clay, lean clay
			OL	Organic silt or clay with low plasticity
	Silt and clay LL>50		MH	Inorganic silt, micaceous or diatomaceous fine sandy or silty soil, elastic silt
			CH	Inorganic clay with high plasticity, fat clay
			OH	Organic clay with medium to high plasticity, organic silt
			Pt	Peat, highly organic soils

Coarse-grained soil:	less than 50% of material passes through No. 200 (0.075mm) sieve size
Fine-grained soil:	more than 50% of material passes No. 200 (0.075mm) sieve size
Gravel:	more than 50% of coarse fraction larger than No. 4 (4.75mm) sieve size
Sand:	more than 50% of coarse fraction smaller than No.4 (4.75mm) sieve size
Less than 5% fines:	GW, GP, SW, SP
More than 12% fines:	GM, GC, SM, SW
Between 5 and 12% fines:	Dual symbols e.g. GW-GM
GW:	$Cu > 41 < Cc < 3$
SW:	$Cu > 61 < Cc < 3$
Fine-grained fraction:	Plot on plasticity chart
Silt:	Beneath A-line or $PI < 4$
Clay:	Above A-line or $PI > 7$
CL-ML:	Above A-line, $4 < PI < 7$

In situ permeability tests have the advantage that a large area of soil, and therefore a more representative sample, can be tested. The effect of preferential flow paths may be assessed. *In situ* permeability tests are not often conducted in geotechnical investigations and data are seldom available. Several methods are available to determine the hydraulic conductivity *in situ*. Daniel (1989) identifies four categories of in situ permeability tests, namely:

- Borehole tests
- Porous probe tests
- Infiltrometers
- Underdrains

He compares nine different in situ permeability tests. The methodologies are described by Daniel (1989). His findings are summarised in **Table 3.8**. The methodology for conducting slug tests is described in a number of geohydrological textbooks such as Fetter (1994).

Table 3.8: In situ permeability tests

Type	Device	Equipment cost	Duration	Direction	Accuracy
Borehole	Slug test	Low	Hours	Horizontal	Medium
	Packer tests	High	Hours	Horizontal	Medium
	Boutwell permaemeter	Low	Days to weeks	Vertical Horizontal	Medium
	Constant head permaemeter	Low	Hours to days	Horizontal	High to Medium
Porous probe	BAT permaemeter	High	Minutes to hours	Horizontal	Medium
Infil-trometer	Open, single- ring	Low	Weeks to months	Vertical	Medium
	Open double-ring	Low	Days to months	Vertical	High
	Closed, single-ring	Low	Weeks to months	Vertical	Medium
	Sealed double-ring	Medium	Weeks to months	Vertical	Very high
	Air-entry	Medium	Hours to days	Vertical	Medium
Under-drain	Lysimeter pan	Low	Weeks to months	Vertical	High

3.6 Availability of geotechnical data

The success with which geotechnical data can be applied to estimate hydrogeological properties depends on the availability and reliability of the geotechnical data. Geotechnical data must be available over large parts of the country and have to be easily accessible to be of use in future hydrogeological studies. In addition, geotechnical data must be available at a reasonable cost.

Standard geotechnical techniques and tests such as soil profile descriptions and soil index tests are conducted during almost every geotechnical investigation. These investigation methods are applied *inter alia* for residential development and may cover large areas. In contrast, the more sophisticated triaxial and double odoemeter tests are only conducted during the design stages of specific structures and therefore represent small site-specific areas. Some types of geotechnical data are more accessible than others. The reliability of estimating geohydrological properties from geotechnical data, depends on the type and quality of the geotechnical data

The availability of geotechnical data, especially data from investigations for residential development, has been researched and published by Milford (1994). Much of the following discussion is based on his information.

Geotechnical data are available at various organisations, which include:

- The Council for Geoscience
- CSIR (Transportek Division)
- Local authorities, regional and metropolitan councils

- Provincial administrations
- Department of Transport
- Private sector

The Council for Geoscience

Over the years, the Council has accumulated substantial amounts of geotechnical data that cover large parts of mainly urban areas in South Africa. The data are presented in different formats, but mostly as engineering geology maps with accompanying reports. Raw data such as soil profile plots and laboratory tests results are included, usually as appendices. All geotechnical reports conducted by the Council are available to the public.

The Council for Geoscience has initiated a digital geotechnical database, ENGEODE, whereby geotechnical data sources are indexed and all soil profiles, together with laboratory test results, are digitally captured (Du Plessis, 1998). This database was set up because of the need for geotechnical data experienced by engineering geologists and other persons operating in the civil engineering field

By March 1998, ENGEODE contained an index of approximately 85 000 soil profiles, mainly reports on housing developments (Croukamp, 1998). Approximately 80 per cent of these soil profiles are from Gauteng. The soil profile descriptions are available in both digital and paper format. Results of laboratory tests (mainly particle-size distribution curves, Unified Soil Classification and Atterberg limits) are usually included with the soil profiles. Very few permeability test results are available, but estimations of saturated hydraulic conductivity values according to the Hazen equation (see Chapter 9) are included. Data on ENGEODE are stored on Oracle databases. Data can be made available on ASCII format and on third party software (notably dot.PLOT) to provide the graphical representation of soil profiles.

The Council of Geoscience has access and control over large quantities of geotechnical data. Unfortunately, these data cover mainly urban areas of South Africa. Geotechnical data are readily available, but there is a cost attached.

CSIR – Transportek

Significant geotechnical data sets are currently in the possession of the Transportek Division of the CSIR. The CSIR has been undertaking the engineering geology mapping of central Gauteng, with emphasis on the dolomite girdle, on a scale of 1:10 000. The mapping is based on the land system and land facet approach. The CSIR has established a GIS database, based on land facet parameters. The database includes generalised soil profiles for each facet, as well as approximately 1 200 additional soil profile descriptions. Most profile descriptions include laboratory results, mainly particle-size distribution curves, Atterberg limits and Unified Soil Classifications. All soil profile descriptions are spatially referenced and many of these can be displayed on and questioned by means of GIS software. Very few permeability studies have been carried out by the CSIR. Estimations of permeability of soil are made by means of tables relating Unified Soil Classification symbols to saturated hydraulic conductivity.

In addition, the CSIR is in possession of data, mainly engineering geology maps indicating construction materials for road construction purposes. These data have previously been collected and maintained by the Department of Transport but this database was closed down in the mid-1980's.

Local authorities, regional and metropolitan councils

Geotechnical data, mainly information regarding geotechnical suitability for residential development, are available from several local authorities and from regional and metropolitan councils. The Greater Johannesburg Metropolitan Council, East Rand Metropolitan Council and the Johannesburg City Council maintain the most extensive geotechnical data sets.

Geotechnical information at the Greater Johannesburg Metropolitan Council comprises several spatial layers comprising speciality geotechnical maps such a dolomite stability map, a landform map and a land use potential/land allocation map.

At least two data sets maintained at the East Rand Metropolitan Council are relevant to this study, namely geotechnical suitability maps for residential development and an undermined land study comprising maps (1:10 000 and 1:5 000) indicating areas of shallow undermining.

The Johannesburg City Council Geotechnical Data Bank contains approximately 2 000 geotechnical reports of varying detail. These cover the greater Johannesburg area. Many reports include soil profiles and laboratory tests. The data are indexed on a cover sheet as well as on a bibliographical reference list. The data bank does not contain digital data. The data are available to the public at minimal reproduction costs.

The Durban Metropolitan Council does not maintain any geotechnical data sets. However, it does have 1:15 000 geological maps, covering the Durban - Westville area. These maps are available from the Surveying Department.

The Cape Town Metropolitan Council also does not maintain any geotechnical data.

Private sector

The private sector has over the years, accumulated substantial quantities of geotechnical data. The private sector (with the exception of mining houses whose data are typical propriety information) is mostly willing to make their information available to other organisations. Copies of all geotechnical investigations are usually indexed and can be accessed by means of the project name, number and location. Although the geotechnical investigations have been conducted in accordance with clients' needs, general geotechnical data, such as soil profile descriptions and index test results, are usually included in the appendices. In addition, the general geological and geotechnical conditions of the specific investigation area are discussed in the report. The investigation areas have usually already been developed by the time the report is accessed, but estimates on the geotechnical characteristics in similar adjacent areas can be made by extrapolation.

3.6.1 Information from other data sources

The assessment of the geotechnical and geohydrological conditions of a specific area requires a thorough understanding of the general conditions of that area. Information on the topography, geology, hydrology, climatology, land use and existing infrastructure has to be available. Many institutions can assist in supplying the relevant information.

A large variety of data collected during geotechnical and hydrogeological investigations that may be used in estimating hydrogeological properties, are available from a number of institutions. These are listed in Table 8.1.

Government Printing Works

A series of topographical sheets on various scales covering the whole of South Africa can be obtained from the Government Printing Works. These include the 1:50 000, 1: 250 000 and 1:500 000 topographical maps and a range of other less relevant maps.

Surveyor-General

A series of aerial photos of various scales covering the whole of South Africa can be obtained from the Surveyor-General. In addition, 1: 10 000 scale othophoto maps, covering most parts of South Africa can also be obtained.

The Council for Geoscience

A 1:1 000 000 regional geological series is available in paper and digital (either CAD or ArcView/ArcInfo) formats. Twenty-seven sheets of the 1:250 000 regional geological series are available in paper format and are in the process of being captured in digital form. An accompanying information booklet on the geology of the specific map can also be obtained. Several 1:50 000 geological sheets of selected areas (mainly the central Witwatersrand area) are in the process of being captured in digital format.

Weather Bureau

There are weather stations at many towns and cities around the country. Meteorological data are recorded, including average monthly minimum and maximum temperatures, average monthly evaporation, average monthly rainfall and cloud cover. The climate statistics are available from the Weather Bureau at minimal cost.

Department of Water Affairs and Forestry (DWAF)

The Directorate of Geohydrology of the DWAF is responsible for maintaining the National Groundwater Database (NGDB). General information regarding boreholes such as their location, longitude and latitude is recorded. Groundwater data such as the depth to groundwater level, groundwater level fluctuations, borehole yield and depth of water strike are also on record. Data can be accessed by co-ordinates and are available free of charge. Digital data can be made available in popular formats such as dBase, Excel, Quattro Pro and Access.

Institute for Soil, Climate and Water (ISCW)

Three data sets of interest are maintained:

- A national land type database
- A national soil profile database
- A soil mapping database

The ISCW land type database consists of land type units surveyed and presented on maps at a scale of 1:250 000. It represents areas with a high degree of uniformity with regard to terrain form, soil pattern and climate (Milford, 1994). It covers 80 per cent of the country. Gaps occur mainly in the Eastern Cape and in the winter rainfall regions.

The soil profiles are classified according to the South African Binomial or Taxonomic Soil Classification Systems. The relevant soil profiles typically extend to a depth of about 1.2 m.

Agricultural soil mapping at a scale of 1:50 000 is available in digital form for the Gauteng area.

ISCW soil profile descriptions and soil classification systems are different from geotechnical descriptions and extend only to 1.2 m in depth, probably describing mostly transported soil, which further limit the geotechnical use of the data.

Soil-water retention data can be used to establish soil-water characteristic curves for different soils, which can assist with the estimated unsaturated geohydrological properties. However, such data are very scarce.

The ISCW frequently uses the Soil Texture Chart to classify soil according to the sand, silt and clay proportions. It is used to differentiate between the different agricultural soils.

Local authorities

Maps indicating the layout of towns and cities are available from most local authorities.

Educational and research institutions

Data on water retention characteristics can be obtained from a number of educational and research institutions which have conducted research in this regard. The University of Natal, University of Fort Hare and the Soil and Irrigation Research Institute have water retention data from research conducted in many parts of the country (Hutson, 1984).

Available geotechnical data and sources are summarised in **Table 3.9** while **Table 3.10** contains information on other data sources.

Table 3.9: Availability of geotechnical and other relevant information (Modified from Keyter; 1994)

Source	Information	Coverage	Format	Accessibility
Council for Geoscience	Engineering geology	Central Wits	Digital	Interpreted information
	Residential development reports	All provinces with the exception of Western, Northern and Eastern Cape	Paper & digital	Interpreted information and soil profiles with lab tests
	ENGEODE	Mainly Gauteng and Port Elizabeth	Paper & digital 60 000 soil profiles 25 000 digital	R40 per soil profile some with lab tests
	Dolomite stability	Central Gauteng	Digital	Interpreted information
CSIR (TRANS-PORTEK)	Engineering geology Problem soils Development suitability	Central Gauteng	Digital	Yes
	Soils database	Central Gauteng	GIS: 1 200 soil profiles	Yes
Gauteng Province	TPA Engineering soils	Gauteng	Digital	Unknown
Greater Johannesburg Metropolitan Council	Geology 1:50 000 Construction materials Landform Dolomite stability Problem soils Land use potential Undermined land	Central Witwatersrand area	Digital	Unknown
East Rand Metropolitan Council	Development suitability Undermined land	East Rand	Digital	
Johannesburg City Council	Geotechnical database	Greater Johannesburg	Paper	Reproduction cost
Department of Transport	Soils engineering maps	Gauteng	Paper	At CSIR

Table 3.10: Other available relevant information

Source	Information	Coverage	Format	Accessibility
General soil data				
ISCW	Land type maps	80% of South Africa	Paper & digital	Interpreted information
	Soil profile database	80% of RSA 200 000 profiles	Paper	Interpreted information
	Soil types	Gauteng 6000 profiles	Paper & digital	Interpreted information
Educational and research institutions	Soil-water retention data	Selected parts in South Africa	Paper	On request
General data				
Government Printing Works	Topographical sheets 1:50 000 1:250 000 1:500 000	Whole of South Africa	Paper	Moderate costs
Surveyor-General	Aerial photos Various scales	Whole of South Africa	Paper & film	Moderate costs
	Orthophotos 1:10 000	Most of South Africa	Paper	Moderate costs
Local authorities	Town layout plans	Most of South African towns	Paper	Most towns free or at reproduction cost
Council for Geoscience	Geology 1:1000 000	100% of RSA	Paper & digital	Moderate costs
	Geology 1:250 000	74% of RSA	Paper	Moderate costs
	Geology 1: 50 000	Gauteng	Paper	Moderate costs
Weather Bureau	Climate statistics	Whole of South Africa	Booklet	Minimal costs
Department of Water Affairs and Forestry	Groundwater data	Whole of South Africa	Digital	Free

CHAPTER 4

RELATIONSHIPS BETWEEN GEOTECHNICAL AND HYDROGEOLOGICAL PROPERTIES

4.1 Estimations of porosity

Porosity data are not collected as frequently as other geotechnical data such as indicator tests. Porosity is an important parameter in the estimation of both saturated and unsaturated hydraulic conductivity. In addition, the soil-water retention characteristics are highly sensitive to porosity. It may be necessary to estimate porosity from other geotechnical data such as soil profile descriptions and particle-size distribution curves. In field soils the porosity depends on a number of factors, the most important being particle-size distribution, bulk density, shape of the grains and mineralogical content.

In coarse-grained soils, soil profile descriptions may provide an indication of the density of the soil. The porosity and void ratio can be calculated if the dry density value is known. However, soil consistency is determined in a very subjective manner, often resulting in inaccurate estimations of primary porosity.

Table 4.1: Typical dry density, porosity and void ratio values for granular soils (Modified from Jennings *et al.*; 1973)

Description	Typical dry density (kg/m3)	Typical porosity	Typical void ratio
		(Specific weight of grains = 2.65)	
Very loose	< 1450	> 0.45	> 0.83
Loose	1450 – 1600	0.45 – 0.40	0.83 – 0.66
Medium dense	1600 – 1750	0.40 – 0.34	0.66 – 0.51
Dense	1750 – 1925	0.34 – 0.27	0.51 – 0.38
Very dense	> 1925	< 0.27	< 0.38

In fine-grained soils, soil consistency is a rough indication of the shear strength of the soil. The shear strength is strongly influenced by moisture content and density. The relationship between soil density and consistency is not reliable and the moisture content has to be considered in order to interpret the soil consistency. Dry, fine-grained soils have a much higher apparent shear strength than wet, fine-grained soils.

Table 4.2: Typical dry density, porosity and void ratio values for cohesive soils (Modified from Mathewson, 1981)

Description	Typical dry density (kg/m3)	Typical porosity (SG of grains = 2.7)	Typical void ratio (SG of grains = 2.7)
Very soft	< 1000	> 0.62	> 1.65
Soft to firm	1000 – 1700	0.36 – 0.62	0.56 – 1.65
Stiff	1700 – 1800	0.32 – 0.36	0.47 – 0.56
Very stiff	> 1800	< 0.32	< 0.47

In the case of an ideal soil consisting of spherically shaped grains of equal diameter, the porosity will be a factor only of the packing of the grains. Porosity values may vary between a maximum of 0.476, in the case of unstable packing to 0.260 in the case of fully compact packing (Davis & De Wiest, 1966). In the case of grains consisting of plate-like structures of identical size, porosity may vary from 0.60 for a box-like structure to 0.00 for ideally stacked plates (Davis & De Wiest, 1966). However, grains in field soils are neither ideally spherical nor plate-like and considerations involving these ideal shapes cannot be directly applied to field soils. The grain shape has a significant effect on porosity, since angular grains may create vault-like structures in the soil, resulting in a 2 to 5 per cent higher porosity value than expected. These vault-like structures may have an even more significant effect on saturated water flow through the soil. The Poiseuille equation indicates that the rate of flow through narrow tubes is very sensitive to the radius of the tubes and therefore also to the radius of pores.

Grain-size distribution has a major effect on porosity, since smaller grains tend to be situated within large pores. The grain-size distribution can be expressed by the coefficient of uniformity. Laboratory results conducted by Hazen (1930) show a definite correlation between porosity and the coefficient of uniformity, as indicated in **Table 4.3**.

Table 4.3: Coefficient of uniformity and corresponding porosity values (presented by Vukovic & Soro, 1992)

C_u	1.8	2.0	2.3	2.3	2.4	7.8	9.0
ε	0.45	0.42	0.44	0.42	0.40	0.32	0.36

Research by Istomina (1957) shows that porosity can be approximated from the coefficient of uniformity by means of the following equation:

$$\varepsilon = 0.255\left(1 + 0.83^{C_u}\right) \qquad [4\text{-}1]$$

However, Istomina has found that significant deviations occur in soils comprising high clay percentages. Equation 4-1 can therefore not be applied if a high percentage of clay is present in the soil.

With the development of the ACRU agrohydrological modelling system, Schulze (1995) indicated that a number of soil properties, including porosity, could be estimated from soil texture classes. These statistically determined relationships have been developed by a number of authors (Rawls; Brakensiek & Saxton, 1982; Schulze George & Angus, 1987; Buitendag, 1990; Everett, 1990). The porosity value range for the twelve agricultural soil types is indicated in **Table 4.4**.

Table 4.4: Estimated porosity values for twelve agricultural soil types (from Schulze 1995)

Soil type	Bulk density (kg/m^3)	Total porosity
Clay	1 220 – 1 370	0.470 – 0.482
Clay loam	1 220 – 1 410	0.474 – 0.456
Loam	1 260 – 1 420	0.512 – 0.480
Loamy sand	1 310 – 1 510	0.452 – 0.477
Silt	N.A.	N.A.
Silt loam	1 130 – 1 340	0.530 – 0.500
Silty clay	1 230 – 1 380	0.476 – 0.480
Silty clay loam	1 250 – 1 400	0.489 – 0.473
Sand	1 320 – 1 500	0.446 – 0.440
Sandy clay	1 350 – 1 530	0.393 – 0.428
Sandy clay loam	1 350 – 1 580	0.435 – 0.405
Sandy loam	1 260 – 1 460	0.486 – 0.466

4.2 Estimations of saturated hydraulic conductivity

Various authors have tried to relate the saturated hydraulic conductivity to descriptions of soil type (Das, 1990; Mathewson, 1981) and these relationships are presented in **Table 4.5**. Since hydraulic conductivity is not entirely dependent on soil type, the predicted saturated hydraulic conductivities are not very accurate. In addition, the percentages of clay fractions present in the profile greatly affect saturated hydraulic conductivity. For example, two soils consisting of sand with clay contents of 10 per cent and 30 per cent respectively can both be described as clayey sand. However, the soil with 30 per cent clay may have a saturated hydraulic conductivity of a few orders of magnitude lower than the soil with 10 per cent clay. In addition, soil types are described subjectively. Saturated hydraulic conductivity values derived from soil-type descriptions may not be very reliable. However, in the absence of more reliable data, saturated hydraulic conductivity values of reasonable reliability can be obtained.

Table 4.5: Estimated hydraulic conductivity values from soil type (modified from Mathewson, 1981)

Soil type	Saturated hydraulic conductivity (m/s)
Gravel	$10^{-1} – 10^{-4}$
Gravel (Well-sorted)	$10^{-1} – 10^{-3}$
Gravel (Poorly sorted)	$10^{-1} – 10^{-4}$
Silty gravel	$10^{-5} – 10^{-8}$
Clayey gravel	$10^{-6} – 10^{-9}$
Sand	$10^{-3} – 10^{-7}$
Coarse sand (Well-sorted)	$10^{-3} – 10^{-5}$
Coarse sand (Poorly sorted)	$10^{-3} – 10^{-5}$
Medium sand (Well-sorted)	$10^{-4} – 10^{-6}$
Medium sand (Poorly sorted)	$10^{-3} – 10^{-5}$
Fine sand (Well-sorted)	$10^{-5} – 10^{-7}$
Fine sand (Poorly sorted)	$10^{-4} – 10^{-6}$
Silty sand	$10^{-6} – 10^{-8}$
Clayey sand	$10^{-7} – 10^{-9}$
Silt	$10^{-6} – 10^{-9}$
Clay (Low plasticity)	$10^{-8} – 10^{-10}$
Clay (High plasticity)	$10^{-9} – 10^{-11}$

A number of authors have attempted to relate saturated hydraulic conductivity to USCS soil groups (Mathewson, 1981; Badenhorst, 1988) and these are summarised in **Table 4.6**.

Table 4.6: Estimation of hydraulic conductivity from USCS soil groups (modified from Mathewson, 1981 and Badenhorst, 1988)

USCS soil Groups	Hydraulic conductivity (m/s)	
	Mathewson	Badenhorst
GP	$10^{-5} - 10^{-2}$	$10^{-5} - 10^{-1}$
GW	$10^{-4} - 10^{-2}$	$10^{-5} - 10^{-3}$
GM	$10^{-8} - 10^{-5}$	$10^{-9} - 10^{-6}$
GC	$10^{-9} - 10^{-6}$	$10^{-10} - 10^{-7}$
SP	$10^{-6} - 10^{-3}$	$10^{-6} - 10^{-3}$
SW	$10^{-7} - 10^{-3}$	$10^{-5} - 10^{-3}$
SM	$10^{-8} - 10^{-6}$	$10^{-9} - 10^{-5}$
SC	$10^{-9} - 10^{-7}$	$10^{-10} - 10^{-6}$
ML	$10^{-9} - 10^{-6}$	$10^{-10} - 10^{-6}$
MH	$10^{-9} - 10^{-7}$	$10^{-11} - 10^{-9}$
CL	$10^{-10} - 10^{-8}$	$10^{-10} - 10^{-8}$
CH	$10^{-11} - 10^{-9}$	$10^{-13} - 10^{-6}$

Although soil classification using the USCS system is much more objective as a means of obtaining geotechnical properties, it does not necessarily follow that precise estimations of hydraulic conductivity can be obtained. Estimated hydraulic conductivities from systematically described soil profiles may be more accurate and precise than estimations from USCS soil groups because of the large variations in hydrogeological properties within many USCS soil groups. The USCS has been developed for engineering purposes and is less applicable to hydrogeological situations.

Carsel and Parrish (1988) conducted normal distribution and joint probability distribution tests for saturated hydraulic conductivity and other hydrogeological properties. These were based on the regression equation developed by Rawls, Brankensiek & Saxton (1982) (Equation 4-7). Joint probability distributions can be used to produce a multivariate normal distribution model for Monte Carlo modelling and other simulation studies. Estimations of the saturated hydraulic conductivity for 12 agricultural texture classes, as determined by Carsel and Parrish (1988) by means of Equation 4-7, are indicated in **Table 4.7.**

Table 4.7: Estimated saturated hydraulic conductivity for twelve agricultural soil types (modified from Carsel & Parrish, 1988 and Schulze, 1995)

Soil type	Estimated saturated hydraulic conductivity (m/s)	
	Carsel & Parrish	Schulze
Clay	5.56×10^{-7}	1.67×10^{-7}
Clay loam	7.22×10^{-7}	6.38×10^{-7}
Loam	2.89×10^{-6}	3.61×10^{-6}
Loamy sand	4.05×10^{-5}	1.69×10^{-5}
Silt	6.94×10^{-7}	N.A.
Silt loam	1.25×10^{-6}	1.89×10^{-6}
Silty clay	5.56×10^{-8}	2.50×10^{-7}
Silty clay loam	1.94×10^{-7}	4.17×10^{-7}
Sand	8.25×10^{-5}	5.83×10^{-5}
Sandy clay	3.33×10^{-7}	3.33×10^{-7}
Sandy clay loam	3.64×10^{-6}	1.19×10^{-6}
Sandy loam	1.23×10^{-5}	7.22×10^{-6}

With the development of the ACRU agrohydrological modelling system, Schulze (1995) has shown that the saturated hydraulic conductivity can be estimated from soil textural classes. Estimations of saturated hydraulic conductivity are also indicated in **Table 4.7**

4.2.1 Estimation of saturated hydraulic conductivity based on empirical relationships

Soil fractions (Soil texture)

In general, the following empirical equation is applicable to predict saturated hydraulic conductivity:

$$K_s = a \cdot f(S, M, C, \varepsilon) \qquad [4\text{-}2]$$

The parameter a is a constant and reflects factors with an effect on saturated hydraulic conductivity other than grain sizes, such as the shape of the grains and packing.

Many authors have related saturated hydraulic conductivity to physical soil properties based on fractions, sand, silt and clay and, in some cases, bulk density (Campbell, 1974; Campbell, 1985; Rawls *et al.*, 1982; Campbell & Shiozawa, 1992). These relationships are expressed as empirical models, many of which have been generated by multiple regression analysis. The more popular equations are the following:

The Campbell equation (1974) is widely used to predict saturated hydraulic conductivity:

$$K_s = a \exp(-6.9C - 3.7M) \qquad [4\text{-}3]$$

This equation is valid for a bulk density value of 1 300 kg/m^3, with grain sizes of 1.025, 0.026 and 0.001 mm for sand, silt and clay respectively.

After extensive research to relate physical soil properties to soil-water retention characteristics, Campbell (1985) points out the relationship between saturated hydraulic conductivity and bulk density, air-entry value and the geometric mean grain diameter. Based on this research, Campbell and Shiozawa (1992) suggested that saturated hydraulic conductivity could merely be expressed as a function of percentages of silt and clay and of the bulk density of the soil. The saturated hydraulic conductivity can be expressed as:

$$K_s = a\left(\frac{1.3}{\rho_b}\right)^{1.3b} \exp(-0.025 - 0.363M - 0.0688C) \qquad [4\text{-}4]$$

where

$$b = \exp(-0.025 - 0.0363M - 0.0688C)^{-0.5} + 0.2\exp\left(0.1332M + 0.47C - \ln^2[\exp(-0.025 - 0.0363M - 0.0688C)]\right)^{0.5} \qquad [4\text{-}5]$$

and a is a constant to be experimentally determined.

Campbell and Shiozawa (1992) also suggest a more simple equation as a means to derive saturated hydraulic conductivity:

$$K_s = 1.5 \times 10^{-5} \exp(-0.07M - 0.167C) \qquad [4\text{-}6]$$

Based on soil-water retention and saturated hydraulic conductivity data collected by Luxmoore and

Sharma (1980), Rawls, Ahuja and Brakensiek (1992) developed the following regression model to predict saturated hydraulic conductivity.

$$K_s = 2.7778\times10^{-6}\exp(19.523\varepsilon - 8.968 - 0.028C + 0.0002S^2 - 0.009C^2 - 8.395\varepsilon^2 + 0.078S\varepsilon - 0.003S^2\varepsilon^2 - 0.019C^2\varepsilon^2 + 0.00002S^2C + 0.027C^2\varepsilon + 0.001S^2\varepsilon - 0.000004C^2S) \quad [4\text{-}7]$$

where the fractions sand and clay and porosity are expressed as percentages. Equation 4-7 has been validated for soils with clay contents ranging from 5 to 60 per cent, sands contents ranging from 5 to 70 per cent and all porosity values representative of field soils.

Particle-size distribution: Coarse grained soils

It has been shown in Chapter 2 that the permeability or intrinsic hydraulic conductivity for water flowing through a narrow tube can be expressed in terms of Poiseuille's law:

$$k = 0.125 \cdot R^2 \quad [4\text{-}8]$$

In the case of fluids flowing through a porous medium, the effective pore diameter, R_e, can be related to the effective grain diameter, d_e, by means of the following equation (Vukovic & Soro, 1992):

$$R_e = c\, f(\varepsilon)\, d_e \quad [4\text{-}9]$$

The parameter, c, is a dimensionless constant depending on a number of porous medium properties (e.g. structure and grain shape), $f(\varepsilon)$ is the function defining the relationship between modelled and actual porous media and d_e is the effective grain diameter related to the tube diameter. Large volumes of the porous media consist of solids through which fluids will not be able to flow. The permeability can be expressed as:

$$k = 0.125\left(c\, f(\varepsilon) d_e\right)^2 \varepsilon \quad [4\text{-}10]$$

The intrinsic hydraulic conductivity is a function of the physical properties of the porous medium. However, Equation 4-10 does not address the effect of the retention forces of the porous media or the physiochemical properties of liquid and porous media. These aspects may significantly influence the hydraulic conductivity in fine-grained soils. However, for homogeneous coarse-grained soils, these aspects may be neglected.

By redefining the constant, c, and the function, $f(\varepsilon)$, Equation 4-10 can be expressed as:

$$k = c_1\, g(\varepsilon) d_e^{\,2} \quad [4\text{-}11]$$

where

$$c_1 = 0.125 \cdot c^2 \quad [4\text{-}12]$$

and

$$g(\varepsilon) = \varepsilon \cdot (f(\varepsilon))^2 \quad [4\text{-}13]$$

Saturated hydraulic conductivity can be expressed as

$$K_s = c_1 \cdot g(\varepsilon) \cdot d_e^{\,2} \frac{\rho g}{\eta} \qquad [4\text{-}14]$$

The effective grain diameter represents the diameter of the grain corresponding to the effective pore diameter in the Poiseuille equation. The effective pore diameter has a significant effect on the saturated hydraulic conductivity of soils. Many researchers have regarded the grain diameter of the smaller part of the soil fraction as the effective pore diameter. Since smaller grains tend to be situated within larger pores, this assumption could be justified. In the case of significant silt and clay contents, saturated hydraulic conductivity will mainly be governed by the fine material fraction.

Saturated hydraulic conductivity varies to a large extent with change in porosity. Vukovic and Soro (1992) show that in the case of sand, saturated hydraulic conductivity may increase by a factor of about 3 for a porosity value increase from 30 to 40 per cent. Since temperature does affect fluid, viscosity, it also has an effect on saturated hydraulic conductivity. In the case of water, the hydraulic conductivity may increase by three per cent for every one degree Celsius increase in temperature (Vukovic & Soro, 1992).

Fluidity, as discussed in Chapter 2, represents the properties of the fluid that effect flow through soil pores. The most important factors with an effect on fluidity are fluid density and viscosity. The viscosity is a function of temperature. The fluidity at 20°C has a value of:

$$f = \frac{\rho_w g}{\eta_{w\,20°C}} = 975124\, m^{-1} s^{-1} \qquad [4\text{-}15]$$

The dimensionless constant, c_1, represents all factors not addressed, the most important probably the shape of the grains. Empirical models frequently assume grains to be spherical and differences in the shape of the grains may have an effect on saturated hydraulic conductivity.

The equation does not consider the effect of electrochemical forces. These forces may have a significant effect on clayey soils. However, in the case of sandy soils with little or no fines, electrochemical forces may be negligible.

Adsorption forces may have a significant effect on saturated hydraulic conductivity, especially if large silt and clay fractions are present. Only the Kozeny-Carman and Zamarin equations take the effect of adsorption into account, by including the specific surface of the soils. Since the saturated hydraulic conductivity basically represents friction forces between water and soil grains, specific surfaces may be a more representative parameter for estimating saturated hydraulic conductivity.

Fourteen frequently used empirical equations were analysed by Vukovic and Soro (1992). The equations have been expressed in the format of Equation 4-14. Predicted hydraulic conductivity was compared to measured hydraulic conductivity and the reliability of the equations was quantified. All fourteen equations discussed can be expressed in the general empirical equation as expressed by Equation 4-14 and are summarised in **Table 4.8**. Detailed descriptions of the fourteen empirical equations are discussed by Vukovic and Soro, (1992) and van Schalkwyk and Vermaak (1999)

Table 4.8: Empirical equations expressed in terms of the general empirical equation (Vukovic & Soro, 1992)

	Author	Coefficient, c_1	Function of porosity, $g(\varepsilon)$	Effective grain diameter, D_e
1	Hazen (1930)	4.717×10^{-9}	$4.6\times10^{-2}(\varepsilon-0.2$	d_{10}
2	Amer & Awad (1974)	$3.63\times10^{-8}\,C_u^{\,0.6}\,d_{10}^{\,0.32}$	$\frac{\varepsilon^3}{(1-\varepsilon)^2}$	d_{10}
3	Shahabi, Das & Tarquin. (1984)	$1.23\times10^{-6}\,C_u^{\,0.735}\,d_{10}^{\,-0.11}$	$\frac{\varepsilon^3}{(1-\varepsilon)^2}$	d_{10}
4	Kenney, Lau & Ofoegbu. (1984)	5.128×10^{-8} *to* 1.026×10^{-6}	1	d_5
5	Slichter (Vukovic & Soro, 1992)	1.038×10^{-7}	$\varepsilon^{3.287}$	d_{10}
6	Terzaghi (Vukovic & Soro, 1992)	2.082×10^{-2} *to* 8.204×10^{-2}	$\left[\frac{\varepsilon-0.13}{\sqrt[3]{1-\varepsilon}}\right]^2$	d_{10}
7	Beyer (Vukovic & Soro, 1992)	$4.615\times10^{-9}\log\frac{500}{C_u}$	1	d_{10}
8	Sauerbrei (Vukovic & Soro, 1992)	3.579×10^{-8}	$\frac{\varepsilon^3}{(1-\varepsilon)^2}$	d_{17}
9	Pavchich (Pravednyi, 1966)	$3.579\times10^{-8}\,C_u^{\,0.333}$	$\frac{\varepsilon^3}{(1-\varepsilon)^2}$	d_{17}
10	USBR (Vukovic & Soro, 1992)	$4.923\times10^{-10}\,d_{20}^{\,0.3}$	1	d_{20}
11	Krüger (Vukovic & Soro, 1992)	5.076×10^{-9}	$\frac{\varepsilon}{(1-\varepsilon)^2}$	$\frac{1}{\sum_{i=1}^{i=n}\frac{2\Delta w_i}{d_i^{\max}+d_i^{\min}}}$
12	Kozeny (Vukovic & Soro, 1992)	6.409×10^{-8}	$\frac{\varepsilon^3}{(1-\varepsilon)^2}$	$\frac{1}{\frac{3\Delta w_1}{2d_1}+\sum_{i=2}^{i=n}\frac{\Delta w_i\left(d_i^{\max}+d_i^{\min}\right)}{2d_i^{\max}d_i^{\min}}}$
13	Zunker (Vukovic & Soro, 1992)	1.377×10^{-8} *to* 4.041×10^{-9}	$\frac{\varepsilon}{1-\varepsilon}$	$\frac{1}{\frac{3\Delta w_1}{2d_1}+\sum_{i=2}^{i=n}\frac{\Delta w_i\left(d_i^{\max}-d_i^{\min}\right)}{d_i^{\max}d_i^{\min}\ln\frac{d_i^{\max}}{d_i^{\min}}}}$
14	Zamarin (Vukovic & Soro, 1992)	8.276×10^{-8}	$\frac{\varepsilon^3}{(1-\varepsilon)^2}$	$\frac{1}{\frac{3\Delta w_1}{2d_1}+\sum_{i=2}^{i=n}\frac{\Delta w_i\left(\ln\frac{d_i^{\max}}{d_i^{\min}}\right)}{d_i^{\max}-d_i^{\min}}}$

Skabalanovich (1961) investigated the reliability of the Hazen (1930), Slichter, Sauerbrei, Kruger, Zunker and Zamarin (Vukovic & Soro, 1992) equations in relation to a sandy aquifer. Saturated hydraulic conductivity values were derived from pumping test evaluations and these were compared to the

predicted saturated hydraulic conductivity for the above-mentioned equations. He found that all equations consistently predicted, on average, lower hydraulic conductivity values than were derived from the pumping tests.

Skabalanovich (1961) showed that in 80 per cent of the cases, calculated hydraulic conductivity values were two times higher or lower than the actual saturated hydraulic conductivity of the water-bearing strata. The Sauerbrei (Vukovic & Soro, 1992) equation yielded the most reliable estimation of saturated hydraulic conductivity, but about 60 per cent of the relevant calculations showed significant deviation. Skabalanovich (1961) concluded that the equations under investigation may not yield reliable estimations of saturated hydraulic conductivity and recommended that the equations should not be used for the site-specific estimation of saturated hydraulic conductivity.

Particle-size distribution, clay fraction and Atterberg limits: Fine-grained soil

Research in deriving empirical equations for saturated hydraulic conductivity in coarse-grained soil is relatively well-established, due largely to numerous investigations into sandy aquifers. In the case of clayey soils, researchers tend to calculate saturated hydraulic conductivity on the basis of permeability tests and research tends to focus in obtaining representative measured values of saturated hydraulic conductivity for use in clay liners and other engineering structures. Little research has been done on deriving saturated hydraulic conductivity from empirical equations. In addition, it is much more difficult to obtain empirical expressions for estimating saturated hydraulic conductivity in clays than in coarse-grained soils (Tavenas, LeBlond, Jean & Leroueil, 1983b).

Taylor (1948) has shown that general equations, which are valid for coarse-grained soils, are not valid for clayey soils. Samarasinghe, Huang and Drnevich (1982) suggest the following empirical equation:

$$K_s = c\frac{e^b}{e+1} \qquad [4\text{-}16]$$

where b and c are experimentally determined constants. Equation 4-16 is applicable to normally consolidated clays, with the value of b typically between 4 and 5 and c a constant indicating soil characteristics. Taylor suggested an empirical linear relationship between the logarithm of saturated hydraulic conductivity and the void ratio:

$$\lg(K_s) = \lg(K_0)\frac{e_0 - e}{C_k} \qquad [4\text{-}17]$$

where C_k is the permeability change index and K_o and e_o respectively are the *in situ* hydraulic conductivity and void ratio values. This equation can be used in consolidation studies where the void ratio and therefore the hydraulic conductivity change as a result of the load applied to the soils. Mesri and Olson (1971) suggest a linear relationship over a very wide range of void ratios:

$$\lg(K_s) = a\lg(e) + b \qquad [4\text{-}18]$$

where a and b are experimentally determined constants. According to Tavenas *et al.* (1983a) equations 4-13, 4-14 and 4-15, all derived from experiments on remoulded clay, may be valid for some clays or certain void ratio ranges but may not be valid in other circumstances.

Hydraulic conductivity in clayey soils is a function of *inter alia* the void ratio of the clay. Tavenas *at al.* (1983a) points out that clay fraction and plasticity index are also significant parameters in determining the hydraulic conductivity. These parameters are related to the *hydraulic conductivity – void ratio* relation by the empirical parameter I_c:

$$I_c = PI + C \qquad [4\text{-}19]$$

where PI is the plasticity index and C is the clay fraction. **Figure 4.1** indicates void ratio versus logarithmic saturated hydraulic conductivity relations as a function of the empirical parameter I_c. **Figure 4.1** can be used as an indication of the saturated hydraulic conductivity of clay soils.

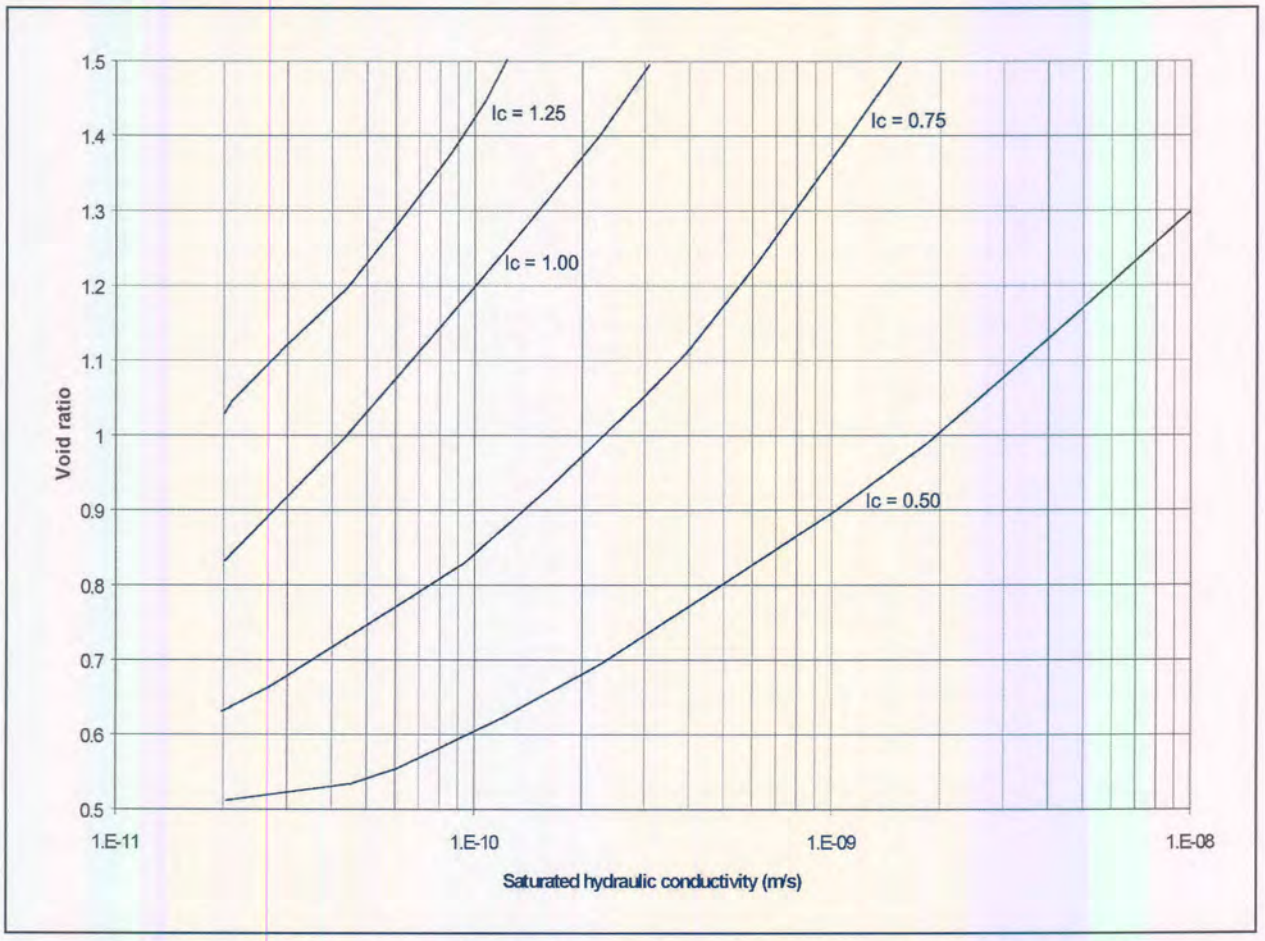

Figure 4.1: Estimation of saturated hydraulic conductivity for fine-grained soils (after Tavenas *et al*, 1983a)

However, the relationship as shown in **Figure 4.1** may not very reliable, since many factors affect saturated hydraulic conductivity in clayey soils.

The rate of consolidation of clay soils under applied stress is partly governed by their permeabilities (Tavenas *et al.*, 1983a). Consolidation tests (in particular conventional step-loaded tests) are routinely conducted during geotechnical investigations. The hydraulic conductivity of soft clays can be determined by observing the initial consolidation rate; the *in situ* void ratio at zero applied pressure under increasing pressure and hence the decreasing void ratio. According to the Terzhagi theory, hydraulic conductivity can be calculated by the equation (Tavenas *et al.*, 1983b):

$$K_s = \frac{C_v(1+e)\sigma_1'}{0.434 \cdot \gamma_w C_c} \qquad [4\text{-}20]$$

where C_v is the coefficient of consolidation, assumed to be a constant, and C_c is the compression index of the clay. The Terzhagi theory makes use of a series of assumptions that do not fit the behaviour of natural clay (Tavenas *et al.*, 1983b). As a result, significant errors of saturated hydraulic conductivity values may occur. Tavenas *et al.* (1983b) proposes that hydraulic conductivity values, obtained by indirect methods,

should not be used in engineering applications. However, these values can be used to get an indication of hydraulic conductivity.

4.2.2 Soil-water retention characteristics

Brutsaert (1967) derives the following relationship with regard to saturated hydraulic conductivity:

$$K_s = c\frac{(\varepsilon-\theta_r)^2}{{\psi_a}^2}\frac{\lambda^2}{(\lambda+1)(\lambda+2)} \qquad [4\text{-}21]$$

where c is a constant representing the effects of the fluid. According to Brutsaert, the theoretically derived constant, c, equals 2.70 in the case of water. The parameter, λ, known as the Brooks and Corey pore size distribution index, is important in describing the soil-water characteristic curve and will be discussed in Section 4.3. Rawls *et al.* (1992) investigated the relationship between soil texture, bulk density and water retention parameters and found that the empirically derived value of the constant c is 0.21, when geometric mean Brooks and Corey pore-size distribution index values are applied. They attained a correlation coefficient of 0.96.

Campbell (1985) suggests that saturated hydraulic conductivity can be calculated by means of the following equation:

$$K_s = \frac{\sigma^2{\theta_s}^2}{2\rho_w{\psi_a}^2(2b+1)(2b+2)} \qquad [4\text{-}22]$$

where b is a pore-size distribution index similar in definition to the Brooks and Corey parameter, but with a different value.

Ahuja, Naney & Williams (1985) show that saturated hydraulic conductivity can be related to water content at -33kPa in terms of the following equation:

$$K_s = 0.00282\cdot(\varepsilon-\theta_{33})^4 \qquad [4\text{-}23]$$

where θ_{33} is the water content at –33 kPa. Experimental studies have indicated that equation 4.23 is suitable for soils with less than 65 percent sand fraction and less than 40 percent clay fraction. According to Rawls *et al.* (1992), equation 4-23 is the best model to use for the study of a wide range of soil properties.

Hutson (1984) developed an empirical equation relating the soil-water characteristic curve to physical soil properties. According to Hutson, the saturated hydraulic conductivity can be estimated from the capillary model developed by Childs & Collis-George (1950):

$$K_s = 5167.36\cdot\frac{\theta_s}{{a_H}^2}\left[\frac{Si^{2b_H}+1}{2b_H+1}-\frac{Si^{2b_H}+2}{2b_H+2}+\frac{(1-Si)^2}{Si^{-2b_H}}\right] \qquad [4\text{-}24]$$

where

$$Si = \frac{2b_H}{1+2b_H} \qquad [4\text{-}25]$$

where a_H and b_H are parameters to be determined experimentally.

4.3 Estimation of soil-water retention characteristics

The theoretical framework for unsaturated flow has been well-established (Chapter 2). However, the direct measurement of unsaturated soil hydraulic properties requires demanding laboratory or field tests. Since it has been found that the indirect determination of unsaturated soil hydraulic properties is adequate for most practical cases (Papagiannakis & Fredlund, 1984), the indirect application of methods to determine unsaturated hydraulic conductivity has become acceptable.

Various models have been developed to determine the unsaturated hydraulic conductivity indirectly from saturated hydraulic conductivity and the soil-water characteristic curve (Burdine, 1953; Millington & Quirk, 1961; Brooks & Corey, 1964; Campbell, 1974; Mualem, 1976; Fredlund Xing & Huang, 1994 and others). These models will be discussed in the following sections. Since the soil-water characteristic curve is used as basis for predicting unsaturated hydraulic conductivity, it is important to describe it accurately.

Soil-water characteristic curves are not readily available in South Africa and many other countries. Laboratory soil-water retention tests can easily be conducted for site- specific investigations but in the case of regional aquifer vulnerability and recharge investigations, soil-water retention data can only be acquired at great cost. In these cases, it may be viable to estimate soil-water retention characteristics from available soil data such as soil fractions and particle-size distribution curves.

4.3.1 Soil fractions

Much research has been conducted to relate soil-water retention data to basic soil properties applying regression analysis (Bartelli & Peters, 1959; Salter, Berry & Williams, 1966; Peterson, Cunningham & Matelski, 1968; Gupta & Larson, 1979; Brakensiek, Engleman & Rawls, 1981; McCeun, Rawls & Brankensiek, 1985; Rawls *et al.*, 1982 and others). Similar regression models have been established in South Africa, especially with regard to soils in certain geographical crop production and irrigation areas. (Van der Merwe, 1973; Hutson, 1984 and others). Much of the early research was conducted at selected soil suctions, most notably at -33 and -1500 kPa. Little statistical evidence has been provided to support the regression models. Gupta and Larson (1979) propose that the regression coefficients can be calculated in terms of the following general regression equation:

$$\theta(\psi) = a_1 S + a_2 M + a_3 C + a_4 OM + a_5 \rho_b \qquad [4\text{-}26]$$

where the regression coefficients at the various soil suction values are indicated in **Table 4.9**:

Table 4.9: Regression coefficients for volumetric water content at various soil suction values (Gupta & Larson, 1979)

Soil suction (kPa)	Regression coefficients					R
	a_1	a_2	a_3	a_4	a_5	
-4	7.053	10.242	10.070	6.333	-321.2	0.950
-7	5.678	9.228	9.135	6.103	-269.6	0.959
-10	5.018	8.548	8.833	4.966	-242.3	0.961
-20	3.890	7.066	8.408	2.817	-187.8	0.962
-33	3.075	5.886	8.039	2.208	-143.4	0.962
-60	2.181	4.557	7.557	2.191	-92.8	0.964
-100	1.563	3.620	7.154	2.388	-57.6	0.966
-200	0.932	2.643	6.636	2.717	-22.1	0.967
-400	0.483	1.943	6.128	2.925	-2.0	0.962
-700	0.214	1.538	5.908	2.855	15.3	0.954
-1000	0.074	1.334	5.802	2.653	21.5	0.951
-1500	0.059	1.142	5.766	2.228	26.7	0.947

Hutson (1984) has established the following general regression model for eight South African soils:

$$\theta(\psi) = b_1 + b_2 C + b_3 M + b_4 \rho_b \qquad [4\text{-}27]$$

where the regression coefficients at the various soil suction values are indicated in **Table 4.10**.

Table 4.10: Regression coefficients for volumetric water content at various soil suction values for South African soils (Hutson, 1984)

Soil suction (kPa)	Regression coefficients				R
	b_1	b_2	b_3	b_4	
10	55.8	3.65	5.54	30.3	0.681
30	-15.5	3.84	5.72	46.3	0.764
100	29.0	3.61	4.41	4.9	0.769
500	158.8	3.47	1.70	-83.8	0.823
1500	602.0	3.22	3.08	-26.0	0.785

Soil-water retention regression models in South Africa have in general been developed for certain geographical regions and may not be applicable to all soils in South Africa. Turner (Hutson, 1984) developed a regression model with correlation coefficients higher than 0.90. However, the regression equation was developed for KwaZulu-Natal clay and clay loam, characterised by high clay contents, low bulk densities and high organic matter, hardly representative of typical South African soils.

4.3.2 Description of the soil-water characteristic curve

Several mathematical functions have been developed to describe and characterise the soil-water characteristic curve. Soil-water retention tests are usually conducted at a series of suction points. The accuracy with which the soil-water characteristic curve is described, will depend on the number of suction points used. The various mathematical functions are fitted through the points, and the values of the fitting parameters can be determined.

The residual water content specifies the upper limit in volumetric water content with a negligible effect on flow in the soil. As such, many researchers have described the soil-water characteristic curve as a function of the reduced water content, also known as the effective degree of saturation:

$$\Theta = \frac{\theta - \theta_r}{\theta_s - \theta_r} \qquad [4\text{-}28]$$

Since it is very difficult to determine the value of the residual water content, many authors regard the residual water content as another fitting parameter rather than to determine it experimentally.

Gardner (1958) proposes that the soil-water characteristic curve can be derived from the following equation:

$$\Theta = \frac{1}{1 + a\psi^n} \qquad [4\text{-}29]$$

The fitting parameter, a, is related to the inverse air-entry value of the soil and denotes the suction value at which air will enter the soil pores. The parameter, n, is related to the slope of the soil-water characteristic curve.

Brooks and Corey (1964) have developed the following function to describe the soil-water characteristic curve:

$$\Theta = \left(\frac{\psi_a}{\psi} \right)^{\lambda} \qquad [4\text{-}30]$$

where the parameter, λ, is known as the Brooks and Corey pore-size distribution index and is a function of the physical soil properties. This parameter is related to the slope of the soil-water characteristic curve.

Farrel and Larson (1972) proposed the following function to describe the soil-water characteristic curve:

$$\psi = \psi_a \exp[\alpha(1 - \Theta)] \qquad [4\text{-}31]$$

Campbell (1974) proposed a function similar to the Brooks and Corey model:

$$\psi = \psi_a \left(\frac{\theta}{\theta_s} \right)^{-b} \qquad [4\text{-}32]$$

where b is a parameter related to the Brooks and Corey pore-size index.

The Brooks & Corey (1964) function does not describe the soil-water characteristic curve accurately in the lower suction (or near-saturated) ranges of the soil-water characteristic curve, Van Genuchten (1980) proposes the following equation, closely related to the Gardner equation:

$$\Theta = \left[\frac{1}{1 + (\alpha\psi)^n} \right]^m \qquad [4\text{-}33]$$

The fitting parameter, α, is related to the inverse air-entry value, the parameter, n, is related to the slope of the soil-water characteristic curve and the parameter, m, is related to the slope of the soil-water characteristic curve at higher suction values.

Based on the Campbell function, Williams, Ross & Bristow (1992) developed the following function to describe the soil-water characteristic curve for a large range of Australian soils:

$$\ln(\Theta) = a + b\ln(\psi) \qquad [4\text{-}34]$$

McKee and Bumb (1984) have developed the following function to describe the soil-water characteristic curve:

$$\Theta = a\exp(c\psi - b) \qquad [4\text{-}35]$$

This equation is also known as the Boltzmann distribution. In order to improve the fit at lower suction values, McKee and Bumb suggest the following modification:

$$\Theta = \frac{1}{1 + a\exp(c\psi - b)} \qquad [4\text{-}36]$$

Hutson (1984) proposes that the soil-water characteristic curve can be described by a function comprising of two parts, i.e., an exponential function (based on the Campbell's function, 1974) and a parabolic function. The parabolic function describes the soil-water characteristic curve at near saturated conditions while the exponential function describes the less saturated conditions. Hutson (1984) identifies a point of inflection, θ_{in}, which occurs on the soil-water characteristic curve and indicates the point between the parabolic and exponential functions.

The soil-water characteristic curve can be described as:

$$\psi = a_H \left(\frac{\theta}{\theta_s} \right)^{-b_H} \quad for\ \psi \geq \psi(\theta_{in}) \qquad [4\text{-}37]$$

and

$$\psi = a_H \left(1 - \frac{\theta}{\theta_s} \right)^{0.5} \left(\frac{\theta_{in}}{\theta_s} \right)^{-b_H} \left(1 - \frac{\theta_{in}}{\theta_s} \right)^{-0.5} \quad for\ \psi(\theta_{in}) \geq \psi \geq 0 \qquad [4\text{-}38]$$

The parameters, a_H, b_H and θ_{in} are determined by curve fitting.

Fredlund and Xing (1994) related the fitting parameters to physical soil properties. They suggest that the following equation can describe the soil-water characteristic curve over the entire soil suction range, up to 1 000 000 kPa, that, according to some researchers (Croney & Coleman, 1961), is the range where the volumetric water content approaches nil. This assumption is supported by thermodynamic considerations.

$$\theta = C(\psi) \frac{\theta_s}{\left\{ \ln\left[e + \left(\frac{\psi}{a} \right)^n \right] \right\}^m} \qquad [4\text{-}39]$$

where e is the natural number 2.71828..., a is the fitting parameter related to the air-entry value, n and m are related to the pore-size function in the lower and higher soil suction ranges respectively. Fredlund and Xing (1994) introduced a correction function, $C(\psi)$, that corresponds to the residual water content. Leong and Rehardjo (1997a) show that a good fit can be obtained in instances where the correction factor is equal to one. The correction factor can be expressed as:

$$C(\psi) = \frac{\ln\left(1 + \frac{\psi}{C_r} \right)}{\ln\left(1 + \frac{1\,000\,000}{C_r} \right)} \qquad [4\text{-}40]$$

According to Leong and Rahardjo (1997), these functions can be grouped into functions that describe typical exponential curves (such as those of Brooks & Corey, 1964; Farrel & Larson, 1972; Williams, Pebble, Williams & Hignett., 1983 and McKee & Bumb, 1984) and functions that describe typical sigmoidal curves (Gardner, 1958; Van Genuchten, 1980; McKee & Bumb, 1984 and Fredlund & Xing, 1994). Leong and Rehardjo (1997a) show that all these equations can be derived from the following generic function:

$$a_1 \Theta^{b1} + a_2 \exp\left(a^3 \Theta^{b_1} \right) = a_4 \psi^{b_2} + a_5 \exp\left(a_6 \psi^{b_2} \right) + a_7 \qquad [4\text{-}41]$$

They show that functions pertaining to typical sigmoidal curves describe the soil-water characteristic curve better than non-sigmoidal functions. They also show that functions with four fitting parameters describe the soil-water characteristic curve better than functions with two or three fitting parameters. The Fredlund and Xing function (Equation 4-39) produces better results than the Van Genuchten function (Equation 4-33). However, in the case of sandy soils, the Van Genuchten function produces better results.

4.3.3 Estimation of parameters that describes the soil-water characteristic curve

Many researchers have developed empirical models describing typical soil-water hydraulic parameters from basic soil data such as soil fractions, bulk density and particle-size distribution curves. In addition, many researchers have developed empirical models describing fitting parameters for various functions of soil-water characteristic curves. They argue that although the fitting parameters for the various soil-water characteristic curve functions are obtained through non-linear regression and other curve-fitting methods, the fitting parameters do have a physical meaning. Leong and Rehardjo (1997a) show that the parameters a and α used in the Gardner (1958), Farrel and Larson (1972), Van Genuchten (1980) and Fredlund and Xing (1994) functions are either directly or inversely related to the air-entry value. Similar relationships of fitting parameters with pore-size distribution and other soil-water hydraulic parameters have been noted.

Rawls *et al.* (1992) propose that the air-entry pressure, ψ_a, the pore-size distribution index, λ, and the residual water content, θ_r (the three unknown parameters in the Brooks and Corey (1964) equation) can be estimated by means of the following regression equations:

$$\psi_a = 0.001\rho_w g \exp(5.340 + 0.185C - 2.484\varepsilon - 0.002C^2 - 0.044S\varepsilon - 0.617C\varepsilon + 0.001S^2\varepsilon^2 - 0.009C^2\varepsilon^2 - 0.00001S^2C + 0.009C^2S - 0.0007S^2\varepsilon + 0.000005C^2S - 0.5\varepsilon^2C) \quad [4\text{-}42]$$

$$\lambda = \exp(-0.784 + 0.018S - 1.062\varepsilon - 0.00005S^2 - 0.003C^2 + 1.111\varepsilon^2 - 0.031S\varepsilon + 0.0003S^2\varepsilon^2 - 0.006C^2\varepsilon^2 - 0.000002S^2C + 0.008C^2\varepsilon - 0.007\varepsilon^2C) \quad [4\text{-}43]$$

$$\theta_r = -0.018 + 0.0009S + 0.005C + 0.029\varepsilon - 0.0002C^2 - 0.001S\varepsilon - 0.0002C^2\varepsilon^2 + 0.0003C^2\varepsilon - 0.002\varepsilon^2C \quad [4\text{-}44]$$

where C is the clay content expressed as a percentage value and is valid for soils with between 5 and 60 per cent clay. S is the sand content expressed as a percentage value and is valid for soils with between 5 and 70 per cent sand.

Rawls *et al.* (1992) propose that the Campbell (1974) constant, b, (Equation 4-32) is related to the Brooks and Corey pore-size distribution index by:

$$b = 1/\lambda \quad [4\text{-}45]$$

They show that the Van Genuchten parameters n and m (Equation 4-33) are also related to the Brooks and Corey pore-size distribution index by:

$$n = \lambda + 1 \quad [4\text{-}46]$$

$$m = \frac{\lambda}{\lambda + 1} \quad [4\text{-}47]$$

Williams *et al.* (1992) have developed eight functions describing the parameters a and b of the Williams *et al.* (1983) equation (Equation 4-34). Williams *et al.* (1992) employed eight frequently measured properties, including a percentage of coarse sand, fine sand, silt and clay, bulk density, organic matter and texture groups, as defined by Northcote (1971) and a structure index, where different values were attributed to structured and intact soils.

Vereecken, Maes, Feyen & Darius (1989) developed multiple regression models to estimate the residual water content, saturated volumetric water content and the Van Genuchten parameters, α and n (Equation

4-33) from basic soil properties. After investigating several closed-form modifications of the Van Genucten equation, Vereecken *et al.* (1989) have concluded that the van Genuchten equation can be expressed with the restriction, $m = 1$ without significant loss of flexibility.

Vereecken *et al.* maintain that the soil-water hydraulic parameters can be expressed as:

$$\theta_s = 0.81 - 0.283\rho_b - 0.001C \quad [4\text{-}48]$$

$$\theta_r = 0.015 + 0.005C + 0.014C_m \quad [4\text{-}49]$$

$$\log(\alpha) = -2.486 + 0.025S - 0.351C_m - 2.617\rho_b - 0.023C \quad [4\text{-}50]$$

$$\log(n) = 0.053 - 0.009S - 0.013C + 0.00015S^2 \quad [4\text{-}51]$$

Vereecken *et al.* (1989) did extensive statistical analysis on the relationships, including a sensitivity analysis. Correlation ranged from 0.84 for saturated volumetric water content to 0.56 for the Van Genuchten fitting parameter, n.

The sensitivity analysis indicated that the saturated volumetric water content was the most sensitive parameter, with a relative sensitivity of 200 for both over- and under-estimations of 30 per cent. The residual water content was the least sensitive parameter, with a relative sensitivity lower than 10 for over- and under-estimations of 90 per cent. The Van Genucten parameters, α and n, were more sensitive for under-estimations than for over-estimations of the parameter value. The parameter, α, was found to be more sensitive than the parameter, n.

Tinjum, Bensen & Blotz (1997) investigated the relationship between soil-water characteristic curves and compacted clay. During the investigation, optimum water contents were determined by means of the Standard Proctor and Modified Proctor Compactive tests. In addition, Atterberg limits were determined. Tinjum *et al.* then determined the relationship between these values and the Van Genuchten parameters n and α (Equation 4-33) by means of stepwise regression. They suggested that the Van Genucten parameters could be expressed as:

$$\log(\alpha) = -1.127 - 0.017PI - 0.092(w - w_{opt}) - 0.263c_{proc} \quad [4\text{-}52]$$

$$n = -1.060 + 0.0002PI - 0.0005(w - w_{opt}) \quad [4\text{-}53]$$

where c_{proc} is a constant indicating the different compaction tests applied. For the Standard Proctor tests the value of the constant is equal to 1, while for the Modified Proctor, the value is equal to -1. Tinjum *et al.* (1997) found a correlation coefficient of 0.76 and 0.65 for α and n respectively. Better correlation could have been obtained if the parameters were correlated with the liquid limit rather than with the plasticity index. Measurements of the plasticity limit are notoriously subjective, resulting in large discrepancies.

Peterson, Moldrup, Jacobsen & Rolsten (1996) found strong relationships between the specific surface area of the soil and water retention at high suction values (1 500 kPa). However, weak relationships at lower suction values were observed. According to Peterson *et al.* (1996), specific surface areas play a dominant role in water retention at high suction values. This is mainly due to the permanent negative charge on clay particles and the polar nature of water. At lower suction values, physical attributes such as structure and packing are likely to overrule the effect of specific surface areas. In contrast to the findings of Peterson *et al.*, Call (1957), Campbell and Shiozawa (1992) and Banin and Amiel (1970) all found strong relationships between specific surface areas and water retention at low suction values. The apparent discrepancy may be due to the higher clay contents of the soils tested by said authors. The clay particles are situated between larger pores of the soil and override the effect of packing in the soil. Peterson *et al.* (1996) found a higher correlation between soil-water retention and specific surface area expressed in volumetric units ($m^2 \cdot m^{-3}$) than in weight units ($m^2 \cdot g^{-1}$). Peterson *et al.* (1996) found a correlation coefficient of 0.70 for 29 soils tested. The correlation coefficient is higher for deeper soils, probably because of less preferential pathways in these zones.

Many authors infer soil-water hydraulic parameters from grain-size distribution data (Jonasson, 1992; Paydar & Cresswell, 1996; Tyler & Wheatcraft, 1992; Smettem, Bristow, Ross, Haverkamp, Cook & Johnson, 1994). It was found that the slope of the soil-water characteristic curve could be related to the slope of the particle-size distribution curve, assuming that both curves conformed to the power law (Chang & Uehara, 1992; Tyler & Wheatcraft, 1992; Smettem *et al.*, 1994). Tyler and Wheatcraft (1992) show that by assuming that the fractal increment obtained from particle-size distribution curves can be used to estimate the fractal dimension of the pore space, the relationship between the slope of the particle-size distribution curve and the slope of the soil-water characteristic curve can be determined by means of:

$$\ln b = -\ln(n_d + 1) \qquad [4\text{-}54]$$

where b is the Campbell parameter (Equation 4-32) related to the slope of the soil-water characteristic curve and n_d represents the slope of the particle-size distribution curve. Chang and Uehara (1992) suggest a linear relationship between the inverse Campbell parameter and the slope of the particle-size distribution curve.

$$\ln b = 0.4 - \ln n_d \qquad [4\text{-}55]$$

Smetten *et al.* (1994) suggest the following linear relationship:

$$\ln b = -0.02 - \ln n_d \qquad [4\text{-}56]$$

If the air-entry value and saturated volumetric water content are known, the Campbell parameter can be estimated and the soil-water characteristic curve can be derived by means of the Campbell equation (Equation 4-32).

4.3.4 Physico-empirical equations relating the soil-water characteristic curve with particle-size distribution curves

Arya and Paris (1981) and Haverkamp and Parlange (1986) propose that the soil-water characteristic curve could be estimated from the particle-size distribution curve. This approach is based on the similarity in shape of the two curves. The similarity in shape can be explained by the LaPlace equation that relates soil suction to pore radii. As water drains from the soil, larger pores are drained first and water retention is dominated by water occurring in smaller pores. Since pore-size distribution is related to grain-size distribution, models based on the LaPlace equation can be applied to estimate the soil-water characteristic curve from the particle-size distribution curve. According to the LaPlace equation and when said fluid is water, soil suction can be expressed as:

$$\psi = \frac{0.146}{R} \qquad [4\text{-}57]$$

At a given soil suction, all pores with a radius size equal to or smaller than the corresponding pore radius are filled with water. Higher soil suction values will result from drainage of pores with radii larger than the corresponding soil suction value. Haverkamp and Parlange (1986) assumed that the relationship between grain diameter and pore radius is expressed by constant, λ_p, representing the packing characteristics of the soil.

$$d = \lambda_p R \qquad [4\text{-}58]$$

Equation 4-58 is only true for uniform soils. In these cases, the packing constant may range from 4.8309 to 8.8889 for pyramidal and tetrahedral arrangements respectively (Gupta & Larson, 1979). However, the arrangements in field soils are much more complicated and the packing parameter is a function mainly of grain-size distribution and bulk density.

According to Arya and Dierolf (1992), the volumetric water content, θ_i, corresponding to the upper limit of the ith grain-size range, can be computed from:

$$\theta_i = \sum_{j=1}^{j=i} V_j \cdot \rho_b \qquad i = 1,2,...,n \qquad [4\text{-}59]$$

where V_j is the volume of soil filled with water. For small particle-size intervals, the average volumetric water content, θ^*_i, corresponding to the midpoint of a given particle size class is:

$$\theta^*_i = (\theta_i + \theta_{i+1})/2 \qquad [4\text{-}60]$$

The corresponding soil suction value, ψ_i, can be obtained by means of the LaPlace equation:

$$\psi_i = \frac{0.146}{R_i} \qquad i = 1,2,...,n \qquad [4\text{-}61]$$

where R_i, is the corresponding pore radius.

Arya and Dierolf (1992) propose that the pore radius can be estimated from the grain diameter by means of the following equation:

$$R_i = \left(\frac{(0.5d_i)^3 4e}{3\alpha} \right)^{0.5} \qquad i = 1,2,...,n \qquad [4\text{-}62]$$

where R_i is pore radius at the ith grain-size range, d_i is the grain diameter and α is a parameter representing the effective pore length associated with each grain, to be determined empirically. The parameter α has been derived from a previous model proposed by Arya and Paris (1981):

$$R_i = 0.5d \left[\frac{4en_i^{(1-\alpha_o)}}{6} \right]^{0.5} \qquad [4\text{-}63]$$

Equation 4.62 suggests that the pore-size is a function of the number on particles, n_i. No physical explanation can be provided for this situation and Arya and Dierolf suggested that the parameter can be replaced by a single empirical parameter, α.

Arya and Dierolf (1992) found that the value for α_i, varied between 3 and 15 mm while the average value was found to be 9.38 mm for all soils tested.

The subsequent implementation of the model with an effective pore length of 9.38 mm indicates a high correlation with measured data. However, the authors do not provide any statistical evidence for the relationship. Arya and Dierolf (1992) are not sure if the effective pore length is related to grain size and, if so, how it varies from soil to soil. In a subsequent sensitivity analysis where the value of the effective pore length is estimated at between 5 and 13 mm., the predicted water content varies only slightly and the curves remain within the range of measured data. Variation of the effective pore length compared to pore radius is therefore negligible.

4.3.5 Application of fractal geometry in soil-water characteristic curves

In the last two decades, many scientists have recognised the scale-invariable or self-similar behaviour of objects and processes. The concepts of fractals, as discussed at length by Mandelbrot (1983) have

revolutionised the way scientists view many natural systems. Fractal geometry views the world as a multitude of scales, each with levels of detail and intricacy. Examples of fractal objects and processes are a rugged coastline, atmospheric turbulence, the fracturing of polycrystalline materials and natural porous media. In each case, the object appears the same, or the process appears to repeat itself in a similar manner regardless of the scale at which the object or process is observed. The understanding of fractal concepts has led to the quantification of many disordered systems.

Tyler and Wheatcraft (1990) show that the soil-water retention function, as expressed by Brooks and Corey (1964), can be developed for the Sierpinski carpet. The fractal function can be expressed as:

$$\frac{\theta}{\theta_s} = \left(\frac{\psi}{\psi_a} \right)^{D-2} \qquad [4\text{-}64]$$

where D represents the fractal dimension of the carpet. In contrast to the exponent function of the Brooks and Corey equation, the Sierpinski carpet exponent, D-2 is physically meaningful and is defined by the recursion algorithm chosen (Tyler & Wheatcraft, 1990). By choosing the Sierpinski model as a model for fractal soil pore space, Tyler and Wheatcraft, in effect, map the three-dimensional soil pore network to a plane (Perrier Rieu, Sposito & De Marsily, 1996).

Rieu and Sposito (1991) have developed a lacunarity model of an aggregated soil based on the space partition of the solid interior into a specific number of parts that are then reduced by a specified factor. The resulting model can be expressed as:

$$\theta(\psi) = \theta_s - 1 + \left(\frac{\psi_{\min}}{\psi} \right)^{3-D} \quad 0 < D < 3 \qquad [4\text{-}65]$$

Rieu and Sposito (1991) found excellent fits to data of six soils varying from sand to clay, with D ranging from 2.758 to 2.986 for sand and clay respectively. Perrier *et al.* (1996) maintain that, although Equations 4-64 and 4-65 do have identical fractal porosities, the two models do not portray soil-water properties in the same way, with the result that significant differences occur in the fractal dimension, D, even though excellent correlation has been achieved for both models.

Tyler and Wheatcraft (1992) show that the Arya and Paris (1981) model (Equation 4-62) can be represented in terms of fractal geometry. According to the original Arya and Paris model the capillary tube length, h_i, associated with particle diameter is calculated by:

$$h_i = d_i N_i \qquad [4\text{-}66]$$

Tyler and Wheatcraft (1992) suggest that the pore space can be scaled by the power law:

$$h_i = F \cdot d^{1-D} \qquad [4\text{-}67]$$

where F can be evaluated if the "ruler" length, N_i, is assumed to be the straight line length of the pore trace. Equation 4-67 can therefore be represented as:

$$h_i = d_i N_i^{\,D} \qquad [4\text{-}68]$$

Turcott (1986) shows that the particle sizes of many geological materials can be expressed by the following fractal power function in the form:

$$N(0.5d_i)^D = c \qquad [4\text{-}69]$$

where c is a constant.

The applications of fractal geometry to soil-water characteristic curves may result in a better understanding and, ultimately, a more accurate estimation of soil-water characteristic curves from readily available soil data. However, much research has yet to be conducted regarding the type of model to be used in these cases. Tyler and Wheatcraft (1992) acknowledge that the theoretical development is not yet adequate. Perrier *et al.* (1996) state that fractal analysis of the water retention curve cannot be carried out without also analysing the underlying fractal object with regard to its geometrical interpretation. Simulations regarding random fractal soil structures show that connectivity is an important aspect in soil hydraulic properties (Perrier, Mullen, Rieu & De Marsily, 1995). The effect of hysteresis should also be considered.

4.4 Estimation of unsaturated hydraulic conductivity

As already stated, the vadose zone is characterised mainly by unsaturated flow. The unsaturated hydraulic conductivity is not a constant, but a function of the volumetric water content that in turn varies in accordance with precipitation events and evapotranspiration. No other soil property shows greater variability than unsaturated hydraulic conductivity. It may vary by up to ten orders of magnitude within a *single* soil horizon, depending on the volumetric water content. Since unsaturated hydraulic conductivity is an important aspect of fluid flow analysis in the vadose zone, it is necessary to be able to determine this property. A continuous record of volumetric water content with time is required to determine travel time and recharge. Unsaturated hydraulic conductivity as a function of volumetric water content can be determined by direct measurements or calculated by indirect procedures and prediction models. Although direct measurement is by far preferable, it is for a number of reasons highly unpractical in most unsaturated flow problem situations:

- Direct measurements are costly and time-consuming.
- Hydraulic properties of soil are hysteretic in nature, i.e. different relationships between unsaturated hydraulic conductivity and volumetric water content exist depending on the wetting or drying process.
- Soil hydraulic properties are highly variable in nature and large amounts of data are required to accurately represent the field value of unsaturated hydraulic conductivity.
- Unsaturated hydraulic conductivity may vary by a few orders of magnitude within the water content range of interest. Most measurement systems cannot efficiently cover the entire range.

(Mualem, 1992)

These restrictions are especially relevant in the case of regional or catchment studies where only basic soil data are available. Several approaches have been followed to estimate the unsaturated hydraulic conductivity by means of indirect methods.

Unsaturated hydraulic conductivity can be expressed as a function of volumetric water content, soil suction or pore-water pressure. Many researchers prefer to express the unsaturated hydraulic conductivity in terms of the relative hydraulic conductivity, by means of the following equation:

$$K_r(\psi) = \frac{K(\psi)}{K_s} \qquad [4\text{-}70]$$

4.4.1 Empirical expressions

Empirical equations are often applied to determine hydraulic properties. No single equation with constant parameters is valid for all types of soil and the parameters have to be adjusted for each particular soil. The parameters of empirical equations are determined by curve-fitting methods. The empirical expressions most frequently applied are listed in **Table 4.11**.

Table 4.11: Empirical equations for determining unsaturated hydraulic conductivity

Equation	Reference	
$K(\psi) = a\lvert\psi\rvert + b$	Richards (1931)	[4-71]
$K_r(\Theta) = \Theta^n \quad where \quad \Theta = \frac{(\theta - \theta_r)}{(\theta_s - \theta_r)}$	Averjanov (1950)	[4-72]
$K(\psi) = \alpha\lvert\psi\rvert^{-n}$	Wind (1955)	[4-73]
$K_r(\psi) = \exp(-\alpha\psi)$	Gardner (1958)	[4-75]
$K(\psi) = \frac{K_s}{a\psi^n + 1}$	Gardner (1958)	[4-76]
$K(\psi) = K_s \quad for\ \psi \le \psi_a$	Brooks and Corey (1964)	[4-77]
$K_r(\psi) = \left(\frac{\psi}{\psi_a}\right)^{-n} \quad for\ \psi \ge \psi_a$	Brooks and Corey (1964)	[4-78]
$K(\psi) = K_s \quad for\ \psi \le \psi_a$	Rijtema (1965)	[4-79]
$K_r(\psi) = \exp[-\alpha(\psi - \psi_a)] \; for\ \psi_a \le \psi \ge \psi_1$	Rijtema (1965)	[4-80]
$K = K_1\left(\frac{\psi}{\psi_1}\right) \quad for\ \psi > \psi_1$	Rijtema (1965)	[4-81]
$K = K_s \exp[\alpha(\theta - \theta_s)]$	Davidson, Stone, Nielson & Larue (1969)	[4-82]
$K = K_s\left(\frac{\theta}{\theta_s}\right)^n$	Campbell (1974)	[4-83]

Mualem (1986) observed that the value of n in Equation 4-72 could be estimated as follows:

n = 3.0 to 3.5 for sands

n = 3.5 to 5.0 for clay, silt and sand mixtures

n = 5.0 to 8.0 for clays

n = 3.5 to 4.0 for well-structured (micro-shattered) soils

It has been shown that many of the fitting parameters used in empirical equations can be derived from readily available soil data such as soil fraction and grain-size distribution data. Likewise, many authors encounter relationships between the fitting parameters used in empirical equations to derive unsaturated hydraulic conductivity and the fitting parameters used in functions to describe the soil-water characteristic curve. Rawls *et al.* (1992) maintain that that the Brooks and Corey equation for unsaturated hydraulic conductivity (Equation 4-30) can be expressed as:

$$K_r(\theta)=\left(\frac{\theta-\theta_r}{\varepsilon-\theta_r}\right)^{3+2\lambda} \quad [4\text{-}84]$$

where λ is the Brooks and Corey pore size index parameter, as defined by Equation 4-30. Rawls *et al.* (1992) found that the Brooks and Corey pore size index parameter, the residual water content and saturated hydraulic conductivity can be estimated from soil fraction data as indicated in Equations 4.30, 4-42, 4-43 and 4-44 respectively. The unsaturated hydraulic conductivity at any volumetric water content can then be determined, provided that porosity and soil fraction data are available.

Rawls *et al.* (1992) found a similar relationship for the Campbell equation (Equation 4-32). According to Rawls *et al.*, the Campbell parameter, *b*, (Equation 4-32) is related to the Brooks and Corey pore size index parameter, λ, by $b=1/\lambda$. Likewise, the Campbell parameter, *b*, is related to the Campbell parameter, *n*, as defined by Equation 4-83. The Campbell empirical equation for unsaturated hydraulic conductivity (Equation 4-83) can be expressed as:

$$K_r(\theta)=\left(\frac{\theta}{\varepsilon}\right)^{3+2/\lambda} \quad [4\text{-}85]$$

As with Equation 4-84, unsaturated hydraulic conductivity as a function of volumetric water content, as described by the Campbell equation, can be estimated, provided that porosity and soil fraction data are available.

The main advantages of empirical equations are that relatively simple mathematical expressions are employed to represent soil hydraulic properties, allowing for a closed-form mathematical solution and thereby simplify analysis. The main disadvantage of empirical expressions in this context is that measured unsaturated hydraulic conductivity at some soil suction values has to be known.

4.4.2 Statistical models

Many researchers have expressed unsaturated hydraulic conductivity in terms of statistical pore-water distribution functions (Purcell, 1949; Gates & Templaar-Lietz, 1950; Childs & Collis-George, 1950; Fatt & Dykstra, 1951; Burdine, 1953; Wyllie & Gardner, 1958; Marshall, 1958; Nielson, Kirkham & Perrier, 1960; Millington & Quirk, 1961; Brutsaert, 1967; Farrel & Larson, 1972; Jackson, 1972; Mualem, 1976; Mualem & Dagan, 1978; Van Genuchten, 1980; Van Genuchten & Nielson, 1985; Fredlund *et al.*, 1994). These models are based on the Hagan-Poiseulle equation and visualise the porous medium as a set of randomly distributed pores. The pores are characterised by their length scale (pore diameter) and the density distribution function, *f(d)*. The total hydraulic conductivity, in accordance with any volumetric water content value is determined by integration along the entire range of liquid-filled pores. Mualem (1992) and Leong and Rehadjo (1997) present an excellent review and theoretical background on the different statistical models.

Childs and Collis-George (1950) investigated the effect of the random distribution of pores on unsaturated hydraulic conductivity. They considered the probability of two sections of a porous medium that were randomly connected in such a way that the larger pores with radius R_1 in one section were connected to smaller pores with radius R_2. The probability, *prob*, is calculated as follows:

$$prob(R_1,R_2)=f(R_1)f(R_2)dR_1\,dR_2 \quad [4\text{-}86]$$

Computations have been simplified in terms of two assumptions:

- The resistance to flow is from the smaller pore radius, R_2.

- There is only one connection between the pores.

By applying the Hagen-Poiseuille equation and Equation 4-86, the discharge flow contributed by the pair of pores under consideration is:

$$dq = M\ prob(R_1, R_2) R_2 \nabla \psi \qquad [4\text{-}87]$$

where M is a constant representing fluid properties and pore geometry. By integrating equation 4-87 with regard to filled pores at any volumetric water content value and applying Darcy's law, the unsaturated hydraulic conductivity can be expressed by means of the following equation:

$$K(\theta) = M\left[\int_{R_2=r_{min}}^{R_2=r(\theta)} \int_{R_1=R_2}^{R_1=r(\theta)} {R_2}^2 f(R_2) f(R_1) dR_1\, dR_2 + \int_{R_2=r_{min}}^{R_2=r(\theta)} \int_{R_1=R_2}^{R_1=r(\theta)} {R_1}^2 f(R_1) f(R_2) dR_2\, dR_1\right] \qquad [4\text{-}88]$$

Childs and Collis-George (1950) proposed transforming the soil-water characteristic curve to a function relating volumetric water content to pore radii based on Kelvin's capillary law and then carrying out the integration. The model proposed by Childs and Collis-George (1950) was subsequently improved by Marshall (1958) and Kunze, Uehara & Graham (1968) to yield:

$$K(\theta_i) = \frac{K_s}{K_{sc}} \frac{\sigma^2 \rho_w g}{2\eta_w} \frac{{\theta_s}^{\zeta}}{n^2} \sum_{j=1}^{m} \left[(2j + 1 - 2i) {\psi_j}^{-2}\right] \qquad [4\text{-}89]$$

where K_{sc} is the calculated saturated hydraulic conductivity and, i is the interval number that increases with decreasing water content. The first interval corresponds to the saturated volumetric water content and the last interval, where i is equal to m to the lowest water content, j is a counter from i to m, n is the total number of intervals between saturated volumetric water content and zero water content and ζ is a constant that accounts for the interaction between pores of various sizes.

Nielson *et al.* (1960) maintain that the computation of unsaturated hydraulic conductivity is significantly improved if an adjusting factor is used to match the computed values with measured saturated hydraulic conductivity. The unsaturated hydraulic conductivity can then be expressed in its analytical form by means of:

$$K(\theta) = \frac{\int_0^{\theta} \frac{(\theta - y)}{\psi^2} dy}{\int_0^{\theta_s} \frac{(\theta - y)}{\psi^2} dy} \qquad [4\text{-}90]$$

where y is a dummy variable (Maulem, 1974; Mualem, 1976).

Burdine (1953) proposes the following equation to calculate relative hydraulic conductivity:

$$K_r(\theta) = \frac{K(\theta)}{K_s} = \Theta^q \frac{\int_{\theta_r}^{\theta} \frac{d\theta}{\psi^2(\theta)}}{\int_{\theta_r}^{\theta_s} \frac{d\theta}{\psi^2(\theta)}} \qquad [4\text{-}91]$$

where q is a correction factor equal to 2.

Mualem (1976) investigated a conceptual model similar to that of Childs and Collis-George (1950) and derived the following equation for predicting relative hydraulic conductivity:

$$K_r(\theta)=\Theta^q\left(\frac{\int_{\theta_r}^{\theta}\frac{d\theta}{\psi(\theta)}}{\int_{\theta_r}^{\theta_s}\frac{d\theta}{\psi(\theta)}}\right)^2 \qquad [4\text{-}92]$$

where q is a correction factor equal to 0.5 but depends on specific soil-fluid properties and may vary considerably for different soils.

Campbell (1974) proposes that unsaturated hydraulic conductivity can be expressed in terms of the Campbell equation (Equation 4-32). The unsaturated hydraulic conductivity can therefore be expressed as:

$$K(\theta)=\frac{\sigma^2{\theta_s}^2}{2\rho_w\eta{\psi_a}^2(2b+1)(2b+2)}\left(\frac{\theta}{\theta_s}\right)^{2b+2} \qquad [4\text{-}93]$$

where b is the Campbell parameter as defined in Equation 4-32.

Van Genuchten (1980) applied Equation 4-33, describing the soil-water characteristic curve, to both the Burdine (1953) and Mualem (1976) equations. Since the Van Genuchten equation is not a closed-form equation, Van Genuchten applied a restriction to the equation, thereby causing the soil-water characteristic curve equation to lose some flexibility, but enabling the calculation of unsaturated hydraulic conductivity to take place. The modified Equation 4-33 can be expressed as:

$$\Theta=\left[\frac{1}{1+(\alpha\psi)^n}\right]^m \quad \text{where} \quad m=1-1/n \quad \text{or} \quad m=1-2/n \qquad [4\text{-}94]$$

where restriction is represented by $m=1-1/n$, unsaturated hydraulic conductivity as a function of soil suction can be expressed in terms of the Mualem (1976) model to yield:

$$K(\psi)=\frac{K_s\left\{1-(\alpha\psi)^{mn}\left[1+(\alpha\psi)^n\right]^{-m}\right\}^2}{\left[1+(\alpha\psi)^n\right]^{m\ell}} \quad \text{and} \quad m=1-1/n \qquad [4\text{-}95]$$

where ℓ corresponds to the correction factor, q, introduced in the Mualem (1976) model with a value of 0.5.

The function can also be expressed in terms of the Burdine (1953) model with the restriction, $m=1-2/n$, to yield:

$$K(\psi)=\frac{1-(\alpha\psi)^{n-2}\left[1+(\alpha\psi)^n\right]^{-m}}{\left[1+(\alpha\psi)^n\right]^{m\ell}} \quad \text{where} \quad m=1-2/n \qquad [4\text{-}96]$$

where ℓ corresponds to the correction factor, q, introduced in the Burdine (1953) model with a value of 2.

Van Genuchten (1980) suggests that the Brooks and Corey pore-size parameter, λ, is related to the van Genuchten parameters m and n through $\lambda=mn$. Rawls *et al.* (1992) maintain that the Van Genucten

parameter, α, is related to the air-entry value, ψ_a through $\alpha = 1/\psi_a$. Equations 4-95 and 4-96 can therefore be expressed as a function of air-entry value, the Brooks and Corey pore-size index and saturated hydraulic conductivity. Rawls *et al.* (1992) indicate that the air-entry value, Brooks and Corey pore-size index parameter and saturated hydraulic conductivity can be estimated from soil fraction data by means of Equations 4-30, 4-42, 4-43 and 4-44 respectively. The unsaturated hydraulic conductivity as a function of volumetric water content can then be estimated, provided that porosity and soil fraction data are available.

Fredlund *et al.* (1994) suggest that a statistical function should be based on the Childs and Collis-George (1950) and Nielson *et al.*(1960) model (Equation 4-90), because of the fact that both the Burdine (1953) and Mualem (1976) models contain a correction factor dependent on the properties of the soil. Fredlund *et al.* (1994) applied the Fredlund and Xing (1994) function (Equation 4-39 and 4-40) to the Nielson *et al.* (1960) model. The Fredlund and Xing function that describing the soil-water characteristic curve, can be expressed as:

$$\theta = C(\psi)\frac{\theta_s}{\left\{\ln\left[e + \left(\frac{\psi}{a}\right)^n\right]\right\}^m} \qquad [4\text{-}97]$$

where $C(\psi)$ is a correction factor that can be expressed as:

$$C(\psi) = \frac{\ln\left(1 + \frac{\psi}{C_r}\right)}{\ln\left(1 + \frac{1\,000\,000}{C_r}\right)} \qquad [4\text{-}98]$$

The Fredlund *et al.* (1994) model that describes the unsaturated hydraulic conductivity as a function by applying the Nielson *et al.* (1960) model (Equation 4-90), can be expressed as:

$$K_r(\psi) = \Theta^q(\psi)\frac{\int_{\ln(\psi)}^{b} \frac{\theta(e^y) - \theta(\psi)}{e^y}\theta'(e^y)dy}{\int_{\ln(\psi_a)}^{b} \frac{\theta(e^y) - \theta_s}{e^y}\theta'(e^y)dy} \qquad [4\text{-}99]$$

where $b = ln(1\ 000\ 000)$, e is the natural number 2.7182..., y is a dummy variable of integration representing the logarithm of soil suction and Θ^q is a correction factor, Θ is the normalised volumetric water content or relative degree of saturation that has been defined as:

$$\Theta = \frac{\theta - \theta_r}{\theta_s - \theta_r} \qquad [4\text{-}100]$$

4.4.3 The effect of hysteresis

It has already been shown that the soil-water characteristic curve is hysteretic by nature, i.e. the shape of the curve differs with regard to wetting and drying cycles. Since the unsaturated hydraulic conductivity is derived from the soil-water characteristic curve, it is clear that the unsaturated hydraulic conductivity will

also exhibit hysteretic behaviour (**Figure 4.2**). Investigations by Nielson and Biggar (1961), Topp (1969) and others showed that the hysteretic behaviour of unsaturated hydraulic conductivity as a function of soil suction, $K(\psi)$, is much more pronounced than in the case of unsaturated hydraulic conductivity as a function of volumetric water content, $K(\theta)$. Topp and Miller (1966) observed, that for the soils tested, the maximum difference in values for the soil-water characteristic curve due to hysteresis was 300 per cent while in the case of $K(\psi)$ hysteretic loops, the difference was 20 000 per cent. In contrast, the difference in values for the $K(\theta)$ hysteretic loops was only 40 per cent. Various other authors have likewise observed this phenomenon (Nielson & Biggar, 1961; Topp, 1969; Talsma, 1970 and others). The hysteretic behaviour of unsaturated hydraulic conductivity is inconsistent with the statistical models that assume each soil to have single pore-size distribution function. From a practical point of view, it is acceptable to use only one branch of the hysteretic loops to compute unsaturated hydraulic conductivity. It is recommended that unsaturated hydraulic conductivity be expressed as a function of volumetric water content to minimise the effect of hysteresis.

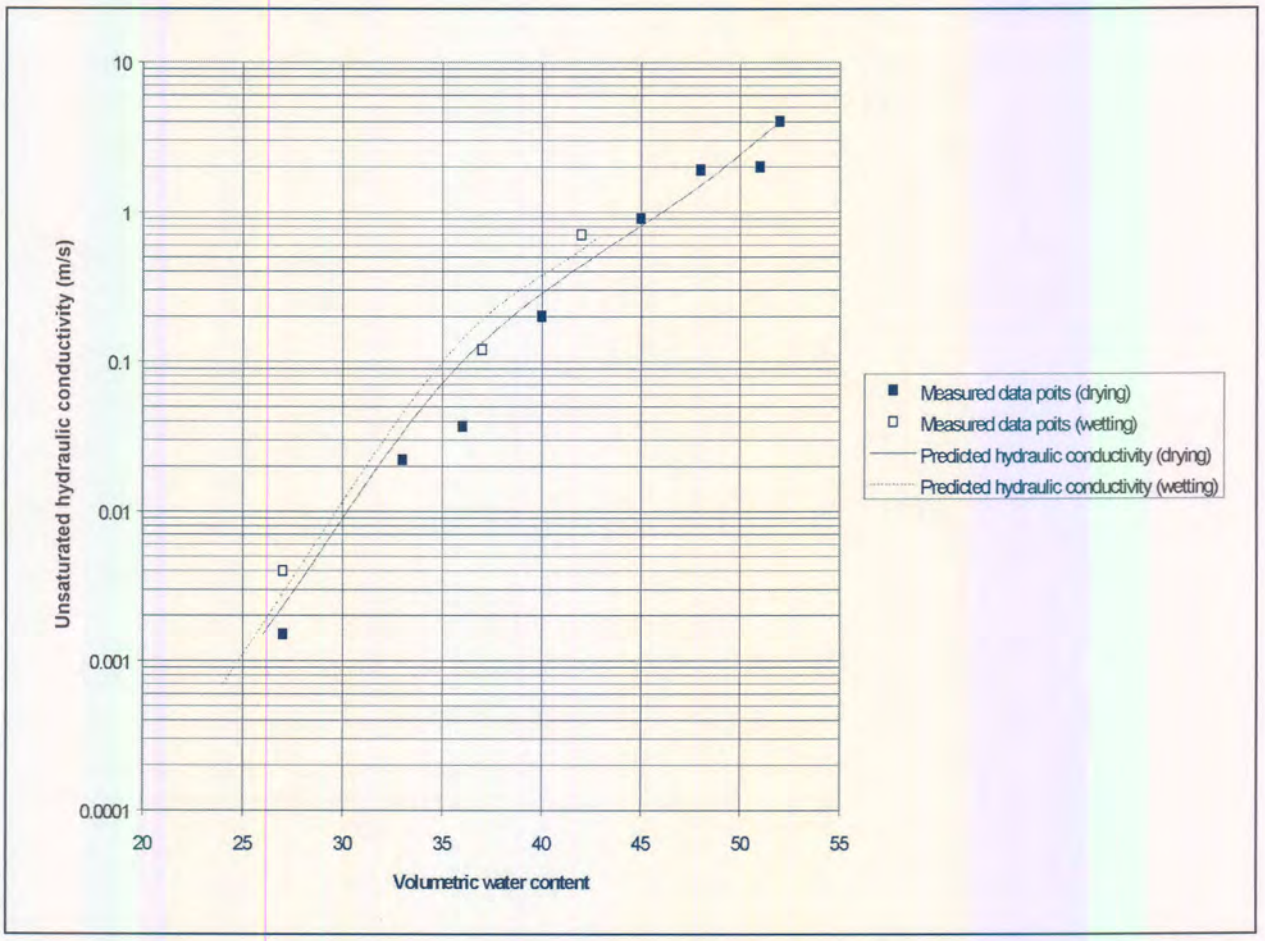

Figure 4.2: Experimentally determined and estimated unsaturated hydraulic conductivity as a function of volumetric water content (after Top and Miller, 1966)

CHAPTER 5

EXPERIMENTAL PROCEDURES AND RESULTS

The experimental procedures conducted during the study comprised the following:

- Analyses of existing hydrogeological data obtained from literature. Data on soil fractions, soil-water retention characteristics and saturated and unsaturated hydraulic conductivities were obtained for soils ranging from coarse sand to clay. Empirical relationships, as described in Chapter 4, were applied to these data and the accuracy and validity of these relationships were assessed.

- Laboratory tests were conducted on three soil types to determine the geotechnical and hydrogeological properties. The geotechnical data were used to predict hydrogeological properties and these were compared to measured hydrogeological properties.

- Field tests were conducted on three soil types to determine the *in situ* hydrogeological properties of these soils. The *in situ* properties were compared to small-scale laboratory results. In addition, the effect of preferential flow, in particular macropore channelling, was assessed for the three soil types.

Because of the number of factors that could influence the hydrogeological properties (including parent rock type, climate, vegetation and time), the research focussed on the characterisation of hydrogeological properties of residual granite. Two experiments were conducted on residual andesite.

5.1 Experimental laboratory and literature studies

Empirical equations relating physical soil properties with hydrogeological properties within the vadose zone were analysed in order to assess the accuracy and reliability of predicted hydrogeological properties. These analyses are mainly based on geohydrological data obtained from literature. The following relationships were investigated:

- Relationship between saturated hydraulic conductivity and physical soil properties (fractions sand, silt and clay, particle-size distribution curves and soil water retention characteristics)

- Analyses of functions describing the soil-water characteristic curve

- Relationship between unsaturated hydraulic conductivity and physical soil properties (fractions sand, silt and clay and particle-size distribution curves)

- Relationship between unsaturated hydraulic conductivity and the soil-water characteristic curve

Various empirical equations were developed (as discussed in Chapter 4) to predict the saturated hydraulic conductivity from sand, silt and clay fractions (soil texture data). In order to assess the reliability of these relationships, the equations were applied to a wide range of literature-based soil data. Basic soil data were obtained from published data sources, such as these published by the Desert Research Institute (1983). A total of 26 data points, representing soils ranging from clay to sand, were applied to the empirical relationships as established in Chapter 4. Saturated hydraulic conductivities were predicted from soil fractions, particle-size distribution curves and soil-water retention data. The predicted values were compared to measured saturated hydraulic conductivity data.

Several mathematical functions describing the soil-water characteristic curve were discussed in Chapter 4. Reliable indirect estimations of unsaturated hydraulic conductivity, based on soil-water retention curves, are only possible on condition that these mathematical functions accurately describe the soil-water characteristic curve. Since the soil-water characteristic curve may be either exponential or sigmoidal in shape (depending on the type of soil), the development of a single function that is valid for all soil-water characteristic curve shapes is complicated.

Several popular functions used to describe the soil-water characteristic curve were tested for five different soil types. These functions were applied to soil-water retention data obtained from literature. A large amount of unsaturated flow data was collected, analysed and published by the Desert Research Institute (1983).

It has already been shown that the soil-water characteristic curves for five soil types can be accurately described by the Van Genucten and Fredlund and Xing functions. These data-sets were further analysed to determine the unsaturated hydraulic conductivity in terms of the Van Genucten and Fredlund *et al.* models. The calculated values were compared to experimentally determined unsaturated hydraulic conductivity values.

5.2 Field experiments

Five extensive field experiments were conducted during the period October 1995 to June 1997. The field experiments were conducted for the following reasons:

- To study the effect of preferential flow and the variability of hydrogeological properties in field soils.
- To study the reliability of existing empirical and other models in estimating the geohydrological properties of field soils

It was impossible to cover all types of residual soils with the field experiments. It was decided to focus on a specific soil and to establish a workable experimental methodology that could be applied in future research. After considering the different types of residual soils, it was decided to focus on residual granite since it covers large parts of South Africa and little is known about its hydrogeological properties. Consequently, Experiments 3, 4 and 5 were conducted on residual granite.

The site of Experiments 1 and 2 is predominantly underlain by andesite of the Hekpoort Formation, Pretoria Group, Transvaal Sequence. Diabase dyke intrusions are also present. Andesite mainly comprises plagioclase with smaller amounts of clino-pyroxene, hornblende and mica. The Weinert N-value for Pretoria is 2.4 (Weinert, 1980). This value suggests predominant chemical weathering and the development of clay minerals such as kaolinite in silica over-saturated rocks and montmorillonite in silica under-saturated rocks.

Experiments 3 and 4 were conducted at Midrand. Experiment 3 was conducted during March 1996, close to the N1 highway near the Samrand onramp. The area was at the time being developed into the Samrand industrial zone. Because of the presence of ferruginised soil with low permeability, a shallow bedrock

and seepage into the testpit, the geohydrological properties could not be derived and the experiment was abandoned.

Experiment 4 was conducted in deeper weathered, less ferruginised soil during the months of April to August 1996. It was conducted close to the New Road and N1 highway intersection, which was under construction at the time.

The sites for Experiments 3 and 4 are underlain by the Halfway House Granite Suite, which mainly comprises granitic gneiss of the Basement Complex. The formation of residual soil has largely been affected by palaeo-climate. Areas above 1 600 m a.m.s.l. are largely remnants of the African erosion cycle, caused by a vertical upliftment of at least 1 000 m that occurred in the early Cretaceous period, which continued for more than 30 million years (Brink, 1979). The very high degree of weathering results in deep residual soil, formation of laterite and even bauxite and intense leaching. The Weinert N-value of 2.4 (Weinert, 1980) suggests predominant chemical weathering, as in the case of Experiments 1 and 2.

The geology at Experiment 4 is representative of the African erosion cycle. Deep residual and completely weathered granite occurs to a depth of more than 10 m. The geology is affected by human activities since the site is in a developed area. The site is also characterised by leached soil layers due to weathering over a long time. Granite corestones are abundant, e.g. the huge granite core stones in the nearby Boulders Shopping Centre. Soil properties have been expected to vary significantly both vertically and horizontally in a soil profile and a very complex flow of water through the residual soil was expected.

The site at experiment 5 is underlain by the Nelspruit Granite Suite. It comprises mostly medium to coarse-grained porphyritic biotite granite of the Basement Complex and is of Swazian age (4 000 to 2 900 Ma). Fine to medium-grained diabase intrusions of Vaalium age (2 100 to 2 700 Ma), occur frequently. The Weinert N-value (1980) is 2.0, suggesting predominant chemical weathering, as is the case in the other experiments.

5.2.1 The effect of preferential pathways and soil variability

Field soils generally comprise distinct layers, developed by the process of pedogenesis. These layers may cause fingering and funnelled flow while macropores, caused by *inter alia* plant-root penetration and desiccation, could cause macropore-channelling

According to the concept of the Representative Elementary Volume (Chapter 4), the effect of preferential flow (if any) should be detected if a sufficiently large representative volume is tested. According to Lauren *et al.* (1988), the REV for soils with macropores is 0.125 m^3 and according to Inoue *et al.* (1988), the REV for soils with cracks is 125 m^3. If no preferential flow is detected in the course of testing these samples, preferential flow paths may still occur in the field soil, but its effect in transporting water and contaminants to the groundwater regime is probably negligible. The exception is highly toxic substances such as pesticides, which could be hazardous even in minute quantities.

Large soil volumes were tested by conducting large-scale *in situ* tests and it was assumed that results will include the effect of preferential flow. In addition, block samples, which do *not* contain any cracks, fissures or biopores, have been carefully selected and the result of these represent matrix flow. In comparing field test results with laboratory results, it could be concluded that higher flow velocities in field soils would suggest the presence of significant preferential flow.

The small laboratory samples used in permeability tests may not be representative of field matrix soils due to the high variability of dry density, soil composition and other properties, resulting in large variations in laboratory-determined hydraulic conductivity values.

5.2.2 Calibration of the neutron probe

A CPN 503 DR hydroprobe® was used to measure *in situ* soil moisture content during the field experiments. The change in moisture content during both infiltration and drainage were measured which assisted in determining geohydrological parameters, such as saturated and unsaturated hydraulic conductivity.

The neutron probe works on the principle of neutron-matter interaction. High-energy neutrons emitted from a radioactive source are thermalised (slowed down) by collisions with atomic nuclei. Hydrogen causes a greater thermalising effect than many other elements found in the soil. The capture of these thermalised neutrons forms the basis for detecting the quantity of water in the soil.

The neutron probe has to be calibrated for the different soil types. The neutron probe calibration method has to take into account both water content and *in situ* density, since both affect neutron probe readings. Actual water contents were obtained by the gravimetric method. Five undisturbed samples were obtained from a site that was covered by a PVC sheet and left for one month to allow drainage to take place. The volume and weight of the samples were determined after which they were oven-dried at 110°C for 48 hours. The dry weights were then determined. Volumetric water contents, θ, were obtained and plotted against the neutron probe readings at the same depth. Linear regression was applied, using the least square method to determine the relationship between neutron probe readings and actual volumetric water content. This method was applied to every soil layer where large differences in soil density were suspected.

5.2.3 Large-Diameter Double-Ring Infiltrometer tests

In order to investigate the effect of preferential flow, Large-Diameter Double-Ring Infiltrometer (LDDRI) tests were conducted at the experimental sites. The test was conducted according to the same principle as traditional double-ring infiltrometer tests, with the exception that the diameters of the rings were three times the size of standard double-ring infiltrometers. The purpose of the larger diameter rings was to test a larger, and therefore, more representative, volume of soil. In addition, a neutron probe was used to determine the depth to wetting front, instead of excavating a hole and visually determining the depth of the wetting front. The advantage was that a number of tests could be conducted at various hydraulic heads and that the reliability of the saturated hydraulic conductivity could be quantified.

LDDRI tests were conducted according to Daniel's method (Daniel, 1989). Two corrugated iron rings, 1.45 and 3.00 m in diameter respectively, were installed concentrically, and embedded approximately 10cm in the soil. The rings were then sealed with a soil/bentonite mixture. A neutron probe access hole was made in the centre of the rings. The hole was equipped with a 2.2m long PVC neutron probe access tube. The PVC tube was sealed by a soil/bentonite mixture. The set-up of the LDDRI test is shown in **Figure 5.1**.

After saturation had been reached, water was kept at a constant head and the infiltration rate of the inner ring was determined. Infiltration rates were determined with water levels kept constant at various heights ranging from 0.05m to 0.25m.

The rate of infiltration, I, can be calculated by means of the following equation:

$$I = \frac{Q}{At} = \frac{q}{A} \qquad [5\text{-}6]$$

The saturated hydraulic conductivity value can be calculated from the following equation:

$$K_s = \frac{I}{i} = \frac{I}{1 + \frac{h}{L_f} + \psi_f} \qquad [5\text{-}7]$$

Figure 5.1: Set-up of the Large-Diameter Double-Ring Infiltration tests

Continuous infiltration for one month at Experiment 2, one week at Experiment 4 and two days at Experiment 5 prior to LDDRI tests, resulted in almost saturated conditions, providing therefore that the effect of soil suction at the wetting front was negligible.

The length of the flow path could be obtained from neutron probe readings. After infiltration of the inner-ring had been measured, neutron probe readings were taken at 5cm intervals. The wetting front could be identified by a distinct decrease in neutron probe counts.

Various assumptions were made with regard to the LDDRI tests (Daniel, 1989):

- The soil is homogeneous and uniformly wetted
- The infiltration rate is high enough to ensure accurate measurements
- Evaporation is negligible
- Seepage beneath the inner ring is one-dimensional
- The swelling process in the soil has been completed
- The effect of boundaries is negligible.

5.2.4 Internal drainage tests

After the LDDRI tests had been completed, the water in the inner and outer rings was allowed to drain. Frequent neutron probe measurements were made to determine the change of water content with time. Potential water losses due to evaporation were limited by covering the site with a canvas tent and by performing tests on deeper soil layers.

The θ-method involves application of the following empirical expressions to determine the relative hydraulic conductivity as a function of water content, θ (Fuller & Moolman, 1989):

$$\theta_s - \theta = \frac{\ln(t)}{\beta} + \frac{1}{\beta} \cdot \ln\left(\frac{\beta K_s}{\alpha z}\right) \quad [5\text{-}8]$$

and

$$K_r(\theta) = \exp[\beta(\theta - \theta_s)] \quad [5\text{-}9]$$

where θ is the volumetric water content, θ_s is water content at saturation, t is time in seconds, K_s is the saturated hydraulic conductivity, K_r is the relative hydraulic conductivity as a function of water content, z is the depth of the soil layer and α and β are constants to be determined experimentally.

Using the data at various depths in Experiment 2 and 4, a linear regression curve was fitted to a plot of (θ_s-θ) vs. ln(t) using the least squares method. The values of β and K_s could then be determined by means of Equation 5-8 and the value of K_r by means of Equation 5-9.

5.3 Experimental procedure

5.3.1 Experiment 1: UP Experimental Farm

The set-up for Experiment 1 is shown in **Figure 5.2**. Three trenches were excavated in a Z-shape as shown in the figure. The southern and western trenches were 4.2 m and 3.9 m deep respectively. Excavation went smoothly and there was no refusal. Another hole, the infiltration source hole, was hand-dug 1.0m away from the southern and western trenches. The hole was 1.00m × 0.75m in area and 1.7m deep.

Six neutron probe access holes with diameters of 50 mm were made around the infiltration source hole and in the side of the western trench as shown in **Figure 5.2**. Access holes no's. 4 and 5 were drilled in the side of the western trench at angles of 45° and 50° respectively. The ends of these access holes were directly beneath the source hole. The holes were drilled with a *Little Beaver* hydraulic 50 mm diameter auger machine. The access holes were equipped with 2.2m PVC access tubes.

The whole experimental set-up was covered by a 5m × 5m canvas tent. The tent prevented evaporation and infiltration from external sources. Background neutron probe readings were made prior to the experiment. The background readings were extended to two weeks because of heavy rain during the first week.

The source hole was filled with water and kept at a constant level of 1 m by means of a ball-valve. The water level was then allowed to drop to 40 cm. Neutron probe readings and visual inspection (including the observation of water flow through the wall of the trench) was performed three times a week.

The experiment was abandoned after the trench walls collapsed. No data with regard to drainage were obtained and it was decided that a second experiment, close to the original site, had to be conducted.

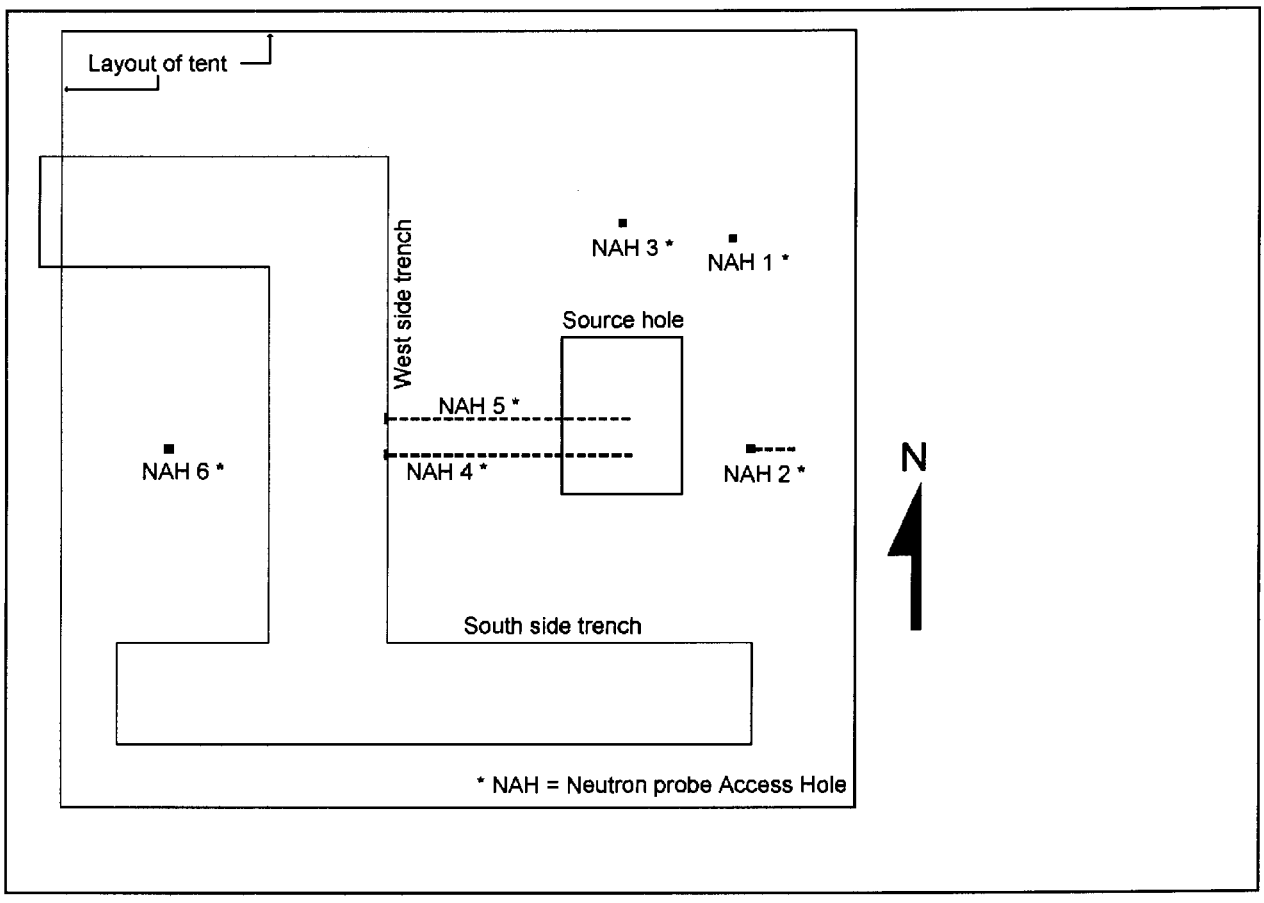

Figure 5.2: Layout of experiment 1

5.3.2 Experiment 2: UP Experimental Farm

For Experiment 2 it was decided that trenches should be excavated after infiltration had taken place. A major disadvantage of this approach was that the travel-time of water along preferential pathways could not be obtained.

A hole, 3.2 m in diameter and 0.6 m deep, was hand-dug to remove the transported material. Equipment for the LDDRI tests was installed and neutron probe background readings were taken. Water was let into both rings and kept at a constant level of 10 cm. Neutron probe readings were taken daily for one week. Constant neutron probe readings implied that saturation had been reached. The water was then allowed to drain for a few hours, after which two LDDRI tests were conducted. Hydraulic conductivity values were determined at hydraulic heads of 0.06 m and 0.25 m respectively. The soil was then allowed to drain and internal drainage tests were conducted by taking neutron probe readings once daily for one month.

After significant drainage, a trench was excavated along one side of the hole to describe the soil profile and obtain samples for geotechnical testing and to calibrate the neutron probe. Water was again let into the inner-ring and the soil profile was observed for preferential flow, but none was detected.

5.3.3 Experiment 3: Shell Ultra City, Midrand

The geology at Experiment 3 comprised of shallow ferruginised soil layer underlain by residual granite and shallow bedrock at about 3m in depth. A hole, 3.2 × 3.2 × 1.5 metres deep was excavated in order to conduct LDDRI tests on residual granite, occurring below the ferruginised layer, because that was more representative of the regional geology. The LDDRI equipment was installed in the soil and the rings

filled with water to a level of 0.20m. After about two weeks, the water level in the rings rose to 0.40 metres because of seepage. The test was abandoned and a new site, with no ferruginised layers and a deeper weathering profile, was identified.

5.3.4 Experiment 4: New Road Interchange, Midrand

Approximately 0.50 metres of transported material was removed and LDDRI equipment was installed in residual soil. After neutron probe background readings had been taken, water was let into the rings and kept at a constant level of about 10cm. Neutron probe readings were taken three to four times a day for one week, until saturation was reached. The water was then allowed to drain for two hours and five LDDRI tests were conducted. The hydraulic head was kept constant at levels varying from 0.09 m to 0.23 m. The water was then allowed to drain and an internal drainage test was conducted by means of neutron readings once a day.

After the internal drainage test, a tracer was discharged into the soil. The tracer consisted of 0.6l commercial food colouring that was diluted with about 2l water that was allowed to drain into the soil for 24 hours. A trench 3.6m deep was then excavated at the place of infiltration and the flow path of the tracer was observed visually and described. A soil profile description was recorded and samples were taken for geotechnical and water retention tests.

5.3.5 Experiment 5: Injaka dam construction site

The top 2 to 3 m of soil was removed during site preparation for grouting tests, conducted close to Experiment 5. The site was levelled and LDDRI equipment was installed in the residual soil. Heavy rains were experienced that lasted for two days but with no significant effect on the test. After neutron probe background readings had been taken, water was let into the rings and kept at a constant level of about 10 cm. Neutron probe readings were taken every hour for about eight hours after which it was continued four times a day. Saturation was reached after 48 hours. The water was then allowed to drain for two hours and six LDDRI tests were conducted. The hydraulic head was kept constant at levels varying from 0.04 m to 0.18 m. The water was then allowed to drain. A test to determine the saturated hydraulic conductivity was conducted, involving the neutron probe readings for the first two hours of drainage and applying the continuity equation.

A trench was excavated close to the inner-ring after which a soil profile description was recorded and samples taken for geotechnical and water retention tests. The inner-ring was again filled with water and the soil profile was observed for preferential flow. However, none was detected.

5.4 Geotechnical tests and results

For the purpose of this study, only the basic geotechnical data, that are generally available at various institutions in South Africa (Milford, 1994) and can be used to estimate important hydrogeological properties over large parts in South Africa, were obtained. These geotechnical tests include:

- Soil profile descriptions
- Laboratory tests to determine the index properties of soil
- Laboratory tests to determine the dry density, water content and specific gravity of the soil
- Permeability tests

In addition to the geotechnical tests, the water retention characteristics of the soil were obtained. These data can be used to establish the hydrogeological properties of unsaturated soil. The determination of soil-water characteristic curves is not a typical geotechnical test, but agricultural water retention data is readily available.

5.4.1 Soil profile descriptions

Soil profile descriptions were recorded at all experimental sites and described according to the guidelines of Jennings *et al.* (1973). In addition, four exploratory large-diameter auger holes were made at the sites of Experiments 1 and 2. Earth cuttings made during the construction of the road onramp at Midrand and the Injaka dam were also studied.

The soil profiles at Experiments 1 and 2 generally comprise a 0.5 m thick, dark-brown, micro-shattered hillwash, overlying a brownish dark-red, firm, silty clay with sand up to about 2.5 m thick. This layer is underlain by reddish yellow, fissured, clayey silt with an increasing sand content to the end of the auger holes at 7 m. Kaolonite clods are discernible at a depth of 1.1m. No water was encountered during the auger drilling, implying that the groundwater surface is deeper than seven metres. Desiccation cracks appeared on trench walls. Plant roots were observed in the soil profile up to a depth of 4 m. The dark-red clayey silt is the result of pedogenesis that destroyed all relict rock structures except for isolated disintegrated quartz veins. The yellow fissured clayey silt was interpreted as completely weathered andesite and the fissures were interpreted as relict bedding or foliation planes. The transition between the red clayey silt and the yellow fissured clayey silt is uneven and gradual. Occasional red 'fingers' intrude into the yellow fissured clayey silt. The depth of this transitional zone varied from 2.0 m to 3.0 m. The finger-like structures were probably caused by preferential weathering along rock joints.

The soil profile at Experiment 3 comprises of about 0.5m, loose to medium dense, clayey fine sand hillwash, underlain by about 2 m of ferruginised residual granite. Shallow granite bedrock was encountered at about 3 m and shallow groundwater at about 2.5 m.

The soil profile at Experiment 4 comprises about 2.0m deep, brownish dark red, very dense to medium dense, clayey, fine sand with gravel; residual granite. This layer is underlain by a 1.0m deep, brownish red mottled yellow and orange, loose, leached, micaceous, medium to coarse sand. The leached layer represents intense weathering, leaching and lessivage over a long period of time, typical of soils developed on the African erosion surface. The leached layer is underlain by a brownish red, orange and yellow, medium dense, micaceous, completely weathered granite. The construction of a new highway onramp at the New Road/N1 intersection revealed a 6m deep and 30m long section through residual and completely weathered granite. The section comprises a dark red oxidised, residual granite and completely weathered granite underlain by greyish white, kaolinitic, completely weathered granite. A clear transition between the greyish white and dark red completely weathered granite and dark red root-like structures extended within the greyish white completely weathered granite. This was probably caused by preferential weathering along discontinuities within granite rock. Large granite corestones were excavated during construction and quartz veins were also visible.

The geology at Experiment 5 comprises more than 10m of deeply weathered, residual and completely weathered granite. A relatively low quartz content was noticeable. The prevailing humid conditions resulted in predominant chemical weathering and the formation of clay minerals in a deep soil profile. The soil profile at Experiment 5 comprised a 2 to 3 metres thick dark red silty sand with clay overlying a white and yellowish light red gravelly sand layer. The top layer was removed during clearing and levelling of the site for preparation of grouting tests. The soil profile was therefore recorded about 4 metres below the natural ground surface.

No distinct soil layers were noticed in the recorded soil profile. Weathering tends to be controlled by relict rock structures and preferential weathering zones and the soil profile was therefore described as different zones rather than the traditional soil layers. The soil profile generally comprises gravelly,

coarse, medium and fine sand with silt. The soil zones differ slightly in colour and silt content, with the exception of a dark red clayey sand pocket and a highly weathered quartz-pegmatite zone. Relict rock fractures could easily be identified from discoloration on the fracture surfaces. Plant-roots frequently occur along these fractures.

A dark red, clayey, fine and medium sand with clay, soil pocket (20 cm × 30 cm) was observed at a depth of about 0.90 metres. This soil pocket differed markedly from the surrounding soil in colour and soil type, but was similar to the top dark red soil layer (that had been removed). A complicated plant-root structure was observed within this soil pocket. It is postulated that this soil pocket has formed due to preferential weathering along a non-resistant weathering zone within the parent rock. The soil weathered to a clayey sand and plant roots took advantage of the higher water content in the clayey soil which resulted in further weathering.

The soil profiles are presented in **Appendix A.**

5.4.2 Geotechnical laboratory tests

A total of 13 disturbed and 37 block samples were obtained from the five experimental areas. 13 indicator tests, 13 basic geotechnical tests consisting of bulk density, moisture content and specific gravity tests and 13 falling-head permeability tests were conducted by the Department of Water Affairs and Forestry's soil materials laboratory. The results are summarised in **Table 5.1.**

Table 5.1: Average values for geotechnical properties of soil samples

	Experiments 1 and 2	**Experiments 3 and 4**	**Experiment 5**
Index properties (%)	**n = 4**	**n = 5**	**n = 4**
Gravel	0.0	22.0	1.00
Sand	26.5	50.8	59.0
Silt	39.5	17.0	28.1
Clay	34.1	7.4	11.8
Liquid limit	44.7	30.2	38.8
Plasticity index	18.5	10.7	13.48
Shrinkage limit	8.9	5.3	5.5
Basic geotechnical properties	**n = 5**	**n=3**	**n=5**
Dry density	1 406 kg/m^3	1668 kg/m^3	1445 kg/m^3
Specific gravity of the solids	2.61	2.64	2.65
Mass water content	24.8%	13.6%	19.12%
Volumetric water content	36.5%	25.8%	27.6%
Porosity	46.2%	36.8%	45.5%
Void ratio	0.86	0.58	0.84
Degree of saturation	79.7%	70.4%	60.73%
Hydraulic conductivity (m/s)	**n=4**	**n=4**	**n=5**
Average value	2.17×10^{-7}	7.64×10^{-8}	1.36×10^{-6}
Median value	7.10×10^{-9}	1.75×10^{-8}	9.80×10^{-7}

n = number of samples

The soil samples in Experiments 1 and 2 comprised well-graded, fine, silty clays. Low liquid and plasticity limits resulted in low activity values, except for samples I-103 and I-107 that were characterised by high liquid and plasticity limits and a high activity value. The samples were classified according to the USCS as silt with sand (ML) to clay with low plasticity with sand (CL), except for samples I-103 and I-107 that were classified as clay with high plasticity with sand (CH) and silt (MH) respectively. The

higher permeability values of sample I-101 can be attributed to by-pass flow of water along the sides of the soil samples during testing.

Soil samples at Experiments 3 and 4, typically comprised well-graded, gravelly clayey sands, some with significant silt contents. All the samples were characterised by low liquid and plasticity limit values and low activity values resulting from the low clay contents. The samples were classified as clayey sands (SC) according to the USCS.

Soil samples at Experiment 5 typically comprised well-graded sands with little silt and clay, the exception being sample I-501, which comprised clayey, fine sand. Sample I-501 was obtained from the dark red clayey sand pocket, and was characterised by a high plasticity index and subsequently a high activity, unlike the other samples, which were characterised by low plasticity indices and low activities. The samples were classified as clayey sands (SC) according to the USCS, with the exception of sample I-501, which was classified as a inorganic clay with high plasticity (CH). It is worthwhile to observe that the soil was classified as a clayey sand, although the sand and silt fraction together amount to only 8 to 10 per cent of the sample weight. This can be explained by the relatively high fine sand fraction (27 to 31 per cent of the sample weight) that is included with the fine fraction.

The geotechnical results are presented in **Appendix B**.

The natural variability of soil properties in field soils was investigated, using statistical analysis of the geotechnical data and calculating the coefficient of variability. The coefficient of variability was used instead of the more traditional standard deviation in order to compare the variability of different soil properties with each other. The results are presented in **Table 5.2**.

Table 5.2: Coefficient of Variability of geotechnical properties

	Coefficient of Variability (%)		
	Experiments 1 and 2	**Experiments 3 and 4**	**Experiment 5**
Index properties	**n = 4**	**n=5**	**n=4**
Gravel	N.A.	12.03	141.42
Sand	22.80	16.26	22.66
Silt	8.23	16.11	6.05
Clay	25.68	68.64	115.10
Liquid limit	19.60	5.46	24.72
Plasticity index	36.24	25.45	67.00
Shrinkage limit	34.27	27.06	79.45
Basic geotechnical properties	**n = 5**	**n=3**	**n=5**
Dry density	4.74	3.33	2.84
Specific gravity of the solids	5.49	0.44	0.63
Mass water content	12.91	2.55	10.67
Volumetric water content	10.24	5.47	10.79
Porosity	6.82	6.10	3.98
Void ratio	11.99	9.44	7.39
Degree of saturation	16.22	11.42	12.29
Hydraulic conductivity	**n=4**	**n=4**	**n=5**
Hydraulic conductivity	194.84	170.00	77.69

n = number of samples

In general, the variability of basic geotechnical properties was low, while that of the index properties was low to medium. The higher variability in Atterberg limits could be caused by the subjective way in which the plasticity and shrinkage limits are determined. The liquid limit, determined in a more objective way, exhibits lower variability. The anomalous variability of the gravel proportion in Experiment 5 and the

clay proportion in Experiments 3 and 4 can be ascribed to very low gravel and clay contents respectively. Although these are highly variable compared to fractions of other soil samples, they are much less variable compared to the compositions of whole samples. The higher variability of index tests in Experiment 5, especially the clay fraction, is the result of the inclusion of sample I-301, exhibiting discrepant soil properties but representing a very small part of the soil profile. The very high variability of hydraulic conductivity values is caused by the combined effect of variability in soil composition, bulk density and other factors influencing hydraulic conductivity. The hydraulic conductivity as determined from laboratory tests is not representative of the field soil. Large-size soil samples or *in situ* tests provided more representative values.

5.4.3 Results of the water retention tests

In addition to geotechnical tests, 11 undisturbed samples were tested by *Central Agricultural Laboratories* in Pelindaba to obtain water retention characteristics. These values could be used to obtain soil-water characteristic curves. The samples were subjected to suction values of 10, 20, 50 and 100 kPa respectively and the volumetric water content was determined at each suction value. The results of these tests are shown in **Table 5.3** and the variability of water retention characteristics is indicated in **Table 5.4**.

Table 5.3: Results of the water retention tests

Suction (kPa)	Average mass water content (%)		
	Experiments 1 and 2	Experiments 3 and 4	Experiment 5
0 (saturated)	31.38	21.00	30.56
10	19.64	10.26	27.04
20	17.81	9.56	23.97
50	15.20	8.47	19.34
100	14.21	7.56	14.99

Table 5.4: Coefficient of Variability of the water retention tests

Suction (kPa)	Coefficient of Variability (%)		
	Experiments 1 and 2	Experiments 3 and 4	Experiment 5
0 (saturated)	8.38	9.21	6.18
10	19.33	8.55	13.69
20	17.38	7.73	11.47
50	16.84	5.80	5.62
100	17.68	8.57	2.21

The soil-water retention tests revealed that, for Experiments 1 and 2, more soil-water has been retained in the soil matrix compared to experiments 3 and 4. Experiments 3 and 4 revealed a rapid decrease in soil-water between saturation and 10 kPa suction. These trends were expected, since water drained rapidly along large pores of the silty sand.

The rapid decrease in soil-water content between saturation and 10 kPa, observed in Experiments 1 and 2, was not expected, and could have been caused by clay minerals with low water retaining properties. The comparatively higher soil-water retention for experiment 5 was also not expected, but could be attributed to clay minerals with higher water retaining properties.

The soil-water retention properties of the soils tested are characterised by moderate to low variability. This indicates that reasonable estimates of soil water retention characteristics can be obtained from soil-water retention tests.

The results of soil-water retention tests are presented in **Appendix B**.

5.5 Results of the *in situ* tests

5.5.1 Infiltration results

Water content profiles at Experiment 1 were characterised by high water contents in shallow zones and lower water contents in deeper zones. The higher water contents in shallower zones can be attributed to light rainfall during the last few days. Heavy rainfall during the first week of background readings resulted in an increase in water content. The fact that the neutron access holes were installed underneath the tent suggested substantial lateral flow. Neutron access holes 4 and 5 were shielded from lateral flow by the trenches and the empty source hole. Water content values in this area remained low, even at deeper zones.

No significant water content changes at neutron access holes 1, 2 and 3 were observed after the source hole had been filled with water because of a high water content after the rainfall events. Significant water content increases were observed at neutron access hole 5 and, for the deeper zones, at neutron access hole 4.

A high rate of water content increase was observed during the first day. The water level in the source hole was kept at 90 cm. The water level was lowered to 40 cm on the second day, resulting in a lower rate of water content increase. The lower rate of water content increase could be attributed to a lower hydraulic gradient leading to a lower infiltration rate.

Since neutron access holes 4 and 5 were installed at an angle, horizontal distances to the source hole varied at different points of measurement. The shallower the point of measurement, the greater the horizontal distance from the source hole. The fact that the rate of water content increase was approximately the same for all points of measurement, suggests substantial lateral flow.

Complete saturation of the soil matrix was observed in the northern bottom part of the western trench wall. The rest of the wall appeared dry. This saturation was probably caused by preferential flow along plant root holes and fissures (Section 5.6.4).

Experiment 2 was performed after a season of heavy rainfall. The soil-water content was therefore high. Slight rises in water content were observed at shallow and medium depths during the first two days. Water content at a depth of 1.64 m was constant, suggesting near-saturated conditions.

No infiltration tests were conducted during Experiment 3.

Experiment 4 was conducted in the dry season and the original soil water content was therefore low. Complete saturation was reached within 24 hours.

Experiment 5 was conducted after three days of heavy rain. The tent was already erected before the rains came. It was found that the rain had no significant effect on the experiment. Infiltration lasted for two days after which the water was allowed to drain. Neutron probe readings were taken every hour after infiltration commenced and subsequently only four times a day after the first day. Saturation at 0.33 m and 1.13 m was reached after 2 hours and 48 hours respectively.

The first two hours of drainage at 0.33 m and, to a lesser degree, at the other depths could be ascribed to water draining primarily through large pores due to the high degree of saturation. The rate of flow was therefore almost equal to saturated flow. The saturated hydraulic conductivity could be determined by applying the continuity equation during the first two hours of draining.

The continuity equation can be expressed as follows:

$$\frac{d\theta}{dt} = \frac{d}{dz} K(\theta) \frac{dh}{dz} \qquad [5\text{-}10]$$

The hydraulic conductivity over the first two hours of draining was calculated at 1.45×10^{-6} m/s. The infiltration results for Experiment 5 are indicated in **Figure 5.3**.

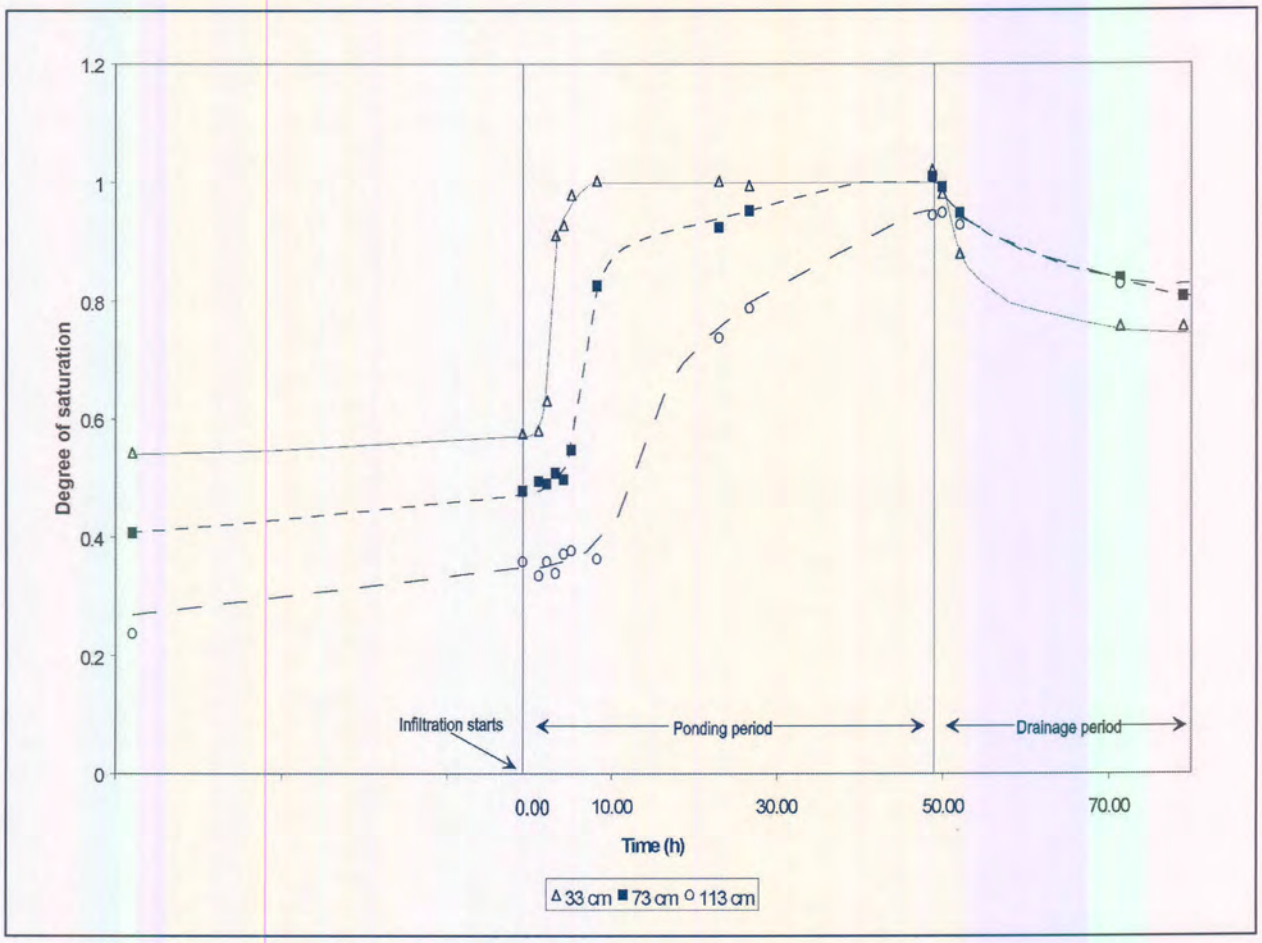

Figure 5.3: Infiltration results at Experiment 5

5.5.2 Results of the Large-Diameter Double-Ring Infiltrometer (LDDRI) tests

The results of the LDDRI tests are summarised in **Table 5.5**.

Table 5.5: Results of the LDDRI tests

	Experiment 2	Experiment 4	Experiment 5
Average hydraulic conductivity (m/s)	2.18×10^{-9}	6.01×10^{-7}	1.91×10^{-6}
Median hydraulic conductivity (m/s)	2.18×10^{-9}	5.59×10^{-7}	1.91×10^{-6}
Coefficient of Variability (%)	N.D.	12.35	15.70
Number of tests	2	5	6

The saturated hydraulic conductivity values, as obtained by the LDDRI tests, are very similar, given the large range of hydraulic heads at which the experiments were conducted. This is confirmed by the low coefficient of variability, which compares well with that of laboratory permeability tests. It also confirms the reliability of LDDRI tests.

5.5.3 Results of the Internal Drainage tests

Two internal drainage tests were conducted during Experiment 2, while one test was conducted during Experiment 4. Curve fitting was conducted by determining the minimum sum of squared residual (SSR) values for the functions. The Generalised Reduced Gradient non-linear optimisation algorithm was applied to determine minimum SSR values, and to determine the values of parameters α and β simultaneously. The results of the internal drainage tests are summarised in **Table 5.6** and in **Figure 5.4**.

Table 5.6: Results of the internal drainage tests

	Experiment 2		Experiment 4
Depth of soil layer, z	0.39	1.14	0.98
Empirical parameter, β	153.716	153.716	102.733
Empirical parameter, α	4.092×10^{-4}	2.017×10^{-2}	1.177×10^{-5}

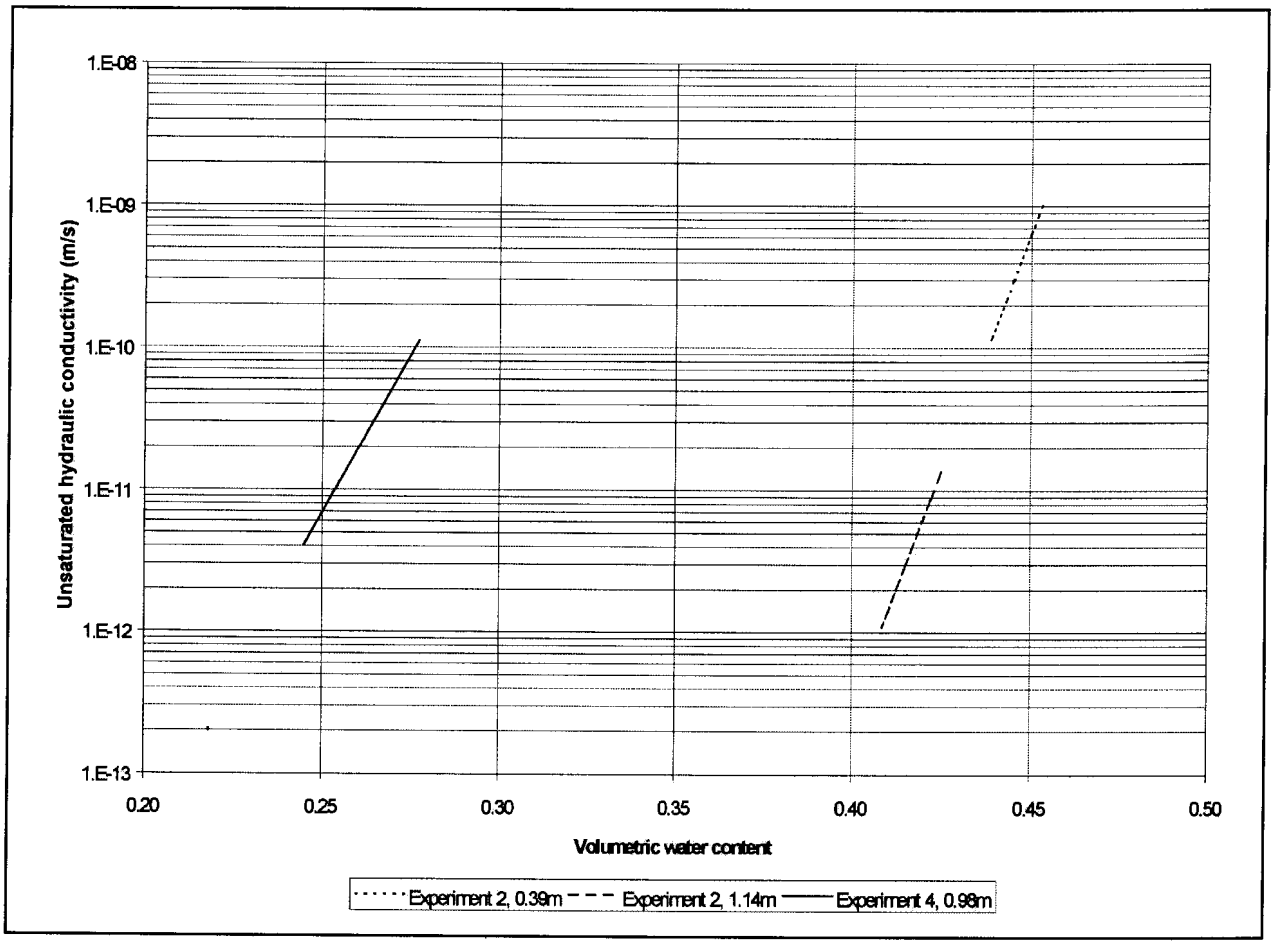

Figure 5.4: Results of the Internal Drainage tests

Equations 5-8 and 5-9 indicate that unsaturated hydraulic conductivity is a function of the empirical parameter β and saturated hydraulic conductivity. The similar parameter β values suggest similar unsaturated hydraulic conductivities for residual soils at depths of 0.39 m and 1.14 m respectively.

The exponential relationship between hydraulic conductivity and water content is in contrast to the typical non-linear sigmoidal relationship generally derived from laboratory and *in situ* tests. This can be ascribed to the form of Equation 5-8, suggesting an exponential relationship.

Because of the simple way in which unsaturated hydraulic conductivity is derived by means of internal drainage methods and the fact that the relationship between soil-suction and water content is ignored, the tests may not yield accurate estimations of unsaturated hydraulic conductivity. In addition, although measurements were taken for more than ten days, little drainage occurred, with the result that unsaturated hydraulic conductivity was derived from a small data range.

5.5.4 Preferential flow

Hydraulic conductivity values derived from laboratory permeability tests were compared with those derived from LDDRI tests. Because of the non-symmetrical shape of the laboratory-determined hydraulic conductivity probability distribution curve and the small amount of data, the effect of preferential flow could not be accurately analysed statistically. However, the effect of preferential flow could be indicated by comparing the median hydraulic conductivity values of the laboratory tests with those of LDDRI tests. The flux increase because of preferential flow is indicated in **Table 5.7**.

Table 5.7: Increase in calculated flux because of preferential flow (hydraulic gradient = 1)

	Experiment 2	Experiment 4	Experiment 5
Median calculated flux of soil matrix (m/s)	7.10×10^{-9}	1.75×10^{-8}	9.80×10^{-7}
Median calculated flux of field soil (m/s)	2.18×10^{-9}	5.59×10^{-7}	1.91×10^{-6}
Calculated factor increase in flux due to preferential flow	None	× 31.9	× 1.95

The variability of hydraulic conductivity should be considered when **Table 5.7** is interpreted. In fact, the hydraulic conductivity of field soils at Experiment 2 is lower than that of the soil matrix. This can be attributed to variable hydraulic conductivity values and subsequent unreliable results. At best, the results proved that preferential flow possibly did not have a significant effect on recharge in field soils at Experiment 2, whereas it possibly had a significant effect on field soils in Experiment 4, while no conclusive evidence was attained that preferential flow had a significant effect on field soils at Experiment 5.

Macropore channelling was observed at Experiment 1. Within 4.5 hours from first filling the source hole, a strong water flow was observed from a plant-root hole, located at the northern bottom part of the western trench wall, 1.97 m deep. The rate of flow was measured at 3×10^{-6} m^3/s. The diameter of the hole was 4 mm. The velocity of water flow can be calculated by means of:

$$v = \frac{q}{A} \qquad [5\text{-}11]$$

where v is the velocity, q is the rate of flow and A is the area perpendicular on water flow. The velocity was therefore calculated at 0.239 m/s.

The preferential flow along plant-root holes and fissures probably caused complete saturation of surrounding soils as was observed at the northern bottom part of the western trench. Water probably flowed into plant-root holes and spread laterally, causing complete saturation of the soil matrix. Flow along fissures was observed in the bottom parts of the western trench. The flow rate could not be measured. Failure of blocks of soil occurred along fissure planes. No other preferential flow was observed in spite of many root-holes along the trench wall.

No preferential flow could be observed at Experiment 2 from the trench wall, excavated near the point of infiltration. The soil was completely saturated. Failure of soil blocks occurred along fissure planes. This suggests preferential flow along these planes.

No preferential flow was observed at Experiment 4 after the inner-ring was filled with water. However, water flow along a plant-root hole was observed within one hour after the inner-ring was filled for the second time. The root hole had a diameter of 5 mm at a depth of 1.10 m. The flow rate was too low to be measured. Within 24 hours, flow along the root hole ceased. No further flow along preferential pathways was observed. The infrequency of flow along the root hole highlighted the dynamic nature of water flow along preferential pathways. The water possibly flushed a soil plug out of its way and water began to flow into the trench. Subsequent transportation of soil particles created another soil plug and water ceased to flow. The complicated nature of water flow can cause difficulties in predicting water flow through macropores.

Tracer tests conducted at Experiment 4 proved that the tracer infiltrated about 15 mm into the soil. The dye was adsorbed strongly by the soil matrix. No macro structures could be identified and no dye was observed along plant-roots, suggesting that no flow of dye took place along preferential pathways.

No preferential flow was observed at Experiment 5.

CHAPTER 6

PREDICTIONS OF GEOHYDROLOGICAL PARAMETERS BASED ON EXPERIMENTAL RESULTS

Based upon data from the literature, the results of laboratory experiments and the results of field experiments, the following correlations were investigated:

- Estimation of porosity from soil profile descriptions, soil-classification tables and empirical equations
- Estimation of saturated hydraulic conductivity from soil profile descriptions, soil-classification tables, empirical equations and soil-water retention characteristics
- Analyses of the various functions describing the soil-water characteristic curve
- Estimation of the unsaturated hydraulic conductivity from empirical equations and soil-water characteristic curves

6.1 Estimations of porosity

Predictions of porosity were made, based on the descriptions of the soil consistency of the various layers at the five experimental sites (Refer to Chapter 4 and Tables 4.1 and 4.2). The predictions of porosity based on soil profile descriptions are summarised in **Table 6.1,** indicating the consistency described for the various horizons.

Table 6.1: Prediction of porosity from soil profile descriptions

Horizon	Description	Predicted porosity	Actual porosity	Prediction
Experiments 1&2				
2	Firm	0.36 – 0.62	0.462	Within range, but wide range of predicted porosity
3	Firm	0.36 – 0.62	0.462	Within range, but wide range of predicted porosity
Experiment 4				
1	Very dense	< 0.34	0.34	Near upper limit
2	Loose	0.40 – 0.45	0.38	Not within range
Experiment 5				
2	Loose	0.40 – 0.45	0.437 – 0.482	Within range, near upper limit
3	Loose	0.40 – 0.45	0.437 – 0.482	Within range, near upper limit
4	Loose	0.40 – 0.45	0.437 – 0.482	Within range, near upper limit

With the exception of the second soil horizon at Experiment 4, accurate predictions of porosity were achieved. However, in the case of Experiments 1 and 2, a wide range of predicted porosity values were suggested, thus rendering predicted values of little use for practical purposes. The wide range was necessary because the consistency of fine-grained soils is influenced by the soil-water content at the time of inspection.

The methods of both Hazen (1930) and Istomina (1957) to predict porosity from the uniformity coefficient were developed for use in uniform soils with little fines. Unfortunately, many of the residual soils that were tested were well-graded with a high percentage of fines. These methods could therefore not be applied in these soils with any accuracy.

Predictions of porosity was made based on the soil textural chart (Schulze, 1995) and these were discussed in Chapter 4. The results are indicated in **Table 6.2**.

Table 6.2: Predicted porosity based on the soil textural chart (Schulze, 1995)

Description	Predicted porosity	Actual porosity	Comment
Experiments 1 and 2			
Silt Loam	0.50-0.53	0.462	Not within range
Silty Clay	0.48	0.462	Near predicted value
Silty Clay Loam	0.47-0.49	0.462	Near lower limit
Experiments 3 and 4			
Sandy Loam	0.47-0.49	0.34-0.38	Not within range
Experiment 5			
Sandy Loam	0.47-0.49	0.437-0.482	Within range

Porosity was under-estimated for most soils, with the exception of sandy loam at experiment 5. In the case of Experiments 1 and 2, the porosity was predicted within 2 to 6 per cent, indicating fairly reliable predictions. Predictions of porosity at experiments 3 and 4 were inaccurate.

6.2 Estimations of saturated hydraulic conductivity

6.2.1 Estimations based on soil profile descriptions and soil classification classes

Saturated hydraulic conductivities were predicted from the soil type description of different residual soils. These predictions were based on the tables compiled by Mathewson (1981). These values were compared to the saturated hydraulic conductivity values, derived from *in situ* LDDRI experiments. The predicted saturated hydraulic conductivity values are summarised in **Table 6.3.**

The measured saturated hydraulic conductivity fell within the predicted range for all residual soils with the exception of the clayey sand of Experiments 3 and 4. A wide range of predicted values is implied for most soil types, especially well-graded sand as found at Experiment 5, thereby significantly limiting its applicability to most hydrogeological investigations.

Table 6.3: Predicted saturated hydraulic conductivity based on soil profile descriptions

Description	Predicted K_s (m/s)	Actual K_s (m/s)	Comment
Experiments 1 and 2			
Silt	$10^{-6} - 10^{-9}$	2.18×10^{-9}	Within range along lower limit
Low plasticity Clay	$10^{-8} - 10^{-11}$	2.18×10^{-9}	Within range
Experiments 3 and 4			
Silty sand	$10^{-6} - 10^{-8}$	5.9×10^{-7}	Within range
Clayey Sand	$10^{-7} - 10^{-9}$	5.9×10^{-7}	Near upper limit
Experiment 5			
Well-graded sand	$10^{-3} - 10^{-7}$	1.91×10^{-6}	Within range, wide range of predicted values

After geotechnical laboratory tests had been conducted on the soil samples, the samples were classified according to the USCS system. Based on this classification, saturated hydraulic conductivities were predicted based on research by Mathewson (1981). The results are summarised in **Table 6.4**:

Table 6.4: Predicted saturated hydraulic conductivity based on USCS soil groups

USCS group	Predicted K_s (m/s)	Actual K_s (m/s)	Comment
Experiments 1 and 2			
CH	$10^{-11} - 10^{-9}$	2.18×10^{-9}	Near upper limit
MH	$10^{-9} - 10^{-7}$	2.18×10^{-9}	Within range along lower limit
Experiment 3 and 4			
SW	$10^{-3} - 10^{-7}$	5.9×10^{-7}	Within range along lower limit
SC	$10^{-7} - 10^{-9}$	5.9×10^{-7}	Near upper limit
Experiment 5			
SC	$10^{-7} - 10^{-9}$	1.91×10^{-6}	Not within range

In general, saturated hydraulic conductivities were not accurately predicted. In the case of CH at Experiment 1 and 2, SC at Experiments 3 and 4 and SC at Experiment 5, saturated hydraulic conductivities were not accurately predicted. In the case of SW at Experiments 3 and 4, a wide range of saturated hydraulic conductivity values were suggested, thereby limiting its applicability in field situations. The reason for these discrepancies can be attributed to the way soil is classified. The USCS system was developed to classify soils according to their geotechnical behaviour, especially with regard to their strength characteristics, not necessarily according to their hydrogeological behaviour. Better predictions of saturated hydraulic conductivity can be derived from soil profile descriptions.

Saturated hydraulic conductivity was predicted based on the soil-textural chart and research by Schulze (1995). The results are indicated in **Table 6.5**.

Table 6.5: Predicted saturated hydraulic conductivity based on the soil textural chart (Schulze, 1995)

Description	Predicted K_s (m/s)	Actual K_s (m/s)	Comment
Experiments 1 and 2			
Silt Loam	1.25×10^{-6} - 2.89×10^{-6}	2.18×10^{-9}	Not within range
Silty Clay	2.50×10^{-7} - 5.56×10^{-8}	2.18×10^{-9}	Near lower limit
Silty Clay Loam	4.17×10^{-7} - $.94 \times 10^{-7}$	2.18×10^{-9}	Not within range
Experiments 3 and 4			
Sandy Loam	1.23×10^{-5} - 7.22×10^{-6}	5.9×10^{-7}	Not within range
Experiment 5			
Sandy Loam	1.23×10^{-5} - 7.22×10^{-6}	1.91×10^{-6}	Near lower limit

The saturated hydraulic conductivity was over-estimated for all soils. In the case of Experiments 1 and 2, saturated hydraulic conductivity was overestimated by a factor of 25 to 1 300. In the case of Experiments 3, 4 and 5, predictions of saturated hydraulic conductivity were more accurate with over-estimations by factors of 4 to 21 recorded. Compared to the results of soil profile descriptions and USCS groups, the values exhibit not as wide range of saturated hydraulic conductivity values and are therefore more reliable.

6.2.2 Empirical equations based on soil fractions

Various empirical equations had been developed (as discussed in Chapter 4) to predict the saturated hydraulic conductivity from sand, silt and clay fractions (soil texture data). In order to assess the reliability of these relationships, the equations have been applied to a wide range of literature-based soil data. A total of 26 data points, representing soils ranging from clay to sand, were applied to the Campbell (1985), Campbell and Shiozawa (1992), and Rawls *et al.* (1982) empirical equations.

In addition, the above-mentioned equations were applied to soil samples obtained from the three experimental sites. The saturated hydraulic conductivity of 13 laboratory samples was determined.

The predicted data were compared to experimentally determined saturated hydraulic conductivity. The results are shown in **Figure 6.1** and the coefficients of correlation are as follows:

Campbell (1985): 0.435

Campbell and Shiozawa (1992): -0.095

Rawls *et al.*(1982): 0.424

Poor correlation coefficients was achieved for the Campbell (1985) and Rawls *et al.* (1982) equations while it appears that no correlation exists in the case of the Campbell and Shiozawa (1992) equation. However, the authors stress the fact that these equations are not valid for all soil types, as confirmed by the results of their investigations.

Better correlation coefficients could be obtained in the case of sand, silty sand and clayey sand, since all these equations have been developed for these soil types. Rawls *et al.* (1982) achieved a correlation coefficient of 0.65 for the soils from which they derived the empirical equation, based on multiple regression techniques. Saturated hydraulic conductivity is greatly influenced by relatively small amounts of silt and clay and the conductivity potential of soils is influenced by the packing and the location of silt and clay in respect of pore connection points.

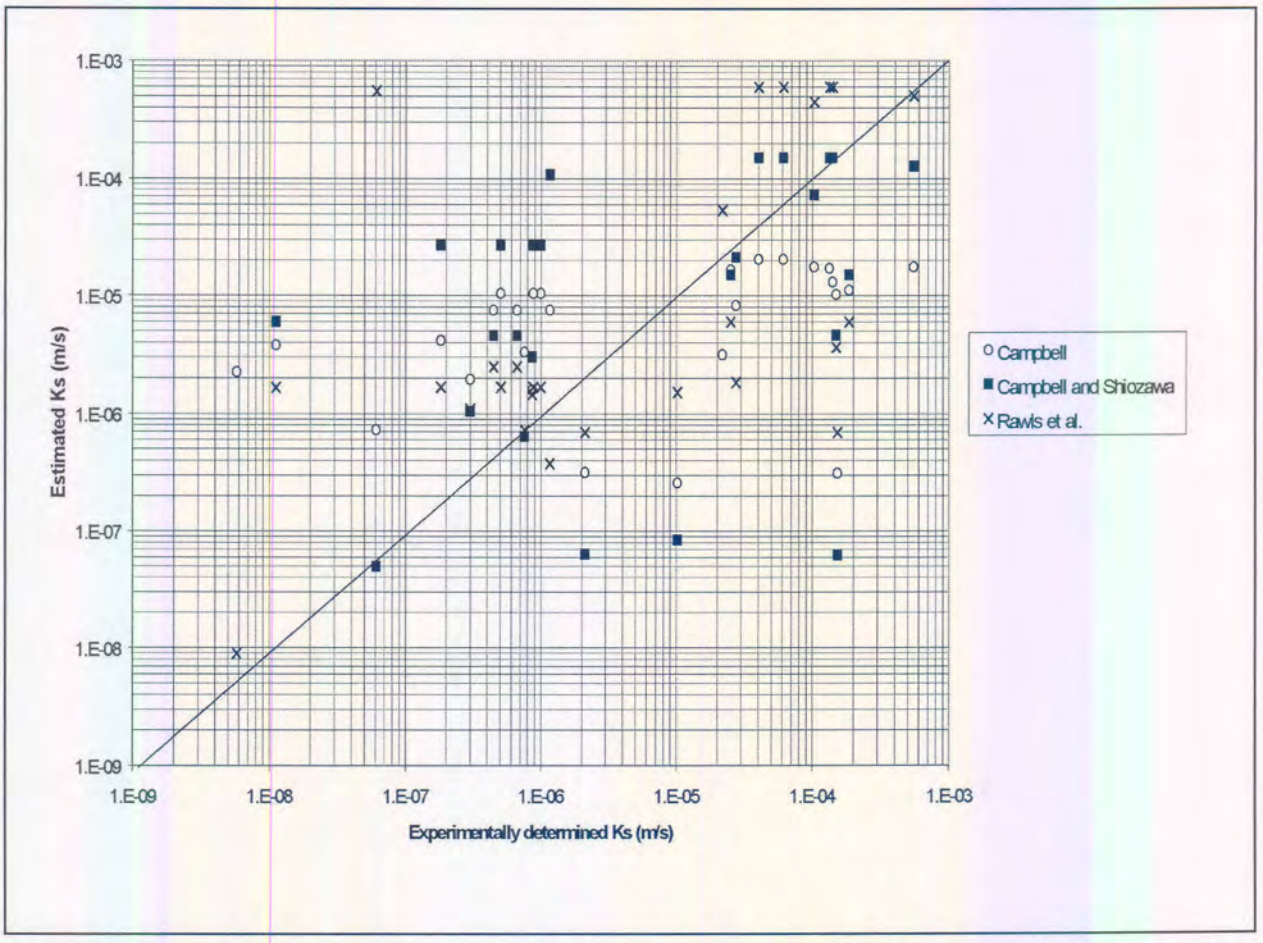

Figure 6.1: Correlation between measured and predicted saturated hydraulic conductivity based on soil fractions

In Chapter 4, it was stated that the parameter, *a*, represents factors such as the shape of grains and grain packing, and this parameter is usually determined from experimental results. Wide ranges of this parameter may indicate inherent inaccuracies of the empirical model. Values of *a* were determined from field experiments and these were compared to the recommended values as derived by the developers of these equations. The results are summarised in **Table 6.6**

Table 6.6: Experimentally derived value and variability of empirical parameter, *a* for popular empirical equations

	Campbell (1985)	Campbell and Shiozawa (1992)	Rawls et al. (1982)
Average value of *a* derived from the experimental sites	2.74×10^{-6}	$5.46 \times ^{-7}$	9.90×10^{-7}
Proposed value for *a*	ND	1.50×10^{-5}	2.78×10^{-6}
Coefficient of variability	114%	126%	120%

Table 6.6 indicates large variations of the empirical parameter, *a*. This indicates that large variations in predicted saturated hydraulic conductivity could occur if the said equations are applied indiscriminately to any soil type. The predicted saturated hydraulic conductivity derived from these equations should therefore be used with caution.

In the case of the Campbell and Shiozawa (1992) equation, the experimentally determined value of parameter *a* differs considerably from that proposed by Campbell and Shiozawa (1992), indicating further

uncertainty about the value of *a*. However, the value proposed by Rawls *et al.* (1982) in their equation is very similar to that determined experimentally, probably indicating a more representative value of *a*.

6.2.3 Empirical equations based on particle-size distribution curves

Literature-based studies

Vukovic and Soro (1992) found that, in the case of fine- to coarse-grained sandy materials, relatively good predictions of saturated hydraulic conductivity could be obtained from the Hazen (1930), Beyer, Sauerbrei and Zunker (Vukovic and Soro, 1992) equations. However, large deviations were recorded in the case of the gravelly sand material, and the equations generally underestimated the saturated hydraulic conductivity. The empirical equations had been developed for sandy materials, characterised by low quantities of fines (generally less than 10 per cent) and a relatively high degree of uniformity (generally less than 5 per cent).

Ten of the fourteen empirical equations under investigation were compared to actual saturated hydraulic conductivity values based on the data from Amer and Awad (1974). In their experiment, Amer and Awad derived an empirical equation from artificially separated soil groups. Basic characteristics of the soil groups are shown in **Table 6.7**. The saturated hydraulic conductivity of each soil group was determined.

Table 6.7: Basic characteristics of the soil groups prepared by Amer and Awad, 1974

	Group 1	Group 2	Group 3	Group 4
d_5 (mm)	0.100 to 0.137	0.171	0.403	0.349 to 0.411
d_{10} (mm)	0.137	0.274	0.460	0.548
d_{17} (mm)	0.137 to 0.141	0.276	0.461	0.553
d_{20} (mm)	0.137 to 0.384	0.438	0.552	0.877
C_u	1 to 21	1 to 5	1 to 5	1 to 4
ε	K determined at 0.293, 0.349, 0.385, 0.411 for each soil group			

The ten empirical equations were applied to each soil group and the saturated hydraulic conductivities were calculated. A large degree of scattering was observed. However, on closer inspection it was observed that some calculated values were strongly correlated to the measured saturated hydraulic conductivity values. A correction factor was calculated for each empirical equation:

$$Correction\ \ factor = \frac{Average\ \ calculated\ \ K}{Experimentally\ \ determined\ \ K} \qquad [6\text{-}1]$$

The correction factor is an indication of the accuracy of the different equations in respect of the different soil groups. A correction factor close to unity indicates accurate predictions of saturated hydraulic conductivity. The correction factors for the ten empirical equations are indicated in **Table 6.8,** varying between 2 and 4 for most equations. The exceptions are the Shahabi *et al.* (1984) and Kenney *et al.* (1984) equations where correction factors of 215 and 22 respectively have been calculated.

Figure 6.2 shows the relationship between experimentally derived and calculated values after the correction factor has been considered. **Figure 6.2** indicates the correlation between calculated and experimentally derived saturated hydraulic conductivity for the ten equations under investigation. In addition, the coefficients of correlation are indicated in **Table 6.8.**

Table 6.8: Correction factors and coefficients of correlation for ten empirical equations

Equation	Correction factor	Coefficient of correlation
Hazen (1930)	3.21	0.7140
Amer and Awad (1974)	1.03	0.9950
Shahabi *et al.* (1984)	215	0.9934
Kenney *et al.* (1984)	22.4	0.8516
Slichter (Vukovic & Soro, 1992)	2.46	0.8701
Terzaghi (Vukovic & Soro, 1992)	2.49	0.8725
Beyer (Vukovic & Soro, 1992)	7.09	0.6099
Sauerbrei (Vukovic & Soro, 1992)	2.93	0.8808
Pavchich (Pravednyi, 1966)	3.89	0.9783
USBR (Vukovic & Soro, 1992)	0.60	0.8119

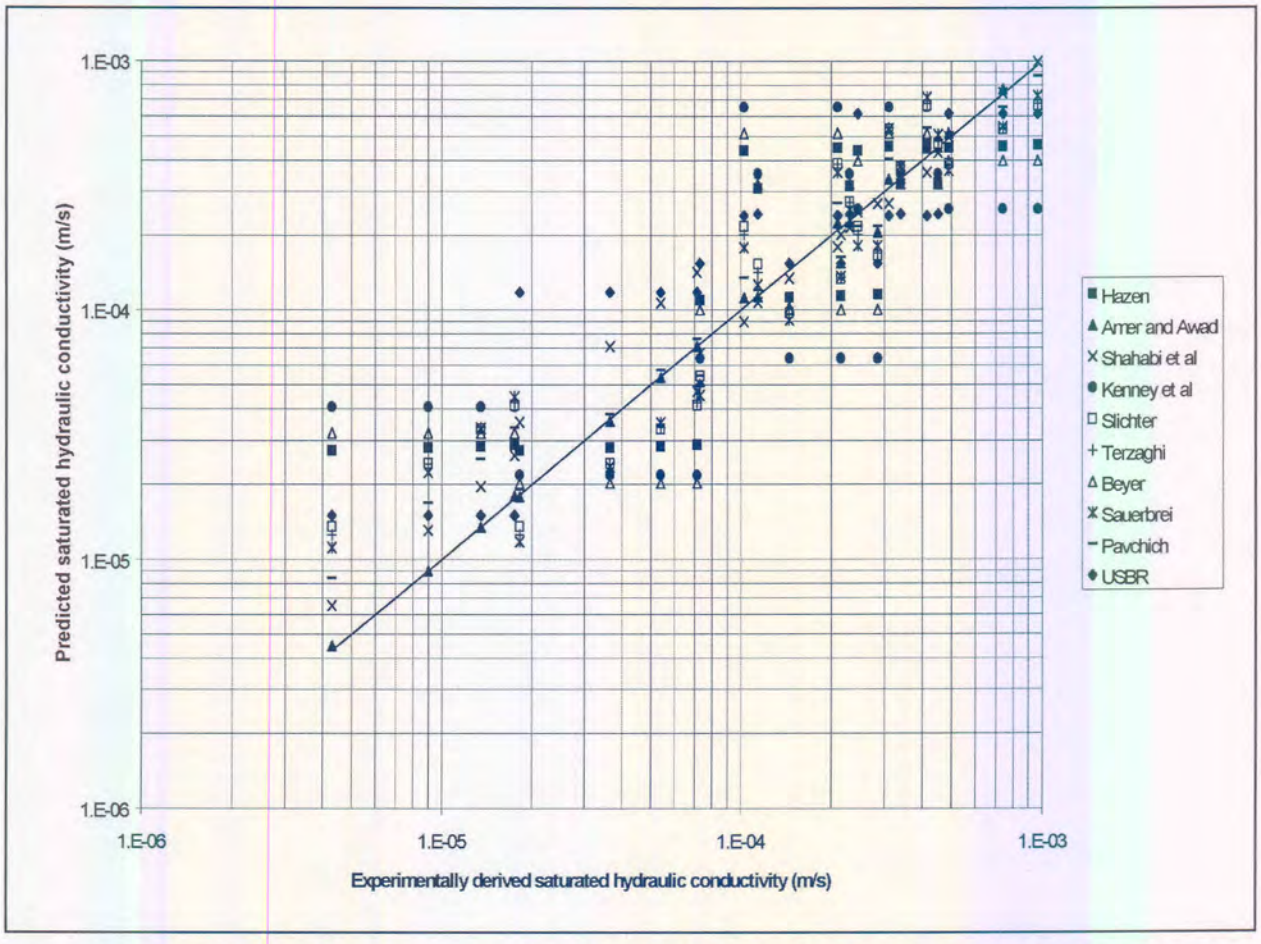

Figure 6.2: Correlation between measured and predicted saturated hydraulic conductivity based on particle size distribution

Equations which incorporate the effect of gradation result in better correlation with saturated hydraulic conductivity. The coefficient of uniformity gives an indication of gradation. The Amer and Awad (1974), Shahabi *et al* (1984), Beyer (Vukovic & Soro, 1992) and Pavchich (Pravednyi, 1966) equations express saturated hydraulic conductivity partly as a function of the coefficient of uniformity. In all of these equations, with the exception of the Beyer equation, a correlation coefficient of more than 0.97 was obtained. The low coefficient of correlation achieved for the Beyer equation could be caused by the fact that the porosity is not considered in this equation.

Experimental studies

Saturated hydraulic conductivity values were derived from the particle-size distributions for residual soils at Experiments 3, 4 and 5. The results of the particle size distributions were applied to ten widely used empirical equations. Predicted saturated hydraulic conductivities were compared to values derived experimentally from *in situ* tests. The results are indicated in **Table 6.9**:

Table 6.9: Predicted saturated hydraulic conductivity for Experiments 3, 4 and 5

Function	Experiment 3 (n=5)		Experiment 5 (n=3)	
	Median K_s (m/s)	Under (-)/Over (+) estimation factor	Median K_s (m/s)	Under (-)/Over (+) estimation factor
Hazen (1930)	2.37×10^{-7}	-2.49	1.25×10^{-7}	-15.23
Amer and Awad (1974)	2.06×10^{-7}	-2.86	2.42×10^{-7}	-7.91
Shahabi *et al* (1984)	4.25×10^{-4}	+721	5.80×10^{-4}	+304
Kenney *et al* (1984)	1.22×10^{-6}	+2.07	1.95×10^{-7}	-9.79
Slichter (Vukovic & Soro, 1992)	1.94×10^{-7}	-3.10	1.91×10^{-7}	-9.98
Terzaghi (Vukovic & Soro, 1992)	1.42×10^{-7}	-3.04	1.99×10^{-7}	-9.59
Beyer (Vukovic & Soro, 1992)	1.42×10^{-7}	-4.17	8.95×10^{-8}	-21.33
Sauerbrei (Vukovic & Soro, 1992)	9.05×10^{-5}	+153	8.71×10^{-5}	+45.6
Pavchich (Pravednyi, 1966)	4.61×10^{-4}	+781	4.29×10^{-4}	+225
USBR (Vukovic & Soro, 1992)	1.95×10^{-5}	+33.07	7.38×10^{-6}	+3.86

The results indicate that large variations (up to a factor of 750) of predicted saturated hydraulic conductivity were obtained. This can be attributed mainly to the fact that all of the developed empirical equations had been developed for uniform sandy soils with little fines. However, in the case of the residual granites investigated, the soils mainly comprise silty, well-graded sand.

Better predictions were derived from the Amer and Awad equation (1974) while the Pavchich (Pravednyi, 1966) and Shahabi *et al.* (1984) equations yielded poor predictions. The poor predictions from the Pavchich equation can be attributed to the fact that the equation had been developed for use in uniform sandy soil and that predicted saturated hydraulic conductivity values are sensitive to the uniformity coefficient.

Average and median predicted saturated hydraulic conductivities, for the ten empirical equations investigated, are indicated in **Table 6.10**. The table indicates that although large variations in predicted saturated hydraulic conductivity were recorded for the various equations, experimentally derived saturated hydraulic conductivity was predicted reasonably accurately for residual soils at Experiments 3 and 4. The large variation in predicted saturated hydraulic conductivity suggests that soil properties other than particle-size distribution and porosity could cause an uncertainty of up to two orders of magnitude for predicted saturated hydraulic conductivity. However, the large variations can also be attributed to the equations' inability to accurately predict saturated hydraulic conductivity as a function of particle-size distribution for a wide range of soil types.

Table 6.10: Predicted saturated hydraulic conductivity for Experiments 3, 4 & 5 based on ten empirical functions

	Experiment 3 & 4	Experiment 5
Average K_s (m/s) (All functions)	1.16×10^{-4}	1.09×10^{-4}
Median K_s (m/s) (All functions)	6.27×10^{-7}	2.73×10^{-7}
***In situ* determined K_s (m/s)**	5.90×10^{-7}	1.91×10^{-6}
Over (+)/under (-) estimation of K_s	+ 2.78	- 7.71
Coefficient of variability (%)	200.8	199.9

As is the case with equations predicting saturated hydraulic conductivity from soil fractions, the generic empirical equation can be expressed as:

$$K_s = a_{gsd} \cdot f(D_e, C_u, \varepsilon) \qquad [6\text{-}2]$$

where D_e, C_u and ε represent effective grain diameter, uniformity coefficient and porosity respectively. The parameter a_{gsd} is a constant and reflects factors other than particle-sizes with an effect on saturated hydraulic conductivity such as the shape of the grains and packing. It is related to the parameter a of empirical equations based on soil fractions. The parameter, a_{gsd}, is derived experimentally and wide ranges of the value could reflect inherent errors regarding the empirical function. In these cases, the parameter will not be a constant, but will vary according to different soil types. The more parameter a_{gsd} varies with regard to different soil types, the greater the inherent errors of the empirical equation.

Table 6.11 indicate the value of parameter a_{gsd} as indicated in literature (a_{gsd}), derived from experiments by Amer and Awad (1974) (a_{gsd1}) and from data collected at Experiments 3 and 5 respectively (a_{gsd3} and a_{gsd5}).

Table 6.11: Experimentally derived values of parameter a_{gsd}

	a_{gsd}	a_{gsd1}	a_{gsd3}	A_{gsd5}	Coefficient of variation
Hazen (1930)	4.72×10^{-9}	1.47×10^{-9}	1.17×10^{-8}	7.19×10^{-8}	147.97
Amer and Awad (1974)	9.54×10^{-9}	9.54×10^{-9}	2.73×10^{-8}	7.54×10^{-8}	102.69
Shahabi *et al* (1984)	1.20×10^{-6}	5.59×10^{-9}	1.66×10^{-9}	3.95×10^{-9}	197.53
Kenney *et al* (1984)	5.00×10^{-8}	2.24×10^{-9}	2.42×10^{-8}	4.90×10^{-7}	164.57
Slichter (Vukovic & Soro, 1992)	1.04×10^{-7}	4.21×10^{-8}	3.21×10^{-7}	1.04×10^{-6}	121.35
Terzaghi (Vukovic & Soro, 1992)	5.00×10^{-2}	2.01×10^{-2}	1.52×10^{-1}	4.80×10^{-1}	119.94
Beyer (Vukovic & Soro, 1992)	4.62×10^{-9}	6.51×10^{-10}	1.92×10^{-8}	9.84×10^{-8}	149.15
Sauerbrei (Vukovic & Soro, 1992)	3.58×10^{-8}	1.22×10^{-8}	2.33×10^{-10}	7.85×10^{-10}	135.75
Pavchich Pravednyi, 1966)	3.58×10^{-9}	9.20×10^{-9}	4.58×10^{-11}	1.59×10^{-10}	149.42
USBR (Vukovic & Soro, 1992)	4.92×10^{-10}	8.22×10^{-10}	1.49×10^{-11}	1.27×10^{-10}	100.79

Table 6.11 shows that the value of parameter a_{gsd} varies greatly for all empirical equations investigated. It indicates that the equations may not be suitable to accurately predict the saturated hydraulic conductivity. The equations showing the least variation are the USBR (Vukovic & Soro, 1992) and Amer and Awad (1974) equations. It indicates that these equations probably offer the most reliable method for predicting saturated hydraulic conductivity for the soils tested. However, these equations still result in highly variable predictions of saturated hydraulic conductivity that may vary by up to one order of magnitude. The equations showing the highest variation include the Shahabi *et al.* (1984) and Kenney *et al* (1984) equations. However, with regard to the Shahabi *et al.* (1984) equation, where the value of parameter a_{gsd} has been derived experimentally from data of Amer and Awad (1974), Experiment 3 and Experiment 5 differ remarkably from those proposed in literature. An incorrect value of a_{gsd} could possibly have been quoted in the literature.

Experimental studies: Fine-grained soils

Saturated hydraulic conductivity is predicted on the basis of the Atterberg limits by applying the method proposed by Tavenas *et al.* (1983a). This method is described in Chapter 4. Because the method is only valid for fine-grained soils, i.e. soils with significant clay content, it was only applied for residual soils at Experiments 1 and 2. The parameter, I_c, a function of both clay content and total PI, was determined for eight soil samples. With the void ratio known, the values were plotted on the diagram as proposed by Tavenas *et al.* and are shown in **Figure 6.3** indicating predicted saturated hydraulic conductivity. The parameter, I_c, and the predicted saturated hydraulic conductivity were statistically analysed and are shown in **Table 6.12**.

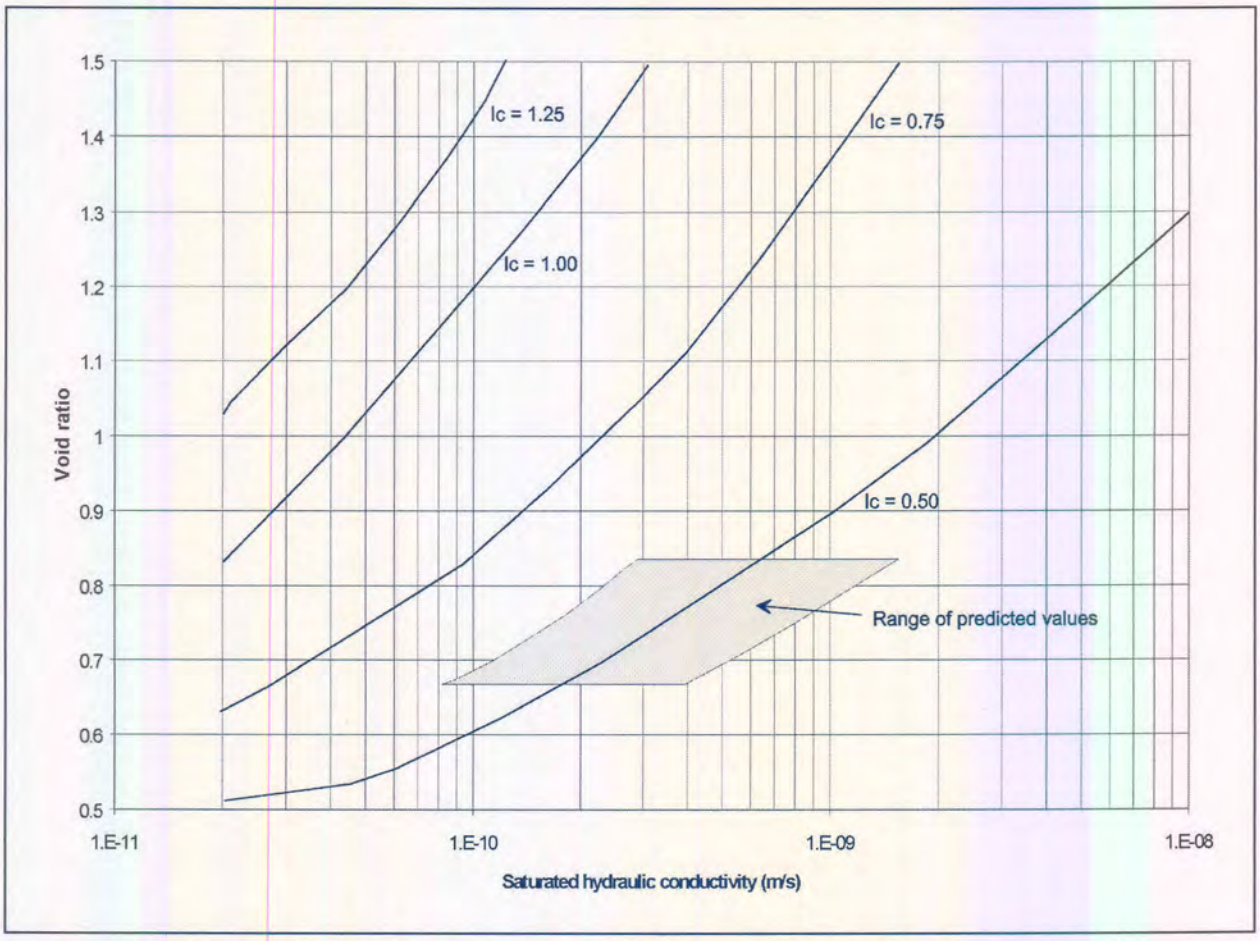

Figure 6.3: Predicted saturated hydraulic conductivity based on Atterberg limits

Table 6.12: Statistical analysis of predicted saturated hydraulic conductivity and parameter, I_c

		Saturated hydraulic conductivity (m/s)	Parameter I_c
Predicted values	Average	7.35×10^{-10}	0.51
	Median	8.05×10^{-10}	0.54
	Maximum	$>1.00 \times 10^{-9}$	0.63
	Minimum	3.70×10^{-10}	0.33
	Coefficient of variation (%)	39.24	21.90
In situ derived median value		2.18×10^{-9}	NA
Sample size		8	8

Predicted saturated hydraulic conductivity values compare well with experimentally derived saturated hydraulic conductivity values as determined by LDDRI tests. The saturated hydraulic conductivity was under-estimated by a factor of about three, which is acceptable, given the large natural spatial variation of saturated hydraulic conductivity. In addition, the variation of predicted saturated hydraulic conductivity is acceptable and compares well with other predictive techniques. The variation of predicted saturated hydraulic conductivity values is similar to the variation of the parameter, I_c, for the eight soil samples analysed.

6.2.4 Predictions of saturated hydraulic conductivity based on soil-water retention data

Various empirical equations have been developed to estimate the saturated hydraulic conductivity from water retention data. These equations were discussed in Chapter 4. In order to assess the reliability of these relationships, the equations were applied to a wide range of literature-based soil data. The data used in the analysis of empirical equations related to soil fraction were also used in this analysis. A total of 26 data points, representing soils ranging from clay to sand, were applied to the Ahuja *et al.* (1985) equation. A correlation coefficient of –0.00165 was achieved, indicating very poor relationship.

In addition to the Ahuja *et al.* (1985) equation, the Brutsaert (1967) and Campbell (1985) equations were applied to five soil types, ranging from sand to clay. The Brooks and Corey (1964) equation was applied to water retention data for the five soil types and the Brooks and Corey pore-size index, residual water content and air-entry values were determined by non-linear regression techniques. These parameters were applied to the Brutsaert (1967) and Campbell (1985) equations and the saturated hydraulic conductivity was determined.

The results indicate very poor correlation between water retention data and saturated hydraulic conductivity, and correlation coefficients of –0.05 and –0.096 respectively were achieved for the Brutsaert (1967) and Campbell (1985) equations.

6.3 Description of the soil-water characteristic curve

Several mathematical functions had been developed to describe the soil-water characteristic curve and these were discussed in Chapter 4. The indirect determination of unsaturated hydraulic conductivity entails integration of these functions. The various models developed to determine unsaturated hydraulic conductivity were also discussed in Chapter 4. Reliable estimations of unsaturated hydraulic conductivity are only possible on condition that these mathematical functions accurately describe the soil-water characteristic curve. Since the soil-water characteristic curve could be either exponential or sigmoidal in shape (depending on the type of soil), the development of a single function that is valid for all soil-water characteristic curve shapes is difficult.

Four popular functions, which describe the soil-water characteristic curve, were tested for five different soil types. The functions applied were:

- The Gardner (1958) function
- The Brooks and Corey (1964) function
- The Van Genuchten (1980) function
- The Fredlund and Xing (1994) function

These functions were applied to soil-water retention data obtained from the literature. Five data sets were selected for further analysis, namely:

- Sand consisting of 0.5 mm to 0.25 mm sand fraction as prepared by Childs and Collis-George (1950) as part of their research for the development of the Childs and Collis-Geoge model to derive unsaturated hydraulic conductivity from soil-water retention data
- Fine sand consisting of soil with grain sizes ranging from 0.8 to 0.05 mm (Vachaud, Gandet & Kuraz, 1974)
- Silty clayey sand (sandy loam) as Elzeftawy and Dempsey (1976) used in their research on steady state-flow in materials for subgrade layers on roads
- Sandy clay-silt (Guelph loam) from the research conducted by Elrick and Bowman (1964)
- Clay consisting of soil with a clay percentage greater than 48 from the research of Neuman, Feddes & Besler (1974)

Curve fitting was conducted by determining the minimum total of squared residual (SSR) values for the functions. The Generalised Reduced Gradient non-linear optimisation algorithm was applied to determine minimum SSR values. The results compared well to curve fitting by applying the Marquardt-Levenberg non-linear optimisation algorithm. Both algorithms required initial values in order to determine optimum parameter values. These values were obtained by trial and error.

The results of the curve fitting are presented in **Figures 6.5** to **6.9** and in **Table 6.13**. Good fit is represented by low SSR values. In addition, correlation coefficients were determined to confirm good fit. SSR values were determined for low, medium and high volumetric water contents to assess the reliability of the functions over the entire soil-water retention range.

Table 6.13: Correlation between experimentally derived soil-water characteristic curves and their related functions

Soil type	Function	SSR at degree of saturation percentages				R^2
		(30%)	(60%)	(90%)	Entire range	
Sand	Gardner (1958)	5.32E-05	2.21E-05	1.65E-04	4.04E-03	0.99190
	Brooks and Corey (1964)	2.36E-05	1.85E-05	3.41E-02	1.89E-04	0.98543
	Van Genuchten (1980)	3.78E-04	5.00E-05	2.21E-05	2.29E-03	0.99657
	Fredlund and Xing (1994)	1.65E-05	5.04E-05	7.66E-06	3.83E-04	0.99923
Fine Sand	Gardner (1958)	3.37E-05	5.15E-05	8.60E-06	4.43E-04	0.99899
	Brooks and Corey (1964)	4.39E-06	1.79E-04	3.66E-02	9.42E-04	0.90465
	Van Genuchten (1980)	1.14E-05	3.03E-05	1.39E-06	2.38E-04	0.99947
	Fredlund and Xing (1994)	3.99E-05	3.77E-05	8.73E-07	5.10E-04	0.99896
Silty-clayey sand	Gardner (1958)	2.09E-05	1.81E-05	1.93E-05	3.89E-04	0.98710
	Brooks and Corey (1964)	1.16E-05	1.63E-04	1.73E-06	4.45E-04	0.98476
	Van Genuchten (1980)	1.97E-05	1.85E-05	2.10E-05	3.54E-04	0.98817
	Fredlund and Xing (1994)	2.31E-05	3.31E-05	2.13E-05	3.59E-04	0.98805
Sandy silt-clay	Gardner (1958)	3.28E-03	1.11E-03	3.23E-02	6.73E-02	0.94548
	Brooks and Corey (1964)	1.26E-05	1.13E-04	1.61E-05	4.31E-04	0.99927
	Van Genuchten (1980)	6.24E-08	4.59E-05	4.66E-05	4.29E-04	0.99928
	Fredlund and Xing (1994)	4.27E-04	2.97E-05	1.31E-03	3.22E-03	0.99518
Clay	Gardner (1958)	3.40E-04	3.64E-05	2.28E-06	1.61E-03	0.99836
	Brooks and Corey (1964)	3.42E-07	4.17E-05	3.25E-04	1.33E-03	0.97117
	Van Genuchten (1980)	7.20E-06	1.97E-04	1.07E-04	6.86E-04	0.99923
	Fredlund and Xing (1994)	1.60E-04	5.20E-05	4.07E-05	5.69E-04	0.99938
Ave-rage	Gardner (1958)	7.45E-04	2.48E-04	6.50E-03	1.48E-02	0.98437
	Brooks and Corey (1964)	1.05E-05	1.03E-04	1.42E-02	6.67E-04	0.96906
	Van Genuchten (1980)	8.34E-05	6.84E-05	3.96E-05	7.99E-04	0.99654
	Fredlund and Xing (1994)	1.33E-04	4.06E-05	2.75E-04	1.01E-03	0.99616

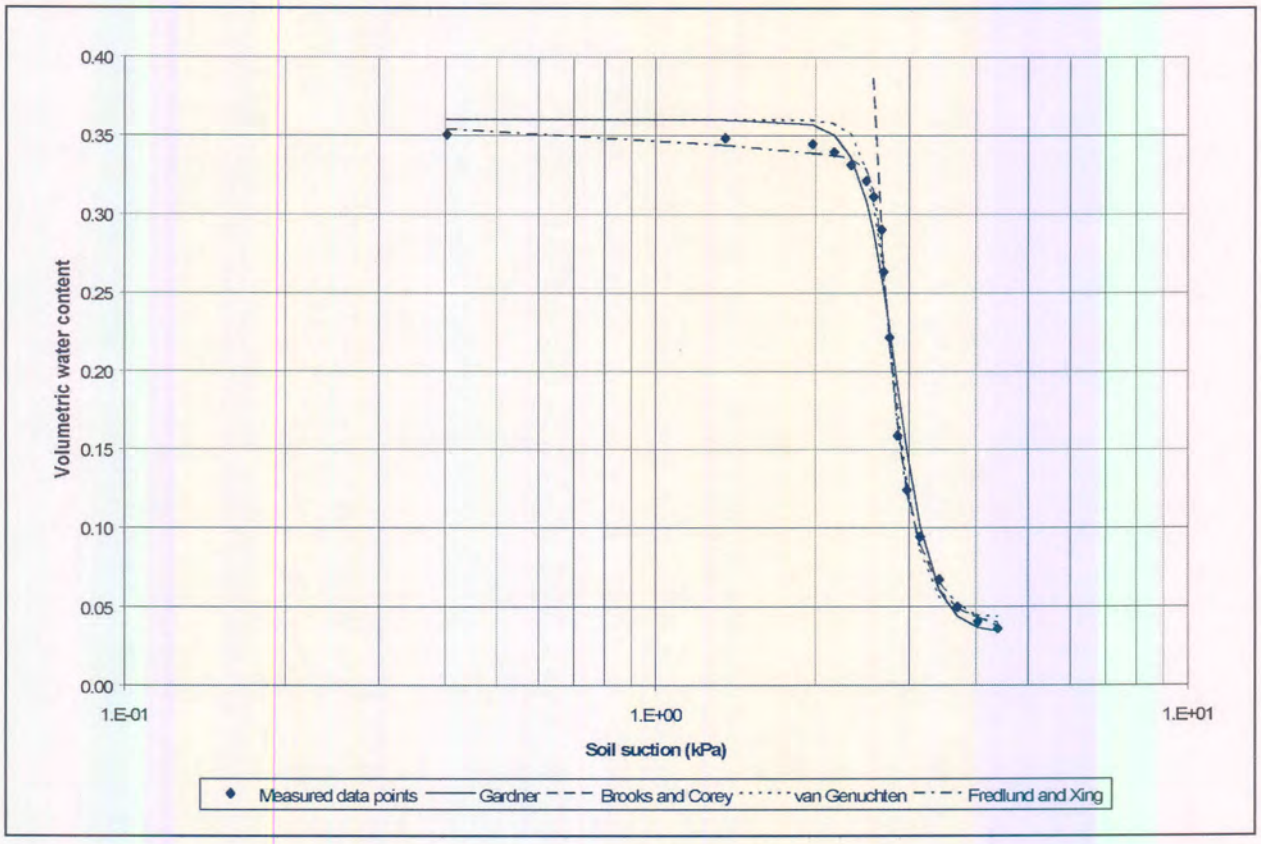

Figure 6.4: Description of the soil-water characteristic curve for sand

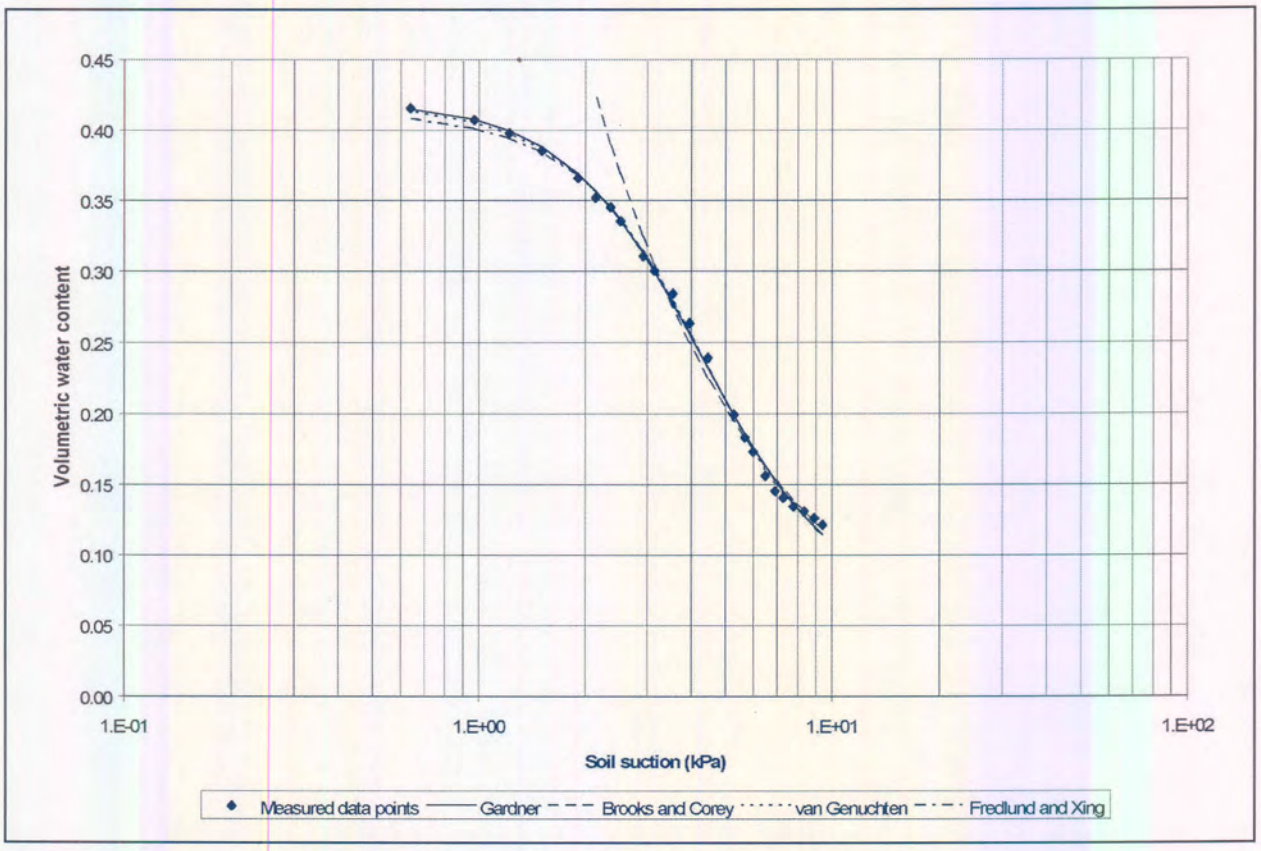

Figure 6.5: Description of the soil-water characteristic curve for fine sand

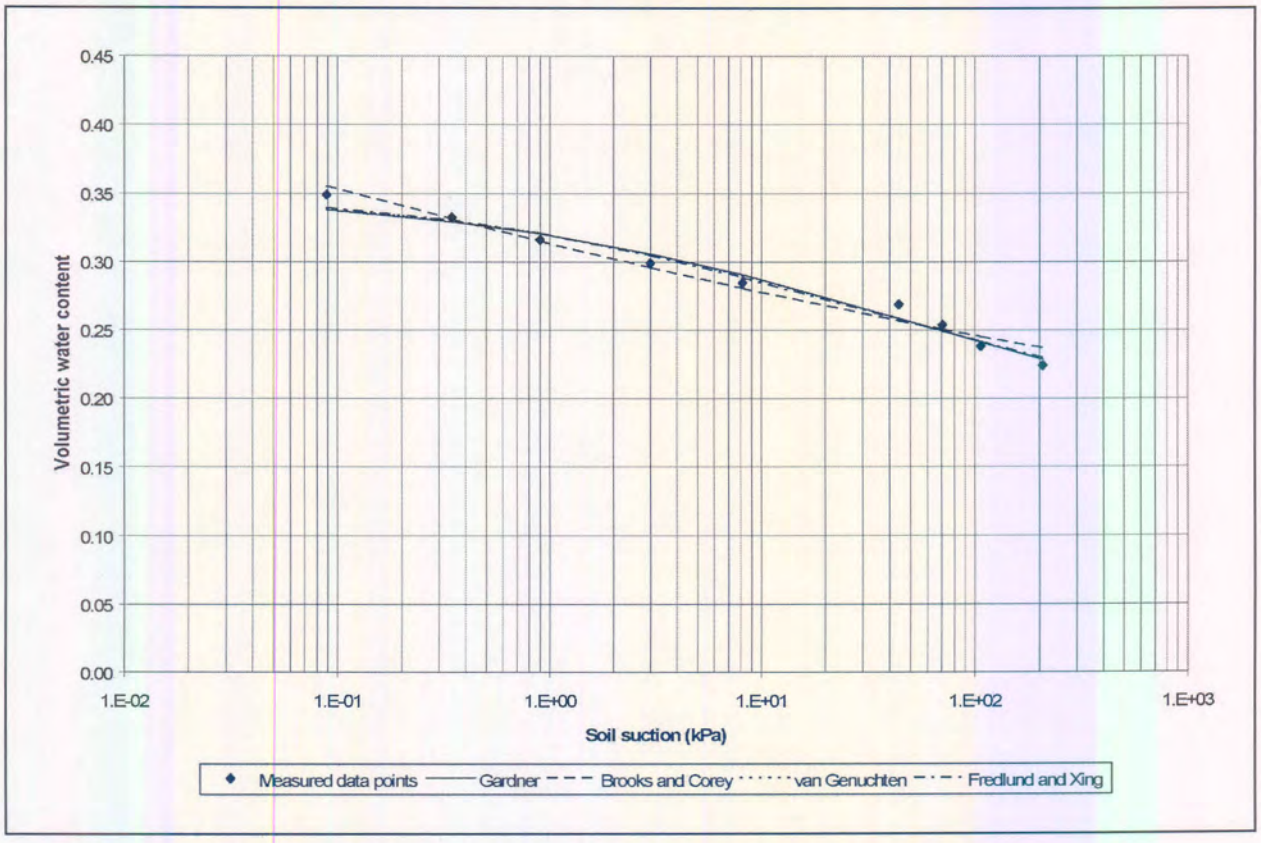

Figure 6.6: Description of the soil-water characteristic curve for silty clayey sand

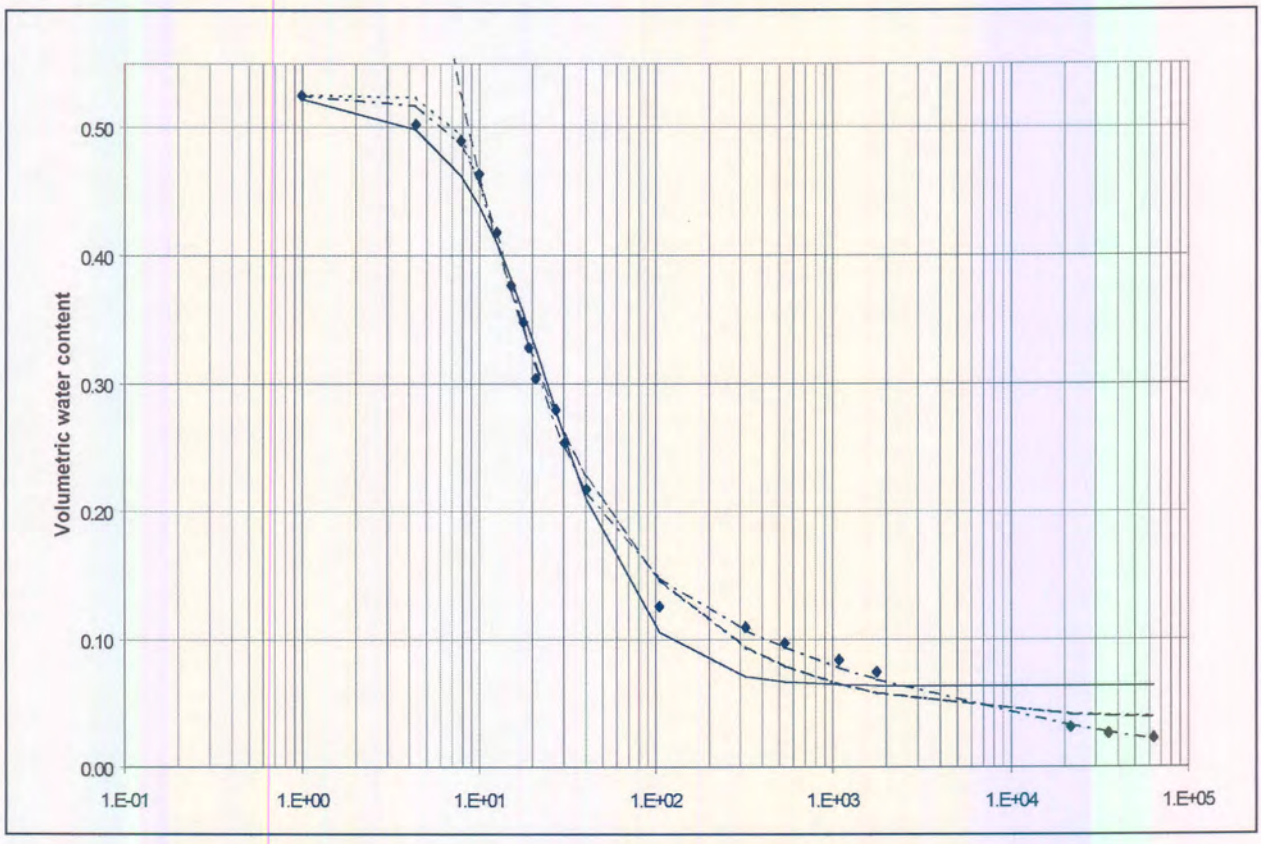

Figure 6.7: Description of the soil-water characteristic curve for sandy silt-clay

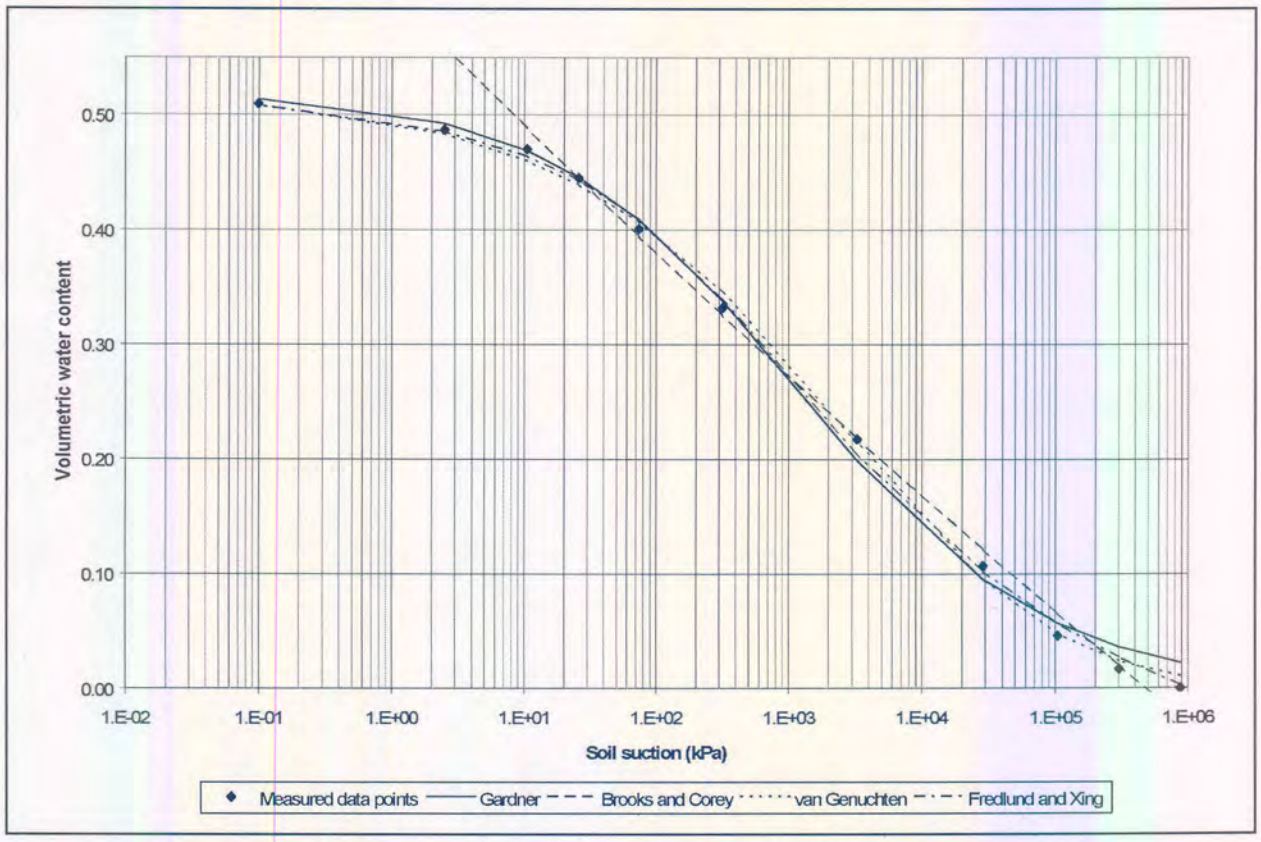

Figure 6.8: Description of the soil-water characteristic curve for clay

Good results were obtained for the four functions applied to the various soil-water retention data sets. Correlation coefficient values ranged from 0.99947 in the case of the Van Genuchten (1980) function applied to soil-water retention data for fine sand to 0.90465 in the case of the Brooks and Corey (1964) function applied to soil-water retention data for fine sand. The Gardner (1958), Van Genuchten (1980) and Fredlund *et al.* (1994) functions best describes sigmoidally shaped soil-water characteristic curves, while the Brooks and Corey (1964) function best describes exponentially shaped soil-water characteristic curves.

The Brooks and Corey (1964) model requires the air-entry value to be known in order to accurately describe the soil-water characteristic curve. Although the air-entry value is difficult to determine experimentally, it can be estimated from initial hand-drawn soil-water characteristic curves.

Good fit was obtained for all five soil-water retention data-sets. The high dependency values between the parameters *m* and *n* in both the Van Genucten (1980) and Fredlund *et al.* (1994) functions suggest that three parameters are probably adequate to describe most soil-water characteristic curves. This is confirmed by the good results obtained from both the Gardner (1958) and Brooks and Corey (1964) functions that only apply three parameters to describe the soil-water characteristic curve. Good results were also obtained by placing a restriction on the *m* parameter of the Van Genucten (1980) function by expressing it as a function of the parameter *n,* and thereby expressing the soil-water characteristic curve in terms of three unknown parameters. The restriction was necessary to obtain a closed function in order to estimate the unsaturated hydraulic conductivity. However, rather poor fit was obtained in the case of sandy silt-clay, as described by the Gardner (1958) function. This can be ascribed to the exponential shape of the specific soil-water characteristic curve while the Gardner (1958) function was developed to describe sigmoidally shaped soil-water characteristic curves. In contrast, best fit was derived by the Brooks and Corey (1964) function, developed to describe mainly exponentially shaped curves. The Brooks and Corey (1964) function was less accurate in estimating soil-water retention at higher suction values. The Brooks and Corey (1964) functions apply two functions to describe the soil-water

characteristic curve, depending on the air-entry value. This results in a kink in the curve at high soil suction levels, inconsistent with experimental data.

6.4 Estimation of the soil-water characteristic curve

6.4.1 Soil fractions

Soil water retention properties can be predicted from soil fractions, based on the methods proposed by Gupta and Larson (1979). This method was discussed in Chapter 4. Volumetric water contents were predicted at a number of soil suction values. These values were compared with measured soil-water characteristic curves as obtained from laboratory water retention tests. The results are presented in **Table 6.14** and **Figures 6.10** to **6.12.**

Table 6.14: Measured and predicted water content at six soil suction values

Soil suction (kPa)	Volumetric water content					Coefficient of variability (%)
	Measured	Average predicted	Median predicted	Maximum predicted	Minimum predicted	
Experiments 1 and 2						
4	0.331	0.482	0.490	0.492	0.456	3.58
10	0.283	0.430	0.441	0.444	0.396	5.35
33	0.237	0.386	0.399	0.412	0.335	8.94
60	0.218	0.365	0.379	0.396	0.308	10.75
100	0.202	0.348	0.361	0.382	0.287	12.07
1000	0.142	0.284	0.297	0.322	0.218	16.02
Experiments 3 and 4						
4	0.206	0.235	0.239	0.252	0.211	7.04
10	0.181	0.179	0.186	0.196	0.151	11.05
33	0.157	0.148	0.147	0.181	0.119	16.51
60	0.145	0.140	0.136	0.179	0.112	19.10
100	0.136	0.134	0.127	0.177	0.106	21.03
1000	0.095	0.106	0.095	0.155	0.082	28.27
Experiment 5						
4	0.428	0.347	0.350	0.354	0.338	2.39
10	0.396	0.271	0.275	0.278	0.260	3.53
33	0.318	0.205	0.209	0.210	0.194	4.49
60	0.266	0.178	0.183	0.183	0.168	4.93
100	0.222	0.159	0.163	0.164	0.149	5.31
1000	0.086	0.102	0.105	0.108	0.094	7.16

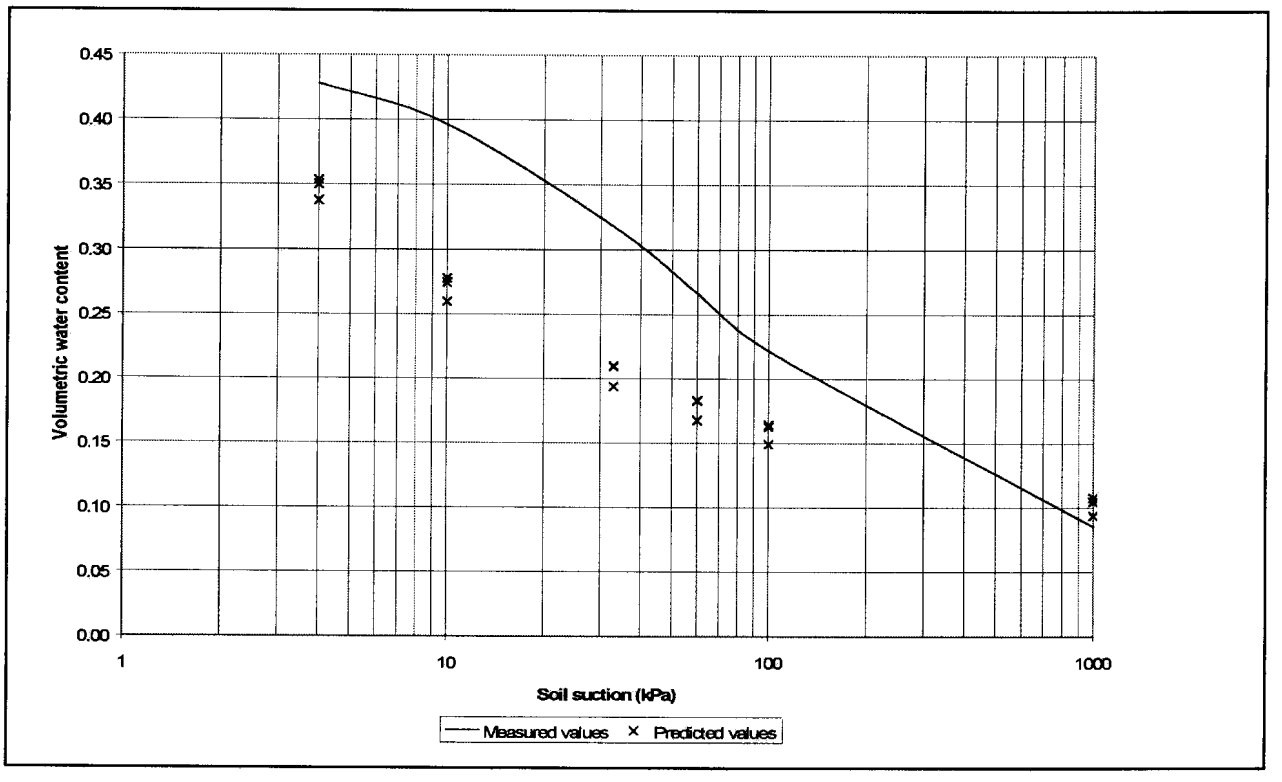

Figure 6.9: Correlation between the measured and predicted soil-water characteristic curve at Experiment 2

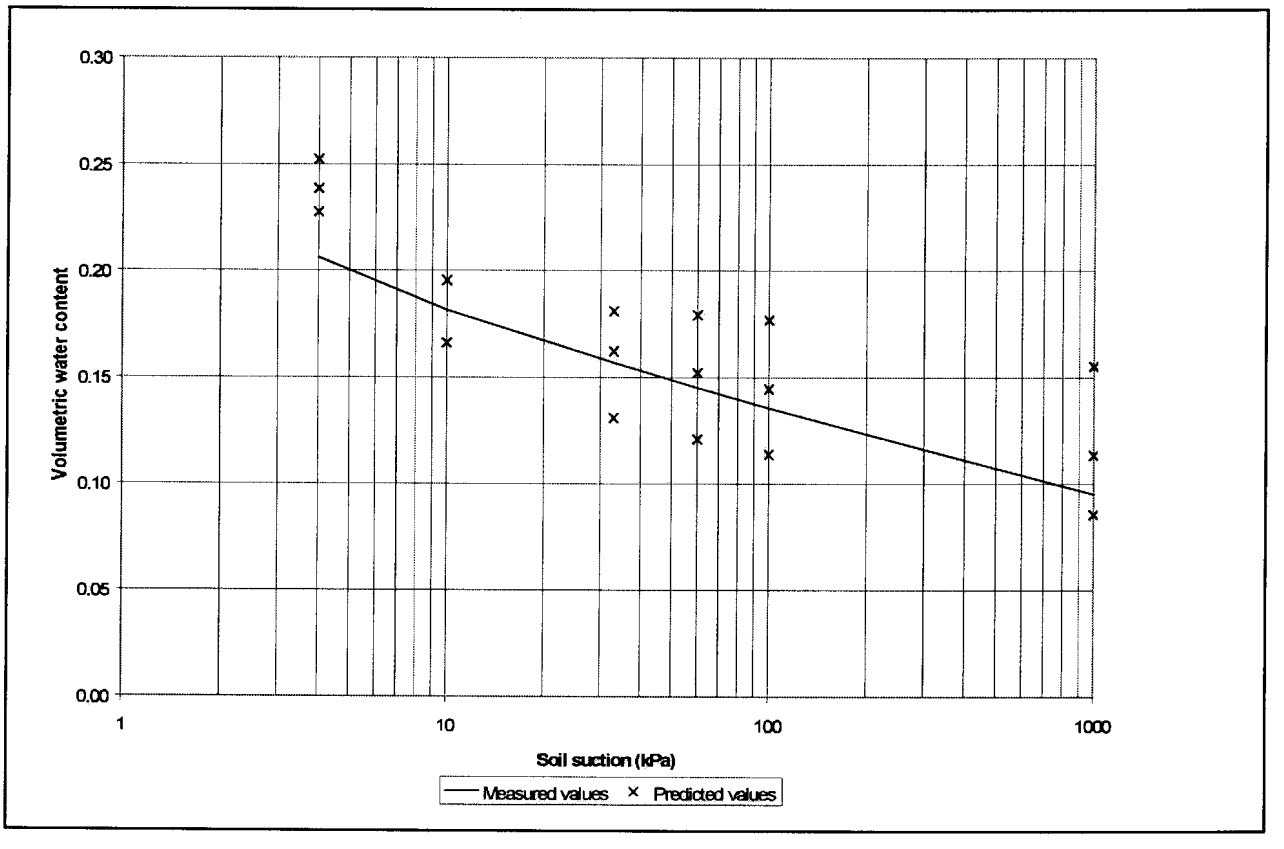

Figure 6.10: Correlation between the measured and predicted soil-water characteristic curve at Experiment 4

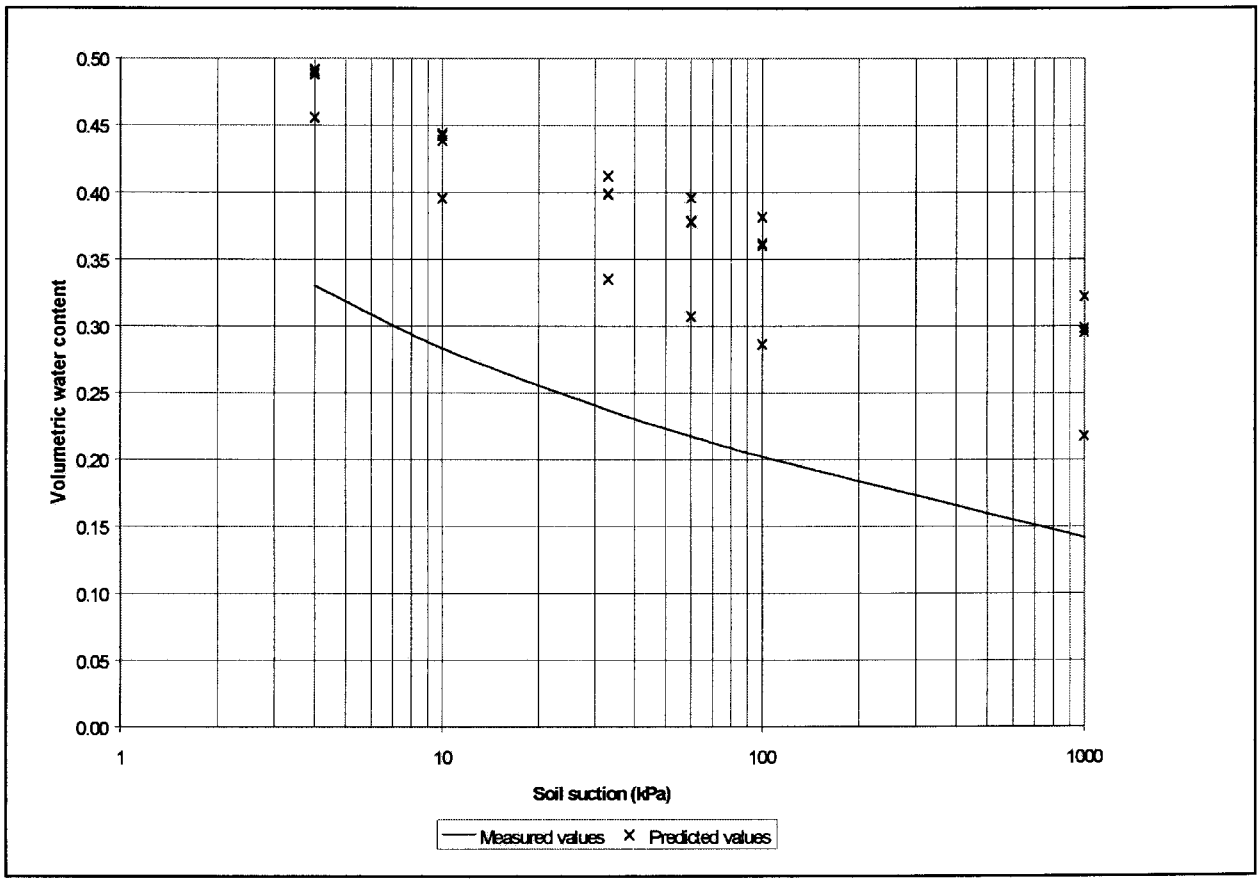

Figure 6.11: Correlation between the measured and predicted soil-water characteristic curve at Experiment 5

Table 6.14 and **Figures 6.10** to **6.12** indicate that in the case of Experiments 3 and 4, the soil-water characteristic curve has been accurately predicted by the Gupta and Larson (1979) regression model. However, less accurate predictions of soil-water characteristic curves were achieved in the case of Experiments 1 and 2 and Experiment 5. This may be caused by the high porosity values of residual soils at Experiments 1, 2 and 5. It appears that the porosity value has a significant effect on soil-water characteristic curves.

6.5 Estimation of unsaturated hydraulic conductivity

6.5.1 Statistical equations

The Van Genuchten (1980) and Fredlund *et al.* (1994) models were applied to estimate unsaturated hydraulic conductivity as a function of volumetric water content. These results were compared to measured unsaturated hydraulic conductivity as obtained from literature.

Soil-water retention data-sets of the five soils referred to in Section 6.4 were fitted to the Van Genuchten (1980) and Fredlund and Xing (1994) functions. In order to obtain a closed-form equation, a restriction was placed on the parameter, *m,* of the Van Genucten (1980) model in terms of:

$$m = 1 - \frac{1}{n} \qquad [6\text{-}3]$$

This resulted in a slight loss of flexibility regarding the Van Genucten (1980) function. However, good fit was obtained when the aid restriction was applied. When the Mualem (1976) model for estimating unsaturated hydraulic conductivity, is applied, unsaturated hydraulic conductivity can be expressed as:

$$K(\psi)=\frac{K_s\left\{1-(\alpha\psi)^{mn}\left[1+(\alpha\psi)^n\right]^{-m}\right\}^2}{\left[1+(\alpha\psi)^n\right]^{m\ell}} \qquad \text{where} \qquad m=1-1/n \qquad [6\text{-}4]$$

Since the volumetric water content is a function of soil suction, unsaturated hydraulic conductivity can be expressed as a function of volumetric water content. The parameter l had been defined as the pore connectivity factor, where Mualem (1976) has suggests a value equal to 0.5.

Fredlund *et al.* (1994) maintain that, by applying the model of Childs and Collis-George (1950) to the Fredlund and Xing (1994) function, unsaturated hydraulic conductivity can be expressed as:

$$K_r(\psi)=\Theta^q(\psi)\frac{\int_{\ln(\psi)}^{b}\frac{\theta(e^y)-\theta(\psi)}{e^y}\theta'(e^y)dy}{\int_{\ln(\psi_a)}^{b}\frac{\theta(e^y)-\theta_s}{e^y}\theta'(e^y)dy} \qquad [6\text{-}5]$$

where b = *ln(1 000 000)*, e is the natural number 2.7182..., y is a dummy variable of integration representing the logarithm of soil suction and Θ^q is a correction factor, where Θ is the normalised volumetric water content or relative degree of saturation as:

$$\Theta=\frac{\theta-\theta_r}{\theta_s-\theta_r} \qquad [6\text{-}6]$$

Fredlund *et al.* (1994) indicate that Equation 6-5 can be solved by numerical integration. The relative hydraulic conductivity as a function of soil suction can be expressed as:

$$K_r(\psi)=\frac{\sum_{i=j}^{N}\frac{\theta(e^{\bar{y}_i})-\theta(\psi)}{e^{\bar{y}_i}}\theta'(e^{\bar{y}_i})}{\sum_{i=1}^{N}\frac{\theta(e^{\bar{y}_i})-\theta_s}{e^{\bar{y}_i}}\theta'(e^{\bar{y}_i})} \qquad [6\text{-}7]$$

where N is the number of intervals and $\bar{y}_i$ is the midpoint of the ith interval.

A computer programme, UNSAT.K was developed in Delphi language to conduct the numerical integration required by the Fredlund *et al.* (1994) model. Soil-water retention data is fitted to the Fredlund and Xing (1994) function and the parameters a, n, m and Cr, required to describe the soil-water characteristic curve, are determined. These values are entered into the computer program. The computer program calculates the volumetric water content and unsaturated hydraulic conductivity at specified soil suction values, applying Equations 6-5 and 6-7.

It has already been shown that the soil-water characteristic curves for five soil types can be accurately described by the Van Genucten (1980) and Fredlund and Xing (1994) functions. These data-sets were further analysed to determine the unsaturated hydraulic conductivity in term of the Van Genucten (1980) and Fredlund *et al.* models. The calculated values were compared to experimentally determined unsaturated hydraulic conductivity values. The results are shown in **Figures 6.12** to **6.15**.

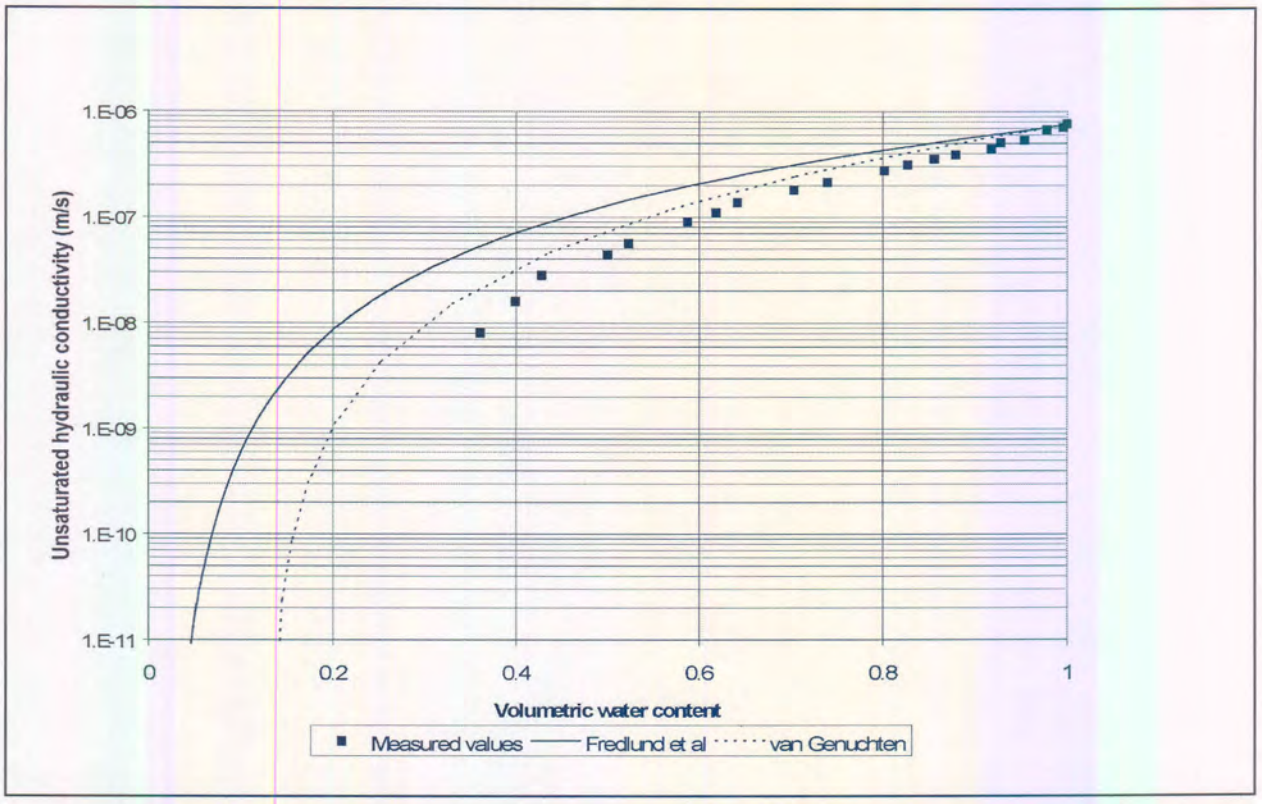

Figure 6.12: Correlation between measured and predicted unsaturated hydraulic conductivity based on soil-water characteristic curves: Sand

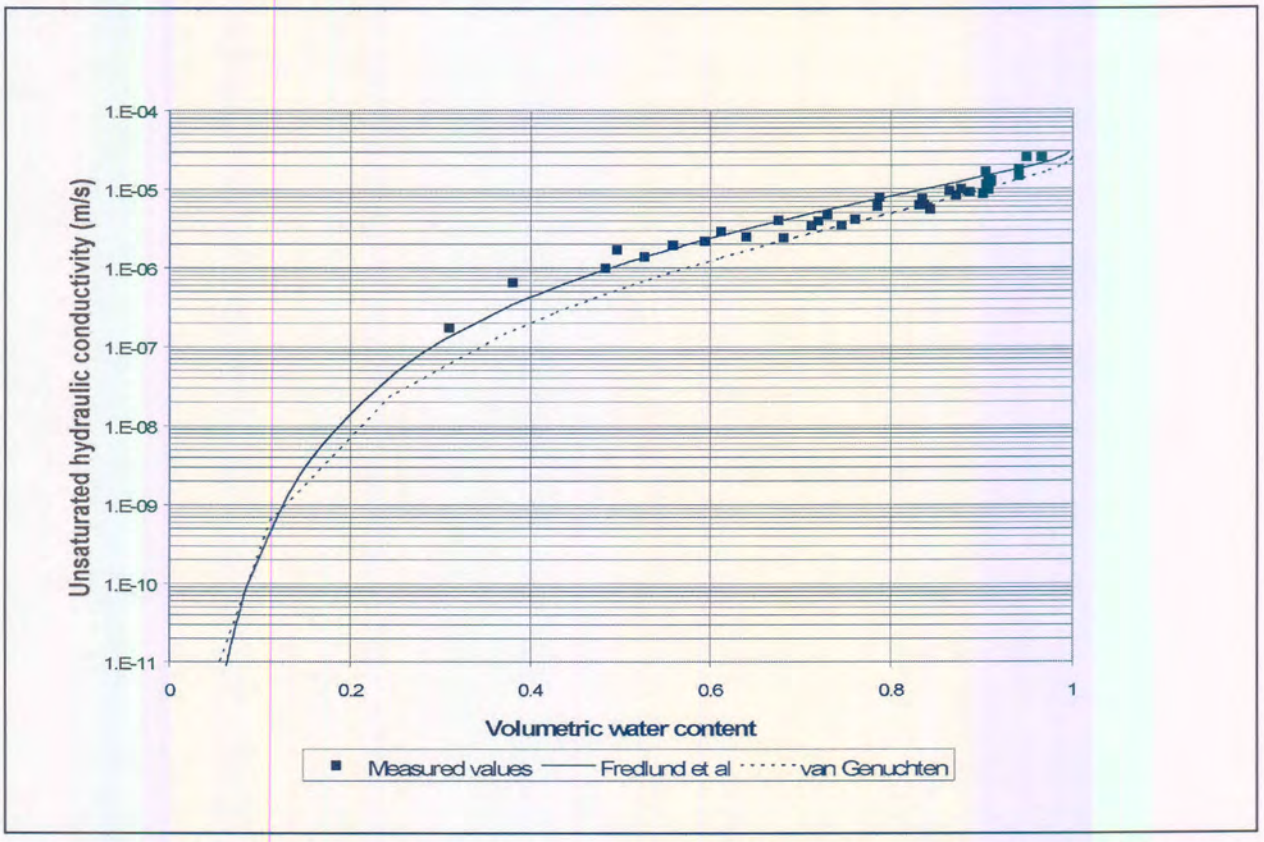

Figure 6.13: Correlation between measured and predicted unsaturated hydraulic conductivity based on soil-water characteristic curves: Fine sand

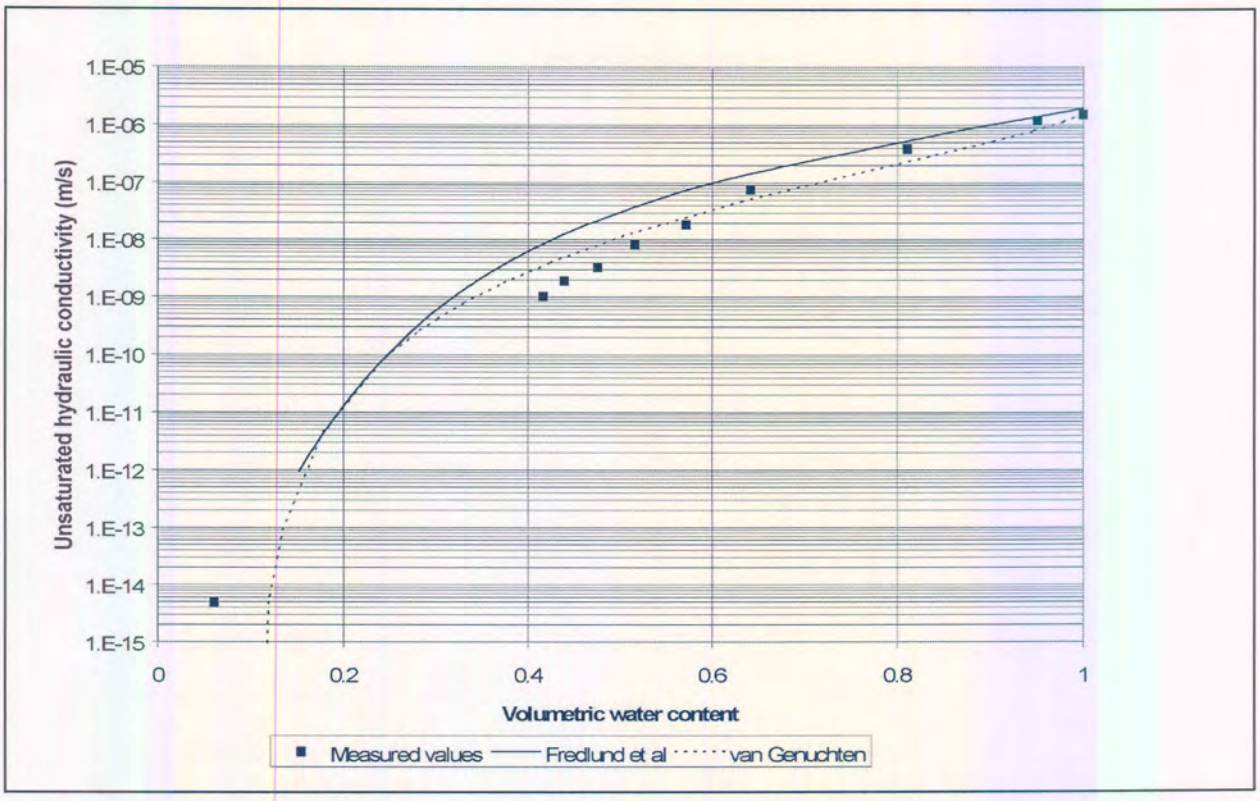

Figure 6.14: Correlation between measured and predicted unsaturated hydraulic conductivity based on soil-water characteristic curves: Sandy silt-clay

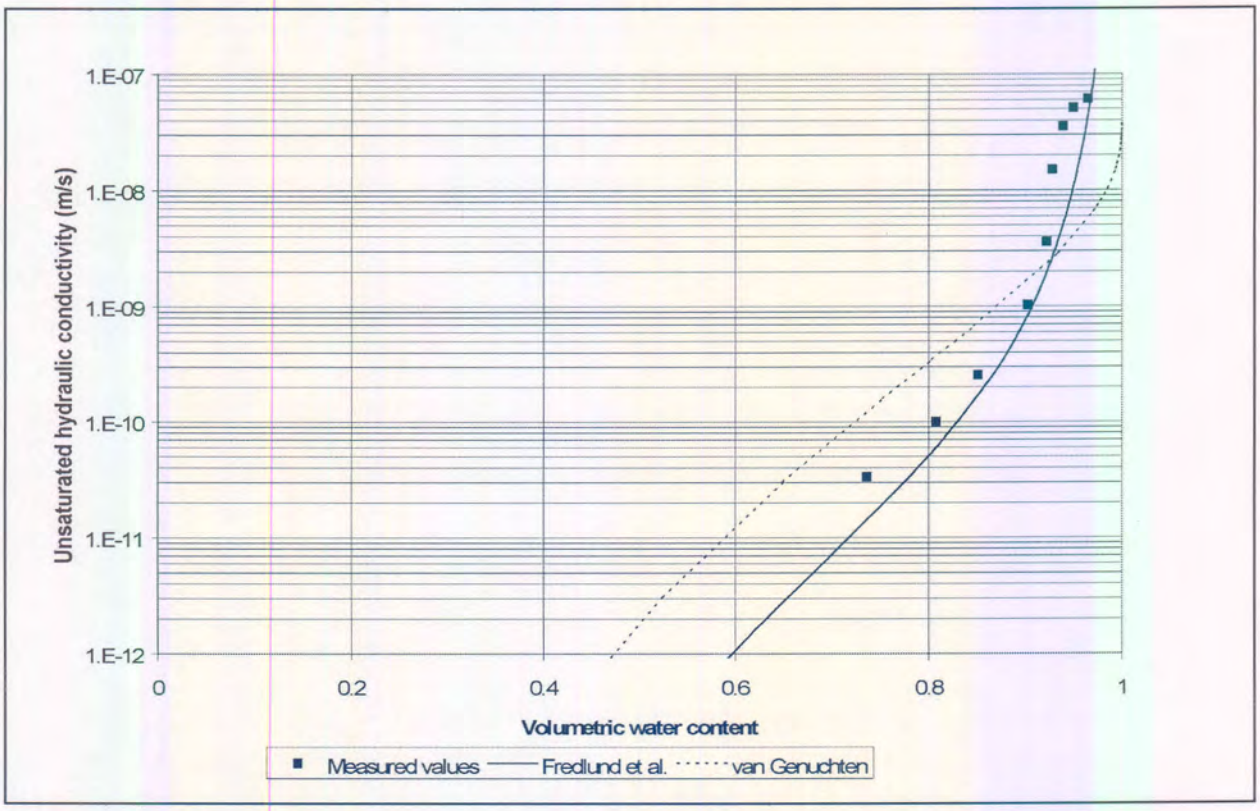

Figure 6.15: Correlation between measured and predicted unsaturated hydraulic conductivity based on soil-water characteristic curves: Clay

Sand

From the above data it can be concluded that the Van Genucten (1980) model can accurately predict the unsaturated hydraulic conductivity. In contrast, the Fredlund *et al.* (1994) model slightly overestimate unsaturated hydraulic conductivity, but the predictions are adequate for most field applications. The unsaturated hydraulic conductivity curve of sand is characterised by a sharp inclination point, indicating that water drains from the large pores and that the retained water is strongly adsorbed to the soil grains. Of interest is the uncharacteristically low saturated hydraulic conductivity measured for the specific sand used in the analyses, which is lower than both the saturated hydraulic conductivity of fine sand and sandy silt-clay. This indicates that saturated hydraulic conductivity is not a function of particle-size distribution only.

Fine sand

Both the Van Genuchten (1980) and Fredlund *et al.* (1994) models accurately predict the unsaturated hydraulic conductivity, with the latter achieving a slightly better correlation. The curve is characterised by a more gradual slope than is the case with sand, indicating that water is retained in the smaller pores and is gradually removed by higher suctions up to about 40 per cent water content, where after the unsaturated hydraulic conductivity decreases rapidly in accordance with the decrease in water content.

Sandy silt-clay

As with the fine sand, both the Van Genuchten (1980) and Fredlund *et al.* (1994) functions fairly accurately describe the unsaturated hydraulic conductivity of sandy silt-clay, although not as accurately as with the fine sand. Deviations between 0 per cent and 40 per cent of water content occur. However, predicted unsaturated hydraulic conductivity is adequate for most field applications.

Clay

The unsaturated hydraulic conductivity curve differs considerably from that of the sand, fine sand and sandy silt-clay. Because of the large surface area of clay minerals, water is strongly adsorbed to the clay minerals and does not drain easily. It can be seen that the Fredlund *et al.* (1994) function gives a much more accurate prediction of unsaturated hydraulic conductivity than the Van Genuchten (1980) function. However, the Fredlund *et al.* (1994) function indicates that the unsaturated hydraulic conductivity values at near-saturated conditions are higher than saturated hydraulic conductivity and that is obviously not possible. With the exception of this inherent error, the Fredlund *et al.* (1994) function accurately predicts the unsaturated hydraulic conductivity of clay.

The correlation coefficients for the various soil types are indicated in **Table 6.15**. It appears that the Van Genuchten (1980) function better represents sandy soils, while the Fredlund *et al.* (1994) function better represents clayey soils. These findings corroborate the findings of Leong & Rehardjo (1997b) that the Fredlund *et al* (1994) function does not predict unsaturated hydraulic conductivity of sandy material as well as the Van Genuchten (1980) model.

Table 6.15: Correlation between estimated and experimentally derived unsaturated hydraulic conductivities (at selected water contents)

Soil type	Coefficient of correlation	
	Van Genuchten	Fredlund *et al.*
Sand	0.9855	0.9657
Fine sand	0.9515	0.9067
Sandy silt-clay	0.9998	1.0000
Clay	0.6535	0.9990

Application of unsaturated hydraulic conductivity models to the field experimental sites

Predictions of unsaturated hydraulic conductivity were made from soil-water characteristic curves based on the models developed by Van Genuchten (1980) and Fredlund *et al.* (1994), as was discussed in the preceding section. The computer program UNSAT.K was applied to determine unsaturated hydraulic conductivity as a function of volumetric water content, based on the permeability and soil-water retention test results for Experiments 1 & 2, 3 & 4 and 5.

After the water retention data had been obtained for residual soils at the respective experimental sites, the data were fitted to soil-water characteristic functions as developed by Van Genuchten (1980) and Fredlund and Xing (1994). The parameters necessary to describe the soil-water characteristic curves were determined. The methodology to determine the fitting parameters from soil-water retention and permeability data was identical to that described in Section 6.3.

With the fitting parameters, saturated hydraulic conductivity and porosity values known, the unsaturated hydraulic conductivity, as a function of water content could be determined. The data were applied to the restricted Van Genuchten (1980) and the Fredlund *et al* (1994) models and these have been discussed in the preceding section.

The results, indicating unsaturated hydraulic conductivity as a function of volumetric water content, are shown in **Table 6.16**.

Table 6.16: Unsaturated hydraulic conductivity at various soil suction values

Soil suction (kPa)	Experiments 1 and 2		Experiments 3 and 4		Experiment 5	
	K (VG)	K (F)	K (VG)	K (F)	K(VG)	K (F)
1.00	1.1×10^{-10}	9.7×10^{-10}	1.4×10^{-8}	5.0×10^{-7}	7.0×10^{-7}	1.2×10^{-6}
5.00	2.6×10^{-12}	1.9×10^{-11}	1.4×10^{-10}	5.4×10^{-10}	2.2×10^{-7}	3.7×10^{-7}
10.00	3.6×10^{-13}	3.4×10^{-12}	1.4×10^{-11}	1.0×10^{-10}	8.4×10^{-8}	1.7×10^{-7}
20.00	4.6×10^{-14}	6.6×10^{-13}	1.4×10^{-12}	2.3×10^{-11}	2.3×10^{-8}	6.1×10^{-8}
50.00	3.0×10^{-15}	8.2×10^{-14}	6.7×10^{-14}	3.4×10^{-12}	2.6×10^{-9}	1.0×10^{-8}
100.0	3.7×10^{-16}	1.8×10^{-14}	6.5×10^{-15}	7.8×10^{-13}	4.0×10^{-10}	1.8×10^{-9}
1000	3.5×10^{-19}	1.2×10^{-16}	2.9×10^{-18}	5.9×10^{-15}	5.9×10^{-13}	2.6×10^{-12}

VG = Van Genuchten (1980)
F = Fredlund *et al* (1994)

Unfortunately, the predicted unsaturated hydraulic conductivities could not be compared to *in situ* values measured at the experimental sites. Because of the simple way in which unsaturated hydraulic conductivity is derived by means of internal drainage tests, accurate estimations of unsaturated hydraulic conductivity may not be attainable. Notwithstanding, unsaturated hydraulic conductivity values for Experiment 4 compare well with that predicted by the Van Genuchten (1980) model. However, discrepancies do occur at higher water contents, which occur due to inherent errors of the Lax-θ method used to determine the unsaturated hydraulic conductivity.

In general, the shape of the unsaturated hydraulic conductivity curve as predicted by the Van Genuchten (1980) and Fredlund *et al.* (1994) functions compare well with each other, even though the predicted unsaturated hydraulic conductivity as derived from the Van Genuchten (1980) model is consistently slightly lower, compared to predicted values derived from the Fredlund *et al.* (1994) function. The similar unsaturated hydraulic conductivity values might indicate that both the Van Genuchten (1980) and Fredlund *et al* (1994) functions were successful in accurately predicting the unsaturated hydraulic conductivity as a function of soil water content.

CHAPTER 7

APPLICATION OF RESULTS ON A REGIONAL SCALE

7.1 Location of the study area

The study area is represented by the orthophoto: 2528 CC 23 Midrand (Halfway House) and covers an area of approximately 25×10^6 m^2. The area includes a major part of Midrand, currently one of the fastest developing nodes in South Africa, where office parks and light industrial complexes are taking advantage of the prime locations along the N1 highway.

In contrast, large portions of the study area comprise smallholdings located side-by-side with light industrial complexes. The smallholding community relies on groundwater for their irrigation and, in places, their domestic needs. Because of the high degree of development, groundwater is vulnerable to a number of potential groundwater-degrading activities. Contamination sources have not been identified since this falls outside the scope of this study. The study area is a unique example of human development dynamics in an urban environment and its impact on groundwater resources.

7.2 The Johannesburg granitoid dome

The Johannesburg Dome, shown in **Figure 7.1**, (also known as the Halfway House or Johannesburg-Pretoria dome) is a dome-like window of ancient granitoid, approximately 750 km^2 in area, situated between Johannesburg and Pretoria in South Africa. It is situated in the central part in the Gauteng Province.

7.2.1 Geology of the Johannesburg Dome

The Johannesburg Dome comprises mainly ancient granitoid. The lack of conformity between the foliations in the granitoids and the overlying rocks implies that the granitoid inlier is not a dome *sensu stricto* (Anhaeusser, 1973). Despite this, the term Johannesburg Dome has been retained in literature. The Johannesburg Dome consists of the following (Hilliard, 1994):

- An archean granitoid dome consisting of Tonalite-Trondjhemite gneisses, banded gneisses, a foliated granodiorite zone and granodiorites (Hilliard, 1994). Greenstone remnants are scattered throughout the basement inlier (Anhaeusser, 1973).

- Rocks of the Witwatersrand and Ventersdorp Supergroups are exposed along the south-eastern margin, and along the southern and south-western margin of the inlier respectively.

- The Black Reef Formation, which forms the base of the Transvaal Sequence, is exposed to the north-eastern, northern and north-western margin of the inlier and lies unconformably on the granitoids and greenstones as well as the rocks of the Witwatersrand and Ventersdorp Supergroups.

- The greenstone remnants that occur scattered throughout the basement inlier are the oldest rocks in the Johannesburg Dome area with an age of 3750-2870 Ma (Swazian Erathem, SACS, 1980). They includes mafic and ultramafic rocks (including the Muldersdrif and Roodekrans ultramafic complexes) altered to serpentinites, a variety of amphibolites, chlorite talc, talc carbonate and talc chlorite shists (Anhaeusser, 1973).

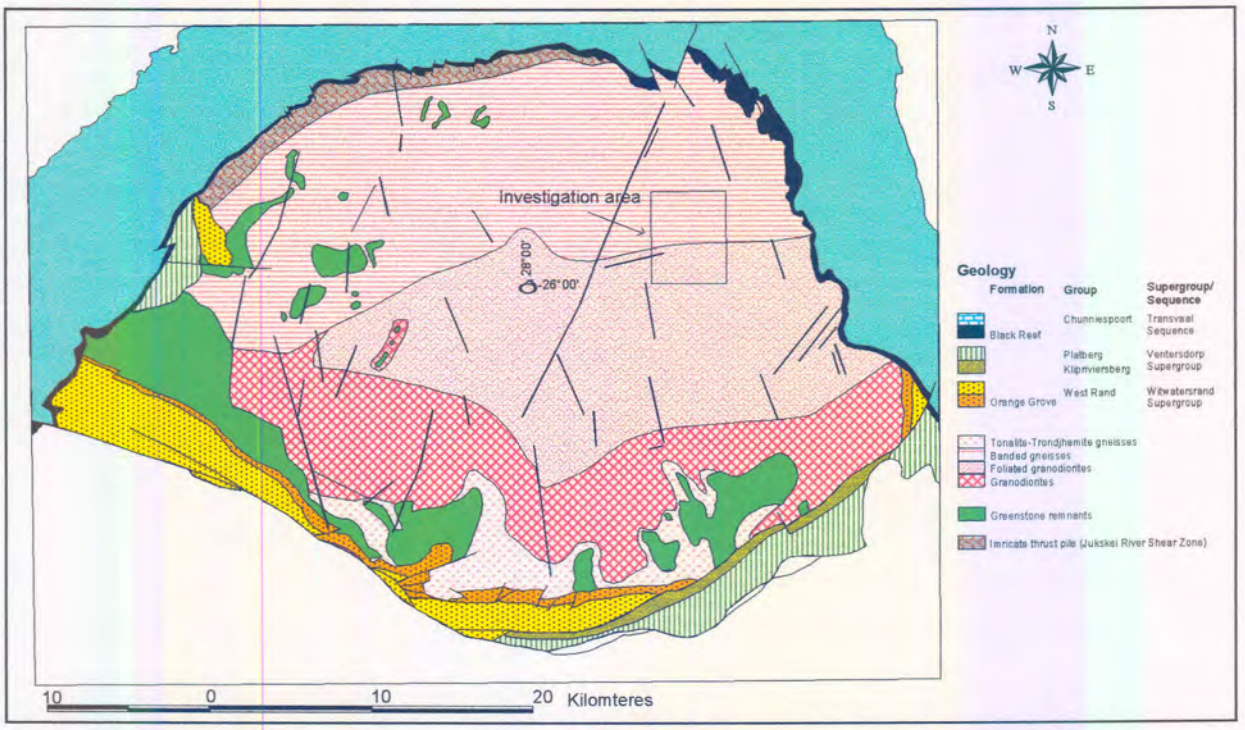

Figure 7.1: Geology of the Johannesburg Granitoid Dome (modified after Hilliard, 1994)

Hilliard (1994), based on the work of Anhaeusser (1973), identified four rock units within the granitoid inlier namely

- Tonalite-Trondjhemite gneisses
- Banded gneisses
- Foliated granodiorites
- Granodiorites

The tonalite-trondjhemite gneisses outcrop in the southern part of the inlier. They intrude the greenstone remnants and contain xenoliths of greenstone fragments (Hilliard, 1994). The gneissic foliation is parallel to the contacts of the greenstone remnants. This phenomenon suggests that the gneissic foliation formed during the intrusion of the tonalite-trondjhemite magma into the greenstone material (Anhaeusser, 1973).

The banded gneisses outcrop in the northern half of the granitoid inlier and consist of gneisses with a strong metamorphic banding defined by alternating quartz-feldspar and biotite rich layers (Hilliard, 1994).

The foliated granodiorites, according to Anhaeusser (1973), form a transitional zone between the granodiorites to the south and the banded gneisses to the north. Hilliard (1994) observed that the

principal rock type of the foliated granodiorites is granodiorite with a weakly-developed gneissic foliation.

Ductile shear zones (previously known as crush zones) developed within all granitoids of the basement inlier. The shear zones are characterised by mylonitic foliation and extensive quartz veining (Hilliard, 1994). Two distinct strike orientations of the shear zones, NE and NNW, have been identified. The shear zones were reactivated as brittle faults after deposition of the Black Reef Formation. Quartz infiltrated the shear zone during the initial ductile deformation and subsequently caused extensive quartz veining during the brittle reactivation of the shear zones (Hilliard, 1994).

7.2.2 Weathering processes

A strong relationship exists between the geology of the granitoids and corestone as well as tor development on the Johannesburg Dome.

MacGregor (1952) observed that tors are largely confined to zones of homogeneous granite. Brink (1979) regards the occurrence of tors in the central part (foliated granodiorite) of the granitoid as a striking example of this hypothesis.

Anhaeusser (1973) arbitrarily delineates the boundaries of the Transitional Zone (foliated granodiorites) by identifying the area in which granitoids show tor development. Hilliard (1994), however, delineates the foliated granodiorite in accordance with the weak to moderate occurrences of gneissic foliations, implying that the foliated granodiorites are closely associated with tor development.

In the study area, this association is striking. The northern part of the study area consists of banded gneisses and no tor development has been observed. The southern part of the study area consists of foliated granodiorite and striking examples of tor development are evident. The best example is probably the Boulders Shopping Centre, which is located on top of huge granitoid boulders.

Because of a lack of correlation between mineralogical composition and topography, Brook (1970) states that the tors can not be explained by rock composition. However, Anhaeusser (1973) postulates that the reasons for tor formation are indeed connected to the geochemical variations between the different granitoids. Brink (1979) contends that the exceptionally high content of microcline feldspar is of paramount importance to the mode of weathering. The occurrence of more resistant microcline in the central part of the inlier causes the rocks to be more susceptible to corestone and tor formation than the granitoids, which contain more sodic feldspar, such as the tonalite gneisses in the southern part of the inlier.

Major shear zones often form prominent linear topographical features. Hilliard (1994) postulates that the resistance in weathering is mainly caused by the extensive quartz veining associated with shear zones and to a lesser degree also by the resistant nature of mylonite.

McKnight (1997) postulates that deep weathering along major structural features may be explained by an advanced hydrolysis of silicate minerals, owing to the increased fracturing, and therefore the increased permeability in this zone. McKnight (1997) observed that deep troughs of highly weathered granitoids trend roughly parallel to bedrock structure. According to McKnight (1997), elongated ridges of shallow bedrock adjacent to deeply weathered troughs, particularly prevalent in the Randburg, Bryanston, and Rivonia areas, conform to the general macro-structural setting of the area. These preferential weathering zones are selectively being exploited by drainage features, with the result that landforms and the drainage pattern in the area are, to a large extent, defined by the underlying structural geological setting.

7.2.3 Geomorphic cycles

The present land surface in the Johannesburg Dome area was affected by the African and Post-African I and II geomorphic cycles.

The African cycle was initiated by a vertical upliftment of at least 1000 m during the Late Jurassic/early Cretaceous period (Brink, 1979). The cycle of erosion lasted more than 100 Ma and resulted in widespread planation. The African erosion event was polycyclic with periods of sedimentation followed by periods of erosion due to regional and global upliftment. However, Partridge & Maud (1987) state that this period should be regarded as a single unit. The long duration of this cycle caused widespread planation, with the surface at two levels, above and below the Great Escarpment. It caused the development of deep residual soil (up to 50 m deep) and extensive kaolinisation. It also caused widespread development of pedocretes. At the end of the cycle, the interior elevation was probably between 500 to 700 m a.m.s.l.

In the Johannesburg Dome area, the African erosion cycle is represented by hill crests higher than approximately 1 600 m a.m.s.l (**Figure 7.2**). These hill crests are manifested generally by five bevelled ridges, extending from the Witwatersrand quartzites in a northern direction towards the Rivonia/Midrand area (McKnight, 1997). One of these ridges is manifested in the investigation area, trending east-west in contrast to the general north-south trend of the ridges.

The ridges are characterised by undulating slightly concave crests and are often underlain by deep kaolinised, leached soils. The residual soil has in places been kaolinised to considerable depth. Feldspars have become thoroughly kaolinised thoroughly leached from the top layers, resulting in a spongy, micaceous, silty sand. The soil horizon is characterised by a very low bulk density and high void ratio and is known to have a collapsible grain structure. Few corestones are present in the profile, which have probably been completely weathered during the erosion cycle. This paleosol, possibly with a thick ferricrete cap, now removed by erosion processes, constitutes a deep weathering front below the African erosion land surface (Partridge & Maud, 1987).

The five ridges preserve a relict scarp structure and large corestones, tors and irregular pinnacles of bedrock have been exposed (McKnight, 1997). McKnight also observed deep kaolinised weathering troughs showing strong correlation with bedrock macrostructure. This zone corresponds to the base of the African Erosion Surface and foliated granodiorite bedrock.

The Post-African I cycle was initiated by an upliftment of 150 m to 300 m and was accompanied by a slight westward tilting. This event took place in the early Miocene period. Erosion carved into the older planar African erosion surface. The degree of weathering was not as intense as with the African erosion cycle but, nevertheless, considerably deep residual soils developed in the humid areas (Brink, 1979). The resulting landscape is not as smooth as that of the African erosion cycle.

In the Johannesburg Dome area, the Post-African I cycle is represented by areas approximately 1400 to 1600 m a.m.s.l. (**Figure 7.2**), generally corresponding with the partly undulating concave upper and middle slopes. Numerous gully heads occur within this zone and are characterised by irregular hardpan ferricrete up to 1.0 m in thickness (McKnight, 1997).

The Post African II cycle was initiated by a major asymmetrical upliftment of the subcontinent co-occurring with a major westward tilting of the land surfaces of the interior and monoclinal warping along the southern and eastern coastal margins. The event caused the formation of the Post African II erosion surface characterised by the incision of coastal gorges and the downcutting and formation of higher terraces along interior rivers.

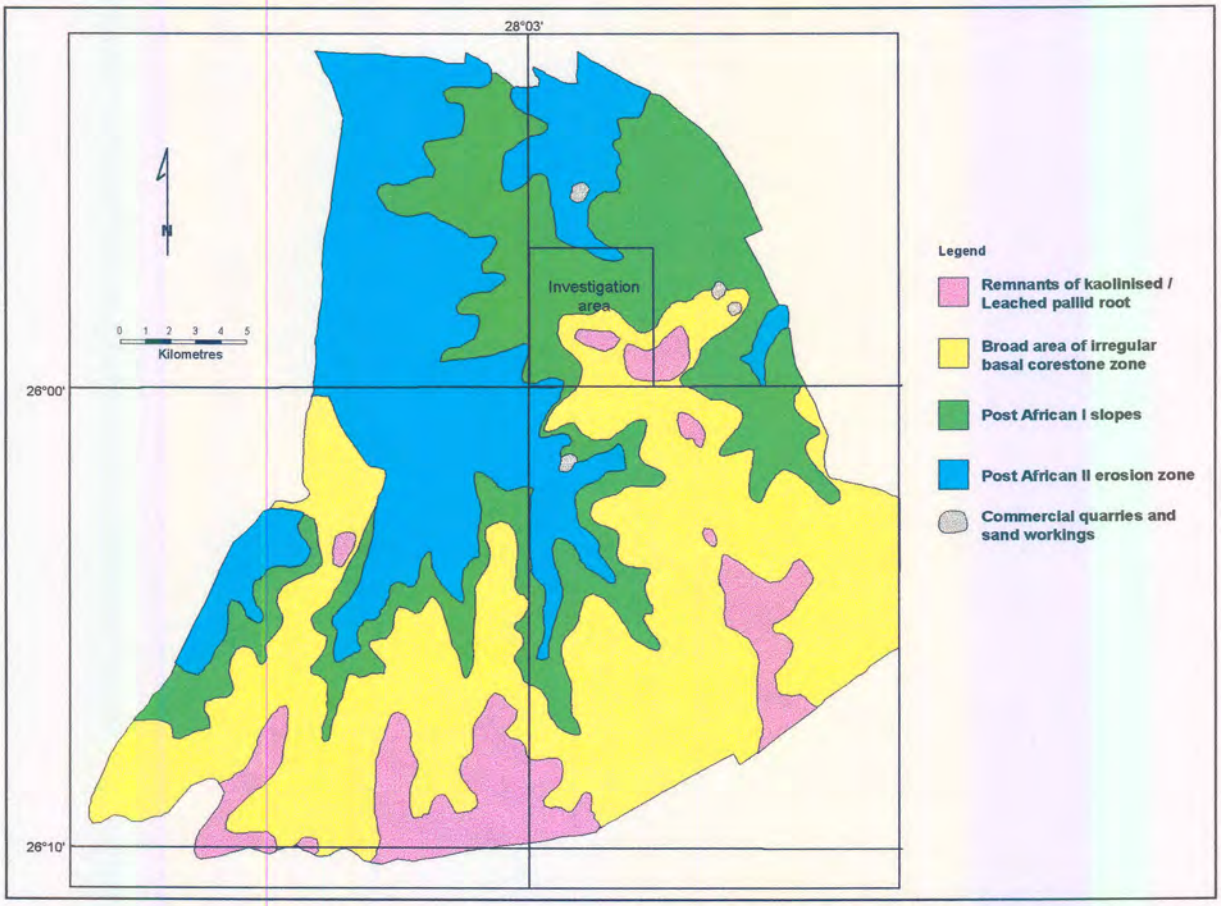

Figure 7.2: Erosion surfaces of the eastern Johannesburg Granitoid Dome (modified after McKnight, 1997)

The late Pliocene upliftment event and the concomitant Post African II erosion cycle caused incision along drainage channels within the undulating Post African I erosion surface of the Johannesburg Dome. The Post African II erosion surface is generally manifested in areas located below 1 500 m a.m.s.l. in particular along the middle and lower slopes along the Johannesburg Dome (McKnight, 1997). These areas are characterised by shallow, relict structured, frequently ferruginised, residual soil profiles. Numerous rock outcrops are present in the Jukskei, Riet, and Kaalfontein streams.

7.2.4 Climate and vegetation

The region is characterised by warm to hot summers and mild winters. Rainfall occurs predominantly in summer and little rainfall is recorded in winter months. The average yearly rainfall is 709 mm. Rainfall occurs mainly in the form of thundershowers. Wind direction is predominantly north-west and the wind velocity is mostly light to intermediate. This climate is typical of the Highveld region.

The indigenous vegetation consists of typical Highveld grass that include *Themeda triandra*, *Trystachya leucothrix*, *Trachypon spicatus* and *Elionurus meticus* (Accocks, 1988). Some exotic trees, mainly *Eucalyptus* and *Acasia Mearinsii* (Black Wattle) also occur in the area.

7.2.5 Surface drainage

Drainage patterns within the Johannesburg Dome area are predominantly controlled by the underlying structural geology. Drainage features, consisting of a number of small streams, flow mainly northwards

in the northern portion of the study area and south westwards in the southern portion. These flow directions are consistent with the local structural trends in the area.

The prominent east-west trending ridge forms a watershed, with the northern streams draining into the Rietspruit River and the southern streams flowing along a number of small streams before they eventually flow into the Jukskei River.

Surface water shows a close interrelationship with the groundwater occurrences, especially groundwater from the shallow weathered aquifer. In turn, the shallow weathered aquifer shows close correlation with seasonal effects. This interrelationship between groundwater and surface water resources is in line with the concepts and philosophy of integrated surface and groundwater systems, supported and currently being implemented as part of the Integrated Catchment Management policies in South Africa.

7.2.6 Groundwater occurrence and potential

The Johannesburg Dome represents a typical hard rock environment. Three aquifer systems can be identified, namely a shallow primary weathered aquifer system and a deep secondary aquifer system occurring in unweathered granitoids and associated with fractures, joints, and other discontinuities within the rock mass. In addition, perched aquifers may occur on hardpan ferricrete and shallow bedrock units.

Although little is known about the groundwater conditions within the Johannesburg Dome, experience in other hard rock environments suggests that groundwater in the deep aquifer will mainly occur along deeply weathered structural features. These zones are fractured and highly permeable, resulting in good borehole yields. However, the surrounding granitoid is virtually impermeable with a very low primary porosity value. The deep secondary aquifer will therefore be recharged mainly from the overlying shallow aquifer systems.

In contrast to the deep aquifer, groundwater in the unconfined shallow aquifer generally occurs within unconsolidated completely weathered and residual granite. Weathering of the granitoid bedrock generally results in an increase in porosity and permeability in relation to unweathered rocks. The increase in size and frequency of pore spaces is mainly caused by mineral dissolution during weathering processes. Porosity in the residual granite is high, typically between 30 and 40 per cent, and permeabilities are medium to low, because of high silt and clay contents. Medium to low borehole yields are expected for boreholes located within the weathered aquifer.

Depending on the weathering mode, transition between residual soil and unweathered bedrock may be either abrupt or gradual. In the case of a gradual transition, the soil profile may possibly include closely jointed, medium to highly weathered, highly permeable granite, situated between the overlying medium to low-permeability residual soil and the underlying impermeable granitoid bedrock. Groundwater preferably flows along these zones and discharges into low-lying drainage channels. In the case of an abrupt transition, medium- to low-permeability residual soil directly overlies impermeable granitoid bedrock, with groundwater perching on top of the bedrock.

In addition to shallow bedrock conditions, groundwater is sometimes perched on low-permeability hardpan ferricrete and clay layers (such as low-permeability clayey residual ultra-mafic rock; greenstone remnants).

As mentioned before, deeply weathered troughs trend roughly parallel to bedrock structure. These preferential weathering zones are being selectively exploited by drainage features, with the result that landforms and the drainage pattern in the area are, to a large extent, defined by the underlying structural geological setting. Areas with high groundwater potential will therefore be located mainly along drainage channels exploiting preferential deeply weathered zones.

The weathered aquifer acts as a storage reservoir, releasing groundwater into fractured zones. The shallow aquifer also discharges into the overlying drainage channels. Perched groundwater along hardpan ferricrete layers also discharges into drainage channels.

7.3 Acquisition and analyses of geotechnical data

The investigation area was extensively investigated by a number of institutions. Both the Council for Geoscience and the CSIR conducted regional engineering geology investigations in the area. Information obtained during these investigations includes a regional engineering geology report (Council for Geoscience, 1998) dealing with engineering geology aspects of large parts of the Johannesburg Dome (including the study area) and the adjacent dolomitic areas and included a large number of soil profile descriptions and geotechnical laboratory results.

The CSIR provided soil profile descriptions and geotechnical laboratory results from their geotechnical database as well as a land facet map of the investigation area. The land facet map was compiled by means of API and captured in a GIS database.

Some private consultants provided geotechnical data, mostly in the form of soil profile descriptions. The geotechnical data accumulated during **Experiments 3** and **4** were also applied to the regional study.

In addition to geotechnical data, borehole data were obtained from the National Groundwater Database of DWAF. A regional borehole census was conducted to supplement groundwater data. Prominent features, such as bedrock outcrop, ferricrete outcrop and seepage zones, were mapped.

7.3.1 Land system classification

The Johannesburg Dome area was one of the first areas in South Africa classified by the land system approach. Several publications on applying the land system approach for engineering geology purposes are based on investigations of the Johannesburg Dome region (Brink & Williams, 1964; Brink & Partridge, 1967; Brink, Partridge, Webster & Williams, 1968; Partridge, 1969, Stiff, 1994, Stiff, 1997). The CSIR published a series of GIS based maps, indicating land facets for the Johannesburg Dome and surrounding areas.

The major part of the Johannesburg Dome is represented by the Kyalami Land System. The Kyalami Land System follows the boundaries of the Johannesburg Dome and is characterised by an undulating landscape with mainly north-southern trending ridges and convex slopes, seldom exceeding 12° (Brink & Partridge, 1967). The land system occurs at an elevation of between 1 400 m to 1 700 m a.m.s.l. In addition, the Boskop and the Muldersdrift Land Systems have also been identified. The Boskop Land System is associated with shear zones (crush zones) within the granitoid rock comprising mylonite. Mylonite is more resistant to weathering than the surrounding rocks, resulting in razorback ridges with a general north-eastern/ south-western trend. The Muldersdrift Land System represents areas underlain by major patches of greenstone remnants scattered throughout the Johannesburg Dome. However, because certain minor patches of greenstone remnants do not display significantly different surfaces than the Kyalami Land System, these areas are included in the Kyalami Land System.

Brink and Partridge (1967) identified a number of land facets and variants comprising the Kyalami Land System. The basic land facets consist of:

- Hill crests that can be recognised between high-lying areas with slopes of less than 2°
- Convex side slopes that can be recognised areas between low and high-lying areas with slopes of less than 12°

- Gully slopes that can be recognised by their location at stream heads and a change in slope relative to the side slope, generally hosting these facets

- Alluvial floodplains and drainage lines occur along non-perennial streams that generally exhibit a sub-parallel drainage pattern

Brink and Partridge (1967) identified a number of variants for each land facet, mostly to differentiate between underlying residual granite and residual basic metamorphic rocks, representing the greenstone remnants scattered throughout the Johannesburg Dome.

In addition, land facets occurring less frequently, such as tors, whalebacks and alluvial terraces occur throughout the Johannesburg Dome. Non-connate facets including pan floors and pan sides remnant of the African Erosion Cycle, dyke ridges and pediment occur within the area.

Brink and Partridge (1967) found close correlation between the land facets and the underlying soils and rocks. Hill crests representing the base of the African Erosion Cycle typically comprise deeply weathered, sometimes kaolinised, leached silty sand. Hill crests representing Post-African Erosion Cycles comprise generally of shallow silty sand residual granite. Hardpan ferricrete is generally associated with gully heads and may also occur in low-lying side slopes.

Land facet classification

Land facets were identified by means of stereoscopic aerial photo interpretation (API). API proved to be a fast and cost effective method of accurately identifying areas with similar physical attributes. The land facet map, as derived from API, is shown in **Figure 7.3**.

The study area is dominated by a major east-west trending ridge that represents remnants of the African Erosion Surface. It forms part of a major north-south trending ridge extending from Venterdorp lavas in the region of Isando to Midrand. Several north-south trending, undulating, slightly convex ridges are clearly visible in the area and correspond to the general macro-structural model.

The structural geology is an important controlling factor in preferential weathering and secondary aquifer development. Drainage features often follow these preferential weathering zones, resulting in linear topographic features as are evident in the study area. Identification of these zones, generally associated with high groundwater potential, is essential since these areas are vulnerable to groundwater contamination. Geological structures were identified by means of API. Geological structural features can generally be readily identified by their linear appearance.

A total of five sets of structural features were identified in the area. The most prominent are the north-south, northeast-southwest and, to a lesser degree, north-northwest south-southeast trending features. These features correspond to the general macro structural model of the Johannesburg Dome (Hilliard, 1994; Anhaeusser, 1973; McKnight, 1997).

The prominent Glen Austin Fracture Zone, identified by McKnight (1997) as a possible major controlling structural feature of the Johannesburg Dome, is not clearly visible in representations of the study area. The sharp contrasts between the weathering and soil characteristics of the areas to the north and those to the south of the study area, observed in numerous engineering geology investigations of the Johannesburg Dome, are manifested in the study area. McKnight (1997) attributes this to the Glen Austin Fracture Zone forming a possible half-graben structure with a downthrow to the south. However, these contrasts do not show direct correlation with the fracture zone.

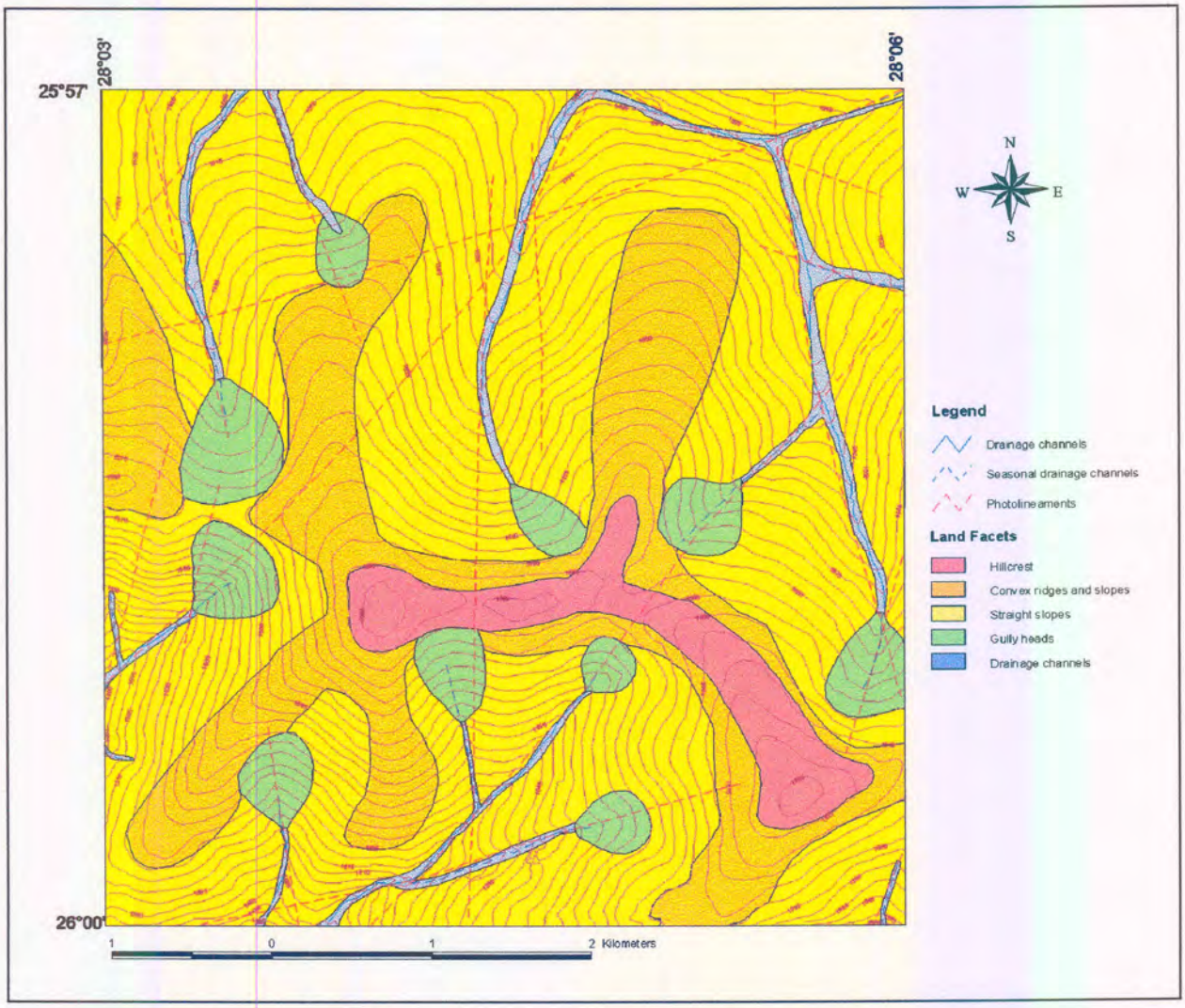

Figure 7.3: Land facet map of the study area as derived by API

The northern portion is generally characterised by undulating terrain with generally shallow residual soils and scattered granitoid outcrops occurring along low-lying drainage channels, such as the Rietspruit River. In contrast, the southern portion is characterised by incised Post African II valleys, as is evident in the Vorna Valley, Carlswald and President Park areas. The area is characterised by deeper weathered soils and a well-defined corestone zone. These differences can be explained by differences in geology and different geomorphic events affecting the weathering patterns in the different areas.

7.3.2 Description of materials

The description of geotechnical material occurring throughout the study area has mainly been based on geotechnical investigations conducted by the Council of Geoscience (1998). A significant geotechnical database was produced, which included large amounts of soil profile descriptions, obtained from the Council for Geoscience, the CSIR and the private sector.

Transported material

Fine colluvium typically comprises the top one metre of a soil profile and occurs along most of the investigation area. It comprises silty to clayey sand with scattered sub-rounded quartz and granite gravel. The soil is often voided and leached.

Hillwash frequently occurs along gully heads and on the lower side slopes adjacent to drainage channels. The hillwash typically comprises a thin layer of silty to clayey sand and is frequently underlain by hardpan ferricrete.

Alluvium occurring along drainage channels typically comprises dark grey, sandy to silty clay, sometimes intercalated with light grey coarse sand. The grey colour indicates saturated reducing conditions.

The gravel pebble marker indicates the transition between residual and transported soils. It may be up to 0.40 m thick and typically comprises a tightly packed to loosely packed sub-rounded and sub-angular quartz and granite gravel in a matrix of frequently ferruginised, silty fine, medium and coarse sand. The overall consistency of the layer is generally medium dense to dense.

Residual granite

The geotechnical characteristics of residual granite are mainly a function of its position within the Kyalami Land System landscape.

A distinction is made between hill crests occurring on the African Erosion Cycle and those on the Post African Erosion Cycles. Hill crests occurring on the former cycle are characterised by deep, kaolinised, highly leached soils. The top pallid highly leached horizon often exhibits a collapsible grain structure.

Hill crests occurring on Post-African Erosion Surfaces comprise a red-brown, stained dark brown and orange-brown, loose to medium dense, voided, silty to clayey sand with fine sub-angular quartz gravel and, sometimes, fine ferricrete concretions. Corestones occur sporadically in the southern portion, while shallow bedrock occurs in the northern portion of the study area.

Convex and straight side slopes comprise red-brown, yellow-brown or grey-brown, loose to medium dense, voided, clayey to silty sand with or without loose to tightly packed coarse, medium and fine ferricrete concretions. Relict rock structures may occur in the soil profile and generally consist of zones of light-grey, loose, clayey sand.

Concave side slopes are not generally defined on the Kayalami Land System (Brink & Partridge, 1967; Stiff, 1994). However, soil profiles on lower-lying areas of the slopes indicate significant differences from soil profiles on upper-slopes. Accordingly, Aucamp (Council for Geoscience, 1998) defines a slightly concave side slope facet occurring on the lower-lying areas on side slopes, close to drainage channels.

The residual material comprises red-brown, stained red, yellow and orange, medium dense to dense, highly ferruginised, silty sand. Hardpan ferricrete frequently occurs at shallow depth. The downward flow of water is impeded by low-permeability material. In addition, gully head areas are characterised by upward hydraulic gradients and groundwater discharge resulting in the development of seepage zones. This groundwater flows mainly in a horizontal direction along the E-horizon, which overlies the ferruginised horizon. The E-horizon comprises shallow, pallid and leached, loose, slightly silty sand.

Apart from concave side-slopes and gully heads, hardpan ferricrete may develop sporadically along convex and straight side slopes and hill crests occurring on Post African erosion surfaces. Hardpan ferricrete may develop either in colluvium or residual granite.

Residual greenstones

Residual greenstones occur sporadically within the Johannesburg dome. The greenstones are generally altered to serpentine shists. The residual material generally comprises orange-brown to olive-green, speckled dark grey, light grey and light red, stiff, occasionally slickensided clay.

Weathering troughs

Not much has been published on the highly weathered material occurring in deep weathering troughs, formed by preferential weathering along geological structures. The material comprises highly weathered, kaolinised and highly permeable granite rock (saprolite) and overlies a medium to slightly weathered, highly fractured granitoid rock.

7.3.3 Statistical analysis

Geotechnical data of the study area as obtained from the Council for Geoscience, the CSIR and the private sector were statistically analysed in order to determine the geotechnical characteristics of the different soil horizons in each land facet type. The geotechnical data were analysed to determine the central tendency of a particular geotechnical property. In addition, the measure of variability was determined. Typical geotechnical properties for the different soil horizons are summarised in **Table 7.1**.

Table 7.1: Typical gravel/sand, silt and clay contents for the different soil horizons

Material		Sand & gravel (%)	Silt (%)	Clay (%)
Hillwash	Average	74	21	4
	Median	76	22	3
	Coefficient of Variability (%)	11.75	31.41	100.80
	Maximum	87	39	20
	Minimum	53	11	1
	Number of samples	16	16	16
Residual granite	Average	72	21	6
	Median	71	22	5
	Coefficient of Variability (%)	18.07	55.87	69.71
	Maximum	92	54	18
	Minimum	40	5	0
	Number of samples	42	42	42
Ferruginous horizon	Average	80	14	6
	Median	81	15	4
	Coefficient of Variability (%)	17.58	59.05	91.52
	Maximum	98	26	15
	Minimum	59	2	0
	Number of samples	5	5	5
Alluvium	Average	42	39	19
	Median	38	43	16
	Coefficient of Variability (%)	58.89	44.90	78.49
	Maximum	81	64	43
	Minimum	16	16	3
	Number of samples	6	6	6

Table 7.1 indicates that, with the exception of alluvium, all materials exhibit similar characteristics concerning sand/gravel, silt and clay contents. Similar trends were observed for grain-size distributions. The materials, with the exception of alluvium, had almost exactly similar average sand/gravel, silt and clay contents.

Variations in soil fraction contents between different testpits were high, especially the clay contents, but similar variations were recorded for all materials. No significant differences in soil fraction contents between soils from different land facets were observed.

It is argued that (with the exception of alluvium, materials originating from intrusive dykes and greenstone remnants) materials within the study area are similar in composition, irrespective of their origin and location within particular land facets. The large variability encountered can be attributed to the fact that samples are not representative of the particular soil horizon and, in the case of clay content, that the general low clay percentage is sensitive to variation analysis. The similarity in soil composition is caused by similar bedrock materials that are subjected to similar weathering processes. However, significant geotechnical differences may exist between the different soil horizons largely caused by leaching and ferricrete development within the different soil horizons.

7.4 Hydrogeological characteristics

Although field evidence is limited, the groundwater characteristics of the area are similar to hard rock environments, namely shallow weathered, low-yielding aquifers and secondary fractured aquifers with a higher yield.

7.4.1 Shallow groundwater

A total of 109 selected soil profile descriptions throughout the study area were analysed in terms of seepage and groundwater levels recorded in the testpits. The following observations were made:

- Of all the soil profile descriptions recorded during the period of May to October, none made any reference to seepage or shallow groundwater conditions encountered during testpit inspection. In contrast, 38 per cent of the soil profile descriptions recorded during the period of November to April recorded seepage or shallow groundwater conditions.

- In three cases, engineering geologists observed that seepage took place after a rainstorm.

- Many residents complained about surface seepage occurring after rainstorms. During field investigations, surface seepage was observed at several places. In all of these cases, hardpan ferricrete or shallow rock outcrop was observed close to the seepage area. Seepage was particularly severe during and just after the 1995/1996 rain season, characterised by above average precipitation.

- In 61 per cent of cases where seepage was observed in testpits, it was observed less than 1.5 metres below surface and before refusal on granite rock or very dense material and in 31 per cent of the cases, seepage was detected at or near refusal depth. The depth of the testpits varied between 1.6 to 6.9 metres.

- In 9 per cent of the cases, water seepage was observed occurring from a ferruginous layer.

The above observations imply a seasonal perched aquifer occurring throughout the study area. The perched aquifer forms during the rainy season and discharges along gully slopes and lower side slopes. Water infiltrates the ground and accumulates either on shallow bedrock or hardpan ferricrete layers. Accumulation of groundwater occurs after rain events and then flows laterally along the low-permeability underlying layer from where it discharges along the ground surface where the low-permeability layers outcrop, generally along gully slopes. A portion of the groundwater evaporates while another portion flows into deeper fractured aquifer systems.

The perched aquifer dries up during the dry season. The little rainfall that infiltrates the perched aquifer is stored in the aquifer before it evaporates. Little surface seepage occurs during the dry months. However,

surface seepage may occur well into the dry season in the case of very wet season in which large amounts of water occur in the perched aquifer systems.

7.4.2 Groundwater recharge and discharge areas

The drainage channels in the study area are hydraulically connected to perched and shallow aquifer systems. All the drainage channels in the area are classified as effluent streams, implying that perched and shallow aquifers discharge into drainage channels. However, in the case of drought, groundwater levels may drop to below the stream level and this may result in the shallow and perched aquifer systems being recharged by the streams.

Gully heads usually represent groundwater discharge areas. Perched groundwater, flowing horizontally along low-permeability ferruginised zones, intersects the side-slopes and results in groundwater being discharged into stream heads. Similar situations may occur in the case of shallow bedrock.

The interrelationship between surface water, shallow and perched aquifer systems and deep aquifer systems in the Johannesburg Dome region has already been discussed. Because of this interrelationship it follows that any interference with either of these systems may result in the other water resources being affected. High groundwater extraction rates from secondary aquifer systems may cause the groundwater level of the shallow aquifer to drop below stream level. This may result in groundwater being recharged by the stream.

To summarise, groundwater discharge areas are mainly associated with drainage channels, flood plains, gully heads and, to a lesser extent, the lower portions of side-slopes. The remainder of the area can be classified as recharge zones. The recharge rate relates closely to the hydrogeological properties of the individual land facet zones

7.4.3 Preferential flow

A number of possible situations with respect to preferential flow were identified.

- Macropore channelling occurring in the top transported soil along biopores, in particular plant root channels and termite holes
- Macropore channelling associated with relict rock structures occurring in residual granite
- Fingering flow occurring within silty sand overlain by a low-permeability ferruginised soil horizon
- Funnelling flow occurring along the interface between low-permeability ferruginised layers and residual material

Not much research was conducted on the mode and extent of preferential flow within the vadose zone. Results from **Experiments 3** and **4** reveal that macropore channelling, in particular macropore channelling along biopores, may occur within the vadose zone. The extent of this type of preferential flow is probably negligible. However, it is possible that significant macropore channelling may occur in certain situations, e.g. where extensive termite activity occurs.

Little is known about the occurrence and extent of fingering and funnelling in the study area. Because of the extensive ferruginous development in the area, it is suspected that funnelled flow along less permeable ferruginous layers may significantly affect the groundwater situation. It is very difficult to determine the extent of these layers. In addition, very little is known about the continuity of ferruginous layers, adding to the uncertainty with regard to this mode of flow.

7.4.4 Borehole census

A borehole census was conducted in the study area in order to obtain a better understanding of the groundwater situation. In spite of the large number of groundwater users present in the area, the borehole census showed a poor response from the smallholding community, which could be ascribed to the fact that many owners could not be reached. It was decided to focus on a few quality responses rather than following a quantitative approach that could be flawed by many errors.

Borehole data were gathered mainly from Glen Austin, Erand, Blue Hills and Carlswald agricultural holdings. Many smallholding residents were connected to municipal services for their water needs. Although many of these residents still used borehole water for gardening and irrigation purposes, some boreholes were not maintained and were subsequently destroyed.

In all cases except one, the quality of the water was described as very good. The poor quality of water encountered in one borehole could be ascribed to rotting vegetation affecting the water quality of the perched aquifer. Although a few residents had the groundwater tested, no water quality results were available. Some residents observed a high lime content in the groundwater.

Depth to groundwater levels varied from ground surface to 25 m. Two distinct groundwater levels could be identified, namely a shallow groundwater level that varied from ground surface to 10 m and a deep groundwater level of more than 10 m. Shallow groundwater conditions were recorded for most of the northern portion corresponding to shallow weathering profiles characteristic of the Post-African erosion surfaces. In contrast, deeper groundwater levels were observed in the more deeply weathered materials in the New Road onramp area, corresponding to the African erosion surface. In many cases, the depth to groundwater surface could not be obtained because many boreholes were equipped with pumps.

Groundwater yield varied from 0.01 to 8.3 l/s. Two boreholes (BH006 and BH008) showed a yield of more than 5 l/s. Both these boreholes could be associated with geological structures as interpreted from aerial photo interpretation. These boreholes possibly represent deeply weathered, high-permeability secondary aquifers.

Based on these observations, it was concluded that there are probably at least three aquifer systems in the study area:

- A shallow seasonal perched aquifer associated with shallow bedrock and highly ferruginised to hardpan ferricrete
- A shallow weathered aquifer associated mainly with deeply weathered silty sand of the African erosion cycle
- A deeply weathered, highly permeable and often high-yielding secondary aquifer associated with geological structures

These aquifer systems showed remarkably good correlation to geomorphic erosion surfaces and land facets within the study area.

7.5 Pedo-transformations

7.5.1 Estimation of saturated hydraulic conductivity

A total of 66 soil samples were collected in the study area from testpits. The soil samples were collected as part of the regional engineering geological mapping of the Midrand/Centurion area conducted by the Council for Geoscience (1998). Foundation indicator tests were conducted and the particle size distributions were determined.

Saturated hydraulic conductivity was estimated applying the empirical equations of Campbell (1985), Campbell and Shiozawa (1992) and Rawls *et al* (1982). These methods were discussed in **Chapter 4**. A correction factor, determined for **Experiment 4**, was included in the equations in order to compensate for factors such as grain shape and packing that vary with each soil type. The results are summarised in **Table 7.2**.

Table 7.2: Estimated saturated hydraulic conductivities as derived from soil fractions

	Campbell	Campbell and Shiozawa	Rawls *et al*
Average estimated K_s (m/s)	5.93×10^{-7}	1.22×10^{-6}	2.96×10^{-7}
Median estimated K_s(m/s)	5.53×10^{-7}	6.69×10^{-7}	2.56×10^{-7}
Coefficient of variation (%)	51.81	116.01	60.16
Maximum estimated K_s(m/s)	1.56×10^{-6}	7.45×10^{-6}	8.44×10^{-7}
Minimum estimated K_s(m/s)	1.04×10^{-7}	1.01×10^{-7}	2.61×10^{-8}
Number of samples	66	66	66
Measured K_s(m/s)	5.90×10^{-7}	5.90×10^{-7}	5.90×10^{-7}
Percentage error	6.35%	-11.86%	56.55%

Table 7.2 shows remarkably good correlation between measured hydraulic conductivity as derived from **Experiment 4** and estimated median hydraulic conductivity as derived from all three empirical equations. However, large variations in estimated hydraulic conductivity were recorded in response to the high variability in the soil compositions of the soil samples. The good correlation between measured and estimated hydraulic conductivity confirms the similarity of soil materials.

In addition to soil fractions, saturated hydraulic conductivity was estimated from grain-size distributions by means of ten popular empirical equations. The application of these empirical equations was discussed in **Chapter 6**. As in the case of the soil fraction equations, a correction factor was included in the empirical equation to compensate for factors such as grain shape and packing. The results are indicated in **Table 7.3**.

Table 7.3: Estimated saturated hydraulic conductivity derived from grain size distribution curves

	Average estimated K_s (m/s)	Median estimated K_s (m/s)	Coefficient of variation	Maximum estimated K_s (m/s)	Minimum estimated K_s (m/s)	Per cent error
Hazen (1930)	2.84×10^{-6}	1.24×10^{-7}	514.53%	9.54×10^{-5}	6.10×10^{-9}	79.05%
Amer & Awad (1974)	4.01×10^{-6}	3.21×10^{-7}	455.79%	1.19×10^{-4}	8.63×10^{-9}	45.62%
Shahabi *et al.* (1984)	9.02×10^{-6}	2.92×10^{-6}	271.44%	1.54×10^{-4}	1.29×10^{-7}	-79.78%
Kenney *et al.* (1984)	1.19×10^{-6}	3.48×10^{-8}	629.61%	4.90×10^{-5}	8.71×10^{-9}	94.10%
Slichter (Vukovic & Soro, 1992)	3.76×10^{-6}	1.64×10^{-7}	514.53%	1.27×10^{-4}	8.10×10^{-9}	72.21%
Tarzaghi (Vukovic & Soro, 1992)	3.82×10^{-6}	1.67×10^{-7}	514.53%	1.29×10^{-4}	8.23×10^{-9}	71.76%
Beyer (Vukovic & Soro, 1992)	2.49×10^{-6}	4.73×10^{-8}	547.58%	8.93×10^{-5}	3.93×10^{-10}	91.99%
Sauerbrei (Vukovic & Soro, 1992)	8.47×10^{-6}	1.32×10^{-6}	355.21%	1.91×10^{-4}	8.47×10^{-9}	-55.42%
Pavchich (Pravednyi, 1966)	1.43×10^{-5}	3.38×10^{-6}	237.69%	2.02×10^{-4}	2.27×10^{-8}	-82.57%
USBR (Vukovic & Soro, 1992)	5.59×10^{-6}	7.20×10^{-7}	287.84%	9.80×10^{-5}	3.20×10^{-9}	-18.06%

n = 43, measured $K_s = 5.90 \times 10^{-7}$ m/s

Table 7.3 indicates a large variability of estimated saturated hydraulic conductivity for all ten empirical equations applied. Many equations show differences of up to five orders of magnitude between the minimum and maximum predicted saturated hydraulic conductivity for the soil samples. Variations in predicted saturated hydraulic conductivity of more than 500 per cent were calculated for the soil samples tested.

7.5.2 Estimation of soil-water retention characteristics

Soil-water retention characteristics were estimated from soil fractions, applying the Gupta and Larson (1979) empirical equation. This method was applied to soils of Experiment 4 and is described in **Chapter 6**. Estimated volumetric water contents at several soil suction values for 43 soil samples obtained from the study area are presented in **Table 7.4**. These estimated values were compared to measured values derived during Experiment 4.

Table 7.4: Estimated volumetric water contents at various suction values

	Estimated volumetric water content at soil suction (kPa)					
	4	**10**	**33**	**60**	**100**	**1000**
Average volumetric water content	0.260	0.199	0.159	0.146	0.137	0.102
Median volumetric water content	0.258	0.196	0.155	0.143	0.134	0.098
Maximum value	0.370	0.326	0.276	0.255	0.239	0.190
Minimum value	0.146	0.098	0.078	0.071	0.066	0.045
Coefficient of variation (%)	17.53%	24.65%	27.42%	27.60%	27.74%	30.99%
Measured value (Experiment 4)	0.206	0.181	0.157	0.145	0.136	0.095
Percentage error	-20.20%	-7.35%	1.11%	1.33%	1.47%	-2.44%
Number of samples	66	66	66	66	66	66

Table 7.4 indicates significantly less variation in estimated volumetric water contents compared to estimated saturated hydraulic conductivity values. These variations correspond to variations in soil fraction composition. This indicates that soil retention characteristics are closely related to grain-size distribution. This trend is further confirmed by the normal distribution curve of the estimated values, as indicated by the similar average and median values. The results confirm that water-retention characteristics are mainly a function of the specific surface of the grains, implying that they are also a function of grain-size distribution, especially for high soil suction values.

With the exception of water contents at a soil suction value of 4 kPa and, to a lesser extent, 10 kPa, estimated volumetric water contents are remarkably similar to the values measured during Experiment 4. This indicates that, although variations occur for different soil samples, water retention characteristics are similar to soils occurring in the study area. The deviations at lower soil suctions occur because of the importance role pore-connectivity and pore-size distribution plays at near saturated conditions, which is not considered by the Gupta & Larson (1979) equation.

7.5.3 Estimation of unsaturated hydraulic conductivity

Unsaturated hydraulic conductivity is mainly a function of both saturated hydraulic conductivity and the soil-water characteristic curve. It has earlier been established that the soil-water retention characteristics and saturated hydraulic conductivity correspond to the results of Experiment 4. It is therefore expected that the unsaturated hydraulic conductivity of residual soils in the study area will be similar to those determined during Experiment 4. The expected variability for unsaturated hydraulic conductivity values in the residual soils is functions of:

- The variability of saturated hydraulic conductivity
- The variability of soil-water retention characteristics
- Variability as a result of errors in describing the soil-water characteristic curve
- Inaccuracies regarding predicted hydraulic conductivity from the soil-water characteristic curve

It has been shown that equations developed by Van Genuchten (1980) and Fredlund and Xing (1994) accurately describe the soil-water characteristic curve. It has also been shown that predicted unsaturated hydraulic conductivity can be accurately predicted from soil-water characteristic curves, provided that the saturated hydraulic conductivity is known. Since it has been shown that major variations occur for estimated hydraulic conductivity, it can be concluded that the variability of unsaturated hydraulic

conductivity will be similar to that of saturated hydraulic conductivity. Unsaturated hydraulic conductivity as derived from Experiment 4 is shown in **Table 7.5**

Table 7.5: Unsaturated hydraulic conductivity at various soil suction values for residual soils in the study area.

Soil suction (kPa)	Experiment 4	
	K (Van Genuchten)	K (Fredlund & Xing)
1.00	1.4×10^{-8}	5.0×10^{-7}
5.00	1.4×10^{-10}	5.4×10^{-10}
10.00	1.4×10^{-11}	1.0×10^{-10}
20.00	1.4×10^{-12}	2.3×10^{-11}
50.00	6.7×10^{-14}	3.4×10^{-12}
100.0	6.5×10^{-15}	7.8×10^{-13}
1000	2.9×10^{-18}	5.9×10^{-15}

7.6 Delineation and characterisation of hydrogeological units

Since the residual soils occurring in the study area were of similar composition and characteristics, the delineation of hydrogeological units had to be based on other physical attributes. The physical attributes identified as having a significant impact on the vadose zone situation include:

- Depth to impermeable bedrock material
- Presence of weathering troughs associated with geological structures
- Depth to shallow groundwater surface
- Presence of a low-permeability ferruginous layer
- Presence of hardpan ferricrete
- Presence of a perched groundwater level associated with low-permeability ferruginous layers or hardpan ferricrete
- Presence of corestones in the soil profile
- Presence of dykes or remnant greenstones

These physical attributes are present in the soil profile and differ from other hydrogeological units mainly because of differences in underlying geology and the geomorphic events to which the soils have been subjected.

The unique hydrogeological units were delineated by means of the land systems approach. The results were incorporated in a GIS system. In addition to the land facet map, the following information was incorporated in the GIS system:

- The bedrock geology, as derived from the geology map compiled by Hilliard (1994)
- The structural geological setting as interpreted by means of aerial photo interpretation
- Outcrop conditions as mapped and compiled by the Council of Geoscience (1998)

- A map indicating areas subjected to different geomorphic events. This map is largely based on work by McKnight (1997)

By incorporating these sources of information in a GIS system, zones exhibiting similar hydrogeological characteristics could be identified. The hydrogeological zones were delineated by overlapping bedrock geology, the land facet, geomorphologic and geotechnical maps. The GIS compiled map was then simplified based on soil profile descriptions. Four major geohydrological zones were identified which closely resemble land facets for the area, namely:

Zone A: Areas representing high-lying topographical features such as hill crests and convex ridges.

Zone B: Areas representing side slopes (upper and lower side slopes) characterised by soil profiles generally deeper than 2m.

Zone C: Areas representing stream heads, gully slopes and side slopes characterised by shallow soil profiles less than 1m deep.

Zone D Drainage channels in which alluvial material has accumulated or where bedrock has been exposed.

The major geohydrological zones were then subdivided into zones corresponding to bedrock geology, geomorphology and geotechnical mapping. Areas depicting zones of similar hydrogeological characteristics are shown in **Drawing 1.**

7.6.1 Description of the hydrogeological zones and assessment of groundwater recharge and vulnerability

The hydrogeological zones identified and delineated are depicted in **Drawing 1**. Typical cross-sections and the interpreted hydrogeological assessment are described below.

A total of 116 soil profiles, obtained from the study area were classified according to their position relevant to the delineated zones as depicted in **Drawing 1**. Typical soil profiles and conceptual unsaturated flow models were established for each of the hydrogeological zones, based on the soil profiles and previous research by, in particular Brink & Partridge (1967), Stiff (1994) and McKnight (1997).

The South African nomenclature defines five weathering stages, as opposed to the traditional six weathering stages defined internationally. Completely weathered rock is described as residual soil in the South African nomenclature while residual soil is often referred to as reworked residual soils. Although the South African nomenclature is probably more descriptive of the material (completely weathered rock is defined as a soil by engineering standards) it is recommended that the international terminology be used to prevent confusion. In this thesis, the international recognised terminology is used with the South African term in brackets, i.e. – completely weathered granite (S.Afr: residual granite).

Zone A1

Zone A1 represents hill crests occurring on the lowered African erosion cycle. The zone corresponds to KYAL0101 (Residual sandy clay with collapsible grain structure on granite) as proposed by Brink & Partridge (1969) and modified by Stiff (1994). It also corresponds to the Interfluve Crest (Remnant of deep kaolinised leached zone) as proposed by McKnight (1997)

A total of 29 soil profiles, representative of Zone A1, had been obtained in the study area. Most of these soil profiles formed part of geotechnical investigations for the construction of medium to large structures, which involved *inter alia* piling. Consequently, many soil profiles were described up to 12m in depth.

Zone A1 soils are characterised by a deep, often kaolinised, highly leached profile. The top pallid, highly leached horizon often exhibits collapsible grain structure.

The hillwash consist of 0.5 to 1.2m of reddish brown to pale brown, loose, intact silty sand with scattered sub-rounded quartz and granite gravel and roots. The soils are often friable, voided and leached. The hillwash is underlain by an often poorly developed pebblemarker. It is typically between 0.1 and 0.3m in thickness and is sometimes absent in the soil profile. It consists typically of a tightly packed to loosely packed sub-rounded and sub-angular quartz and granite gravel in a matrix of frequently ferruginised, silty fine, medium and coarse sand. The overall consistency of the layer is medium dense to dense.

The residual granite underlying the pebble marker consists of orange-brown to red-brown, loose to medium dense, voided, silty to clayey sand with fine sub-angular quartz gravel and, sometimes, fine ferricrete concretions. The consistency of the soils generally increases with depth, becoming medium dense to dense, with medium dense soil comprising the top approximately 1.0 m of residual granite. The collapsible grain structure of this pallid root zone, and its associated geotechnical problems, has been well documented. According to Partridge and Maud (1987), extensive weathering during the African erosion cycle resulted in the development of highly leached soils, probably with a thick ferricrete cap. The soils therefore represent the base of a thick ferricrete layer, which has since been eroded away.

The orange-brown to red brown leached soil layer is often underlain by extensive pale brown, to yellow, soft sandy clay with occasional fine quartz gravel. This completely weathered (S.Afr: residual) kaolinised zone represents extensive *in situ* chemical weathering of the granitioid rock. Nearly all minerals, with the exception of quartz, have been weathered to kaolinite (with some minerals first weathered to montmorillonite and then to kaolinite) under humid climatic conditions, typical of the paleo-climate during the early Miocene age. Fingers of leached, reddish brown, residual granite were observed, extending into the kaolinised zone along preferential weathering zones.

The orange brown, leached layer is generally underlain by pale grey to pale brown, veined and pegmatitic in places, highly weathered, often jointed, very soft granitoid rock. These zones correspond to the kaolinised zones, but have not been weathered to a similar extent. Occasional moderately weathered corestones occur within the soil profile. The thickness of the highly weathered zone varies significantly (0 to 4m).

The weathering profile is approximately 10m in thickness. The weathering profile is noticeably consistent in its thickness, given the typical heterogeneous nature of these profiles. Groundwater occurs approximately 8m below ground surface and is perched on the impermeable bedrock material.

Flow through the vadose zone is complex. The preferential weathering zones are important aspects in flow through these zones. The conceptual unsaturated groundwater flow model is represented in **Figure 7.4**. The medium to high permeability of the soils implies that recharge events will be related closely to rainfall events. During infiltration, water will move predominantly along the more permeable preferential weathering zones as indicated by **Figure 7.4**. In periods between rainfall events, groundwater will mainly be recharged (though on a limited scale) along the less permeable (though characterised by higher water-retaining properties) sandy clay. The jointed, highly to medium weathered rocks, although possibly highly permeable, will have little effect on the recharge rate, because flow through joints will depend on the flow rate through overlying soils. High flow velocities will occur along these joints, resulting in lower travel times and hence higher vulnerability. This effect will be overshadowed by the predominant flow along preferential weathering zones.

However, it is expected that the main pathway of water within the phreatic zone will be along highly permeable, medium to highly weathered, jointed, soft rock zones. Flow along these zones will be mainly horizontal. This zone could:

i Provide base flow to streams,

ii Result in seepage along lower slopes characterised by a shallow bedrock or ferricrete layers or

iii Recharge deeper fractured aquifer systems.

The fact that seepage has occurred in several places within the study zone for several months after the particularly wet 1995/1996 rain season indicates that the weathered zones act as a storage zone.

Areas underlain by Zone A1 are recharge areas almost without exception. In general, it can be concluded that the shallow aquifer systems are vulnerable to pollution due to the low travelling times. Since fractured aquifer systems are generally associated with linear drainage features in the study area, it can be concluded that the potential for groundwater will be low. However, the zones are important since these zones act as water storage and are recharging deeper aquifer systems.

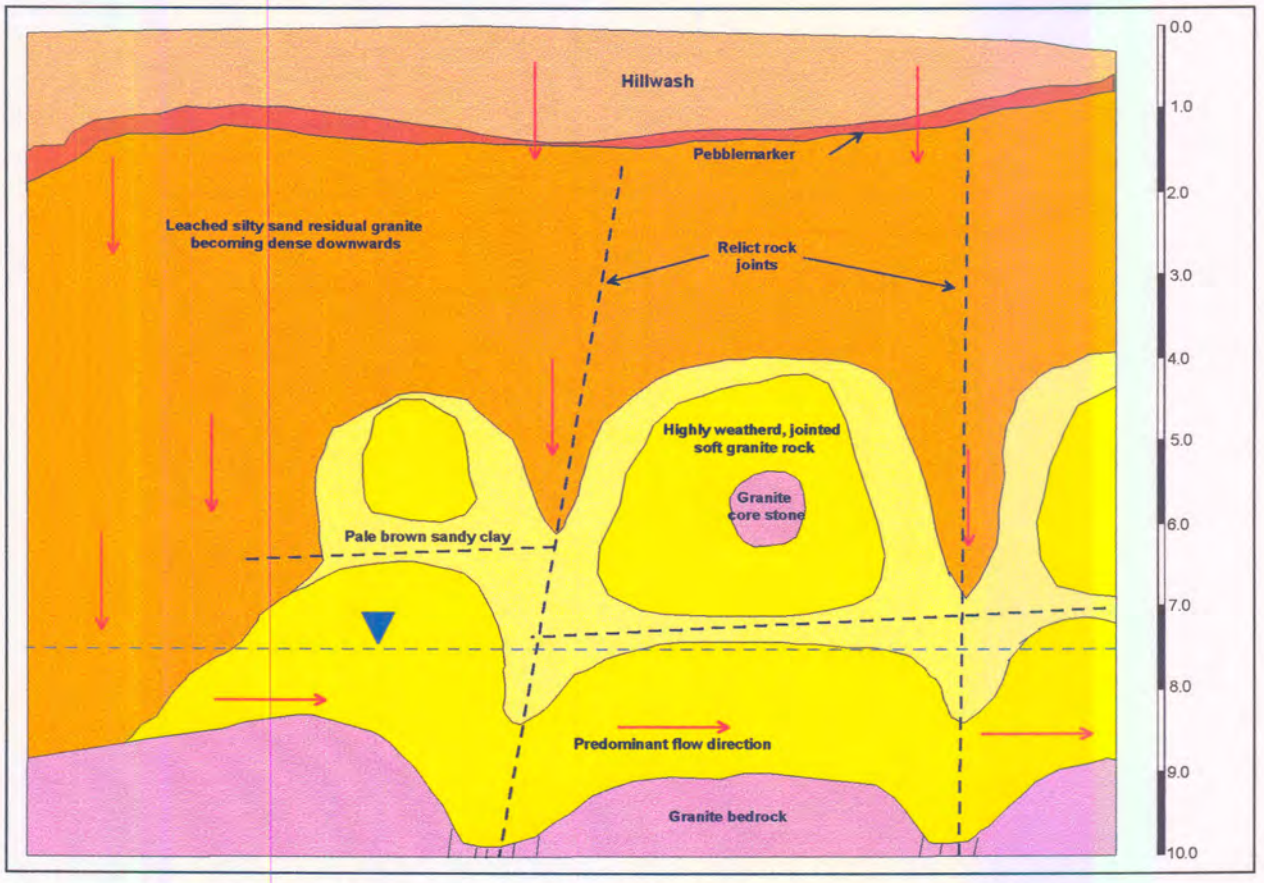

Figure 7.4: Typical soil profile and conceptual unsaturated groundwater model for Zone A1

Zone A2

Zone A2 represents concave ridges within the study area. These areas generally occur along topographic highs with the ridges sloping mainly northwards or southwards towards low-lying drainage channels. The zone corresponds to KYAL0101 (Residual sandy clay with collapsible grain structure on granite) as proposed by Brink & Partridge (1967) and modified by Stiff (1994). It also corresponds partly to the Interfluve Crest (Remnant of deep kaolinised leached zone) and partly to the Scarp and Shelf (basal corestones zone) as proposed by McKnight (1997). A total of 18 soil profiles, representative of Zone A2, were obtained in the study area.

As in Zone A1, Zone A2 soils are characterised by a deep highly leached profile. The top pallid, highly leached horizon often exhibits collapsible grain structure. Zone A2 also represents the transitional zone

between Zones A1 and B1/B2 and between Zones A1 and C1. Consequently, soil profiles are highly variable, with soil depths ranging from 0.2m to deeper than 2.5m and refusal on either hardpan ferricrete or soft rock granite. The central parts of Zone A2 are generally more representative of Zone A1, while the edges of the zone are more representative to Zones B1, B2 and C1.

The hillwash consists of 0.2 to 0.7m of reddish brown to pale brown, loose, intact silty sand with scattered sub-rounded quartz and granite gravel and roots. The soils are often friable, voided and leached. The hillwash is underlain by a pebblemarker, sometimes absent or poorly developed and sometimes well developed, with a thickness between 0.1 and 0.4m. It typically consists of a tightly packed to loosely packed sub-rounded and sub-angular quartz and granite gravel in a matrix of frequently ferruginised, silty fine, medium and coarse sand. The overall consistency of the layer is medium dense to dense.

A total of 17 per cent of soil profiles recorded refusal on hardpan ferricrete. These profiles were recorded close to the contact with Zone C1 (gully slope). Refusal occurred between 0.4m and 1.1m from ground surface. The hardpan ferricrete comprises orange-brown, mottled black and dark yellow, medium hard ferricrete. The hillwash and residual granite overlying the hardpan ferricrete are grey-brown, very loose to loose, voided, silty sand with sporadic quartz gravel.

A total of 44 per cent of soil profiles recorded refused on very soft rock granite. These profiles were recorded close to the contact with Zone B1 (straight slope). A typical soil profile comprises hillwash and pebble marker overlying a pale orange-brown to pale grey, sometimes weakly cemented ferruginous, loose to dense, silty sand, residual granite (S.Afr: reworked residual granite). This layer is generally underlain by pale orange brown, dense to very dense, relict jointed, silty sand completely weathered granite (S.Afr: residual granite)

A total of 39 per cent of soil profiles recorded no refusal to approximately 2.0m depth. These profiles were mainly recorded along the central parts of Zone A2. A typical soil profile comprises hillwash and pebble marker overlying reddish brown, voided, sometimes weakly cemented ferruginous, loose to dense, silty sand, completely weathered granite (S.Afr: residual granite).

Seepage was recorded in only on test pit. It is possible that the groundwater level occurs at depths greater than 2m.

Flow through the vadose zone is expected to be complex and flow characteristics depends on the underlying soil profile. In general, it is expected that flow in the central parts of convex ridges will be similar to Zone A1, i.e., water infiltrates predominantly along the more permeable preferential weathering zones. As in Zone A1, water will be perched on top of impermeable granite rock and will then flow down-slope along the more permeable jointed highly weathered granite.

Along the edges of Zone A1, representing transition to Zones B1 and C1, highly weathered granite is absent from the profile and the shallow bedrock occurs at approximately 2m depth. The fact that no water has been encountered during recording of the soil profile indicates that limited water is stored within these layers. Water either flows down-slope to drainage areas or is removed by evapotranspiration processes. Flow within soils characterised by hardpan ferricrete layers will be similar to that of Zone C1 and will be described in the relevant section.

The conceptual unsaturated groundwater model for Zone A2 is shown in **Figure 7.5**. The medium to high permeability of the soils implies that recharge events will be closely related to rainfall events. The high permeability of soils also implies high evapotranspiration rates. However, in the case of very high evapotranspiration rates, the top soil layers will dry out rapidly. This will result in a significant decrease in hydraulic conductivity and consequently, the upward movement of water from deeper more saturated zones will be impeded. In the case that water is perched on shallow bedrock or hardpan ferricrete, evapotranspiration processes will remove the perched water.

Areas underlain by Zone A2 are almost without exception recharge areas, the exceptions being very shallow soils where seepage may occur, thereby acting as a discharge point. In general, it can be

concluded that the shallow aquifer systems are vulnerable to pollution due to the low travelling times. Since fractured aquifer systems are generally associated with linear drainage features in the study area, it can be concluded that the potential for groundwater will be low. However, linear features, that could represent fractured zones with a high potential for groundwater, occasionally cross Zone A2 areas at several topographic saddles.

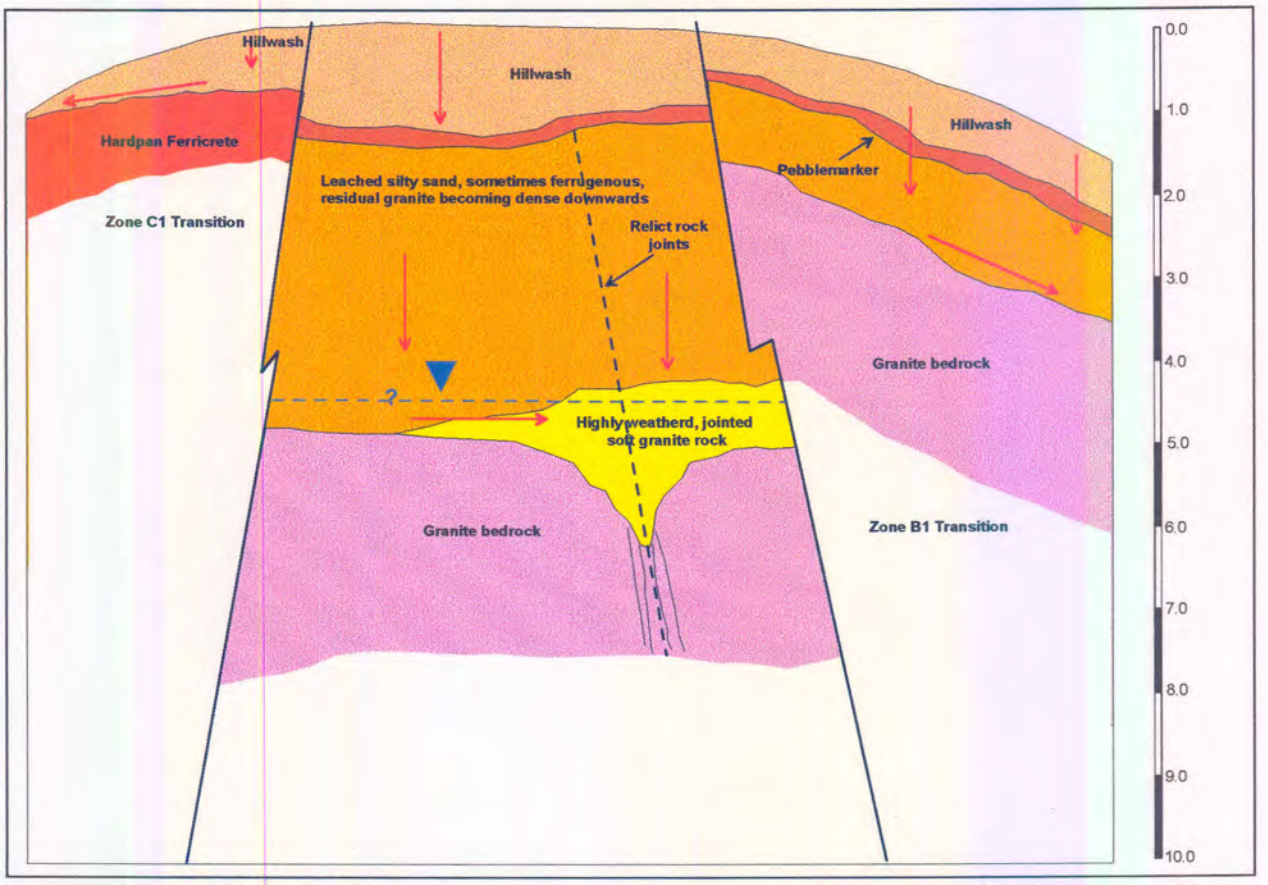

Figure 7.5: Typical soil profile and conceptual unsaturated groundwater model for Zone A2

Zone A3

Zone A3 represents the upper slopes occurring south of the dominant east-west ridge in the study area. The lower boundary of this zone is defined by the 1550m contour level and represents the approximate base of the African erosion surface. The zone is entirely underlain by foliated granodiorites (Hilliard, 1994) also known as the transitional zone (Anhaeusser, 1973). Zone A3 does not occur along the northern parts of the investigation area (underlain by banded gneisses), even though large parts occur above the 1550m contour line. The zone corresponds to KYAL0203 (Convex side slope, hillwash on residual granite) as proposed by Brink & Partridge (1967) and modified by Stiff (1994). It also corresponds to the Scarp & Shelf (African Base with corestones) as proposed by McKnight (1997).

Only two soil profiles, representative of Zone A3, were obtained. The soil profiles have been recorded up to 2.0m in depth, which is not representative of a typical soil profile for Zone A3. Consequently, expected physical and hydrogeological characteristics of this zone are mostly based on work by McKnight (1997). The development of corestones and tors along the foliated granodiorite has been discussed in **Section 7.2.2**.

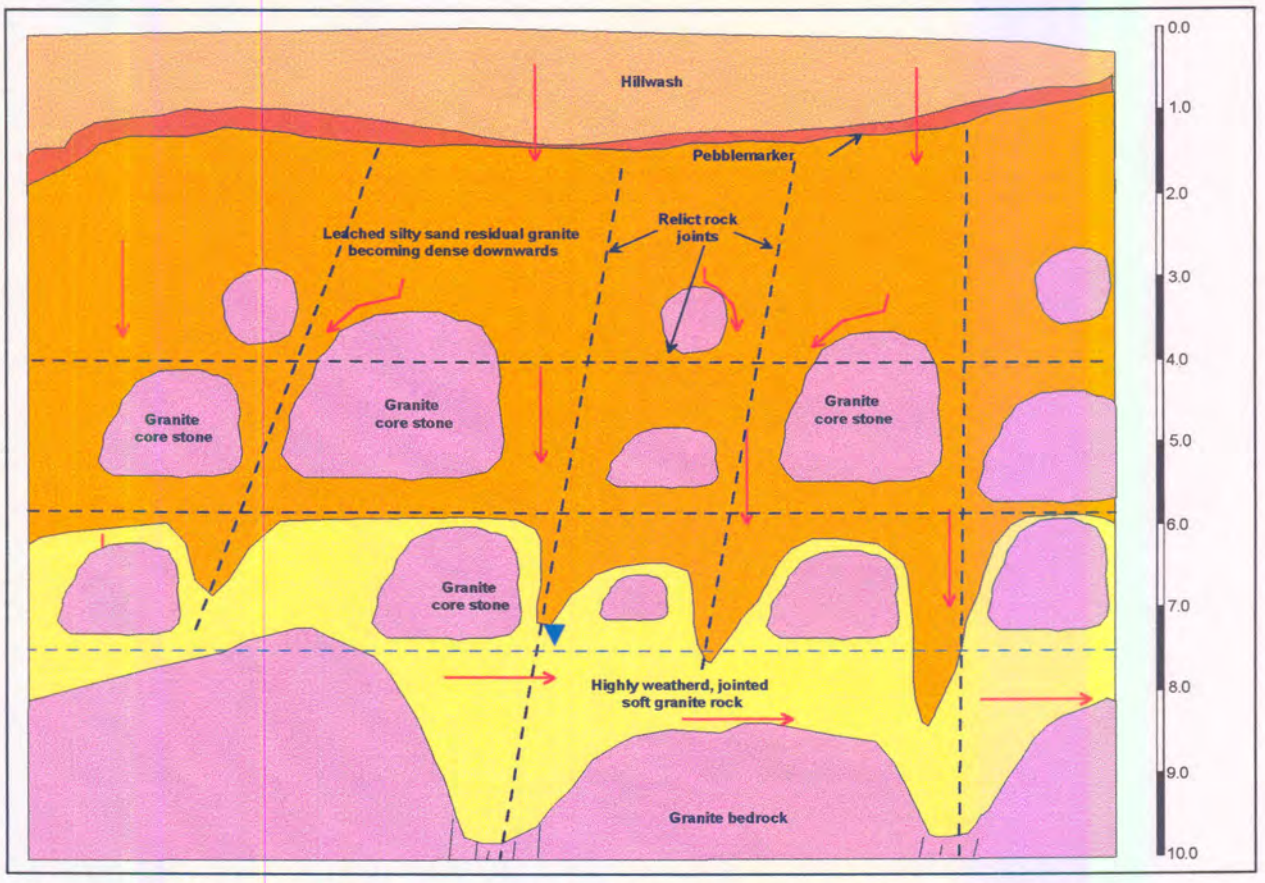

Figure 7.6: Typical soil profile and conceptual unsaturated groundwater model for Zone A3

Zone A3 is characterised by a deep, sometimes leached, soil profile. Corestones frequently occur in the profile. The size and frequency of corestones is highly variable and corresponds to the structure of the underlying bedrock. In essence, the weathering profile is similar to that of Zone A1, except that the extent of weathering is less pronounced. Consequently, top soil layers have in general not been as extensively leached and corestones have developed.

The hillwash consist of approximately 0.4m of greyish brown, loose, intact silty sand with scattered sub-rounded quartz and granite gravel and roots. The soils are often friable, voided and leached. The hillwash is underlain by a pebblemarker, sometimes absent or poorly developed and sometimes well developed, with a thickness of approximately 0.1m. It typically consists of a tightly packed to loosely packed sub-rounded and sub-angular quartz and granite gravel in a matrix of silty fine, medium and coarse sand. The overall consistency of the layer is medium dense to dense.

Flow through the unsaturated soil profile is mainly along preferential weathering zones. The conceptual unsaturated groundwater flow model is represented in **Figure 7.6**. The medium to high permeable nature of the soils implies that recharge events will closely be related to rainfall events. During infiltration, water flows predominantly along the more permeable preferential weathering zones. The infiltrating water is channelled pass the impermeable corestones as indicated in **Figure 7.6**. This results in extensive leaching between corestones.

The main pathway of water within the phreatic zone is along high-permeable medium to highly weathered jointed soft rock zones. Flow along these zones is mainly horizontal. This zone

i Provide base flow to streams

ii Results in seepage along lower slopes characterised by a shallow bedrock or ferricrete layers or

iii could recharge deeper fractured aquifer systems.

Areas underlain by Zone A3 are mostly recharge areas. In general, it can be concluded that the shallow aquifer systems are vulnerable to pollution due to the low travelling times. Since fractured aquifer systems are generally associated with linear drainage features in the study area, it can be concluded that the potential for groundwater will be low. However, it has been stated that these zones could act as water storage and could recharge deeper aquifer systems.

Zone B1

Zone B1 represents straight to slightly convex slopes within the study area, excluding areas occurring south of the dominant east-west ridge above 1550m. Zone B1 covers the largest portion of the study area. The zone corresponds to KYAL0203 (Convex side slope, hillwash on residual granite) as proposed by Brink & Partridge (1967) and modified by Stiff (1994). It also corresponds partly to the Concave Upper/Middle Slope (Zone C) as proposed by McKnight (1997). Zone B1 occurs on the Post African I erosion surface.

A total of 38 soil profiles, representative of Zone B1, were obtained in the study area. Most of these soil profiles formed part of geotechnical investigations for residential development and small office developments and consequently, soil profiles had been described only up to approximately 2.5m in depth.

Zone B1 soils are characterised by their variability in physical soil profile attributes. The soil profiles are deeply weathered, underlain by shallow granite rock or underlain by shallow hardpan ferricrete. In contrast to Zone A2 soils, there appears to be no correlation between the physical soil profile characteristics and its position in relation to other morphology units. This implies that the hydrogeological characteristics of this zone can not be predicted and will depend on site-specific situations.

The hillwash and pebble marker layers are similar in appearance to that observed in Zones A1, A2 and A3 soils.

A total of 42 per cent of all soil profiles did not record refusal up to approximately 2.5m. A typical soil profile comprises hillwash and pebble marker overlying reddish brown, voided, ferruginous, loose to dense, silty sand completely weathered granite (S.Afr: residual granite). Ferruginous layers occur in all these soil profiles. The ferruginous layers generally occur between 0.2 and 0.6m below ground surface and their thickness could range between 0.2m to 2.3m

The ferruginous zones comprises either scattered ferricrete nodules, weakly to well cemented ferricrete concretions, honeycomb ferricrete or boulder ferricrete. The boulder ferricrete indicates weathering of ferricrete layers. According to McKnight (1997), the residual ferruginised soil layers could have developed under wet paleo-climate conditions and because the ferricrete is slowly dissolving under present climatic conditions.

A total of 37 per cent of all soil profiles recorded refusal on pale brown to grey, soft to hard, highly weathered to moderately weathered granitoid rock. A typical soil profile comprises hillwash and pebble marker overlying a reddish brown to pale grey, sometimes ferruginous, medium dense to very dense, silty sand, residual granite (S.Afr: reworked residual granite). This layer is generally underlain by pale orange brown, dense to very dense, sometimes micaceous, relict jointed, silty sand, completely weathered granite (S.Afr: residual granite). Ferruginous soil layers were recorded in only three of these soil profiles. The ferruginous soil layers comprises either nodular ferricrete or boulder ferricrete.

A total of 21 per cent of all soil profiles recorded refusal on hardpan ferricrete. Refusal occurred between 0.2m and 1.3m from ground surface. The hardpan ferricrete comprises orange brown, mottled black and dark yellow, medium hard ferricrete. The hillwash and residual granite overlying the hardpan ferricrete are described as grey-brown, very loose to loose, voided, silty sand with sporadic quartz gravel. The residual granite and overlying pebble marker are often ferruginised.

The variability in soil profile descriptions closely resembles that of Zone A2. However, in contrast to Zone A2 soils, seepage was recorded in 37 per cent of all soil profiles described. This supports the hypothesis that water generally flows down-slope along Zone A2 towards Zone B1. The perched aquifers in Zone B1 are being recharged by rainfall, runoff and down-slope seepage originating from Zone A2. This net recharge effect exceeds evapotranspiration. However, given the seasonal rainfall patterns, it is expected that most water in the perched aquifer will either evaporate or discharge into drainage channels during the dry winter months. This hypothesis is supported by the fact that no seepage had been encountered in most soil profiles recorded during the dry season.

In the case of shallow bedrock, the highly weathered granite is generally absent from the profile and the shallow bedrock occurs at approximately at a depth of 2m. Water either flows down-slope to drainage areas or is removed by evapotranspiration processes. Flow within soils characterised by hardpan ferricrete layers will be similar to that of Zone C1 and will be described in the relevant section.

The conceptual unsaturated groundwater model for Zone B1 is shown in **Figure 7.7**. The medium to high permeability soils and the shallow weathering profile implies that recharge events will closely be related to rainfall events. As with Zone A2, the high permeability of soils also implies high evapotranspiration rates.

Areas underlain by Zone B1 are mostly recharge areas, the exceptions being very shallow soils where seepage can occur, thereby acting as discharge points. In general, it can be concluded that the shallow aquifer systems are vulnerable to pollution due to the low travelling times. Since fractured aquifer systems are generally associated with linear drainage features in the study area, it can be concluded that the potential for groundwater will be low. However, linear features, which may represent fractured zones with a high potential for groundwater, occasionally occur within Zone B1.

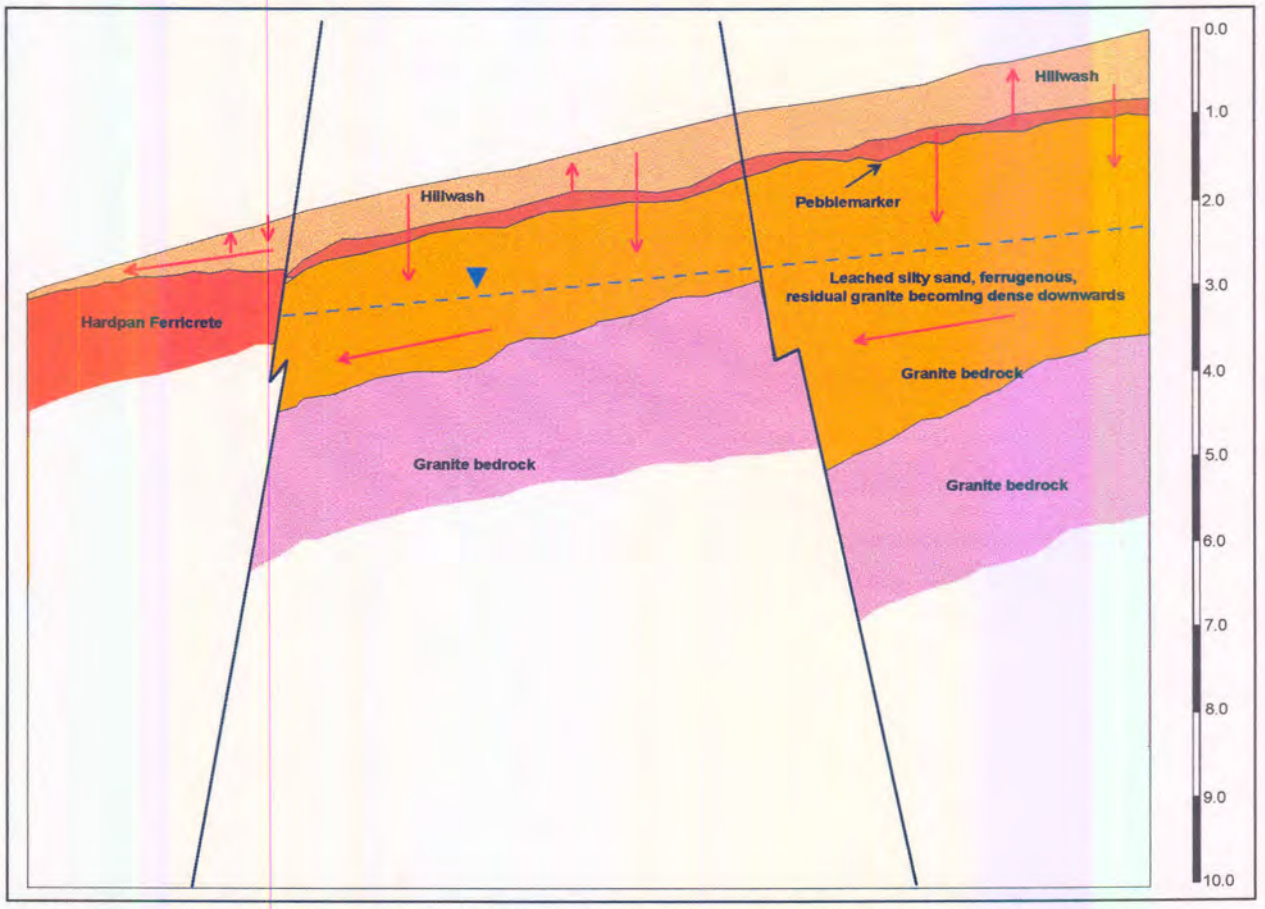

Figure 7.7: Typical soil profile and conceptual unsaturated groundwater model for Zone B1

Zone B2

Zone B2 represents a narrow band of slightly convex lower slopes, adjacent to drainage features within the study area. The zone corresponds to KYAL0203 (Convex side slope, hillwash on residual granite) as proposed by Brink & Partridge (1967) and modified by Stiff (1994). It also partly corresponds to the Concave Upper/Middle Slope (Zone C) as proposed by McKnight (1997). Lower side slopes are not distinguished from middle and upper slopes for geotechnical purposes, except when possible flooding zones are indicated. This can be attributed to the fact that the soil profile characteristics are similar to that of the middle and upper slopes. However, it has been envisaged that the hydrogeological characteristics of Zone B2 will differ significantly from the upper slopes. Zone B2 occurs on the Post African I erosion surface.

A total of 6 soil profiles, representative of Zone B2, were obtained in the study area. Most of these soil profiles formed part of geotechnical investigations for residential development and small office developments and consequently, soil profiles have been described only up to approximately 2.5m in depth.

Hardpan ferricrete had been recorded in five of the six soil profiles. Although the sample number is too small to deduce valid conclusions, it would appear that shallow hardpan ferricrete is a prominent feature in Zone B2 soils.

The hillwash layers appears to be similar in appearance to that observed in other soil zones. However, the pebble marker appears to be either absent or poorly developed. Since Zone B2 soils are located at the forefront of active erosion processes, i.e., close to eroding drainage channels, it is possible that the pebble marker has been eroded away.

A typical soil profile consists of hillwash, between 0.2 and 0.7m in thickness, overlying light grey to yellowish grey loose to very loose, voided, silty sand. Occasional ferricrete nodules occur in the layer, which is approximately 0.5m in thickness. The loose residual granite is underlain by hardpan ferricrete, approximately 0.4 to 1.4m from ground surface.

Although no soil profiles were obtained in the southern parts of the study area, visual inspection revealed tor development along lower slopes, close to drainage features. It is postulated that significant erosion occurred along these areas, thereby exposing corestones that developed in the soil profile along Zone A3 areas. The Boulders shopping centre, built on top of large granitoid boulders, is partly located in a Zone B2 area. Tors were also identified along other areas within Zone B2 and alongside Zone A3 areas, though extensive development has shadowed many of the tors. It is significant that the observed large boulders are confined to the southern parts of the study area, underlain by foliated granodiorite, while no boulders were observed in the northern parts of the study area, which are underlain by banded gneiss.

No seepage was recorded in any of the test pits, contradictory to expectations. However, all of these soil profiles were recorded during the end of the dry season and it is postulated that the water had either been discharged in the drainage channel, or was removed by evapotranspiration processes during the dry season. It is expected that surface seepage will occur over large parts of the area during the rain season, especially after significant rainfall events. This presumption is supported by visual observations made during the borehole census in the area. Widespread seepage was observed along Zone B2 areas, especially in the region of borehole BH008. According to the residents, seepage generally occurs during the rainy season.

The conceptual unsaturated groundwater model for Zone B2 is shown in **Figure 7.8**. Water flows rapidly on top of impermeable ferricrete layers within the permeable loose residual granite and hillwash. The zone is recharged by rainfall, surface runoff and seepage originating from Zone B1. During wet weather conditions, surface seepage occurs and Zone B2 therefore acts as a discharge zone. Zone B2 is therefore a major contributor of base flow to small streams. Since sub-surface seepage is a major recharge factor for Zone B2 areas, long periods of surface seepage are expected after significant rainfall events.

Areas underlain by Zone B2 are generally recharge areas during dry weather conditions and may change to discharge areas during wet weather conditions. The impermeable ferricrete layer acts as a barrier against aquifer contamination but surface water features could be highly vulnerable to contamination since these areas are a major contributor of base flow to surface water bodies. Since secondary fractured aquifer zones are generally associated with drainage features, it can be concluded that these aquifers are also vulnerable to contamination.

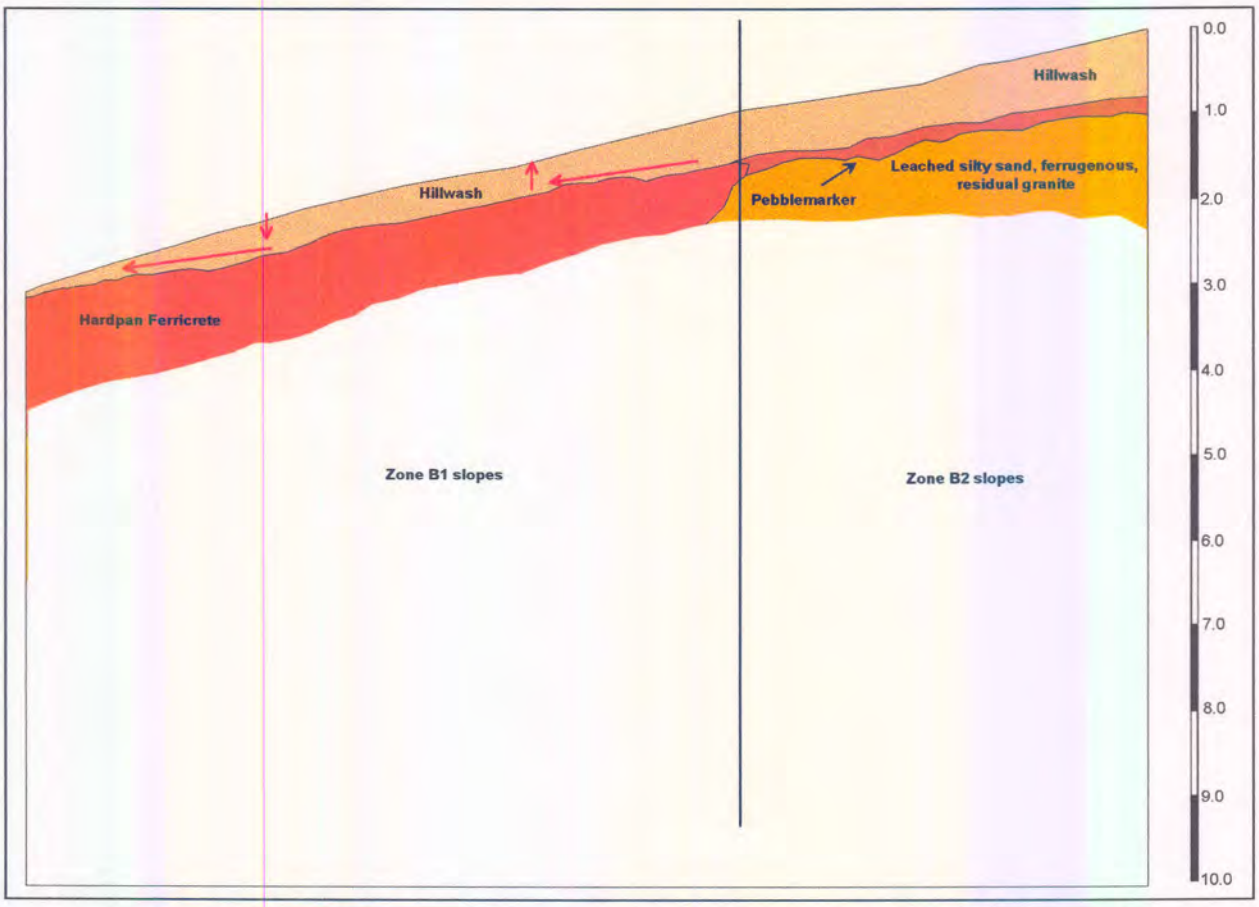

Figure 7.8: Typical soil profile and conceptual unsaturated groundwater model for Zone B2

Zone B3

Zone B3 represents slightly convex slopes occurring below the 1 500m contour line, and is representative of the Post African II erosion surface. The zone corresponds to KYAL0203 (Convex side slope, hillwash on residual granite) as proposed by Brink & Partridge (1967) and modified by Stiff (1994). It also corresponds partly to the Middle/Lower Slope (Zone D) as proposed by McKnight (1997). Zone B3 is confined to the far northern and far southern areas in the study area.

No soil profiles representative of Zone B3 were obtained in the study area. As such, the physical and hydrogeological characteristics of this zone were deduced from soil profiles occurring outside the study area, within areas representative of Zone B3.

A large proportion of soil profiles occurring in Zone B3, recorded refusal on shallow, pale brown, soft to medium hard, highly to moderately weathered granitoid rock. Shallow bedrock is a prominent feature in Zone B3 soils.

The hillwash and pebble marker layers are similar in appearance to that observed in other soil zones. A typical soil profile consists of hillwash, between 0.1 and 0.4m in thickness, and a pebble marker consisting of tightly packed to loosely packed sub-rounded and sub-angular quartz and granite gravel in a

matrix of silty fine, medium and coarse sand. These layers are underlain by yellowish brown to orange brown, medium dense to very dense, relict jointed, micaceous, silty sand. Occasional ferricrete nodules occur in the top residual granite layer. Granite bedrock occurs approximately between 1.3m and 2.9m below ground surface.

Seepage was observed in some of the test pits, approximately 2m below ground surface.

The conceptual unsaturated groundwater model for Zone B3 is shown in **Figure 7.9**. Water flows rapidly on top of impermeable bedrock within the completely weathered granite (S.Afr: residual granite). The zone is recharged by rainfall, surface runoff and seepage originating from Zone B1.

Areas underlain by Zone B3 are mostly recharge areas, but surface seepage occurs in areas underlain by very shallow bedrock or bedrock outcrops. The perched aquifers in Zone B3 are being recharged by rainfall, runoff and down-slope seepage originating from Zone B1. This net recharge effect may exceed evapotranspiration, but given the highly seasonal nature of South African rainfall, it is expected that most water in the perched aquifer will either evaporate or discharge into drainage channels during the dry winter months.

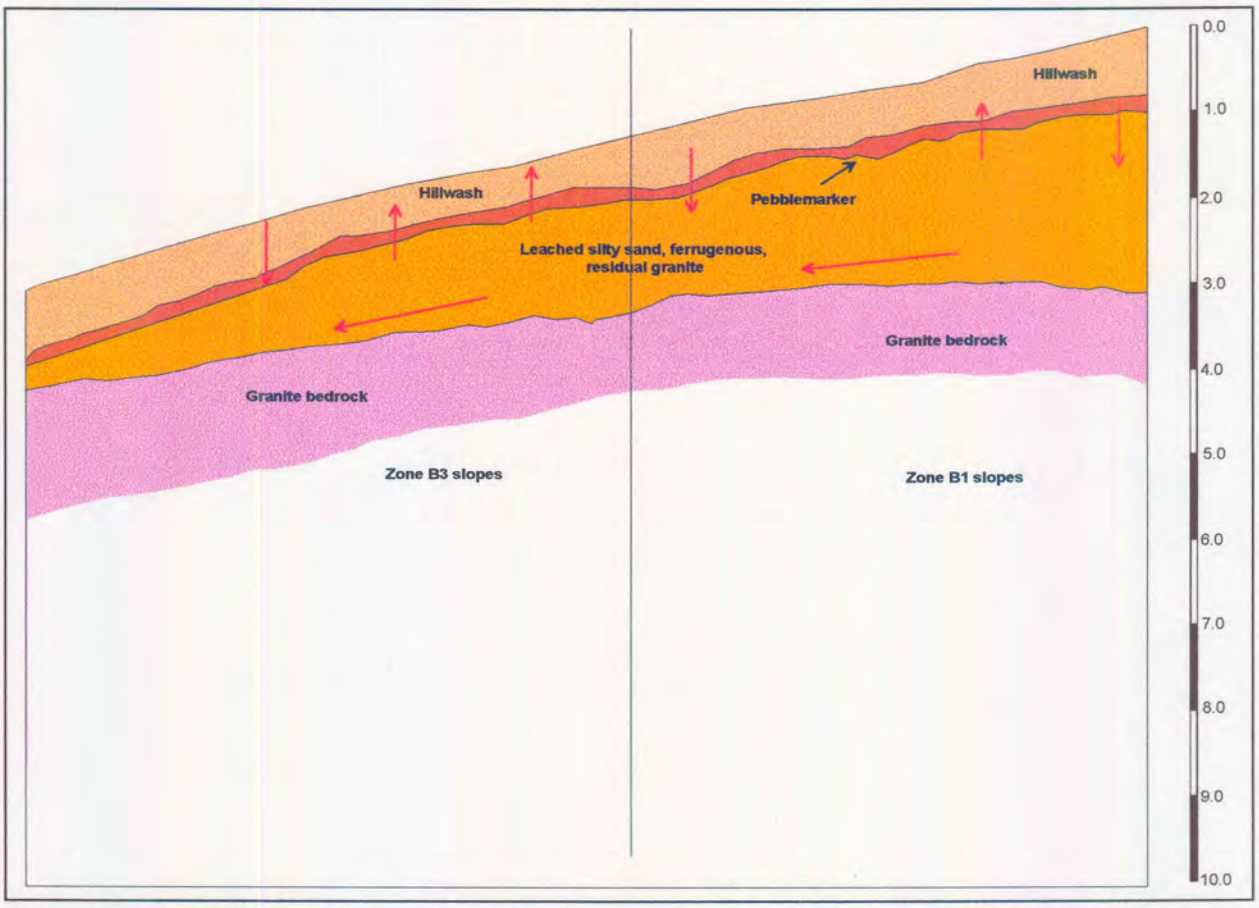

Figure 7.9: Typical soil profile and conceptual unsaturated groundwater model for Zone B3

Zone C1

Zone C1 represents areas occurring along stream heads in the investigation area. The zone corresponds to KYAL0501 (sandy gully wash derived from granite) as proposed by Brink & Partridge (1967) and modified by Stiff (1994). It also corresponds partly to the Concave Middle/Lower Slope (Zone D) as proposed by McKnight (1997). Gully heads are readily identifiable in Aerial Photo Interpretation.

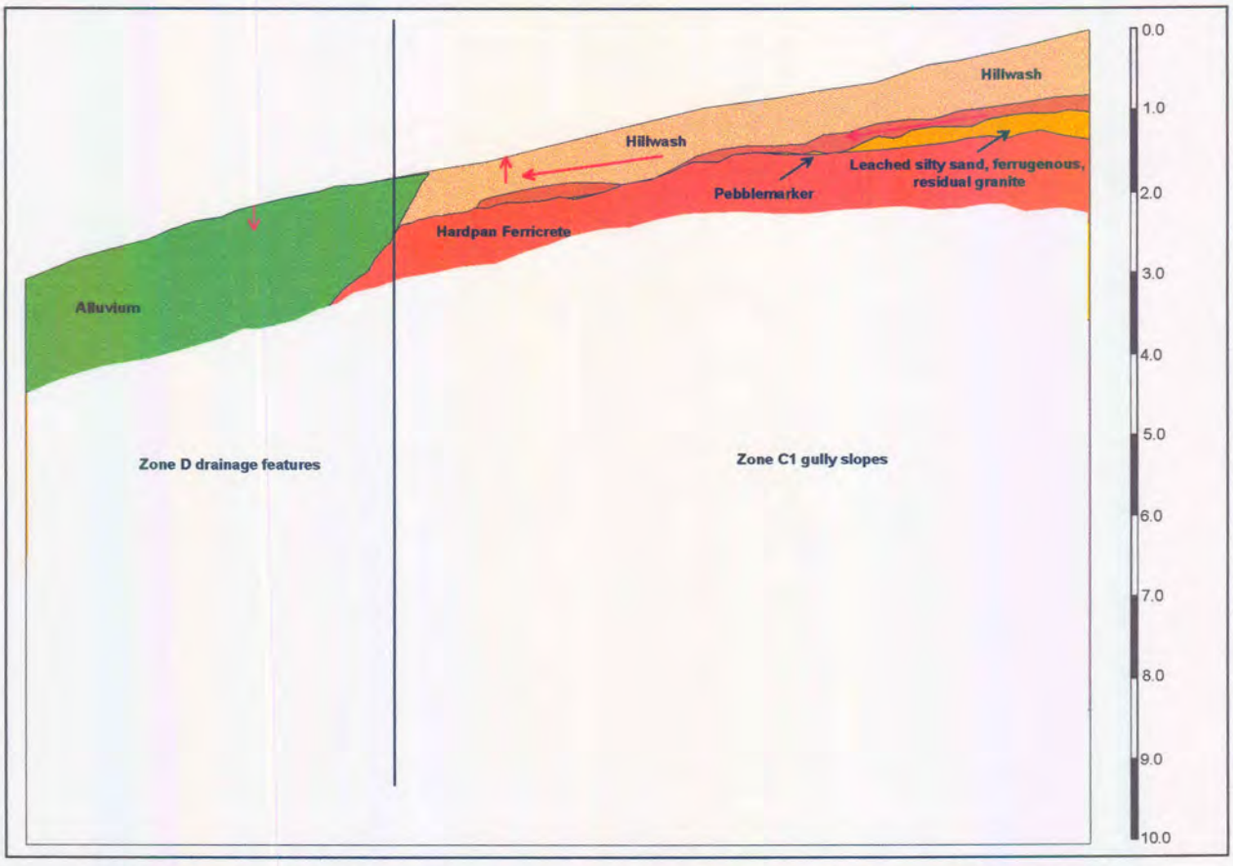

Figure 7.10: Typical soil profile and conceptual unsaturated groundwater model for Zone C1

Zones C2 and C3

It has been recognised that the depth to impermeable ferricrete/bedrock layers is one of most important aspects in assessing the hydrogeological characteristics of the vadose zone. As such, these factors had been incorporated in the GIS map and are indicated as Zones C2 and C3 in **Drawing 1**. Expected shallow soil profiles had been mapped during a regional geotechnical investigation, which includes the investigation area. Mapping was based on the soil profile descriptions and the frequency of bedrock outcrops in the area. Zones C2 and C3 differ from other hydrogeological units in that their boundaries were not derived from by means of aerial photo interpretation. The zones occur mainly adjacent to Zones B1, A2 and A3.

Zone C2 areas are characterised by occasional bedrock or ferricrete outcrops. Based on soil profiles in these zones, it is expected that hardpan ferricrete or granite bedrock will occur between 1.0 and 3.0m below ground surface. Zone C3 areas are characterised by frequent bedrock or ferricrete outcrops. Based on soil profiles within these zones, it is expected that hardpan ferricrete or granite bedrock will occur within 1.5m below ground surface.

A total of 11 soil profiles, representative of Zones C2 and C3 were obtained. All of these soil profiles formed part of geotechnical investigations for residential development and small office developments and consequently, soil profiles had been described only up to approximately 2.5m in depth.

Only 3 of the 11 soil profiles are representative of Zone C2. Of these three soil profiles, one was recorded in residual greenstone material, one recorded refusal at 0.7m on hardpan ferricrete and one recorded no refusal up to 1.8m in depth. The assumption that soil depths of between 1.0m and 3.0m occur within Zone C2 areas could therefore not be verified

A total of 8 soil profiles are representative of Zone C3. Hardpan ferricrete was recorded in 7 of the 8 profiles between 0.1m and 1.3m from ground surface. It would therefore appear that the presumption that shallow profiles can be expected in areas characterised by frequent hardpan ferricrete/bedrock outcrops is true.

The soil profile generally consists of hillwash, between 0.1m and 0.5m in thickness, overlying a pebblemarker. Residual granite is typically absent from the soil profile and the pebble marker is sometimes also absent in the case of very shallow soil profiles.

The hillwash typically consists of yellowish to greyish brown, loose to very loose, voided, silty to clayey sand with sporadic quartz gravel. The underlying pebble marker consists of tightly packed to loosely packed sub-rounded and sub-angular quartz and granite gravel in a matrix of ferruginous, silty fine, medium and coarse sand.

The conceptual unsaturated groundwater model for Zones C2 and C3 is shown in **Figure 7.11**. The flow mechanisms are expected to be similar to that of Zones C1 and B2. Water flows rapidly on top of impermeable ferricrete layers within the high-permeability, loose, residual granite and hillwash. During wet weather conditions, surface seepage occurs and Zones C2 and C3 which act as a discharge zone.

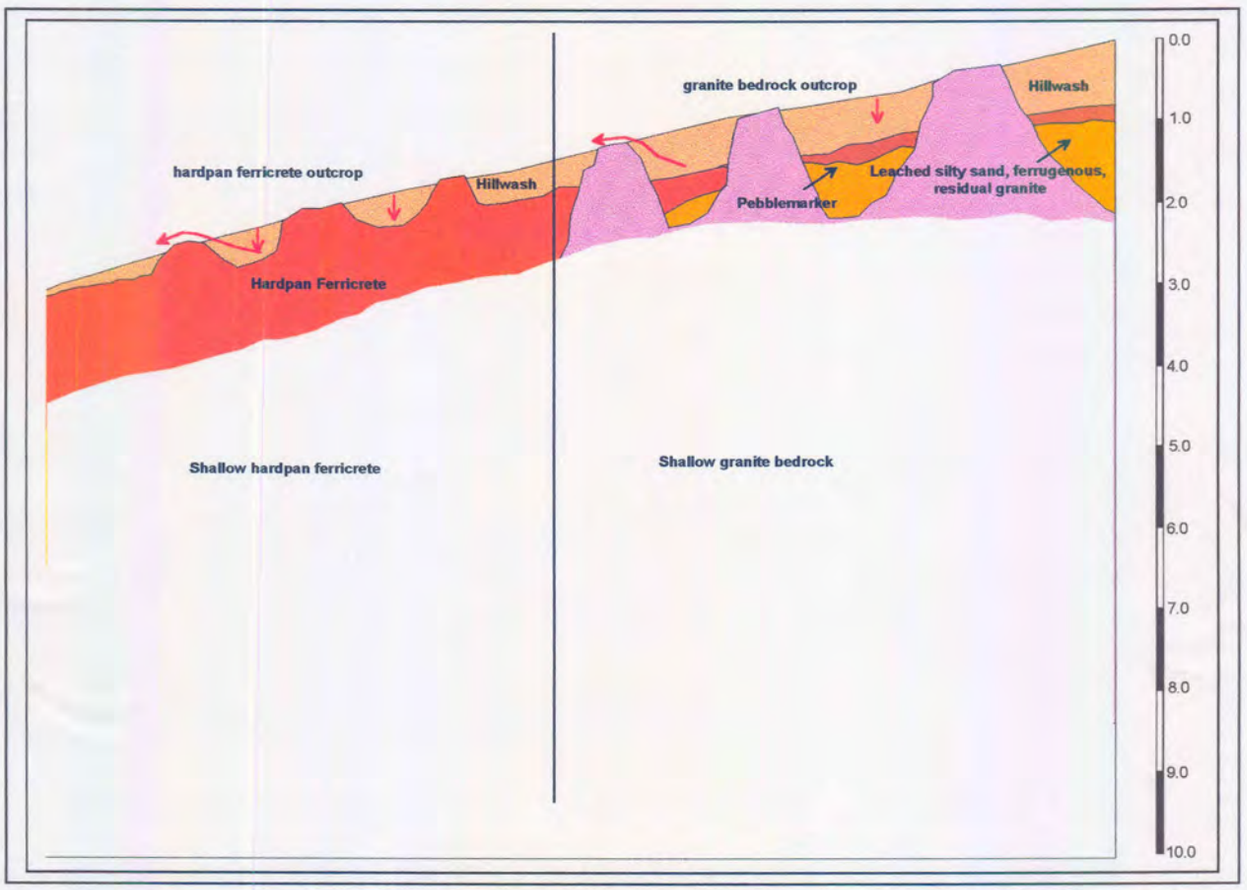

Figure 7.11: Typical soil profile and conceptual unsaturated groundwater model for Zones C2 and C3

Areas underlain by Zone C3 are generally recharge areas during dry weather conditions and could change to discharge areas during wet weather conditions. The impermeable ferricrete layer acts as a barrier to aquifer contamination. However, surface runoff will manifest in streams and it can be concluded that surface water features could be vulnerable to contamination.

Zone D

Zone D represents drainage lines in the investigation area. The zone corresponds to KYAL07 (alluvial floodplain) as proposed by Brink & Partridge (1967) and modified by Stiff (1994). Drainage features are readily identifiable in aerial photo interpretation. The drainage lines generally occur as linear features and conform to the underlying structural geology.

Only 2 soil profiles, representative of Zone D, were obtained in the study area. These soil profiles form part of geotechnical investigations for residential development and small office developments and consequently, soil profiles had been described only up to approximately 2.5m in depth.

A field investigation revealed that major drainage lines are generally located on extensive alluvium. The alluvium generally comprises alternating dark grey, firm, sometimes fissured or micro-shattered, sandy clay and light grey, loose, fine sand.

Gully wash frequently underlies minor drainage lines. The gully wash generally comprises dark grey loose clayey sand becoming more clayey deeper in the soil profile.

Granitoid rock outcrops within the Rietspruit located in the northern parts of the investigation area. These areas are located on the Post African II erosion surface, characterised by shallow bedrock. According to McKnight (1997), granitoid bedrock frequently occurs in drainage channels located on the Post African II erosion surface.

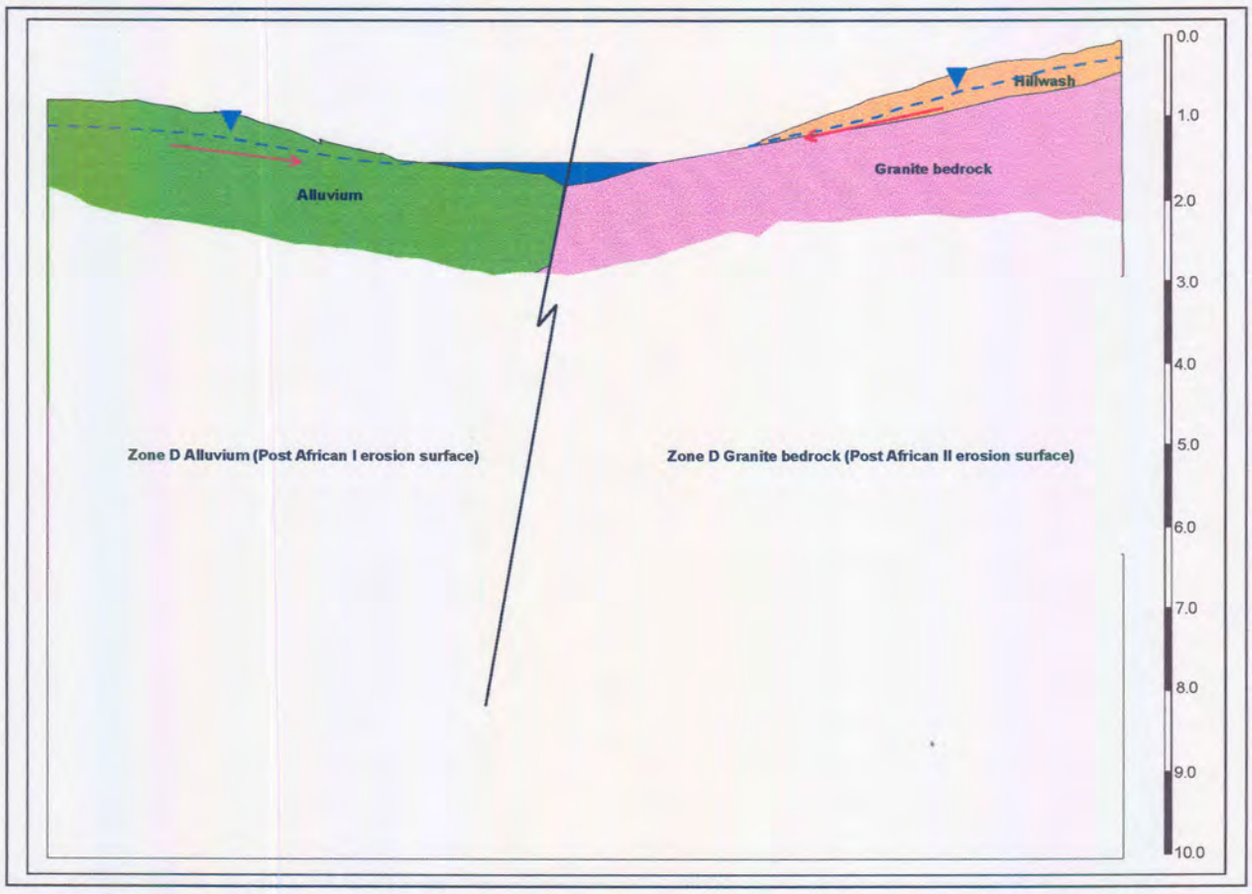

Figure 7.12: Typical soil profile and conceptual unsaturated groundwater model for Zone D

The conceptual unsaturated groundwater model for Zone D is shown in **Figure 7.12**. Zone D areas are generally discharge areas. Rainfall infiltrates soils in higher lying areas and flows down-slope after

A total of 10 soil profiles, representative of Zone C1, were obtained in the study area. Most of these soil profiles formed part of geotechnical investigations for residential development and small office developments and consequently, soil profiles were described only up to approximately 2.5m in depth.

Hardpan ferricrete was recorded in 8 of the 10 soil profiles. Although the sample number is too small to deduce valid conclusions, it appears that shallow hardpan ferricrete is a prominent feature in Zone C1 soils.

The hillwash layer is between 0.2m and 0.6m in thickness and typically consists of yellowish to greyish brown, loose to very loose, voided, silty sand with sporadic quartz gravel. The underlying pebble marker consists of tightly packed to loosely packed sub-rounded and sub-angular quartz and granite gravel in a matrix of ferruginous, silty fine, medium and coarse sand. The pebblemarker is frequently either absent or poorly developed.

In some cases, the hardpan ferricrete has developed directly underneath the pebblemarker or hillwash. In many cases, the transported soil is underlain by reddish to orange brown, very loose to medium dense, ferruginous, silty sand residual granite. The hardpan ferricrete occurs between 0.2m and 1.0m in depth below the ground surface.

No seepage was recorded in any of the test pits, contradictory to what was expected. However, all of these soil profiles had been recorded during the end of the dry season and it is postulated that the water was either discharged in the drainage channel, or removed by evapotranspiration processes during the dry season. It is expected that surface seepage will occur over large parts of the area during the rain season, especially after significant rainfall events. Widespread seepage was observed along Zone C1 areas during the rainy season.

The conceptual unsaturated groundwater model for Zone C1 is shown in **Figure 7.10**. In general, Zone C1 is similar in appearance to Zone B2. The flow mechanisms are also expected to be similar. Water flows rapidly on top of impermeable ferricrete layers within the permeable, loose, residual granite and hillwash. The zone is recharged by rainfall, surface runoff and seepage originating from Zone B1. During wet weather conditions, surface seepage occurs and Zone C1 therefore acts as a discharge zone. Zone C1 is therefore, like Zone B2, a major contributor of base flow to small streams. Since subsurface seepage is a major recharge factor in Zone C1 areas, long periods of surface seepage are expected after significant rainfall events.

Areas underlain by Zone C1 are generally recharge areas during the dry season and changes to discharge areas during the wet seasons. The impermeable ferricrete layer acts as a barrier against aquifer contamination but surface water features are highly vulnerable to contamination since these areas are a major contributor of base flow to surface water bodies. Since secondary fractured aquifer zones are generally associated with drainage features, it can be concluded that these aquifers are also vulnerable to contamination.

Springs originating from gully heads are sometimes used for feedstock watering, irrigation and domestic purposes.

which it discharges into streams. Minor streams are frequently seasonal in nature, implying that limited recharge occurs along these areas during dry weather conditions. In addition, fractured aquifer systems are frequently associated with the drainage features. As such, a lowering in groundwater levels in these areas can be expected during high borehole abstraction rates, resulting in the aquifer being recharged by the stream. In cases where surface water is contaminated, the fractured aquifer could also become contaminated.

The streams are obviously vulnerable to pollution.

CHAPTER 8

DISCUSSION, CONCLUSIONS AND RECOMMENDATIONS

8.1 Discussion

The theoretical aspects regarding saturated and unsaturated flow are well researched. Most of the knowledge regarding the vadose zone has been collected by hydrogeologists, soil scientists and, more recently geotechnical (and geological) engineers and engineering geologists. However, this knowledge is mostly based on investigations in shallow transported soil and very little research has been conducted in deeper residual soils and rocks. Very little is known about the hydrogeological properties of deep residual soils and these aspects need further investigation.

Many practising geohydrologists and engineering geologists lack knowledge of flow processes in the vadose zone. As a result, important aspects in groundwater recharge and contamination investigations may be overlooked. These aspects may also be overlooked during investigation of engineering structures that may affect groundwater quality, such as waste disposal sites, cemeteries and low-cost housing.

Although preferential flow has been identified as an important contributor to groundwater recharge as early as 1882, it was only in the 1980's that preferential flow processes began to be investigated in detail. It is very difficult to estimate flow through preferential pathways. Much progress has been achieved in understanding preferential flow processes. Although conventional, Darcian-based one-dimensional flow equations have been verified in laboratory and field tests, little research has been conducted on flow through residual soils. From recharge studies conducted in South Africa, it is argued that preferential flow may be an important aspect in groundwater recharge and contamination of groundwater resources.

Many relationships between hydrogeological properties and hydrogeological data were found in literature. Soil profile descriptions are the most versatile of all geotechnical data sources and a number of hydrogeological properties can be derived. The literature study has shown that estimations of hydrogeological properties, especially hydraulic conductivity, are not very reliable. To the author's knowledge, no attempt has been made to describe soil profiles in terms of their hydrogeological characteristics. Such descriptions could greatly assist in the understanding of flow processes in field soils and may result in more accurate assessments of hydrogeological properties. This is especially true in the case of preferential flow processes.

Poor relationships between saturated hydraulic conductivity and soil-water retention characteristics have been observed. This can be ascribed to soil-water characteristics being largely a factor of the specific surface (and thus size) of the soil grains, while saturated hydraulic conductivity is largely a function of large soil pore conduits.

Soil-water retention characteristics can be estimated from geotechnical data, in particular from soil fractions and grain size distribution curves. The literature survey has revealed that the Van Genuchten (1980) and Fredlund and Xing (1994) functions can best describe soil water characteristic curves for a large range of soil types and these have been verified by the experimental results.

The relationships between soil-water characteristic curves and unsaturated hydraulic conductivity have been well researched. Excellent estimations of unsaturated hydraulic conductivity can be obtained, provided that the saturated hydraulic conductivity is known and that the soil-water characteristic curve is well described by the Van Genuchten (1980) and other functions. This has been confirmed by the experimental results showing that the Van Genuchten (1980) and Fredlund et al (1994) models can accurately predict the unsaturated hydraulic conductivity. It appears that the Van Genuchten (1980) model best describes sandy soils while the Fredlund *et al* (1994) model best describes clayey soils. These trends should be confirmed.

The results of saturated hydraulic conductivity achieved by Large-Diameter Double Ring Infiltrometer tests confirm the reliability of this test. In contrast, the high variability of saturated hydraulic conductivity achieved from laboratory tests proves that the samples tested were not representative of the field soils. The experiments indicate that saturated hydraulic conductivity can accurately be obtained by means of *in situ* tests. However, laboratory permeability test results indicate that accurate values of saturated hydraulic conductivity may be obtained, provided that a representative number of samples are tested and that these tests are conducted on undisturbed samples.

One major advantage of conducting large-scale *in situ* tests is that preferential pathways may be intercepted, thereby acknowledging the effect of preferential flow. The field experiments indicate that preferential flow, in particular macropore channelling, is probably not a significant factor in water flow through residual granite on the scale tested. However, limited preferential flow has been observed at all experimental sites.

It is important to note that experiments have been conducted on limited soil types and on limited scales. Fingering and funnelled preferential flow types have not been tested. Observations made at the experimental sites cannot be extrapolated to other soil types. Additional research has to be conducted on a wider range of soils and on larger scales in order to determine the effect of preferential flow in field soils. Preferential flow is probably more pronounced in fine-grained soils due to their low permeability. Layered and heterogeneous field soils may also be prone to preferential flow.

Internal Drainage methods may not yield accurate estimations of unsaturated hydraulic conductivity. In addition, unsaturated hydraulic conductivity can only be derived for a small data range, depending on the drainage rate of soils. Alternatively, unsaturated hydraulic conductivity can be obtained indirectly, provided that the soil-water characteristic curve for field soils can be obtained by simultaneously measuring the water content and soil suction of field soils during drainage or wetting (e.g. by means of neutron probes and tensiometers).

Land pattern techniques proved to be a successful tool in delineating field soils of similar hydrogeological characteristics. In both the geotechnical and soil science fraternities, these techniques have been used with success in identifying soils with similar characteristics. From the geotechnical point of view, land pattern classification techniques enable engineering geologists to identify possible problem soil areas. Although some examples have been found in literature where remote sensing techniques have been employed in hydrogeological investigations (of the vadose zone), these techniques are not as well entrenched as in geotechnical investigations. There exists excellent potential to exploit land pattern techniques for hydrogeological investigations.

Land pattern classification techniques have been applied successfully to differentiate between zones of similar hydrogeological properties for the test area in Midrand. Movement of water within the vadose zone is greatly affected by the distribution of shallow rock and hardpan ferricrete in the area and seasonal perched water levels often develop on these low permeable materials. Residual soil properties are remarkably similar throughout the study area, with the exception of alluvium located in

drainage channels. This can be ascribed to the similar geology underlying these soils. Differentiation between zones of similar hydrogeological properties is mainly based on the distribution of shallow rock and hardpan ferricrete. It is anticipated that these factors will control flow of water through the vadose zone in other hard rock environments.

8.2 Conclusions

The research has shown that the geohydrological characteristics of residual soils in the vadose zone can be determined from frequently available geotechnical data and by applying modified geotechnical methods. Three aspects, important in flow of water through the vadose zone, have been addressed during the course of the study namely:

- Saturated and unsaturated flow through the soil matrix
- Preferential flow
- The spatial distribution and delineation of zones with similar hydrogeological characteristics.

These aspects account for scaling in the vadose zone. Unsaturated flow through the soil matrix represents characteristics of a particular soil horizon. Preferential flow represents flow through a soil profile and can generally be observed in testpits and trenches. The spatial distribution of the hydrogeological units can be identified via land classification techniques such as aerial photo interpretation.

8.2.1 Saturated and unsaturated flow through the soil matrix

The research focussed in predicting the following hydrogeological properties:

- Porosity
- Saturated hydraulic conductivity
- Soil-water retention characteristics
- Unsaturated hydraulic conductivity

The porosity of field soils can be estimated from soil profile descriptions, soil fractions and soil classification systems. In many cases, porosity can be estimated within the range of predicted values. However, the tables and empirical equations, which are used to predict porosity, allow for a wide range of porosity values, especially for fine-grained material. This renders predicted porosity values of little use for site-specific investigations. Porosity and saturated volumetric water content (which are almost equal to each other) are important aspects to be considered in the estimation of soil-water retention characteristics, saturated hydraulic conductivity and unsaturated hydraulic conductivity, as had been indicated from sensitivity analyses by Vereecken *et al.* (1989). Accurate estimations of these parameters are only possible on condition that the *in situ* porosity has been determined experimentally. If not, it is suggested that a probabilistic approach should be followed to account for uncertainties regarding porosity. Estimated porosity values can be used during the feasibility stage or for the compilation of regional groundwater recharge or vulnerability maps.

No other soil property varies as greatly as the saturated hydraulic conductivity, which may vary by more than ten orders of magnitude for field soils ranging from coarse gravel to clay. Considering that flow through the saturated soils is directly proportional to saturated hydraulic conductivity, it is

obvious that an accurate determination of *in situ* saturated hydraulic is crucial in the assessment of flow through soils.

Saturated hydraulic conductivity can be estimated from soil profile descriptions, soil fractions, particle size distribution curves, Atterberg limits and soil classification systems. As with porosity, saturated hydraulic conductivity is frequently estimated within the range of predicted values. However, as with porosity, the tables and empirical equations which are used to predict saturated hydraulic conductivity, allow for a wide range of saturated hydraulic conductivity values. Considering the variability of saturated hydraulic conductivity and the sensitivity of this parameter in the assessment of flow through soils, predicted values are of no use for site-specific investigations and of little use during the feasibility stage.

The fact that saturated hydraulic conductivity had been estimated within the range of predicted values suggests that it is related to the grain-size distribution of field soils. However, many other factors, such as packing, the shape of the grains and pore channel geometry, affects saturated hydraulic conductivity and accounts for approximately two orders of magnitude variation of the predicted value.

Since saturated hydraulic conductivity is related to grain-size distribution, its value will be affected by variations in grain-size distributions. Soil samples, which are used to determine grain-size distributions, are not necessarily representative of the soil matrix, as is shown by the variability of sand, silt and clay fractions, obtained from similar soil horizons. The same reasons may account for the variations in laboratory permeability tests conducted on undisturbed soil samples, besides experimental error. Accurate determination of saturated hydraulic conductivity can only be achieved by conducting applicable *in situ* tests, and only if a representative soil area is tested. Small-diameter infiltrometer tests may not yield accurate determination of *in situ* hydraulic conductivity.

Predictions of soil-water retention characteristics from geotechnical data proved to be more accurate compared to saturated hydraulic conductivity and porosity. The accuracy of these predictions depends on the porosity value. The accuracy of these predictions can be improved if the porosity has been determined experimentally. Good predictions are possible in the high suction range, where soil-water retention is mainly a factor of specific soil surfaces, and therefore grain-size distributions. Poor predictions are usually associated along the low suction ranges, where water retention is affected by the pore-size distribution.

As with saturated hydraulic conductivity, predictions of soil-water retention characteristics are affected by variations in grain size distribution. Soil samples used to determine grain-size distribution are not necessarily representative of the specific soil horizon and as such, predicted soil-water retention characteristics may also not be representative. Predictions of soil-water retention characteristics can be used during the feasibility stages of the investigation or in the compilation of groundwater recharge and vulnerability maps.

Variations in unsaturated hydraulic conductivity are even more pronounced compared to saturated hydraulic conductivity and variations of up to twenty orders of magnitude can occur within a single soil horizon. These variations may occur within a small soil suction range, as is the case with a sandy soil. Most empirical models used to predict unsaturated hydraulic conductivity are based on the assumption that saturated hydraulic conductivity and some aspects of soil water retention characteristics are known. Predictions of unsaturated hydraulic conductivity, based on estimated saturated hydraulic conductivity, are useless considering the inherent variability of both properties and that errors in predicted saturated hydraulic conductivity are amplified when used to predict unsaturated hydraulic conductivity. Experimentally derived saturated hydraulic conductivity and a good estimation of soil-water characteristics are a prerequisite for accurate predictions of unsaturated hydraulic conductivity.

In the case that saturated hydraulic conductivity and soil-water retention characteristics are known, unsaturated hydraulic conductivity can be estimated by statistical methods. Accurate predictions of unsaturated hydraulic conductivity can be made, provided that the soil-water characteristic curve

accurately describes soil-water retention characteristics. Sigmoidal functions, such as the Van Genuchten (1980) and Fredlund & Xing (1994) functions, accurately describe soil-water retention characteristics. The former function is more accurate in sandy soils and the latter is more accurate in clayey soils. Accurate predictions of unsaturated hydraulic conductivity can be achieved with the exception of soils characterised by a bi-modal pore-size distribution and soils where preferential flow is dominant. These predictions can be used during site-specific investigations, thereby eliminating the need for time-consuming and expensive laboratory tests.

8.2.2 Preferential flow

Preferential flow was observed in three of the five field-tests, substantiating the opinion held by several authors that preferential flow occurs in most soil types. The field experiments focussed in addressing macropore channelling and other preferential flow mechanisms, such as fingering and funnelled flow were not addressed.

Preferential flow observed during the field experiments occurred mainly in bio-pores, specifically relict plant root holes. These flow paths occurred at depths between approximately 1.0 and 2.0 metres below ground surface, suggesting that preferential flow may extent much deeper than previously thought. The complexity of preferential flow was also highlighted during the field experiments. The connectivity of preferential flow paths is an important aspect, with preferential flow taking place in very few flow paths.

Preferential flow is more pronounced in fine-grained soils, which are usually characterised by low permeability. Preferential flow may constitute a larger portion of flow through the soil profile compared to coarse-grained soils. In addition, certain preferential flow paths are caused by desiccation cracking and aggregation and these processes are more pronounced in fine-grained soils.

The quantification of preferential flow is extremely difficult, if not impossible. However, the research has shown that the preferential flow paths, in particular macropore channels, can be identified by inspection of the soil profile. Soils prone to preferential flow can then be identified. Very little is known on preferential flow mechanisms and it is suggested that a probabilistic approach should be followed in quantifying preferential flow

8.2.3 The spatial distribution and delineation of zones with similar hydrogeological characteristics

The delineation of zones with similar geotechnical characteristics, using land pattern techniques, is hailed as an important milestone in the engineering geological science. The research has shown that the same principles can be applied for delineating zones of similar hydrogeological characteristics, and that these techniques can arguably be used with greater effect for differentiating between zones of similar geohydrological characteristics.

The hydrogeological characteristics of units within the study area were successfully identified using the land system classification approach. Geohydrological characteristics of some units can be much more accurately predicted than those of other units. Shortcomings were identified in the accurate delineation of boundaries along the identified units. The geohydrological characteristics of areas located close to these boundaries should be interpreted with caution.

The research have shown that the geohydrological characteristics are functions mainly of underlying geology, geomorphologic history and pedogenic processes. The spatial distribution areas characterised by similarities of any of these aspects can be identified using land pattern classification techniques. The research has shown that accurate predictions of geohydrological characteristics is possible, based on:

- An understanding on weathering processes for different geological materials
- An understanding of the geomorphologic history to which these rocks were subjected
- An understanding of pedogenic processes

The hydrogeological characteristics can be predicted fairly accurately using mainly aerial photos, geological and topographical maps. The hydrogeological properties can be confirmed by conducting a field investigation in specific areas and these properties can then be extrapolated to areas with similar land patterns.

The construction of conceptual hydrogeological models for each identified hydrogeological unit is essential in understanding the hydrogeological setting. For example, the main variables affecting flow in the vadose zone within the study area include:

- Occurrence and depth of shallow bedrock
- Depth to groundwater surface
- Occurrence of ferruginised layers and hardpan ferricrete
- Occurrence of perched aquifers.

The geohydrological properties of the materials are not as important to differentiate between the geohydrological units within the study area and this can be mainly be attributed to the fact that these soils have been derived only from granitoid bedrock. However, the geohydrological properties can be an important aspect in areas underlain by complex geology.

8.3 Recommendations

It is proposed that additional research should be conducted on the following aspects:

- Methods to identify soils prone to preferential flow. The research should be aimed at methods for quantifying the water moving through the vadose zone. It has been shown that preferential flow, in particular macropore channelling, occurs in the soils tested. Although it has been shown that the extent of preferential flow in the soils tested is probably not significant, little has been achieved in quantifying preferential flow. It is postulated that preferential flow may be the main mode of transport in many South African soils, especially fine-grained soils.
- Unsaturated zone modelling. With the knowledge gained during the course of this investigation, current unsaturated flow models can be improved to include methods for estimating groundwater flow and recharge from geotechnical data sources. These models may be included in conventional groundwater models in order to derive more accurate estimations of recharge. Currently, large uncertainties revolve around the values of recharge to be attributed to specific soil types.
- Integrated groundwater and surface water models. At present, little is known about the unique relationship between surface and groundwater systems. The research has shown that, in the case of the study area, perched aquifer systems are an important aspect in contributing to surface water base flow. It is also highly vulnerable to contamination. These aspects should be further investigated.
- Solute transport and attenuation in the vadose zone. Solutes are mainly transported by means of advection. The results of this research enable researchers to more accurately describe the flow

through the vadose zone based on geotechnical data. However, little is known about solute transport and attenuation processes in the vadose zone.

- Vadose zone monitoring. The international trend in investigations regarding features that may impact negatively on the groundwater is to monitor soil moisture in the vadose zone in order to detect constituents before they enter the groundwater regime. It is proposed that vadose monitoring programmes should be implemented in South Africa in order to prevent expensive remediation programmes after groundwater contamination has already taken place.

CHAPTER 9

REFERENCES

AASHTO 1974. American Association of State Highway and Transportation Officials. Standard specifications for transportation materials and methods of sampling and testing; Part 1: Testing (11th Edition). Washington D.C.

ACCOCKS, J.P.H.1988. Veld types of South Africa. Memoirs of the Botanical Survey of South Africa. No. 57. Pretoria: Government Printer, Pretoria

ASSOCIATION OF ENGINEERING GEOLOGISTS. Committee on core logging, 1976 – A guide to core-logging for rock engineering. Proceedings of a symposium on Exploration for rock Engineering, 1976 :71 – 86.

AHUJA, L.R., NANEY, W.J. AND WILLIAMS, R.D. (1985) Estimating soil water characteristics from simpler properties or limited data. Soil Science. Society of American Journal, 49:1100-1105?

ALLER, L., BENNET, T., LEHR, T.H., PETTY, R.J. & HACKETT, G. 1987. *DRASTIC: A standardized system for evaluating ground water pollution potential using hydrogeologic settings*, EPA/600/2-87-036:455. Ada: US Environmental Protection Agency.

AMER, A.M. & AWAD, A.A. 1974. Permeability of cohesionless soils. Journal of the Geotechnical Division, 100(GT12): 1309-1316.

ANHAEUSSER, C.R., 1973 The geology and geochemistry of the archean granites and gneisses of the Johannesburg-Pretoria Dome. Special Publication of the Geological Society of South Africa, 3: 361-385.

ARYA, L.M. & DIEROLF, T.S. 1992. Predicting soil moisture characteristics from particle-size distributions: An improved method to calculate pore radii from particle radii. (In: Van Genuchten, M. Th., Leij, F.J. & Lund, L.J. eds. Proceedings of an International Workshop on Indirect Methods for Estimating the Hydraulic Properties of Unsaturated Soils. Riverside: California, 11-13 October , 1989: 115-142.)

ARYA, L.M. & PARIS, J.F. 1981. A physicoempirical model to predict the soil moisture characteristic from particle-size distribution and bulk density data. Soil Science Society of . America. Journal, 45: 1023-1030.

ASTM (various dates) American Society for Testing and Materials, 1916 Race Street, Philadelphia, Pa. 19103

AVERJANOV, S.F. 1950. *About permeability of subsurface soils in case of incomplete saturation*, English Collection, Vol. 7. (As quoted by Fredlund *et al.* Predicting the permeability function for

unsaturated soils using the soil-water characteristic curve. Canadian. Geotechnical Journal, 31: 533-546.)

BADENHORST, D.B. (1988) Die ontwerp van grond- en rotsvuldamstrukture. Unpublished MSc Dissertation, University of Pretoria.

BANIN, A. & AMIEL, A. 1970. A correlative study of the chemical and physical properties of a group of natural soils of Israel. Geoderma. 3:185-198

BARTELLI, L.J. & PETERS, D.B. 1959. Integrating soil moisture characteristics with classification units of some Illinois soils. Soil Science Society of America. Proceedings, 23:15-29

BEAR, J. 1979. *Hydraulics of Groundwater*. McGraw-Hill, Book Co., New York

BEAVEN, P.J. 1994. Keynote address. (In: South African Institute of Engineering Geologists.Report on the Proceedings of the Fourth Symposium on Terrain Evaluation and Data Storage: Midrand.)

BELL, F.G. 1993. *Engineering geology*. London: Blackwell Scientific Publications.

BEVEN, K. & GERMANN, P. 1982. Macropores and water flow in soils. Water Resources Research, 18(5): 1311-1325.

BODMAN, G.B. & COLMAN, E.A. 1943. Moisture and energy conditions during the downward entry of water into soils. Proceedings of the Soil Science Society of America, 8: 116-122.

BRADY, N.C. 1974. *The Nature and Properties of Soils*. New York: Macmillan Publishing Co. Inc.

BRANKENSIEK, D.L., ENGLEMAN, R.L. & RAWLS, W.J. 1981. Variation within texture classes of soil water parameters. Transactions American Society of Agricultural Engineering, 24:335-339

BRAUNE, E. 1990. Groundwater: The hidden solution to SA's dwindling water supply. Engineering News, June 1990: 18-19.

BRAUNE, E. & DZIEMBOWSKI, Z.M. 1997. Towards integrated groundwater and surface water management. (In: Report of the Proceedings: Eighth South African National Hydrology Symposium: Held in November 1997 at the University of Pretoria.)

BREDENKAMP, D.B., BOTHA, L.J., VAN TONDER, G.J. & VAN RENSBURG, H.J. 1995. Manual on the quantitative estimation of groundwater recharge and aquifer storativity. (Prepared for the Water Research Commission, Report No. TT 73/95, Pretoria.)

BRINK, A.B.A. 1979. *Engineering geology of Southern Africa*, Vol. 1. Pretoria: Building Publications.

BRINK, A.B.A. & PARTRIDGE, T.C. 1967. Kyalami land system: An example of physiographic classification for the storage of terrain data. (Proceedings of the Fourth Regional Conference for Africa on Soil Mechanics and Foundation Engineering: Held in 1967 in Cape Town.)

BRINK, A.B.A. & WILLIAMS, A.A.B. 1964. Soil engineering mapping for roads in South Africa. Pretoria: CSIR, Research Report No 227).

BRINK, A.B.A., PARTRIDGE, T.C., WEBSTER, R & Williams, A.A.B. 1968. Land classification and data storage for the engineering usage of natural materials. (Proceedings of the Fourth Conference of the Australian Road Research Board, 4(2):1624-1647.)

BROOK, G.A. 1970. An investigation into the origin and evolution of two inselberg landscapes in the Transvaal. M.Sc. thesis, University of the Witwatersrand, Johannesburg

BROOKS, R.H & COREY, A.T. 1964. Hydraulic properties of porous medium. Hydrology Paper 3, Colorado State University, Colorado.

BRUTSAERT, W. 1967. Some methods of calculating unsaturated hydraulic conductivity. Transactions American Society of Agricultural Engineering, 100:400-404

BSI 1990. British Standards 1377: Methods of testing for Soils for Civil Engineering purposes. British Standards Institution, London.

BUITENDAG, I. 1990. Modelling infiltration under different tilled conditions. Unpublished MScEng dissertation. Department of Agricultural Engineering, University of Natal, Pietermaritzburg.

BURDINE, N.T. 1953 Relative permeability calculations from pore-size distribution data. Petrolium Transactions, American Institute of Mining Engineering, 198:71-77

CALL, F. 1957. Soil fumigation IV. Sorption of ethylene dibromide on soils at field capacity. Journal of the Science of Food and Agriculture, 8:137-142

CAMPBELL, G.S. 1974. A simple model for determining unsaturated conductivity from moisture retention data. Soil Science, 117: 311-314.

CAMPBELL, G.S. 1985. Soil Physics with basics; Transport models for soil-plant systems. Elsevier, New York.

CAMPBELL, G.S. & SHIOZAWA, S. 1992. Prediction of hydraulic properties of soils using particle-size distribution and bulk density data. In: Van Genuchten, M. Th., Leij, F.J. & Lund, L.J. eds. Proceedings of the International Workshop on Indirect Methods for Estimating the Hydraulic Properties of Unsaturated Soils. Riverside; California, 11-13 October, 1989: 317 - 328

CARSEL, R.F. & PARRISH, R.S. 1988. Developing joint probability distribution of soil water retention characteristics. Water Resources Research, 24: 755-769.

CHANG, H. & UEHARA, G. 1992. Application of fractal geometry to estimate soil hydraulic properties from the particle-size distribution. (In: Van Genuchten, M.Th., Leij, F.J. & Lund, L.J. eds. Proceedings of the International Workshop on Indirect Methods for Estimating the Hydraulic Properties of Unsaturated Soils.Riverside: California, 11-13 October 1989: 125-138

CHILDS, E.C. 1969. *An introduction to the physical basis of soil water phenomena.* London: Wiley.

CHILDS, E.C. & COLLIS-GEORGE, G.N. 1950. The permeability of porous materials. (In: Proceedings of the Royal Society of London; Series A, 201: 392-405.)

CHORLEY, R.J., SCHUMM, A. & SUGDEN, D.E. 1984. *Geomorphology.* Methuen & Co. Ltd. London.

CHRISTIAN, S.C. & STEWART, G.A. 1953. Survey of the Katherine-Darwin region. Land Research Series, No.1. Melbourne: CSIRO.

CIVITA, M. 1990. (In Italian) La vautazione della vulnerabilita degli acquiferi all'inquinamento. (Proc. 1st Conv. Naz "Protezione e Gestione delle Acque Sottorrane: Metodologie, Techologie, e Obiettivi" Marano sul Panaro 3:39-86.)

COGELS, O. G. 1983. Heterogeneity and representativity of sampling in the study of soil microstructure by the mercury intrusion method. Agriculture Water Management, 6:203-211.

CRONEY, D. & COLEMANN, J.D. 1961. Pore pressure and suction in soils. In: Proceedings of the Conference on Pore Pressure and Suction in Soils. London: Butterworths. (As quoted by Fredlund *et al.* Predicting the permeability function for unsaturated soils using the soil-water characteristic curve. Canadian Geotechnical Journal, 31:533-546.)

CROUKAMP, L. 1998. Personal communication.

COUNCIL FOR GEOSCIENCE, 1998. *Regionale ingenieursgeologiese karteringsverslag van 'n area in die Centurion-Midrand gebied.* Pretoria: Raad vir Geowetenskappe.

DANIEL, D.E. 1989. In situ hydraulic conductivity tests for compacted clay. Journal of Geotechnical Engineering, 115(9): 1205-1226.

DARCY, H. 1856. *Les fontaines publiques de la villa de Dijon.* Paris: Dalmont.

DAS, B.M.1990. 2nd ed. *Principles of geotechnical engineering*. Boston: Kent Publishing Company.

DAVIDSON, J.M., STONE, L.R., NIELSON, D.R. & LARUE, M.E. 1969. Field measurement and use of soil-water properties. Water Resources Research, 5: 1312-1321. (As quoted by Fredlund *et al.* Predicting the permeability function for unsaturated soils using the soil-water characteristic curve. Canadian Geotechnical. Journal, 31:533-546.)

DAVIS, S.N. & DE WIEST, J.M. 1966. *Hydrogeology*. New York: Wiley.

DE BEER, M 1991. Use of the Dynamic Cone Penetrometer (DCP) in the Design of Road Structures. Proceedings, Geotechnics in the African Environment. Rotterdam, Balkema: 167-176

DEPARTMENT OF WATER AFFAIRS AND FORESTRY. 1986. *Management of water resources in the Republic of South Africa.* Cape Town: CTP Book Printers.

DESERT RESEARCH INSTITUTE. 1983. *Unsaturated flow properties data catalog,* Vol. 1. University of Nevada: Water Resources Center.

DU PLESSIS, A. 1998 Personal communication.

EDWORTHY, K. J. 1989. Waste disposal and groundwater management. Journal for the IWEM 3:109-115.

ELGES, H.F.W.K. 1985. Dispersive Soils. Transactions of the South African Institution of Civil Engineers, Special Issue: Problem soils in South Africa, 27(1): 347-353

ELRICK, D.E. & BOWMAN, D.H. 1964. Note on a improved apparatus for soil moisture flow measurements. Soil Science Society of American Proceedings: 450-453

ELZEFTAWY, A, & DEMPSEY, B.J. (1976) Unsaturated Transient and Steady State Flow of Moisture in Subgrade Soil. Transportation Research Record 612. Transportation Research Board, National Academy of Science.

EVERETT, L.G., WILSON, L.G. & HOYLMAN, E.W. 1984. *Vadose zone monitoring for hazardous waste*. New Jersey: Noyes Data Corporation.

EVERETT, M.J. 1990. The modification and verification of a one dimensional soil water flow model. Unpublished MSc dissertation. Department of Agricultural Engineering, University of Natal, Pietermaritzburg.

FARREL, D.A. & LARSON, W.E. 1972. Modelling the pore structure of a porous medium. Water Resources Research, 3: 699-706.

FATT, I. & DYKSTRA, H. 1951. Relative permeabilities studies. Transactions of the American Institute of Mining, Metallurgical and Petroleum Engineers, 192:249-255.

FEDDES, R.A., KOWALIK, P.J. & ZARADNY, H. 1978. Evapotranspiration. In Modelling flow and transport in the unsaturated zone: Short course, 13-17 May 1991, Delft, The Netherlands.

FERNANDEZ, F. & QUIGLEY, R.M. 1985. Hydraulic conductivity of natural clays permeated with simple liquid hydrocarbons. Canadain Geotechnical Journal, 22:205-214.

FETTER, C.W. 1994. *Applied hydrogeology.* 3rd ed. Upper Saddle River, NJ.: Prentice Hall.

FLURY, M., FLÜRER, H., JURY, W. A. & LEUENBERGER, J. 1994. Susceptibility of soils to preferential flow of water: A field study. Water Resources Research, 30(7): 1945-1954.

FOSTER, S.S.D. 1987. Fundamental concepts in aquifer vulnerability, pollution risk and protection strategy. In Vulnerability of Soil and groundwater to pollutants (W van Ouijenbooden & H.G van Waegeningh, eds) TNO Committee on hydrologican research, The Hague, Proceedings and Information, 38: 69-86

FREDLUND, D.G. & XING, A. 1994. Equations for the soil-water characteristic curve. Canadian Geotechnical Journal,. 31: 521-532.

FREDLUND, D.G., XING, A. & HUANG, S. 1994. Predicting the permeability function for unsaturated soils using the soil-water characteristic curve. Canadian Geotechnical Journal, 31:533-546.

FREEZE, R.A. (1969) The mechanism of natural groundwater recharge and discharge. 1. One-dimensional, vertical, unsteady, unsaturated flow above a recharging or discharging groundwater flow system. WRR 5:153-171

FREEZE, R.A. & CHERRY, J.A. 1979. *Groundwater.* Englewood Cliffs, N.J.: Prentice Hall.

FULLER, K.D. & MOOLMAN, J.H. 1989. An evaluation of simplified field methods for estimating soil hydraulic conductivity. Suid-Afrikaanse Tydskrif vir Plant en Grond, 6(1):64-69.

GARDNER, W. R. 1958. Some steady state solutions of the unsaturated moisture flow equation with application to evaporation from a water table. Soil Science 85:228-232. (As quoted by Fredlund *et al.* Predicting the permeability function for unsaturated soils using the soil-water characteristic curve. Canadian Geotechnical Journal, 31:533-546).

GATES, J.I. & TEMPLAAR-LIETZ, W.T. 1950. Relative permeabilities of California cores by the capillary-pressure method, drilling and production practice. American Petroleum Institute Quaterly: 285-298.

GEOLOGICAL SOCIETY ENGINEERING GROUP WORKING PARTY. 1990. Tropical residual soils. Quaterly Journal of Engineering Geology, 23: 1-101.

GREEN, W.H & AMPT, G. 1911. Studies of soil physics and the flow of air and water through soils. Journal of Agricultural Science, 4: 1-24

GUPTA, S.C. & LARSON, W.E. 1979. Estimating soil water retention characteristics from particle size distribution, organic matter percent and bulk density. Water Resources Research, 15(6): 1633-1635.

HAVERKAMP, R. & PARLANGE, J.-Y. 1986. Predicting the water retention curve from particle-size distribution: 1. Sandy soils without organic matter. Soil Science, 142(6): 325-339.

HAZEN, A. 1930. *Water supply. American civil engineers handbook.* New York: Wiley. (As quoted by Das, B. M. 1990. 2nd ed. *Principles of geotechnical engineering.* Boston: Kent Publishing Company.)

HEARNE, G.A., WIREMAN, M. & CAMPBELL, A. 1991. Vulnerability of groundwater in the Greater Denver Area. (Draft publication of the US Geological Survey, Denver, Colorado.)

HELLING, C.S. & GISH, T. J. 1991. Physical and chemical processes affecting preferential flow. (In: Gish, T. J. & Shirmohammadi, A. eds. 1991. Preferential flow. Proceedings of National Symposium of the American Society of Agricultural Engineers, St. Joseph, MI, pp. 77.)

HILLEL, D. 1980. *Fundamentals of soil physics.* New York: Academic Press.

HILLEL, D. & ELRICK, D.E. 1990. Scaling in Soil Physics, Principles and Applications: Proceedings of a symposium sponsored by Division S-1 of the Soil Science Society of America, Special publication Number 25. 18 Oct 1989, Las Vegas, NV.

HILLIARD, P. 1994. The structural evolution of the Johannesburg Dome, Kaapvaal Craton, South Africa. Pretoria: University of Pretoria (M. Sc. dissertation).

HOLTZ, R.D. & KOVACS, W.D. 1981. *An introduction to geotechnical engineering.* Englewood Cliffs, N.J.: Prentice Hall.

HORTON, R.E. 1933. The role of infiltration in the hydrologic cycle, Trans. AGU, 14: 446-460

HOULSBY, A.C. 1976. Routine interpretation of the Lugeon water-test. Quarterly Journal of Engineering Geology, 9:303-313

HUTSON, J.L. 1984. Estimation of hydrological properties of South African soils. Pietermaritzburg: University of Natal (Ph. D. thesis).

INOUE, H., HASEGAWA, S. & MIYAZAKI, T., 1988. Lateral flow of water in an extremely cracked crop field, Transactions Japan Society of Irrigation Drainage and Reclamation Engineering, 134:51-59.

ISTOMINA, V.S. 1957. *Seepage stability of the soil.* Translated from Russian. Moscow

JACKSON, R.D. 1972. On the calculation of hydraulic conductivity. Proceedings Soil Science Society of America, 36:380-382.

JENNINGS, J.E., BRINK, A.B.A. & WILLIAMS, A.A.B. 1973. Revised guide to soil profiling for civil engineering purposes in Southern Africa. Die Siviele Ingenieur in Suid-Afrika, Jan. 1973.

JONASSON, S.A. 1992. Estimation of the Van Genuchten parameters from grain-size distribution. In: Van Genuchten, M. Th., Leij, F.J. & Lund, L.J. eds. 1992: Proceedings of an International Workshop on Indirect Methods for Estimating the Hydraulic Properties of Unsaturated Soils. Riverside; California, 11-13 October 1989: 443-452.

KENNEY, T.C., LAU, D. & OFOEGBU, G.I. 1984 Permeability of compacted granular materials. Canadian Geotechnical Journal, 21(4):726-729. (As quoted by Das, B. M. 1990. 2nd ed. *Principles of geotechnical engineering*. Boston: Kent Publishing Company.)

KEYTER, G.J. (1995) Preliminary guidelines for the development of a national geotechnical database. CSIR Division of Building Technology, Internal Report BE415/002, Pretoria

KIRCHNER, J., VAN TONDER, G.J. & LUKAS, E. 1991. The exploitation potential of Karoo aquifers. Water Research Commission Report, 170/2/91, Pretoria.

KRAMER, J.H & KELLER, B. 1995. Understanding the geological framework of the vadose zone and its effect on storage and transmission of fluids. In Wilson, LG, Brevett, L.G. & Cullen, S.J. eds. Handbook of vadose zone characterisation monitoring. Lewis; Boca Raton, Florida: 137-158

KUNG, K. -J. S. 1990. Preferential flow in a sandy vadose zone: 2. Mechanisms and implications. Geoderma, 46: 59-71.

KUNZE, R.J., UEHARA, G. & Graham, K. 1968. Factors important in the calculations of hydraulic conductivity. Proceedings Soil Science Society of America, 32:760-765

LAUREN, J. G., WAGNENT, R, J., BOUMA, J. & WOSTEN, J. H. M. 1988. Variability of saturated hydraulic conductivity in a glassaquic hapludalf with macropores. Soil Science, 145(1): 20-28.

LE GRAND, H.E. 1983. A standardized system for evaluating waste-disposal sites. National Water Well Association, Dublin, Ohio, USA: 49

LEONG, E.C. & REHARDJO, H. 1997a. Review of soil-water characteristic curve equations. Journal of Geotechnical and Geoenvironmental Engineering, 123 (12): 1106-1117

LEONG, E.C. & REHARDJO, H. 1997b. Permeability functions of unsaturated soils. Journal of Geotechnical and Geoenvironmental Engineering, 123 (12): 1118-1126

LERNER, D.N., ISSAR, A. & SIMMERS, I. 1990. A guide to the understanding and estimating of natural recharge. IAH Publication, 9. Hannover: Heise.

LEVIN, M. 1988. A geohydrological appraisal of the Vaalputs radioactive waste disposal facility in Namaqualand, South Africa. Bloemfontein: University of Orange Free State (Ph. D. thesis).

LUXMOORE, R.J. & SHARMA, M.L. 1980. Runoff responses to soil heterogeneity: Experimental and simulation comparisons for two contrasting watersheds. Water Resources Research, 16: 671-684.

MABULA, M.C. 1997. Extent of non-Darcian flow through soils. (In: South African Institute of Engineering Geologists. Proceedings of Geology for Engineering, Urban Planning and the Environment; Midrand, South Africa, 12-14 November, 1997

MacGREGOR, A.M. 1952. Some milestones in the precambrian of Southern Rhodesia. (Proceedings of the Geological Society of South Africa, 54:27-71).

MANDELBROT, B.B. 1983. *The fractal geometry of nature*. San Fransisco: Freeman.

MARSHALL,T.J. 1958. A relation between permeability and size-distribution of pores. Journal of Soil Science, 9:1-8

MARTIN, J.P. & KOERNER, R.M. 1984a. The influence of vadose zone conditions in groundwater pollution; Part I: Basic principles and static conditions. Journal of Hazardous Materials, 8: 349-366.

MARTIN, J.P. & KOERNER, R.M. 1984b. The influence of vadose zone conditions in groundwater pollution; Part II: Fluid movement. Journal of Hazardous Materials, 9:181-207.

MATHEWSON, C.C. 1981. *Engineering geology*. Columbus, Ohio: Merrill Publishing Company.

McBRIDE, M.B. 1994. Environmental chemistry of soils, Oxford University Press, Oxford.

McCUEN, R.H., RAWLS, W.J. & BRANKENSIEK, D.L. 1981. Statistical analysis of the Brooks-Corey and and the Green-Ampt parameters across soil texture. Water Resources Research, 17: 1005-1013.

McKEE, C.R. & BUMB, A.C. 1984. The importance of unsaturated flow parameters in designing a monitoring system for hazardous wastes and environmental emergencies. Proceedings Hazardous Material Controle Research Institute National Conference: 50-58

McKNIGHT, C. 1997. The Sandton-Midrand soil catena, a legacy of polycyclic weathering and erosion. (In: South African Institute of Engineering Geologists. Geology for Engineering, Urban Planning and the Environment Proceedings: Midrand, South Africa, 12-14 November 1997

MELZER, K.J. & SMOLTCZYK, U. 1982. Dynamic Penetration Testing, State-of-the-Art Report. Proceedings, 2nd European Symposium on penetration Testing (ESOPT II), Amsterdam: 191-202

MESRI, G. & OLSON, R.E. 1971. Mechanics controlling the permeability of clays. Clays and Clay Minerals, 19: 151-158.

MILFORD, R.V. 1994. The availability of terrain information in South Africa. (In: South African Institute of Engineering Geologists. 1994: Proceedings of the Fourth Symposium on Terrain Evaluation and Data Storage: Held at Midrand.)

MILLER, E.E. & MILLER, R.D. 1956. Physical theory for capillary flow phenomena. Journal of Applied Physics, 27: 324-332.

MILLER, R.J. & LOW, P.F. 1963. Threshold gradient for water flow in clay systems. Proceedings Soil Science Society of America, 27: 605-609

MILLINGTON, R.J. & QUIRK, J.P. 1961. Permeability of porous solids. Transactions Faraday Society, 57:1200-1206.

MIYAZAKI, T. 1993. *Water flow* in *soils*. New York: Marcel Dekker.

MONKHOUSE, F.J., STEYN, J.N. & BOSHOFF, L.P. 1983. *A Dictionary of Geography: Southern African Edition*. De Jager Haum Publishers, Pretoria.

MUALEM, Y. 1974. Hydraulic properties of unsaturated porous media: a critical review and new models of hysteresis and prediction of the hydraulic conductivity. Technion Project No. 38/74, Israel Institute of Technology, Haifa.

MUALEM, Y. 1976. A new model for predicting the hydraulic conductivity of unsaturated porous media. Water Resources Research, 12: 513-522.

MUALEM, Y. 1986. Hydraulic conductivity of unsaturated soils: Prediction and formulas. In: Klut, A. ed. Methods of soil analysis. Part 1. Physical and mineralogical methods. Agron. Monogr. 9 (2nd ed) American Society of Agronomy, Madison, Wisconsin 799-4823.

MUALEM, Y. 1992. Modeling the hydraulic conductivity of unsaturated porous media. In: Van Genuchten, M. Th., Leij, F.J. & Lund, L.J. eds. 1992: Proceedings of an International Workshop on Indirect Methods for Estimating the Hydraulic Properties of Unsaturated Soils. Riverside; California, 11-13 October 1989:15-36

MUALEM, Y. & DAGAN, G. 1978. Hydraulic conductivity of the soils: Unified approach to the statistical models. Soil Science Society of America Journal, 42:392-395

MURPHY, K. & STIFF, J.S. 1994. The use of GIS spatial databases for terrain evaluation. (In: South African Institute of Engineering Geologists, 1994: Proceedings of the Fourth Symposium on Terrain Evaluation and Data Storage, Midrand.)

NEUMAN, S.P., FEDDES, R.A. & BRESLER, E. (1974) Finite Element Simulation of flow in Saturated-Unsaturated soils considering water uptake by Plants. In Development of methods, tools and solutions for unsaturated flow. Third Annual Report (Part 1) Hydrodynamics and Hydraulic Eng. Laboratory, Israel Institute of Technology. Haifa, Israel.

NIELSON, D.R. & BIGGAR, J.W. 1961. Measuring capillary conductivity. Soil Science, 92: 192-193.

NIELSON, D.R., KIRKHAM, D. & PERRIER, E.R. 1960. Soil capillary conductivity: Comparison of measured and calculated values. Soil Science of American Proceedings, 24:157-160

NORTHCOTE, K.H. 1971. 4th ed. *A factual key for the recognition of Australian soils.*Glenside, SA: Rellim Technical Publications.

PAPAGIANNAKIS; A.T. & FREDLUND, D.G. 1984. A steady state model for flow in saturated-unsaturated soils. Canadian Geotechnical Journal, 21: 419-430

PARSONS, R. & JOLLY, J. 1994. The development of a systematic method for evaluating site suitability for waste disposal based on geohydrological criteria. WRC Report No. 485/1/94, Pretoria.

PARTRIDGE, T.C. 1969. Some geomorphic units in the Transvaal and their significance in physical development. Durban: University of Natal (Ph.D. thesis).

PARTRIDGE, T.C. 1994. The land system and land type classifications: comparisons and applications in the Southern African context. (In: South African Institute of Engineering Geologists, 1994: Proceedings of the Fourth Symposium on Terrain Evaluation and Data Storage: Midrand.)

PARTRIDGE, T.C. & MAUD, R.R. 1987. Geomorphic evolution of Southern Africa since the Mesozoic. South African Journal of Geology, 90(2):179-208

PAYDAR, Z. & CRESSWELL, P. 1996. Water retention in Australian soils. II: Prediction using particle size, bulk density, and other properties. Australian Journal of Soil Research, 34:679-693.

PENMAN, H.L. 1948. Natural evaporation from open water, bare soil and grass. Proceedings of the Royal Society, A193: 120-145.

PENMAN, H.L. 1963. Vegetation and Hydrology. Commonwealth Agricultural Bureaux, Farnham Royal.

PERRIER, E., RIEU, M., SPOSITO, G. & De MARSILY, G. 1996. Models of the water retention curve for soils with a fractal pore size distribution. Water Resources Research, 32(10):3025-3031.

PERRIER, E., MULLON, C., RIEU, M. & DE MARSILY, G. 1995. Computer construction of fractal soil structures: Simulation and their hydraulic and shrinkage properties. Water Resources Research, 31: 2927-2943.

SCHEIDEGGER, A.E. 1957. *The physics of flow through porous media.* Toronto: University of Toronto.

SCHULZE, R.E. 1995. *Hydrology and Agrohydrology: A text to accompany the ACRU 3.00 agrohydrological modelling system.* Water Research Commission, Pretoria, Report TT69/95

SCHULZE, R.E. GEORGE, W.J. & ANGUS, G.R. 1987. Unpublished recommended values of soil water retention constants. Department of Agricultural Engineering, University of Natal, Pietermaritzburg.

SHAHABI, A.A., DAS, B.M. & TARQUIN, A.J. 1984. An empirical relation for coefficient of permeability for sand. In: Proceedings of the Fourth Australia-New Zealand Conference on Geomechanics, 1:54-57.

SILILO, O.T.N., CONRAD, J.E., MURPHY, K.O'H., TREDOUX, G., EIGENHUIS, B., FERGUSON, M.C.D. & MOOLMAN, J.H. 1997. Investigation of the contaminant attenuation characteristics of the soil aquifer system with special emphasis on the vadose zone. Draft Final Report, WRC Project No. K5/572, Pretoria.

SIMMERS, I. ed. 1988. Estimation of natural groundwater recharge. NATO ASI Series C, Vol. 222. (In: Proceedings of the NATO Advanced Research Workshop: Held in March 1947 at Antalaya in Turkey. Dordrecht: Reidel Publishing Company.)

SKABALANOVICH, I.A. (1961) (in Russian) First Ukranian Convention of Hydrogeologists in Kiev

SMETTEM, K.J.R., BRISTOW, K.L., ROSS, P.J., HAVERKAMP, R., COOK, S.E. & JOHNSON, A.K.L. 1994. Trends in water balance modelling at field scale using Richard's equation. (In: International Conference of Scientific Research Integration 1994: Trends in Hydrology, 1: 383-402. Trivandrum. India

SOUTH AFRICAN COMMITTEE OF STRATIGRAPHY. 1980. *Stratigraphy of South Africa. Handbook 8.* Part 1: Litostratigraphy of the Republic of South Africa, South West Africa/Namibia and the Republics of Bophuthatswana, Transkei and Venda. Pretoria: Council for Geoscience.

SPOSITO, G. & JURY, W.A. 1990. Miller Similitude and Generalized Scaling Analysis. In Hillel, D. & Elrick, D.E. eds. 1990. Scaling in Soil Physics, Principles and Applications: Proceedings of a symposium sponsored by Division S-1 of the Soil Science Society of America, Special publication Number 25. 18 Oct 1989, Las Vegas, NV.

STEENHUIS, T.S. & PERLANGE, J.Y. 1990. Preferential flow in structured and sandy soil. (In: Gish, T. J. & Shirmohammadi, A. eds. 1991. Preferential flow. Proceedings of National Symposium of the American Society of Agricultural Engineers, St. Joseph, MI, pp. 77.)

STIFF, J.S. 1994. Terrain evaluation for urban development. In: South African Institute of Engineering Geologists. Proceedings of the Fourth Symposium on Terrain Evaluation and Data Storage: Midrand.

STIFF, J.S. 1997. Status quo of engineering geological investigation for urban planning and development. In: South African Institute of Engineering Geologists. Proceedings of Workshop on Geology for Engineering, Urban Planning and the Environment: Midrand.

SWARTZENDRUBER, D. 1962. Non Darcy behaviour in liquid saturated porous media. Journal of Geophysical Research, 67:5205-5213.

TALSMA, T. 1970. Hysteresis in in two sands and the independent domain model. Water Resources Research, 6: 964-970.

TAVENAS, F., JEAN, P., LEBLOND, P. & LEROUEIL, S. 1983a. The permeability of natural soft clays. Part I: Methods of laboratory measurement. Canadian Geotechnical Journal, 20:629-644.

TAVENAS, F., JEAN, P., LEBLOND, P. & LEROUEIL, S. 1983b. The permeability of natural soft clays. Part II: Permeability characteristics. Canadian Geotechnical Journal, 20:645-660

TAYLOR, D.W. 1948. *Fundamentals of soil mechanics*. New York: Wiley. (As quoted by Tavenas *et al.* 1983 The permeability of natural soft clays. Part II: Permeability characteristics. Canadian Geotechnical Journal, 20:645-660.

THORTON, S.F., LERNER, D.N., BRIGHT, M.I. & TELLMAN, J.H. 1993. The role of attenuation in landfill liners. Proceedings of the Fourth International Landfill Symposium: Held at Cagliari, Italy 11-15 October 1993, pp 407-416. (As quoted in Seimons *et al.* 1994. Investigation of the contaminant attenuation capacity of the soil/aquifer system with special emphasis on the vadose zone. Progress report. WRC Project No. K5/572, Stellenbosh.)

TINJUM, J.M., BENSON, C.H. & BLOTZ, L.R. 1997. Soil-water characteristic curves for compacted clays. Journal of Geotechnical and Geoenvironmental Engineering, 123(11): 1060-1069.

TOKUNAGA, K. & SATO, T. 1975. The fundamental studies on the sampling method. II: On the variation in the distribution of the physical properties of soils found in large area farm land, Transactions Japan Society of Irrigation and Drainage Reclamation Engineers, 55:1-8

TOPP, G.C. 1969. Soil water hysteresis measured in a sandy loam compared with hysteretic domain model. Soil Science Society of America Proceedings, 33:645-651.

TOPP, G.C. & MILLER, E.E. 1966. Hysteretic moisture characteristics and hydraulic conductivities for glass-bead media. Soil Science Society of America Proceedings, 30:156-162

TURCOTT, D.L. 1986. Fractals and Fragmentations. Journal of Geophysical Research, 91(2): 1921-1926

TYLER, S.W. & WHEATCRAFT, S.W. 1990. Fractal processes in soil water retention. Water Resources Research, 26: 1047-1054.

TYLER, S.W. & WHEATCRAFT, S.W. 1992. Fractal aspects of soil porosity. (In: : Van Genuchten, M. Th., Leij, F.J. & Lund, L.J. eds. 1992: Proceedings of an International Workshop on Indirect Methods for Estimating the Hydraulic Properties of Unsaturated soils. Riverside; California, 11-13 October 1989: 53-65

UNESCO 1984. *Ground water in hard rocks*. United Nations.

UNLU, K., KEMBLOWSKI, M.W., PARKER, J.C., STEVENS, D., CHONG, P.K. & KAMIL, I. 1992. A screening model for affects of land-disposed waste on groundwater quality. Journal of Contaminant Hydrology, 11:27-49 (As quoted in Parsons & Jolly 1994. The development of a systematic method for evaluating site suitability for waste disposal based on geohydrological criteria. WRC Report No. 485/1/94, Pretoria.)

VACHAUD, G., GANDET, J.P. & KURAZ, V. 1974. Air and water flow during ponded infiltration in a vertical bounded column of soil. Journal of Hydrology, 22: 89-108

VAN DER MERWE, A.J. 1973. Physico-chemical relationships of selected OFS soils: A statistical approach based on taxonomic criteria. Bloemfontein: University of the Orange Free State (Ph.D. thesis).

VAN GENUCHTEN, M.Th. 1980. A closed-form equation for predicting the hydraulic conductivity of unsaturated soils. Soil Science Society of America Journal, 44:892-898

VAN GENUCHTEN, M.Th. & NIELSON, D.R. 1985. On describing and predicting the hydraulic properties of unsaturated soils. Annales Geophysisae, 3(5): 615-628.

VAN SCHALKWYK, A. & VERMAAK, J.J.G. 1999. The Relationship between the Geotechnical and Hydrogeological Properties of Residual Soils and rocks in the Vadose Zone. Project No. K5/701/0/1, Draft final report to the Water Research Commission, Pretoria.

VAN TONDER, G.J. & KIRCHNER, J. 1990. Estimation of natural groundwater recharge in the Karoo aquifers of South Africa. Journal of Hydrology, 121:395-419.

VEREECKEN, H., MAES, J., FEYEN, J. & DARIUS, P. 1989. Estimating the soil moisture retention characteristic from texture, bulk density, and carbon content. Soil Science, 148(6): 389-403.

VRBA, J. & ZAPOROZEC, A. 1994. Guidebook on mapping groundwater vulnerability. International association of hydrogeologists, Vol.16. Verlug Heinz Heise: Hannover.

VUKOVIC, M. & SORO, A. 1992. *Determination of hydraulic conductivity of porous media from grain-size composition*. Littleton, Colorado: Water Resources Publications.

WARD, R.C. 1975. *Principles of hydrology*. 2nd ed. London: McGraw-Hill.

WARRICK, A.W. 1990. Application of Scaling to the Characterization of Spatial Variability in Soils. In Hillel, D. & Elrick, D.E. eds. 1990. Scaling in Soil Physics, Principles and Applications: Proceedings of a symposium sponsored by Division S-1 of the Soil Science Society of America, Special publication Number 25. 18 Oct 1989, Las Vegas, NV.

WARRICK, A.W., MULLEN, G.J. & NIELSON, D.R. 1977. Scaling field-measured soil hydraulic properties using a similar media concept. Water Resources Research, 13: 355-362.

WATES, J.A., RYKAART, E.M., VERMAAK, J.J.G. & BEZUIDENHOUT, N 1999. The performance of natural soil covers in rehabilitating opencast coal mines and waste dumps in South Africa. Draft Water Research Commission Report, Pretoria.

WEINERT, H.H. 1980. *The natural road construction materials of Southern Africa*. Pretoria: Academia.

WHITE, R.E. 1989. *Introduction to the principles and practices of soil science*. Second Edition. Blackwell Scientific Publications: Boston.

WIERENGA; P.J. 1995. Water and Solute Transportation Storage In Wilson, L.G., Everett, L.G. & Gollen, S.J. Handbook of vadose characterisation zone and monitoring. Lewis Publishers, Boca Rarton, Florida

WILLIAMS, J., PEBBLE, R.E., WILLIAMS, W.T. & HIGNETT, C.T. 1983. The influence of texture, structure and clay mineralogy on the soil moisture chacteristic. Australian Journal of Soil Research, 21:15-32

WILLIAMS, J., ROSS, P.J. & BRISTOW, K.L. 1992. Prediction of the Campbell water retention function from texture, structure and organic matter. (In: Van Genuchten, M. Th., Leij, F.J. & Lund, L.J. eds. 1992: Proceedings of the International Workshop on Indirect Methods for Estimating the Hydraulic Properties of Unsaturated soils. Riverside; California, 11-13 October 1989: 427-442

WIND, G.P. 1961. Capillary rise and some applications of the theory of moisture movement in unsaturated soils. Institute for Land and Water Management Resources: Technical Bulletin, 22.

WIND, G.P. 1955. Field experiment concerning capillary rise of moisture in heavy clay soil. Netherlands Journal of Agricultural Science, 3:60-69

WOOD, E. F., SIVAPALAN, M., BEVEN, K. & BAND, L. 1988. Effects of spatial variability and scales with implications to hydrologic modelling. Journal of Hydrology, 102: 29-47.

WYLLIE M.R.J. & GARDNER, G.H.F. 1958. The generalized Kozeny-Carman equation 11. A novel approach to problems of fluid flow. World Oil Production Section, 146:210-228

YOUNGS, E.G. 1990. Application of Scaling to Soil-Water Movement Considering Hysteresis. In Hillel, D. & Elrick, D.E. eds. 1990. Scaling in Soil Physics, Principles and Applications: Proceedings of a symposium sponsored by Division S-1 of the Soil Science Society of America, Special publication Number 25. 18 Oct 1989, Las Vegas, NV.

DRAWING 1

2528CC 23 MIDRAND : HYDROGEOLOGICAL UNITS

APPENDIX A

Soil profile descriptions

UNIVERSITEIT VAN PRETORIA
UNIVERSITY OF PRETORIA
YUNIBESITHI YA PRETORIA

VADOSE ZONE CHARACTERISATION
UP EXPERIMENTAL FARM

HOLE No: TP1
Sheet 1 of 1

JOB NUMBER: 4222

Scale 1:20

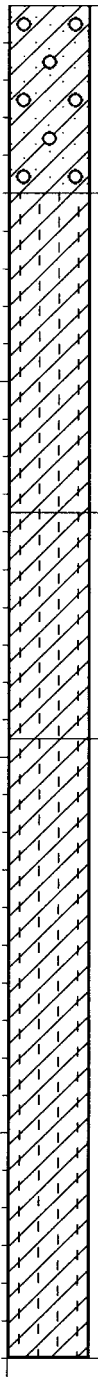

0.00

Slightly moist, Dark reddish brown, soft, microshattered sandy gravelly (quartz and andesite) CLAY and plant roots - **Hillwash.**

0.50

Slightly moist, brownish dark red with black blotches, yellowish brown when wet, stiff, intact, silty CLAY with sand - **Residual andesite, Hekpoort Formation.**

1.35

Slightly moist, brownish dark red and reddish yellow blotched (becoming more yellowish downward) with black blots and stripes, stiff, intact, silty CLAY with sand (Two zones of highly weathered angular quartz on depth 1.60 and 1.95m) - probably relict quartz veins - **Residual andesite Hekpoort Formation.**

1.95

Slightly moist, reddish yellow with brownish dark red and black blots and stripes, firm, fissured (coloured black and brownish dark red on sides), silty CLAY with sand - **Residual andesite Hekpoort Formation.**

3.60

NOTES

1) No water seepage.

2) No refusal.

CONTRACTOR :
MACHINE : TLB
DRILLED BY :
PROFILED BY : Jan Vermaak
TYPE SET BY : YJvV
SETUP FILE : STANDARD.SET

CLIENT : WRC
INCLINATION :
DIAM :
DATE PROFILED : 17 March 1997
DATE : 14/02/00 14:35
TEXT : C:\profiles\WRC.TXT

ELEVATION :
X-COORD :
Y-COORD :

HOLE No: TP1
Pretoria

dot.PLOT 3030 J&W Inc

UNIVERSITEIT VAN PRETORIA
UNIVERSITY OF PRETORIA
YUNIBESITHI YA PRETORIA

VADOSE ZONE CHARACTERISATION
UP EXPERIMENTAL FARM

HOLE No: TP 2
Sheet 1 of 1

JOB NUMBER: 4222

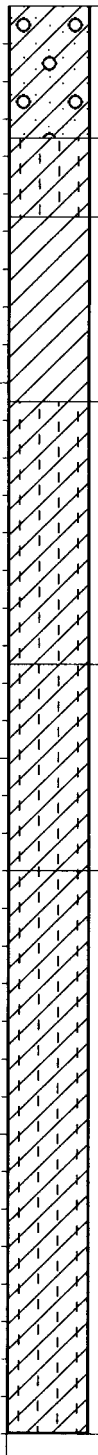

0.00	Dry, reddish dark brown, soft, microshattered, sandy gravelly (about 30 per cent rounded quartz and andesite up to 5cm diameter) CLAY; plant roots - **Hillwash**.
0.35	Dry, reddish dark brown with black blots, firm, intact, silty CLAY with sand - **Residual andesite Hekpoort Formation**.
0.56	Slightly moist, reddish dark brown with white blots, stiff, intact, CLAY with sand - White blots represent kaolinisation - **Residual andesite Hekpoort Formation**.
1.05	Slightly moist, reddish dark brown and reddish yellow blotched with black and white blots and black stripes, stiff, intact, silty CLAY with sand (two 1cm thick zones of highly weathered angular quartz at depth 1.40 and 1.74m) - probably relict quartz veins - **Residual andesite Hekpoort Formation**.
1.75	Slightly moist, reddish yellow to pale downward with reddish dark brown blots and stripes, firm, fissured (coloured black and reddish dark brown - relict rock joints) silty CLAY with sand - **Residual andesite Hekpoort Formation**.
2.30	Slightly moist, pale yellow with reddish dark brown blots and stripes, firm, fissured coloured reddish dark brown and black on relict rock joints, silty clay with sand - **Residual andesite Hekpoort Formation**.
3.80	

NOTES

1) No water seepage.

2) No refusal.

CONTRACTOR :
MACHINE : TLB
DRILLED BY :
PROFILED BY : Jan Vermaak
TYPE SET BY : YJvV
SETUP FILE : STANDARD.SET

CLIENT : WRC
INCLINATION :
DIAM :
DATE PROFILED : 17 March 1997
DATE : 14/02/00 14:35
TEXT : C:\profiles\WRC.TXT

ELEVATION :
X-COORD :
Y-COORD :

HOLE No: TP 2

dot.PLOT 3030 J&W Inc

UNIVERSITEIT VAN PRETORIA
UNIVERSITY OF PRETORIA
YUNIBESITHI YA PRETORIA

VADOSE ZONE CHARACTERISATION
UP EXPERIMENTAL FARM

HOLE No: TP 3
Sheet 1 of 1

JOB NUMBER: 4222

Scale 1:15

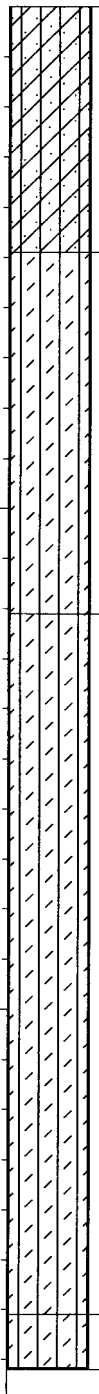

0.00 Moist, reddish dark brown, firm, intact, sandy SILT - CLAY with coarse gravel and cobbles (quartz and andesite) at 0.38 - 0.49m - gravelmarker; plant roots - **Hillwash**.

0.49 Moist, brownish dark red, firm, intact, clayey SILT with sand and scattered black ferruginous nodules; plant roots - **Residual andesite, Hekpoort Formation**.

1.21 Moist, brownish dark red, firm, intact, clayey SILT with sand **Residual andesite Hekpoort Formation**.

2.61 Moist, brownish dark red and greyish yellow, firm, fissured clayey SILT with sand and up to 0.15m diameter highly weathered andesite rocks - **Highly weathered andesite, Hekpoort Formation**.

2.72

NOTES

1) No water seepage.

2) No refusal.

CONTRACTOR :
MACHINE : TLB
DRILLED BY :
PROFILED BY : Jan Vermaak
TYPE SET BY : YJvV
SETUP FILE : STANDARD.SET

CLIENT : WRC
INCLINATION :
DIAM :
DATE PROFILED : 17 March 1997
DATE : 14/02/00 14:35
TEXT : C:\profiles\WRC.TXT

ELEVATION :
X-COORD :
Y-COORD :

HOLE No: TP 3

dot.PLOT 3030 J&W Inc

UNIVERSITEIT VAN PRETORIA
UNIVERSITY OF PRETORIA
YUNIBESITHI YA PRETORIA

VADOSE ZONE CHARACTERISATION
UP EXPERIMENTAL FARM

HOLE No: TP 4
Sheet 1 of 1

JOB NUMBER: 4222

Scale 1:20

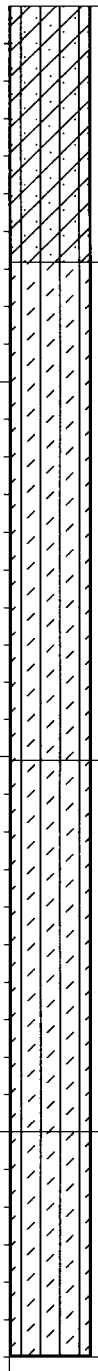

0.00 — Moist, reddish dark brown, firm, intact, sandy SILT and CLAY with gravel (quartz and andesite) at 0.40 - 0.68m - gravelmarker; plant roots - **Hillwash.**

0.68 — Moist, brownish dark red and yellowish dark red, firm, intact, clayey SILT with sand, relict quartz veins - **Residual andesite, Hekpoort Formation.**

2.01 — Moist, brownish dark red and yellowish dark red, firm, intact, clayey SILT with sand - **Residual andesite, Hekpoort Formation.**

3.00 — Very moist, yellowish dark red, soft, fissured, clayey SILT with sand - **Highly weathered andesite, Hekpoort Formation.**

3.60

NOTES

1) Water seepage due to close by point of infiltration.

2) No refusal.

CONTRACTOR :
MACHINE : TLB
DRILLED BY :
PROFILED BY : Jan Vermaak
TYPE SET BY : YJvV
SETUP FILE : STANDARD.SET

CLIENT : WRC
INCLINATION :
DIAM :
DATE PROFILED : 17 March 1997
DATE : 14/02/00 14:35
TEXT : C:\profiles\WRC.TXT

ELEVATION :
X-COORD :
Y-COORD :

HOLE No: TP 4

dot.PLOT 3030 J&W Inc

UNIVERSITEIT VAN PRETORIA
UNIVERSITY OF PRETORIA
YUNIBESITHI YA PRETORIA

VADOSE ZONE CHARACTERISATION
NEW ROAD BRIDGE

HOLE No: TP 1a
Sheet 1 of 1

JOB NUMBER: 4222

Scale 1:20

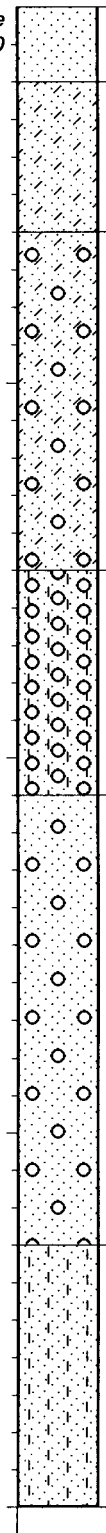

0.00 Moist, brownish grey, very loose, voided, medium to fine SAND with gravel and plant roots - **Fill.**

0.20 Moist, dark red, dense to very dense clayey fine SAND with rounded quartz gravel - **Residual granite.**

0.60 Moist, dark red, dense gravelly clayey fine SAND - **Residual granite.**

1.50 Moist to very moist, dark red with orange mottles, medium dense to dense, slightly leached, silty fine SAND with quartz gravel - **Residual granite.**

2.10 Very moist, brownish red with orange and yellow mottles, loose to very loose, leached, micaceous, gravelly medium coarse SAND with silt - **Residual granite.**

3.30 Very moist, brownish red yellow and orange, medium dense, micaceous, silty fine SAND with silt - **Residual granite.**

4.00

NOTES

1) No seepage.

2) No refusal.

CONTRACTOR :
MACHINE : TLB
DRILLED BY :
PROFILED BY : Jan Vermaak

TYPE SET BY : YJvV
SETUP FILE : STANDARD.SET

CLIENT : WRC
INCLINATION :
DIAM :
DATE PROFILED : 17 March 1997

DATE : 14/02/00 14:35
TEXT : C:\profiles\WRC.TXT

ELEVATION :
X-COORD :
Y-COORD :

HOLE No: TP 1a
Midrand

dot.PLOT 3030 J&W Inc

UNIVERSITEIT VAN PRETORIA
UNIVERSITY OF PRETORIA
YUNIBESITHI YA PRETORIA

VADOSE ZONE CHARACTERISATION
INJAKA DAM SITE

HOLE No: TP 1b
Sheet 1 of 1

JOB NUMBER: 4222

Scale 1:15

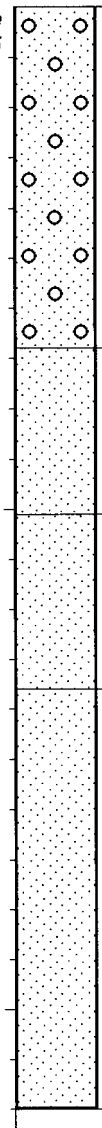

0.00

Moist, white and yellowish light red with dark red stripes, medium dense, gravelly SAND with silt and clay, few plant roots - **Residual granite.**

0.68

Moist, yellowish red and white with dark red stripes, loose to medium dense SAND with silt and clay. Dark red soil pockets comprising silty sand and clay caused by preferential weathering along relict rock structures - **Residual granite.**

1.01

Moist, light red, yellow and white with dark red stripes, loose to medium dense, SAND with silt and clay - **Residual granite.**

1.36

Moist, white and yellowish light red with dark red stripes, loose to medium dense, SAND with silt and clay - **Residual granite.**

2.20

NOTES

1) No seepage.

2) No refusal.

3) No distinct layering.

CONTRACTOR :
MACHINE : TLB
DRILLED BY :
PROFILED BY : Jan Vermaak

TYPE SET BY : YJvV
SETUP FILE : STANDARD.SET

CLIENT : WRC
INCLINATION :
DIAM :
DATE PROFILED : 17 March 1997

DATE : 14/02/00 14:35
TEXT : C:\profiles\WRC.TXT

ELEVATION :
X-COORD :
Y-COORD :

HOLE No: TP 1b
Injaka

dot.PLOT 3030 J&W Inc

APPENDIX B

Geotechnical and soil-water retention test results

Department of Water Affairs and Forestry:
Soil materials laboratory

Index tests (Per cent passing)

Sieve size (mm)	Experiments 1 & 2 18 April 1996				Experiment 3 & 4 7 August 1996				Experiments 5 11 April 1997				
	I01	I02	I03	I04	I01	I02	I03	I04	I01	I02	I03	I04	I05
4.750	100	100	100	100	94	98	99	97	94	98	99	97	98
2.000	96	100	100	100	69	75	81	72	69	75	81	72	77
0.425	72	95	97	97	45	48	46	35	45	48	46	35	38
0.150	57	89	90	86	39	36	31	23	39	36	31	23	25
0.075	51	84	84	75	34	28	24	17	34	28	24	17	19
0.050	44	74	67	63	31	26	22	15	31	26	22	15	19
0.005	26	48	42	32	18	10	7	5	18	10	7	5	7
0.002	22	42	36	26	16	8	5	4	16	8	5	4	4

Geotechnical tests

Test	Experiments 1 & 2 18 April 1996		Experiment 3 & 4 7 August 1996		Experiments 5 11 April 1997	
Dry Density (kg/m^3)	Kald 001	1407	D 001	1640	D 001	1437
	Kald 002	1452	D 002	2165	D 002	1493
	Kald 003	1318	D 003	1632	D 003	1388
	Kald 004	1368	D 004	1732	D 004	1431
	Kald 005	1487			Cal 001	1475
Moisture content (kg/kg)	Kald 001	0.288	D 001	0.138	D 001	0.211
	Kald 002	0.215	D 002	0.000	D 002	0.165
	Kald 003	0.253	D 003	0.132	D 003	0.189
	Kald 004	0.268	D 004	0.138	D 004	0.179
	Kald 005	0.217			Cal 001	0.212
Specific gravity	Kald 001	2.60	D 001	2.65	D 001	2.64
	Kald 002	2.60	D 002	2.64	D 002	Not tested
	Kald 003	2.55	D 003	2.63	D 003	2.68
	Kald 004	2.60	D 004	2.63	D 004	2.66
	Kald 005	2.72			Cal 001	2.64
Void ratio	Kald 001	0.85	D 001	0.62	D 001	0.837
	Kald 002	0.79	D 002	0.22	D 002	Not tested
	Kald 003	0.94	D 003	0.61	D 003	0.931
	Kald 004	0.91	D 004	0.52	D 004	0.859
	Kald 005	0.83			Cal 001	0.790

Constant head and falling head permeability tests (cm/s)

Experiments 1 & 2 18 April 1996		Experiment 3 & 4 7 August 1996		Experiments 5 11 April 1997	
PB001	2.6×10^{-7}	PB001	4.9×10^{-8}	PB001	3.4×10^{-4}
PB002	3.2×10^{-7}	PB002	No test	PB002	3.4×10^{-5}
PB003	1.1×10^{-6}	PB003	3.3×10^{-6}	PB002	9.7×10^{-5}
		PB001a	2.7×10^{-5}	PB002	1.1×10^{-4}
		PB002a	2.0×10^{-7}	PB002	9.8×10^{-4}

Central Agricultural Laboratories

Soil-water retention tests (Per cent water content, kg/kg)

Soil suction (kPa)	Experiments 1 & 2 18 April 1996				Experiment 3 & 4 7 August 1996			Experiments 5 11 April 1997			
	WR 001	WR 002	WR 003	WR 004	WR 001	WR 002	WR 003	WR 001	WR 002	WR 003	WR 004
10	14.01	22.04	20.70	21.80	10.01	11.23	9.53	22.89	27.04	16.65	13.38
20	13.25	18.56	19.49	19.95	9.29	10.40	9.00	20.10	23.27	17.41	12.67
50	11.49	15.75	16.25	17.32	8.75	8.75	7.90	16.65	20.08	17.12	13.22
100	10.50	15.13	15.16	16.06	8.27	7.41	7.00	13.38	19.82	16.15	12.94